Mid-Cenozoic Cool-Water Carbonate Facies And Their Diagenetic History, St. Vincent Basin, South Australia

BASIM SHUBBER

Thesis submitted for the degree of
Doctor of Philosophy in Geology

THE UNIVERSITY OF ADELAIDE
Department of Geology and Geophysics

November 1996

CONTENTS

CHAPTER 4

DIAGENESIS

CHAPTER 5

DOLOMITE

CHAPTER 6

SUMMARY AND CONCLUSIONS

ABSTRACT

Cool-water carbonates form on platforms constrained by bottom water temperatures below approximately 20°C. Mid- to high-latitude, shallow-water, unrimmed shelves and distally-steepend ramps, as well as deep-water slopes in low-latitude regions, are typical cool-water carbonate settings. This study addresses the style and cause of cyclicity in the cool-water, bryozoan-dominated Port Vincent Limestone, through facies analyses and reconstruction of their palaeoenvironments. The study also describes the diagenetic processes and interprets the environments in which the rocks altered. The Oligocene-Miocene Port Vincent Limestone is one of several Tertiary units exposed along coastal cliffs on the western side of the St. Vincent Basin, on the southern Australian continental margin. It is a friable, highly-porous, bryozoan calcarenite punctuated by several 0.5-1 m thick layers of hard, bryozoan calcarenite. These lithological and petrophysical characteristics are related to primary depositional facies, and were later accentuated by selective diagenesis. The outcropping succession is divided into three informal members. The lower member is comprised of two facies, a bryozoan-miliolid-echinoid packstone/rudstone and a bryozoan-bivalve floatstone. The middle member is comprised of five, metre-scale, hardground-bounded, asymmetric, warming-upward subtidal cycles. The upper member is comprised of fine, highly-abraded, bryozoan-*Eponides* grainstone facies. Facies analysis indicates that the Port Vincent Limestone was deposited on a transgressive cool-water carbonate ramp, extending from the inner ramp to an outer middle ramp. Cyclicity suggests that episodic warmer water periods occurred several times during deposition of the Port Vincent Limestone. The warming-upward cycles represent fourth-order parasequences that developed during high frequency fourth-order sealevel fluctuations and are superimposed on a longer term third-order cycle. The three building units (facies) of each parasequence represent three distinctive systems tracts.

This study confirms that cool-water carbonates have low diagenetic potential and yield little $CaCO_3$ for cementation. Cement is limited and precipitated in three diagenetic environments: the seafloor, shallow-burial, and meteoric. Seafloor cementation was synsedimentary, affecting each depositional cycle separately, whereas later shallow-burial and meteoric cementation affected the entire succession. Seafloor cement precipitated from oxidising marine water on or just below the seafloor. At the top of each depositional cycle,

microbioclastic internal-micrite partially infills inter- and intragranular pores, and also overlies the aforementioned seafloor cement. This diagenetic sequence is seen in each successive depositional cycle. After shallow burial, a zoned, brightly-luminescent cement precipitated in pore spaces around the synsedimentary cement and in fractures that cut across pre-cemented echinoid fragments. Later, the rocks were exposed to the shallow meteoric realm, where they underwent minor dissolution and the formation of two cement fabrics, both of which occur in minor amounts. The first is a non-luminescent, syntaxial overgrowth consisting of several thin, dull- to brightly-luminescent zones. The second is a blocky cement composed of: (a) non- to dull-luminescent, non-equicrystalline mosaic, which precipitated within an active, fresh-water phreatic zone. (b) an equicrystalline mosaics, with thin bright- to dull-luminescent intercrystalline boundaries, which precipitated within a relatively stagnant fresh-water phreatic zone. The source for cement is produced by mild intergranular pressure solution, and marine and meteoric dissolution.

The Port Vincent Limestone is locally altered to dolostone and dolomitic limestone. Sucrosic dolomite completely or partially replaces original matrix and most grains. Isotopic and geochemical data suggest that dolomitisation occurred during mid-Cenozoic time, after shallow burial, resulting from fluctuating mixtures of marine water. The dolomite is non-stoichiometric, composed of 41.6 mol% $MgCO_3$, 53 mol% $CaCO_3$, 5.4 mol% $FeCO_3$, and has elevated Sr, Al, and Na concentrations. Crystals show several dull- to bright-luminescent concentric zones, which indicate variable compositional ratios of the dolomitising fluid. Boundaries between adjacent zones are straight and sharp, and sectoral zonations are absent, suggesting no dissolution took place during crystal growth. Dolomite dissolution was fabric selective, affecting a few crystal centres and iron-poor concentric zones, producing thin, rhomb-shaped, intracrystalline voids that are now empty or partially filled with iron oxide. Traces of calcite precipitated in a few intracrystalline micropores, demonstrate a two-step dedolomitisation process.

This study provides significant insight for studies on other cool-water carbonate accumulations throughout the geologic record. Of particular importance, the cool-water model effectively serves for interpreting the diagenetic pathways in ancient calcitic facies, and can be applied towards directing the course of exploration for hydrocarbons and economic ore deposits.

STATEMENT

This work contains no material which has been accepted for the award of any other degree or diploma in any university or other tertiary institution and, to the best of my knowledge and belief, contains no material previously published or written by another person, except where due reference has been made in the text.

I give consent to this copy of my thesis, when deposited in the University Library, being available for loan and photocopying.

Basim Shubber, November 1996

ACKNOWLEDGEMENTS

In undertaking work towards this thesis I have benefited greatly from assistance, advice, and technical and financial support provided by a number of individuals and organisations. This research was made possible by an Australian Overseas Postgraduate Research Scholarship (OPRS) and a University of Adelaide scholarship, to which I am most grateful.

Thanks are due to Dr. Yvonne Bone, Dr. Brian McGowran and Professor Noel P. James for their supervision of the project, their friendly advice and continuous encouragement, their tireless reviews of drafts of the manuscript, and their numerous lively discussions about the project and science in general. Dr. Yvonne Bone entrusted me with many teaching duties, which offered significant scientific and financial benefits. I sincerely thank Yvonne for her support and friendship that extended beyond university boundaries, making my family and I feel at home and welcomed in Australia.

Thanks are due to Drs. Steve Hageman and Qianyu Li for their critical discussions and valuable input into the thesis. I acknowledge the support and advice from Dr. Victor Gostin and Professor Patrick James regarding general thesis matters and for helping the progression of my studies during my time at the Department of Geology and Geophysics.

Staff members of the University of Adelaide provided technical support throughout the study, in particular from the Department of Geology and Geophysics I thank: Rick Barrett for photography and computing assistance, John Stanley and Keith Turnbull for geochemistry, Wayne Mussared and Geoff Trevelyan for preparation of thin sections, Sophia Craddock, Mary Odlum and Gerald Buttfield for their friendly assistance over the years; and from the Centre for Electron Microscopy and Microstructure Analysis (CEMMSA) John Terlet and Huw Rosser.

Much time was spent in the field, for this aspect of the study I am grateful to Mark and Chris Hicks from Port Vincent, for their support and friendship.

To my friends, I give special thanks for their friendship, company and joys over the years of university life in Adelaide, especially Qianyu Li, Steve Hageman, Graham Moss, Tony Mazzoleni, Ghazy Kreshan, Lal Mendis, and Paul Polito.

As ever, my deepest gratitude goes to my parents for their inexhaustible support through all stages of my education. Special thanks to my wife Intisar for her support during my university career, and to the little Shubbers, Zaid, Saif and Hayder for giving up many evenings and weekends.

..... ***Basim***

Chapter 1

INTRODUCTION

1. COOL-WATER CARBONATES

1.1 Definition And General Characteristics:

Cool-water carbonates form on platforms that are constrained by bottom water temperatures below approximately 20°C. Accordingly, mid- to high-latitude, shallow-water, unrimmed shelves and distally-steepened ramps are typical cool-water carbonate settings (Fig. 1.1). Cool-water carbonates may also form in low-latitude regions on deep-water slopes and basin settings (Brookfield, 1988; James and Choquette, 1990a).

The principle characteristics of cool-water carbonate sediments and their depositional and diagenetic environments are distinctive, and contrast significantly from those described in classical warm-water (tropical) carbonate models (e.g., Wilson, 1975; Flügel, 1982; Nelson et al., 1982; Nelson 1988; Henrich et al., 1995). Cool-water carbonate deposition occurs mostly on high-energy unrimmed shelves (cf. James and Kendall, 1992) that are swept by onshore waves due to the lack of a barrier along their deeper offshore margin (Nelson, 1988; Jones and Desrochers, 1992; Bone and James, 1993). Such shelves may be effected by processes similar to those acting on distally-steepend ramps (Read, 1985; Ginsburg and James, 1974), or homoclinal ramps (Ahr, 1973; Read, 1980 & 1985; Burchette and Wright, 1992).

Unlike chlorozoan-dominated warm-water carbonates (Fig. 1.2), cool-water carbonates are almost exclusively biogenic, dominated by aphotic skeletal associations like the foramol (Lees and Buller, 1972) and bryomol (Nelson et al., 1988a) assemblages of bryozoans, foraminifers, echinoids, bivalves, gastropods, and brachiopods. Cool-water carbonate sediments contain little amounts of carbonate mud, which often times is distributed locally, thus textures are dominantly grainstones and rudstones. This mud, however, differs from that present in tropical carbonates in that it has not originated through disintegration of calcareous green algae during initial deposition, but is either a product of bioerosion,

accumulation of nannofossils, or direct precipitation. Consequently, the mud in cool-water carbonates is dominantly calcite in composition, rather than aragonite.

Constituents are commonly made of calcite with variable amounts of Mg rather than aragonite and high-Mg calcite. As a consequence, cool-water carbonate sediments and rocks have low diagenetic potential and will yield little $CaCO_3$ for cementation during meteoric diagenesis. Seafloor cementation however, is common and its products are manifest in the form of distinctive hardgrounds in otherwise friable and highly porous calcarenites. Local as well as large scale dolomitisation is common in many cool-water carbonate sequences (e.g., James et al., 1993; Shubber et al., 1996).

1.2 Previous Work on Cool-Water Carbonates:

Interest in cool-water carbonates has been growing since the unconventional views of Chave (1967) acknowledged the precipitation of carbonate sediments beyond the tropics, and related their existence to low terrigenous supply rather than temperature. Following Chave's ideas, a series of research studies on modern and ancient cool-water carbonates begun detailing many attributes of these distinctive sediments from regions around southern Australia and New Zealand (e.g., Connolly and von der Borch, 1967; Wass et al. 1970; Nelson, 1978, 1988; Nelson et al., 1982; Rao, 1981a, 1981b; Jones and Davies, 1983; McGowran and Beecroft, 1985; Gostin, et al. 1988; Reeckmann, 1988; Kamp, et al. 1990; James and Bone, 1991, 1992; James, et al. 1992, 1993, 1994; Boreen, et al. 1993, Bernecker et al., 1995; Nicolaides, 1995). More recently a number of studies addressing the facies and depositional environments of cool-water carbonates from the northern hemisphere have been introduced (e.g., Scoffin, 1988; Henrich et al., 1995; Carey et al., 1995).

2. STUDY OBJECTIVES

The continental margin of southern Australia is the largest region of cool-water carbonate deposition on a shelf in the modern ocean. This area has been the site of almost continuous

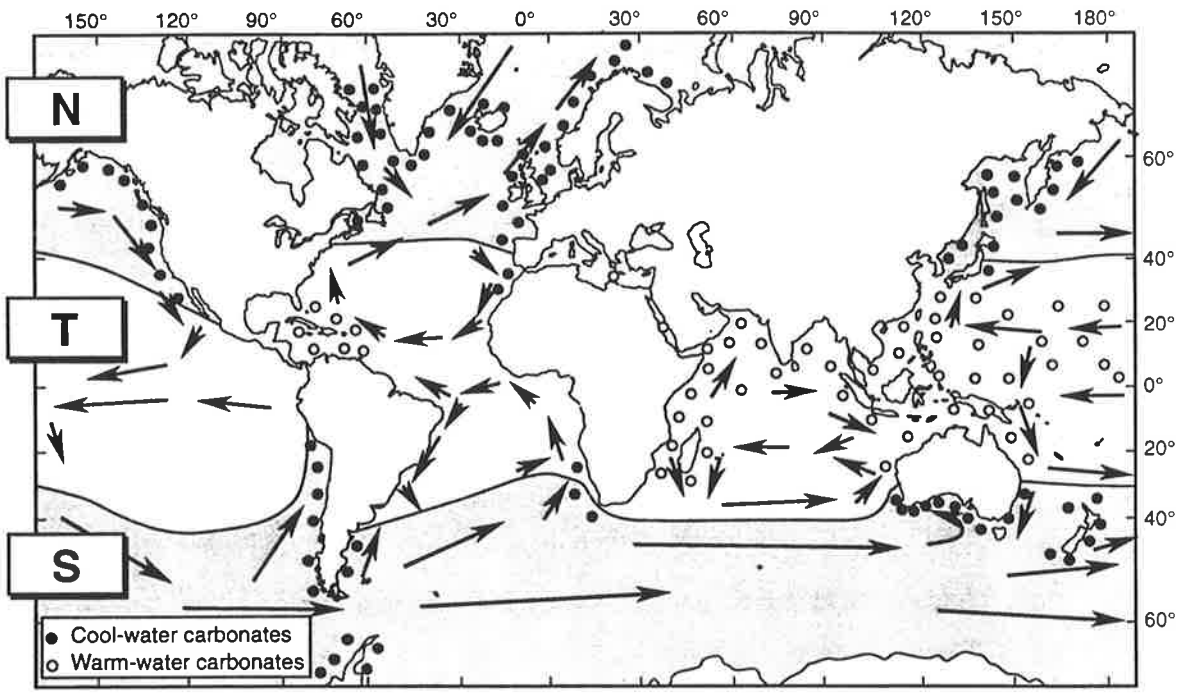

Figure 1.1: Global distribution of modern cool-water and warm-water (tropical) carbonates. N, S = northern and southern cool-water carbonate belts; T = Tropical, warm water carbonate belt. Modified from Henrich et al., 1995.

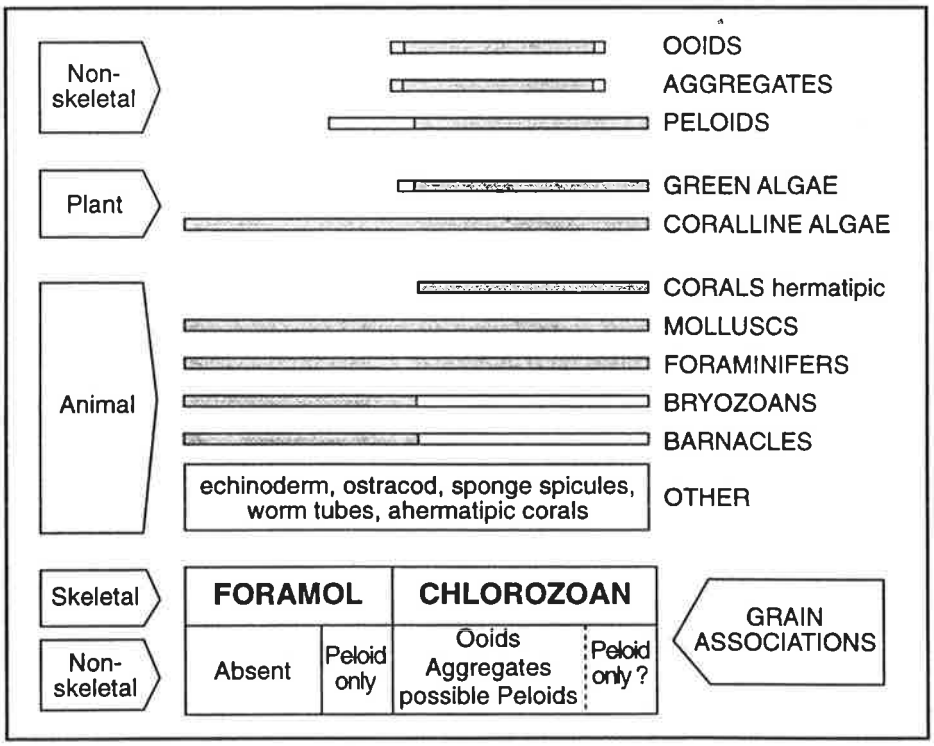

Figure 1.2: Comparison of foramol and chlorozoan carbonate assemblages. From Lees and Buller, 1972.

cool-water carbonate deposition since the Eocene. Eocene to Miocene strata outcrop in several shallow onshore basins like the St. Vincent Basin in South Australia (Stuart, 1970; Lindsay, 1981, 1985; Cooper, 1985; Lindsay and McGowran, 1986; James and Bone, 1989, 1994; McGowran and Li, 1994; Boreen and James, 1995). It is now 26 years since the comprehensive study of Stuart (1970) was published. Although at that time Stuart addressed many questions, many others remained unanswered, and/or need to be updated to meet current demands.

This study describes and interprets the depositional facies, reconstructs the depositional environments, and addresses the style and cause of cyclicity in the Cenozoic Port Vincent Limestone in the St. Vincent Basin. Diagenetic products and environments in which most alterations occurred are described. The diagenetic history of this limestone succession is revealed from the sequence of cementation. The study also documents the presence of dolomite in the Port Vincent Limestone and provides an assessment on the style, composition, mode of origin and diagenetic history of these dolomites.

It is hoped that this study of Cenozic limestones will provide significant insight for studies on other cool-water carbonate accumulations of similar or older age. Of particular importance, the cool-water model effectively serves for interpreting the diagenetic pathways in ancient calcitic facies, and can be applied towards directing the course of exploration for hydrocarbons and economic ore deposits.

3. METHODS

Rock samples were collected from 15 measured stratigraphic sections at a sampling interval of 50 cm. Additional sub-samples were taken where significant physical variation occurred. General carbonate sedimentology terms are after Reijers and Hsü (1986). Granulometric properties were described using Miall's (1990 p. 27) classification list (Fig. 1.3). Carbonate depositional textures were described following the genetic classification of Dunham (1962). Dunham's classification offers environmental interpretations based on relations between

Limiting particle diameter				Clastic rocks			Carbonate rocks	
							Transported constituents	Authigenic constituents
m	mm	ϕ units[b]	Micrometers (μm)					
	2048	−11		V. large	Boulders	Gravel	V. coarse calcirudite	Extremely coarsely crystalline
1	1024	−10		Large				
	512	− 9		Medium				
	256	− 8		Small				
	128	− 7		Large	Cobbles			
10^{-1}	64	− 6		Small				
	32	− 5		V. coarse	Pebbles		Coarse calcirudite	
	16	− 4		Coarse				
10^{-2}	8	− 3		Medium			Medium calcirudite	
	4	− 2		Fine				
	2	− 1		V. fine			Fine calcirudite	Very coarsely crystalline
10^{-3}	1	0		V. coarse	Sand		Coarse calcarenite	Coarsely crystalline
	1/2	+ 1	500	Coarse			Medium calcarenite	
	1/4	+ 2	250	Medium			Fine calcarenite	Medium crystalline
10^{-4}	1/8	+ 3	125	Fine			V. fine calcarenite	
	1/16	+ 4	62	V. fine			Coarse calcilutite	Finely crystalline
	1/32	+ 5	31	V. coarse	Silt		Medium calcilutite	
	1/64	+ 6	16	Coarse			Fine calcilutite	Very finely crystalline
10^{-5}	1/128	+ 7	8	Medium			V. fine calcilutite	
	1/256	+ 8	4	Fine				Aphanocrystalline
	1/512	+ 9	2	V. fine				
10^{-6}					Clay/mud			

Figure 1.3: Grain size classification for clastic and carbonate rocks constituents. Miall (1990).

BRYOZOA GROWTH FORMS					
GROWTH FORM NAME		SHAPE	NELSON et al. 1988	CLASSIFICATION Cheilostome	Cyclostome
ERECT RIGID	1. FENESTRATE		ER ERfe	Reteporiform	Reticulate diastoporiform
	1a. *Adeona* sp.	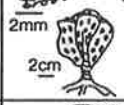	ERfe	Reteporiform	———
	2. FOLIOSE	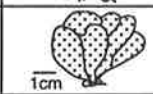	ERfo	Escharifform	Bilaminar diastoporiform
	3. FLAT ROBUST BRANCHING		ERro	Adeoniform	———
	4. DELICATE BRANCHING	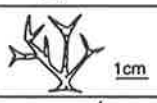	ERde	Vinculariiform	Idmidroniform, Pustuliporiform, Cavarid diastoporiform, Homeriform, Lichenoporiform
ERECT FLEXIBLE	5. ARTICULATED BRANCHING	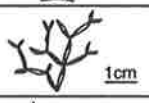	EF	Cellariform	Crisiform
	6. ARTICULATED ZOOIDAL	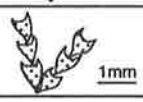	———	Catenicelliform	———
7. ENCRUSTING			ENul	Membraniporiform	Stomatoporiform
8. NODULAR/ ARBORESCENT		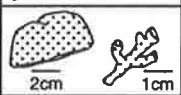	ENml	Celleporiform	Atractosoeciform Cerioporiform
9. VAGRANT		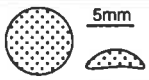	FL	Lunulitiform	———

Figure 1.4: Bryozoan classification scheme, the growth-form approach. Bone and James, 1993.

grains, fabric, and hydraulic processes. Bryozoans were identified using the bryozoan growth-form classification of Bone and James (1993) (Fig. 1.4; Appendix A-1). Other principle constituents were identified with the aid of descriptions given in Milliman (1974), Bathurst (1975), Flügel (1982), Ludbrook (1984), Smith (1984), Kruse and Philip (1985), Murray (1985), McNamara et al. (1986), Boardman et al. (1987) and Nelson et al. (1988b). Fine constituents were identified by scanning electron microscopy. Facies were recognised by field observations and laboratory analysis. Quantification of constituents using point counting by volume % (grain-bulk, Dunham, 1962) was performed on a number of selected thin sections to accentuate critical facies differences (also see Flügel 1982, p. 241). Porosity type follows the classification of Choquette and Pray (1970).

Mineralogy of constituents was identified by a Philips PW 1050 x-ray diffractometer (XRD). All samples were spiked with quartz to provide a reference peak for accurate measurements of the calcite peak. Positions of peaks were measured to the nearest 0.01° 2-theta, using the computer program XPLOT. The derived angular values were then entered into a computer program to obtain the mole % $MgCO_3$ proportions within the calcite. Calibration is based on Goldsmith et al. (1961).

Transmitted-light microscopy and cathodoluminescence (CL) were carried out on 199 polished thin sections. CL characteristics of calcite cements and dolomite (Appendix A-2) were studied by examining 40 polished sections (100 μm thick), using a Technosyn 8200 luminoscope. An additional 31 standard thin sections were stained for chemical assessment and differentiation using the technique of Dickson (1966). Selected dolomite samples were examined by backscattered electron images (BSE), produced from a Philips XL 20 scanning electron microscope (SEM) equipped with an energy-dispersive x-ray system (SEM-EDS). Chemical analyses were conducted through dry methods using polished sections, where selected spots were identified using a Cameca SX51 electron microprobe with three wavelength dispersive spectrometers, used under accelerating voltage of 15 kV and specimen current of 20 nA, beam size ranged between 1-2 microns.

Carbon and oxygen isotope analyses were performed on a few pure limestone and dolomite samples, using an Optima stable isotope mass spectrometer (Fisons Instruments) equipped with an Isocarb automated preparation system. Values of $\delta^{13}C$ and $\delta^{18}O$ relative to PDB were determined from CO_2 released from calcite or dolomite dissolved in 100% H_3PO_4 at 90°C, then corrected to 25°C. The isotopic ratios were reported in delta notation (per mill ‰) relative to Peedee Formation Belemnite (PDB). The $^{87}Sr/^{86}Sr$ ratios were performed by Professor Kurt Kyser, at Queen's University, Canada.

Out of nearly 2000 onshore and offshore bore holes drilled on the western margin of the St. Vincent Basin, only six had cutting samples from Tertiary strata. Unfortunately the suitability of the bore holes for detailed facies studies is reduced as the cutting samples were affected by considerable down hole contamination. Nevertheless, well reports provided critical stratigraphic references.

4. REGIONAL SETTING

4.1 St. Vincent Basin:

The Cenozoic St. Vincent Basin is a structural intracratonic graben complex (Stuart, 1969, 1970). It formed during the Middle Eocene, as a consequence of sudden and rapid acceleration in the rate of separation between Australia and Antarctica (Cooper, 1985). Prior to the Middle Eocene the area was a land mass undergoing weathering and erosion (Daily et al., 1976). The basin covers an area of 15,000 km^2, extending for about 250 km from north to south and 100 km from east to west (Fig. 1.5). It is bounded by uplifted basement blocks of the Mount Lofty Ranges in the east, the low up-faulted central Yorke Peninsula in the west and north, and the uplifted Kangaroo Island in the south (Stuart, 1969; Ludbrook, 1980). The basin is connected from the north east to the Pirie Basin via a corridor in the Crystal Brook area (Kremor, 1986-*in* Alley and Lindsay, 1995). Several, tectonically related, sub-basins comprise the St. Vincent Basin. The largest is the Adelaide Plains Sub-basin and others, including the Golden Grove, Noarlunga and Willunga sub-basins.

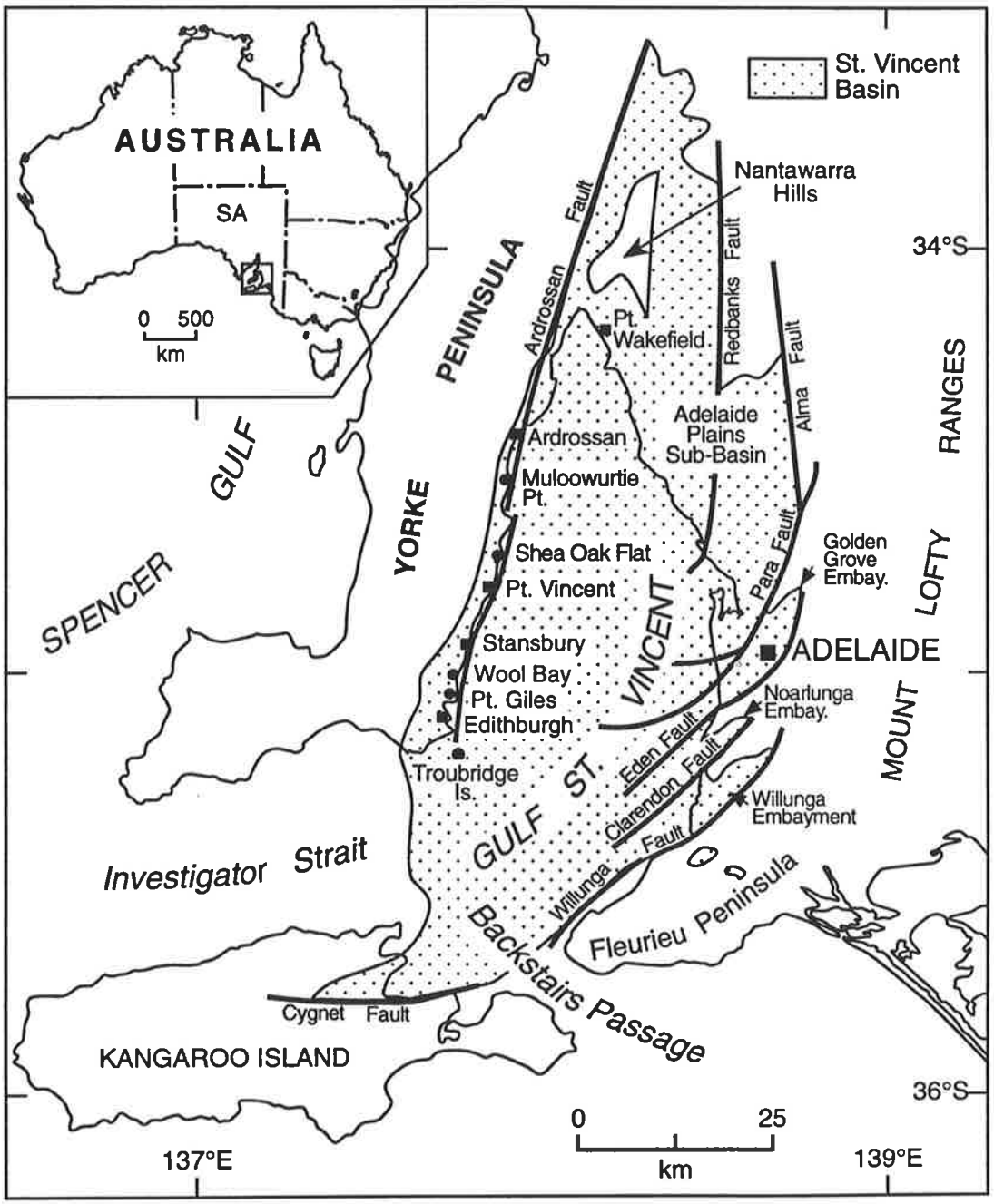

Figure 1.5: The Cenozoic St. Vincent Basin of South Australia and its major embayments and faults.

Today, approximately 60% of the basin lies beneath Gulf St. Vincent. It is an active region of modern carbonate sediment production and accumulation (Gostin, et al., 1988).

Sedimentation in the basin commenced during Middle Eocene time with fluviatile deposits followed by significant carbonate and mixed siliciclastic accumulation. Up to 600 m of Cenozoic sediments accumulated in the St. Vincent Basin (Daily et al., 1976; BMR, 1979). Several Cenozoic units are exposed along coastal cliffs on both the eastern and western sides of the basin. Sub-crop as well as off-shore units can be traced via a limited number of bore holes. Cenozoic successions west of the basin are the thinnest due to their distant position from the main tectonically-controlled depositional centre. The rocks are mainly shallow-marine, cool-water carbonates with minor, but significant, terrigenous clastic units. The fact that the basin lay within high-latitude regions, coupled with its relatively close geographic position to Antarctica, did not prevent warm-water incursions from lower latitudes.

4.2 Yorke Peninsula:

Yorke Peninsula is a low north-south trending horst, separating St. Vincent Gulf from Spencer Gulf (Crawford, 1965). Cenozoic beds of the St. Vincent Basin are intermittently exposed in easily accessible coastal cliffs for approximately 85 km along the east coast of Yorke Peninsula, from south of Ardrossan to Edithburgh. The Port Vincent Limestone is intermittently exposed for approximately 50 km from south of Shea Oak Flat to south of Edithburgh (Fig. 1.6). Apart from a few quarries and open mines, inland surface geological investigation is hindered by an omnipresent blanket of Quaternary calcrete.

4.3 Palaeogeography:

Except for northward drifting, the general palaeogeography of the St. Vincent Basin is similar to that of today. The present geographically disconnected Kangaroo Island, Flinders, and Mount Lofty Ranges were, during the Late Cambrian-Early Ordovician, part of a continuous great mountain chain termed the Delamerides (Thomson, 1969; Daily et al., 1976, 1979).

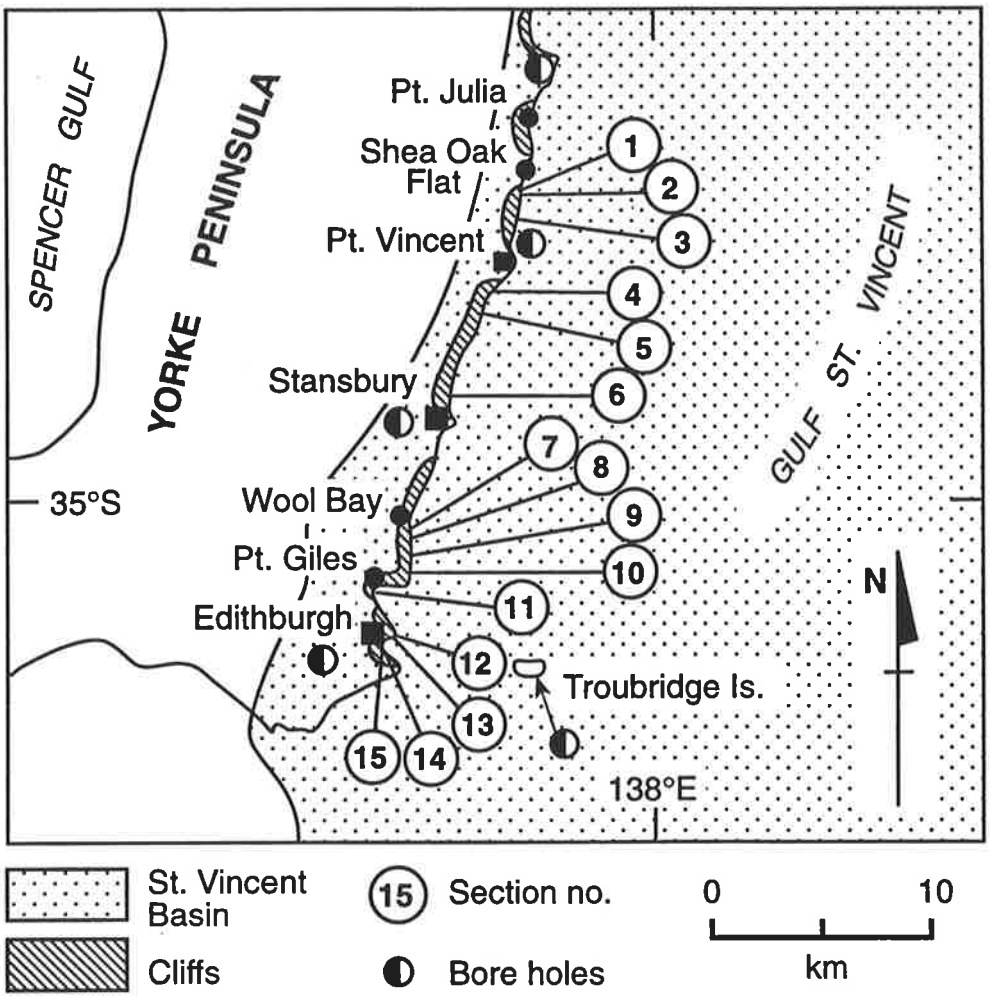

Figure 1.6: Location map showing studied sections of the Port Vincent Limestone outcrops on the east coast of Yorke Peninsula.

During Early Palaeocene time a phase of slow northward drifting of Australia from Antarctica reached its final stage, and brought most of the southern half of the Australian plate into the position of 60° S latitude. There is no evidence of marine transgressions during this time (McGowran, 1991), and the Cretaceous - Tertiary boundary is unconformable reflecting a major eustatic fall in sealevel at the end of the Cretaceous. This phase was followed by a sudden and more rapid separation between Australia and Antarctica during the Middle Eocene, drifting the continent 10° further north. There is no evidence of sedimentation in southern Australia during late Early - early Middle Eocene (McGowran, 1989a).

The St. Vincent Basin received its first deposits in the Middle Eocene, in the form of terrigenous non marine sediments (Alley and Lindsay, 1995). Widespread deposition commenced during three marine transgressions, and a phase of decelerated drifting prevailed throughout until the Late Miocene bringing the continent into lower latitudes (McGowran, 1989a, 1991; McGowran et al., 1992; Veevers et al., 1991).

Widespread carbonate deposition continued during the Early Oligocene in the St. Vincent Basin and most of the southern basins. Deposition in the St. Vincent Basin ceased by the late Early Oligocene as a consequence of the global sealevel fall of approximately 125 m and the development of ice sheets in Antarctica (Haq et al., 1987; Shackleton, 1986).

Carbonate deposition resumed in the St. Vincent Basin following a rapid transgression during the Late Oligocene - Early Miocene. During this time and through the early Middle Miocene at least six transgressive episodes affected southern Australia, and are evident from several glaucony rich layers, and horizons containing warm-water extratropical large benthic foraminifers (McGowran, 1979; Alley and Lindsay, 1995). The St. Vincent Basin became exposed at the end of this stage, due to falling sealevel followed by uplift which is evident from the low-angle unconformity that separates Oligocene - Miocene strata from the overlying Pliocene strata. Deposition of the Port Vincent Limestone ceased while the basin was lying south of latitude 50° S.

Oceanic access to the St. Vincent Basin during most of the Cenozoic is believed to be provided by Investigator Strait (Glaessner and Wade, 1958), and Backstairs Passage (Cooper and Lindsay, 1978). This is supported by the presence of isolated exposures of Late Eocene, Oligocene, and Early Miocene marine deposits along both entrances and northern Kangaroo Island (Howchin, 1903; Glaessner and Wade, 1958; Ludbrook, 1963a; Lindsay, 1972, 1983; McGowran, 1973, 1978; Milnes et al., 1983).

4.4 Palaeoclimate:

The St. Vincent Basin passed across several climatic belts during its northward drift from high latitudes to lower latitudes. As a consequence, carbonate sediments of the St. Vincent Basin accumulated under contrasting climatic conditions, ranging from cool-temperate during the late Middle Eocene and Oligocene to warm-temperate and subtropical during significant parts of the Miocene.

Palynological and palynofloral evidence indicate widespread cool-temperate rain forests during the Early Palaeocene in most of southern Australia (Alley and Clarke, 1992), with temperatures around 18°C during the Middle Eocene (Alley and Lindsay, 1995).

The late Middle Eocene Epoch marks the beginning of a gradual but remarkable climatic change (referred to as the Terminal Eocene Event) since the end of the globally-warm, glacial-free, late Cretaceous. Oxygen isotope palaeotemperature curves and micropalaeontological evidence from southern Australia indicate significant climatic cooling across the Eocene-Oligocene boundary, with several short-lived warmer episodes interrupting this overall cooling event (Shackleton and Kennett, 1975; McGowran and Beecroft, 1985). Lindsay and McGowran (1986) stress that this climatic event did not cause a catastrophic change among the foraminiferal community in the St. Vincent Basin. Cool - temperate rain forests prevailed in most of the southern parts of South Australia during the latest Eocene to Early Oligocene (Alley and Lindsay, 1995).

As the rate of separation between Australia and Antarctica increased, seawater temperature elevated. By the end of Oligocene time, a climatic warming initiated and continued to the end of the Lower Miocene Epoch, when cooling was established again. Three warm intervals, separated by two miniglaciations, were recorded from the Miocene succession of South Australia:- the lower Early Miocene, the middle Early Miocene, and the upper Early Miocene to the Middle Miocene (McGowran and Li, 1994). Supported by oxygen isotope analysis data and the presence of large benthic foraminifers, the late Early Miocene and the early Middle Miocene have been regarded as the warmest interval of the Neogene (Shackleton and Kennett, 1975; McGowran, 1979; Wolfe and Poore, 1982; Adams et al., 1990).

Surface water temperature, at 47-52°S latitude, in the southern ocean fell from 20°C in the Early Eocene to 11°C in the Late Eocene. Cooling continued during the Early Oligocene, with temperatures dropping to 7°C. Bottom water temperatures were 2-3°C less (Shackelton and Kennett, 1975). Water temperature rose by about 3°C during the Early Miocene followed by a fall and a later rise at the beginning of the early Middle Miocene (Shackelton and Kennett, 1975).

The oxygen-isotope temperature curve of Devereux (1967) and a palaeontologically based climate curve (Hornibrook, 1971) indicate climatic cooling at the beginning of the late Eocene through the Oligocene during the Tertiary in New Zealand. During the last two decades, minor differences have occurred in interpreting the cause and dating the timing and duration of these cooling events. However, there seems to be a general agreement on a cooling event in the Tertiary. Globally, palaeoclimatic evidence clearly indicates a gradual temperature decline during the late Middle Eocene across the Eocene/Oligocene boundary and earliest Oligocene (Frakes, 1986; Wei, 1991; Berggren and Prothero 1992; Miller, 1992).

5. PREVIOUS STUDIES

The name St. Vincent Basin was introduced by Glaessner and Wade (1958), replacing the former Adelaide Basin of Howchin and Parr (1938); Glaessner (1953). The St. Vincent

Basin has been the subject of numerous stratigraphic studies, most of which centred on the basin's eastern margin, with particular emphasis on the systematics of stratigraphy. In contrast, the geology of the basin's western margin received less attention, with far fewer studies addressing the Tertiary stratigraphy and sedimentology.

The foundation for many studies on the Tertiary of the region were laid down by earlier workers like Tepper (1879), Howchin (1886, 1903, 1911) and Tate (1888, 1890). Early views on the region's tectonic framework were introduced by Benson (1911), who related Kangaroo Island and the Mount Lofty Ranges to the same tectonic network. Howchin (1911) indicated the existence of a graben, and considered the Tertiary sediments downthrown towards Gulf St. Vincent. Building on these views, Fenner (1927, 1930) considered that the Mount Lofty Ranges and Yorke Peninsula were two horst structures. Glaessner (1953), Campana and Wilson (1954) and Glaessner and Wade (1958) all rejected the notion that a Tertiary sea covered vast parts of the Mount Lofty Ranges, as initially proposed by Fenner (1927).

The first reconnaissance geological survey was conducted by King (1956). In the following years, the Tertiary stratigraphic knowledge of the region was enriched by various geological studies, and a number of reports from stratigraphic and exploration bore holes (e.g., Glaessner 1953, 1959; Wade, 1959; Ludbrook 1954, 1961a, 1963a, 1963b, 1964; Lindsay 1967, 1969; and Harris 1966). A valuable contribution by Crawford (1965) presented significant aspects of the Tertiary stratigraphy, structure, tectonics and economic geology of Yorke Peninsula. Increased detail on the Tertiary stratigraphy, particularly of the western part of the St. Vincent Basin, was introduced by Stuart (1969, 1970). Stuart presented the time-rock stratigraphic units of the Cenozoic strata exposed on the eastern coast of York Peninsula, describing type sections and suggesting new rock names. He also addressed the geological history and tectonic activity which took place in the St. Vincent Basin during the Tertiary. Subsequently, most work focused on the eastern part of the St. Vincent Basin (e.g., Lindsay, 1981, 1985; Harris, 1985; McGowran and Beecroft, 1985; Moss, 1995),

except for Stafford (1987) who reported a general geological coverage of Yorke Peninsula, briefly outlining some of Stuarts (1970) earlier work on the Tertiary succession.

Recently Alley and Lindsay (1995) published a comprehensive summary on the Tertiary "southern marine basins" of South Australia. The study updates much of the early work and presents significant results obtained from extensive exploration and investigation carried out by a team of geologists at the South Australian Department of Mines and Energy. The study covered the eastern part of the St. Vincent Basin thoroughly but did not update earlier information regarding the western side of the basin.

Chapter 2

STRATIGRAPHY

1. INTRODUCTION

This chapter describes and illustrates the stratigraphic relationships of the Port Vincent Limestone in the Cenozoic St. Vincent Basin. The origin and significance of lithostratigraphic sequences and their relation to previous and current studies of sealevel fluctuation are discussed and interpreted in the context of sequence stratigraphy (chapter 3).

Local stratigraphic correlation is compiled from 15 outcrop sections (Figs. 1.6, 2.1; Appendices B-2 to B-6). For a regional stratigraphic framework, the local stratigraphy is correlated with reference stratigraphic successions from various southern Australian Cenozoic basins (Fig. 2.2).

2. GENERAL STRATIGRAPHY

2.1 Distribution and Thickness:

The bryozoan-dominated Port Vincent Limestone occurs along the western margin of the St. Vincent Basin (Fig. 1.5). Beds are intermittently exposed for approximately 50 km along the east coast of Yorke Peninsula (Fig. 1.6). They crop out from a location about 600 m south of Shea Oak Flat southwards until they disappear below the surface just south of Edithburgh (Fig. 2.1; plates 2.1-A, B, C; 3.2-A, B; 4.3-A; 4.4-A, B; 5.1-A, B). Lithostratigraphic correlation is easily established between these outcrops, despite several physical discontinuities.

The limestone has a maximum thickness of 125 m in a bore hole on Troubridge Island. A thickness of 49 m was recorded from the Black Point stratigraphic well No. 1A, 33 m in Port Vincent No. 1 stratigraphic well, 35 m in Stansbury stratigraphic bore hole, and 9 m in Stansbury West No.1 well (Ludbrook, 1961a, 1963b, 1964; Steel, 1963; Watts and Gausden, 1966). The limestone rapidly thins to zero in the western, northern and north western directions. Only 3 m are exposed in coastal sections south of Shea Oak Flat.

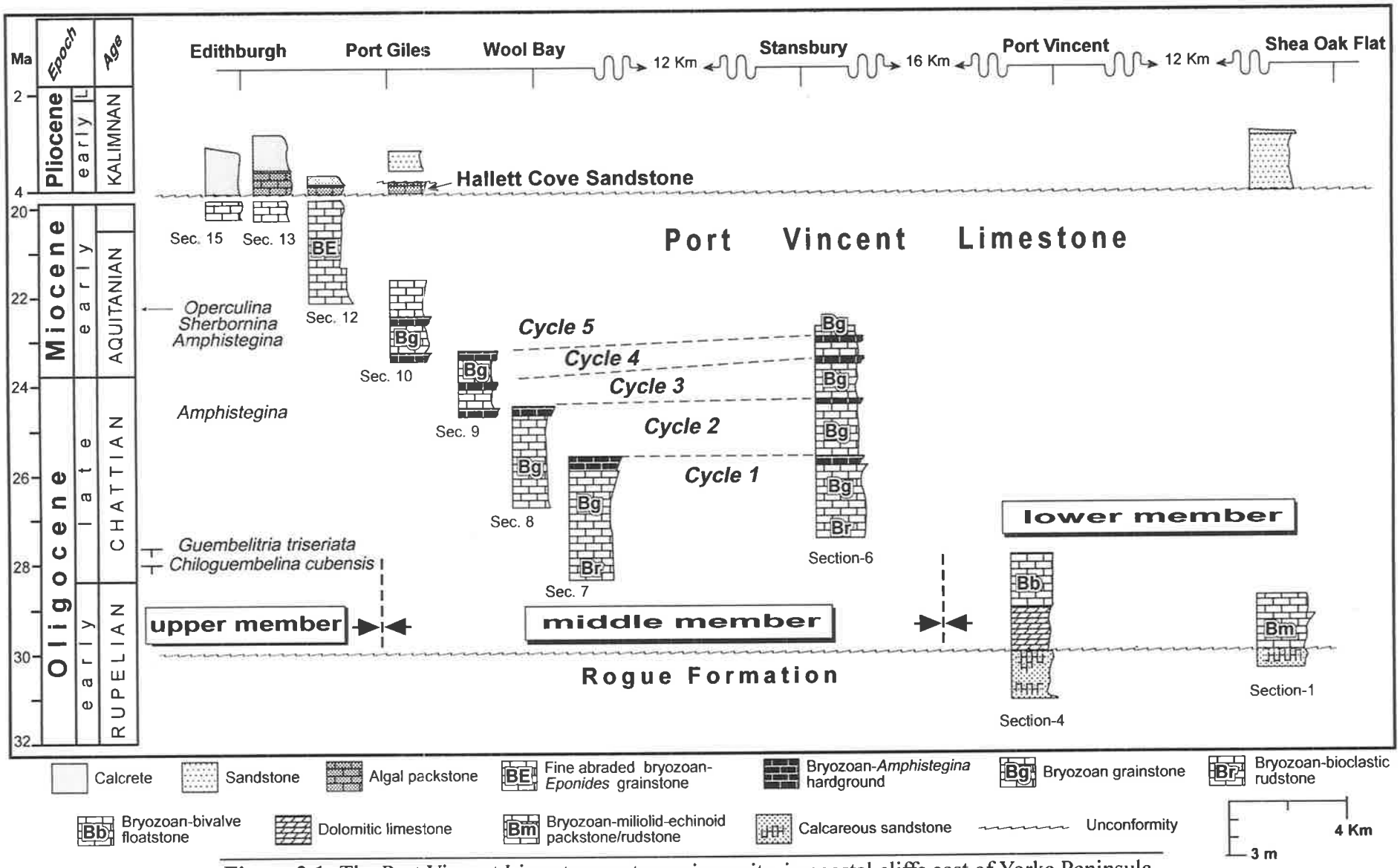

Figure 2.1: The Port Vincent Limestone outcropping units, in coastal cliffs east of Yorke Peninsula.

Exposures between Stansbury and Wool Bay (middle member), range from 12 to 15 m in thickness. From south of Giles Point to south of Edithburgh (upper member) thicknesses range from 3 to 6.5 m (Fig. 2.1, Appendix B-6). The limestone has not been recorded from the central or northern parts of Yorke Peninsula. Bore holes confirm that the Port Vincent Limestone thins and terminates 10 - 25 km inland from the east coast. Thinning is both depositional and erosional. Beds are nearly horizontal, with a very gentle southerly dip. The name Port Vincent Limestone was first applied by Stuart (1969). Prior to Stuart the same units were referred to as the Port Willunga beds (Ludbrook, 1961a, 1963a, 1964; Crawford, 1965).

2.2 Age and Boundaries:

In coastal areas, the rocks are mainly Oligocene to Lower Miocene in age, whereas units in the Troubridge Island bore hole extend from Late Eocene to Middle Miocene age, and in the Black Point bore hole they are Lower Miocene in age (Stuart, 1969, 1970, and references within).

Age determination in this study is in close agreement with Stuart's age ranges, based on the following evidence: (1) *Globigerinatheka index* is present immediately below the unconformity separating the Rogue Formation from the dolomitised part of the Port Vincent Limestone south of Port Vincent, but was not observed above in the Port Vincent Limestone dolomite. Top *Globigerinatheka index* indicates a Late Eocene age (Lindsay, 1985; McGowran and Beecroft, 1986). (2) The planktonic foraminifers *Chiloguembelina cubensis, Guembelitria stavensis*, and *Globigerina* sp. are prominent in the dolomitised beds (plate 5.6-A). *Chiloguembelina cubensis* and *Guembelitria triseriata* are also present north of Stansbury at the base of the succession. McGowran and Beecroft (1985) place top *Guembelitria* within zone P.21, early in the Late Oligocene. *Chiloguembelina cubensis* Zone marks the early Late Oligocene/Early Miocene boundary (McGowran and Beecroft, 1985). Therefore, the lower part of the Port Vincent Limestone succession, which extends

from Shea Oak Flat to Port Giles and includes the lower member and the bottom part of the middle member, is uppermost Early Oligocene to Late Oligocene in age (Figs. 2.1, 3.3).

The Port Vincent Limestone succession is obscured by absence of exposure (~ 4 km) between Giles Point and Edithburgh. Correlation in this case is rendered possible by foraminiferal zonation which suggests that the upper third of the Port Vincent Limestone succession at Port Giles and that at Edithburgh are of the same age. *Sherbornina* sp. and *Operculina* sp. are present in samples from both locations, while *Amphistegina* sp. were recorded from below in the hardgrounds extending from Stansbury to Port Giles (cycle tops in the middle member). According to Stuart (1969 - Text Figure 14), the last appearance of *Sherbornina* is in the Early Miocene whereas *Operculina* extends into the Middle Miocene. Other studies however, show *Operculina* extending only into the Early Miocene (e.g., McGowran, 1979; Heath and McGowran, 1984). Consistent in trend with these age ranges is the absence of the large benthic foraminifer *Lepidocyclina*. *Lepidocyclina* appears late in the Early Miocene (McGowran, 1979, 1986).

From the above faunal evidence it is concluded that the Oligocene/Miocene boundary is located somewhere between the *Amphistegina* set of hardgrounds and the *Operculina* zone. The youngest exposed beds of the Port Vincent Limestone are Early Miocene in age. These are exposed at the top of the section at Port Giles and extend southward to Edithburgh.

The Port Vincent Limestone unconformably overlies the Eocene Rogue Formation. It is unconformably overlain by the Pliocene Hallett Cove Sandstone in the south, and by Quaternary sediments in the north (Fig. 2.1) (Crawford, 1965; Stuart, 1970; Cooper, 1985; Alley and Lindsay, 1995). These boundaries are further discussed in the proceeding section.

2.3 Composite Stratigraphy in the St. Vincent Basin:

Tertiary strata overlie highly weathered Precambrian basement rocks in most parts of the St. Vincent Basin, with the remainder locally overlying Cambrian limestones (plate 2.2-A) or Permian Cape Jervis Formation on the basins eastern margin. No Mesozoic strata have been recorded underlying Cenozoic sediments (Daily et al., 1976; Alley and Lindsay, 1995).

The record of alternating marine transgressions and regressions during Late Eocene - Middle Miocene time is reflected by the diversity of rock units and sequence boundaries observed in the stratigraphic succession of the St. Vincent Basin. Tertiary sedimentation commenced with Middle to Late Eocene basal fluviatile sediments (North Maslin Sand and Clinton Coal Measures equivalent), and ceased with the deposition of Late Pliocene fossiliferous sandstones and arenaceous limestones (Hallett Cove Sandstone). The interval between these two units is stacked with a variety of shallow marine siliciclastic, cool-water carbonates, and nonmarine deposits (Reynolds, 1953; Stuart, 1970; Lindsay, 1981, 1985; Cooper, 1985; Lindsay and McGowran, 1986; McGowran and Beecroft, 1986). The most complete Tertiary successions are exposed in coastal cliffs on the eastern and western margins of the basin, in the Willunga Embayment and in eastern Yorke Peninsula respectively. The following section aims to present a composite stratigraphic succession for the Port Vincent Limestone in the St. Vincent Basin. However the complete Tertiary succession on eastern Yorke Peninsula is briefly presented here to place the Port Vincent Limestone in a geological context. Figure 2.2 illustrates intrabasinal correlation as well as correlation with strata in other Tertiary southern and southeastern Australian Basins.

Tertiary strata on the western margin of the St. Vincent Basin are exposed in semicontinuous coastal cliffs along the east coast of Yorke Peninsula. These successions are thin due to their distal position relative to the main tectonically controlled depositional centre (Cooper, 1985; M. Sandiford pers. com.). The Tertiary stratigraphy along the east

coast of Yorke Peninsula has been described by Stuart (1969, 1970), and is described below with further reference to field observations made in this study.

The succession begins with thin fluviatile sands and pebbles, which are correlated with the Middle to Late Eocene portion of the Clinton Coal Measures in the north west part of the basin (Crawford, 1965). These Tertiary fluviatile sediments are recorded from the Black Point bore hole, and in coastal areas a one-metre thick layer is exposed at the base of the cliffs, mid way between Rogue and Muloowurtie Points (plate 2.2-B). The succeeding Muloowurtie Formation and its Quartoo Sand Member (Stuart, 1970) unconformably overlies these fluviatile sediments, if present, or the Cambrian Kulpara Limestone (plate 2.2-A, B). The Muloowurtie Formation is a marine sequence, 12 m thick, consisting of ochre-yellow microbioclastic wackestone, quartz sand, and fine calcareous and glauconitic quartz sand (plate 2.2-C). A thin sequence of lagoonal silts and quartz sands, defined by Stuart (1970) as the Throoka Silts, disconformably overlies the Muloowurtie Formation, and is disconformably overlain by sediments of the Rogue Formation. The Late Eocene-Oligocene Rogue Formation is a marine sequence dominated by siliciclastic sediments (plate 2.4-D), including several characteristic hard silicified bands (30-50 cm thick) which contain numerous *Turritella* sp. and sponge spicules (plate 2.3-A, B, C). The formation is intermittently exposed in coastal cliffs from Rogue Point to approximately 7 km south of Port Vincent, and has a maximum thickness of 52 m in the Black Point bore hole. Two dark green, glaucony-rich sandstone and mudstone, beds of the Port Julia Greensand Member punctuate the stratigraphic succession of the Rogue Formation extending from Port Julia to south of Shea Oak Flat. The two beds are approximately 1 m vertically apart at Shea Oak Flat. The lower is 40-50 cm thick, and the upper is 10-20 cm thick (plate 2.4-A, B). Type sections of the Late Eocene Muloowurtie Formation, Throoka Silts, and Late Eocene/Oligocene Rogue Formation are present at Muloowurtie Point (Stuart, 1970).

Early Oligocene beds of the Port Vincent Limestone unconformably overlie the Rogue Formation (plate 2.4-C) between Shea Oak Flat and Port Vincent. These beds are

Figure 2.2: Tertiary Stratigraphy of The St. Vincent Basin, and other Southern/Southeastern Basins.

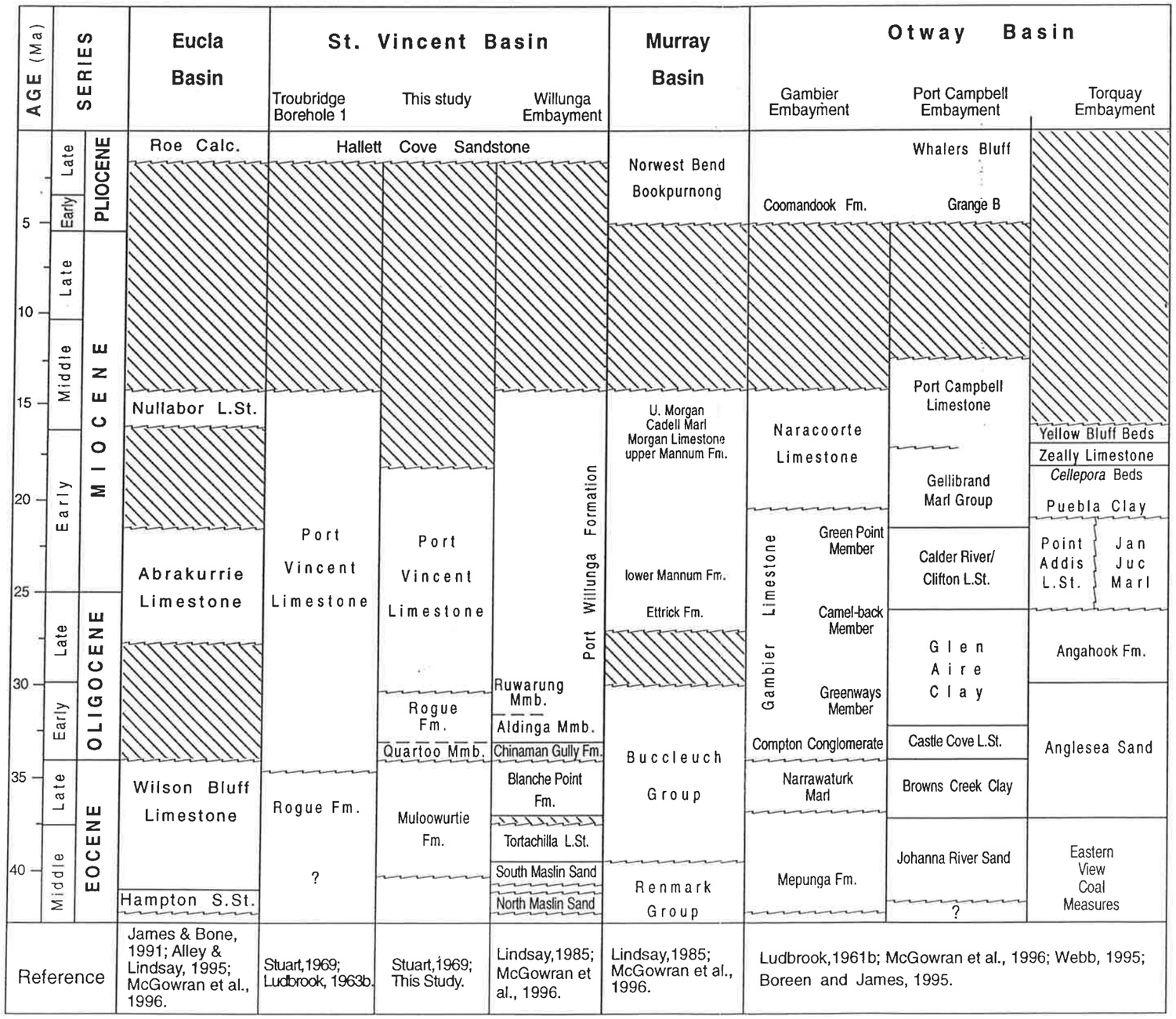

correlated with the Oligocene part of the bryozoan-rich Port Willunga Formation on the eastern side of the St. Vincent Basin (Stuart, 1970). A low angle unconformity separates the Early Miocene Port Vincent strata from the Pleistocene Ardrossan Clays and Sandrock in the northern area (between Shea Oak Flat and Wool Bay), and the Late Pliocene marine sediments of the Hallett Cove Sandstone in the southern area extending between Port Giles and Edithburgh (Fig. 2.1; plate 2.5-A, B). The Hallett Cove Sandstone is composed of fossiliferous sandstones and arenaceous limestones rich in *Marginopora vertebralis* (plate 2.5-C), molluscs, coralline algae, and oysters. The latter increase in abundance southwards, forming an oyster dominated-bed, less than 1 m thick, which is exposed approximately 2.5 km south of Port Giles.

Only the Late Oligocene part of the Willunga Formation is exposed in coastal cliffs along the Willunga Embayment. The Oligocene/Miocene sediments are found in bore holes in the Willunga Embayment and the Adelaide Plains sub-basin (Lindsay, 1981, 1985; Moss, 1995). The coarse grained bryozoan, chert-bearing, Ruwarung Member (Cooper, 1977), has no equivalent lithostratigraphic unit on Yorke Peninsula. However, some similarities are present in the stratigraphic succession exposed on both sides of the St. Vincent Basin. One example is the common occurrence of silica rich beds in the Eocene/Oligocene Blanche Point Formation and the Rogue Formation, suggesting deposition from silica-rich oceans during the Middle/Late Eocene (McGowran, 1989b).

The separation of Australia from Antarctica resulted in a series of marine transgressions into the southern marine basins, and the deposition of considerable thicknesses of marine sediments. Thus, the Tertiary stratigraphic record is largely similar in all basins. The succession begins with early Tertiary non-marine terrigenous sediments, and passes vertically and laterally (seawards) into marine cool-water limestones (Alley and Lindsay, 1995). Figure 2.2 summarises the stratigraphic record in the St. Vincent Basin and other Tertiary southern and southeastern Australian Basins.

Plate 2.1:

A- The Port Vincent Limestone succession, exposed in coastal cliffs south of Shea Oak Flat. The rocks appearing in this location are the bryozoan miliolid-echinoid packstone/rudstone facies of the lower member. Scale indicated by arrow = 1 m.

B- The Port Vincent Limestone middle member exposed north of Stansbury (section 6). This section is composed of warming-upward, subtidal, hardground-bounded, carbonate cycles.

C- The Port Vincent Limestone succession, exposed in coastal cliffs south of Edithburgh. Rocks in this location are composed of fine, highly-abraded bryozoan-*Eponides* grainstone facies which comprise the upper member.


A


B


C

Plate 2.2:

A- The Tertiary Muloowurtie Formation (M) unconformably overlying the Cambrian Kulpara Limestone (K) south of Muloowurtie Point. Scale indicated by arrow = 1 m.

B- Basal fluviatile sediments (sands and pebbles) unconformably overlain by the Tertiary Muloowurtie Formation (M) on the western side of the St. Vincent Basin, south of Muloowurtie Point. Scale = 1 m.

C- Thin section photomicrograph (plain light) showing microbioclastic wackestone, quartz sand, and fine calcareous and glauconitic quartz sand of the Muloowurtie Formation exposed at Muloowurtie Point.


M
K
A


M
M
B

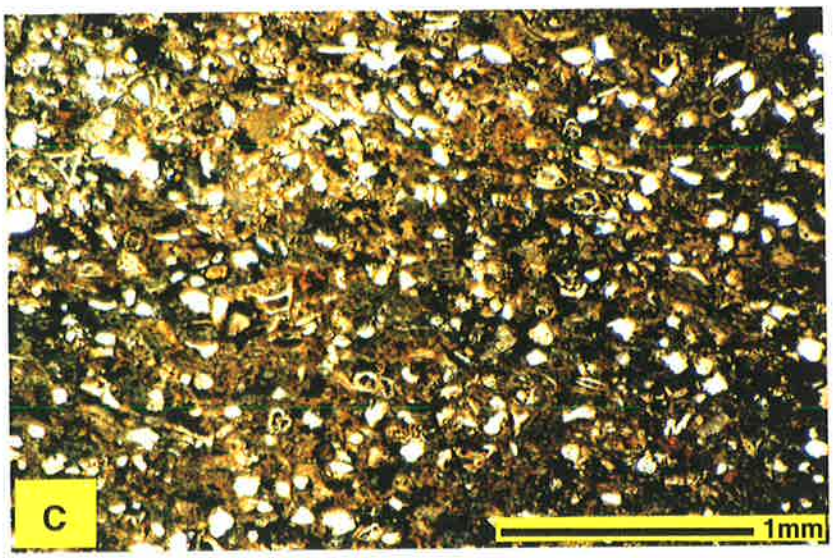
C
1mm

Plate 2.3:

A, B- Late Eocene-Oligocene Rogue Formation exposed south of Rouge Point. The formation contains several characteristic hard silicified 30-50 cm thick bands (arrows in photo A), which contain numerous *Turritella* sp. (B). Scale in photo A = 2 m.

C- Thin section photomicrograph (plain light) showing sponge spicules (arrows) and peloids (P), which are common in the lower part of the Rogue Formation exposed at Rogue Point.


A


B
2 cm

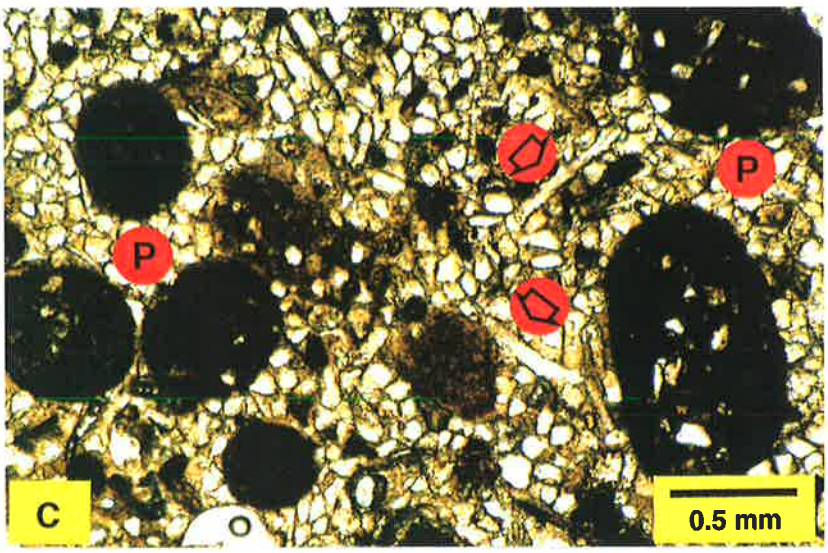
C
P
P
0.5 mm

Plate 2.4:

A- Dark green beds of the Port Julia Greensand Member (arrows) punctuating the Rogue Formation, south of Shea Oak Flat (section 3). The two beds are approximately 1 m vertically apart; the lower is 40-50 cm thick, and the upper is 10-20 cm thick. Scale = 2 m.

B- Thin section photomicrograph (plain light) showing glaucony-rich sandstone and mudstone of the Port Julia Greensand Member.

C- Early Oligocene beds of the Port Vincent Limestone (P) unconformably overlying the Rogue Formation (R), south of Port Vincent township. Scale (bottom left corner) = 1 m.

D- Thin section photomicrograph (plain light) of a sample from the top of the marine Rogue Formation where the quartz sandstone seen in plate 2.3-C becomes enriched in calcareous constituents, e.g., fragments of delicate branching (d) and articulated branching (a) bryozoan growth forms.

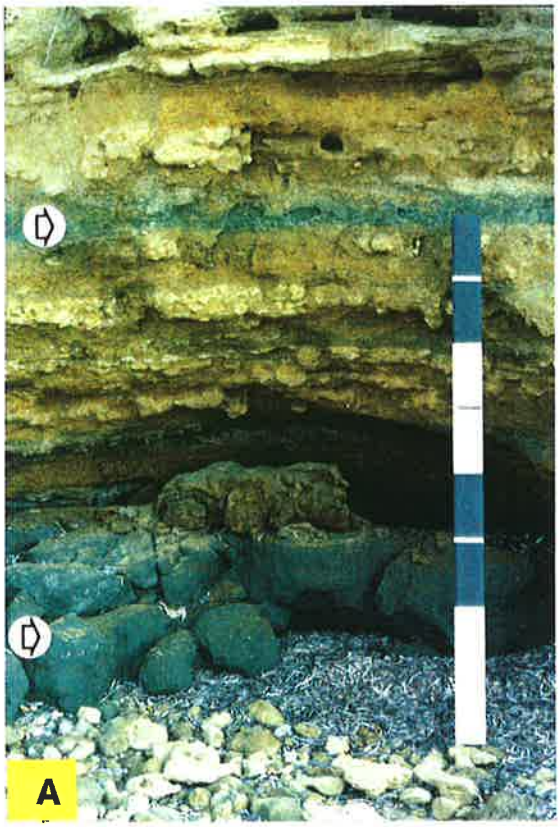
A

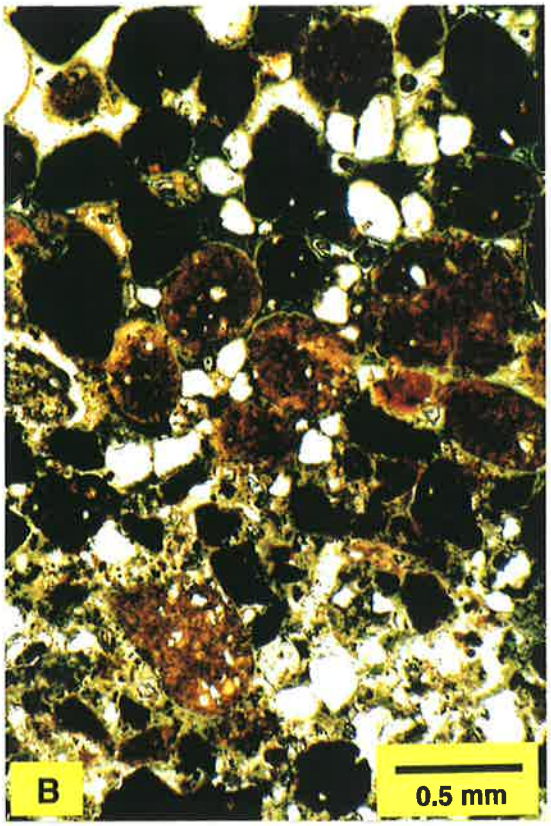
B
0.5 mm


P
R
C

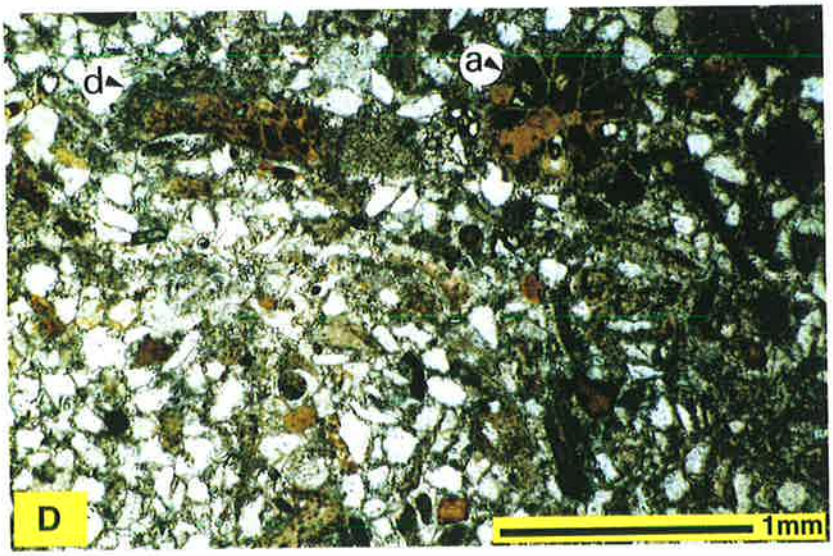
d
a
D
1mm

Plate 2.5:

A- Unconformity surface (arrows) between the Port Vincent Limestone (P) and the overlying Pliocene Hallett Cove Sandstone (H) at section 15 south of Edithburgh.

B- Thin section photomicrograph (plain light) for the unconformity surface illustrated in photo A above, showing the fine, highly abraded bryozoan-*Eponides* grainstone facies of the Port Vincent Limestone (P), and the overlying sediments of the Hallett Cove Sandstone (H).

C- Thin section photomicrograph (plain light) showing large benthic foraminifer *Marginopora vertebralis* filled with intragranular cement in the Hallett Cove Sandstone at Edithburgh (section 15).

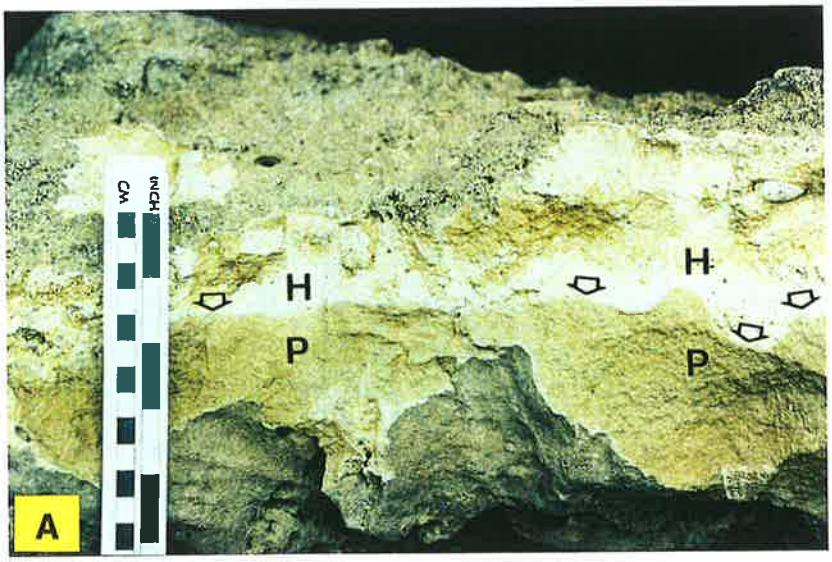
CM
INCH
H
P
H
P
A


2mm
H
P
B

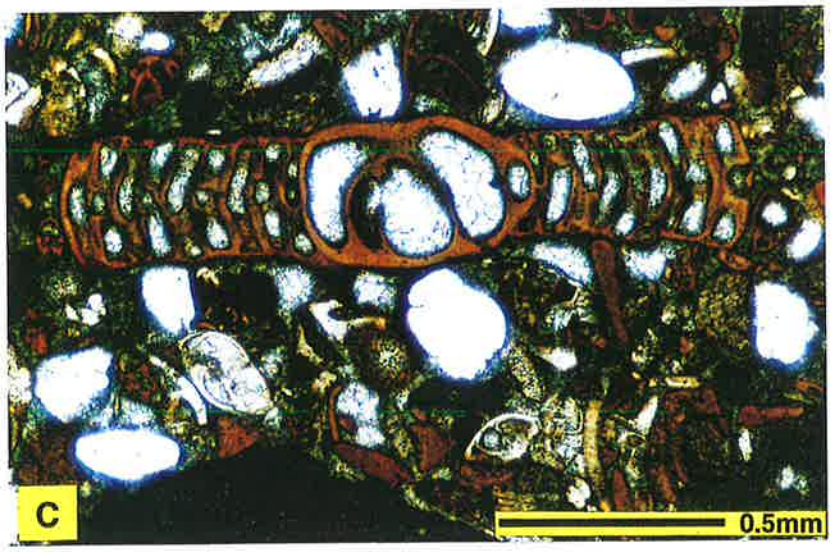
0.5mm
C

Chapter 3

FACIES & CYCLICITY

1. INTRODUCTION

The term "facies" is defined as: "...a body of rock characterised by a particular combination of lithology, physical and biological structures that bestow an aspect (facies) different from the bodies of rock above, below and laterally adjacent" (Walker, 1992). Facies of the Port Vincent Limestone were determined by field observations and laboratory analyses, including point counting. Early diagenetic features were also included to aid in facies definition. All facies are bryozoan dominant but are differentiated on the basis of bryozoan growth forms and other associated components. Rocks contain little carbonate mud both as depositional seafloor micrite, and internal micrite (cf. Ried et al., 1990). Facies classification is kept as simple as possible in order to avoid the complexities associated with multiple subdivisions that may overshadow primary patterns in facies analysis. Ultimately, each facies has its own environmental interpretation, which reflects aspects of its depositional environment.

2. PORT VINCENT LIMESTONE

The Port Vincent Limestone spreads along the western margin of the St. Vincent Basin (Fig. 1.5). Beds are nearly horizontal, with a very gentle southerly dip and are intermittently exposed for approximately 50 km along the east coast of Yorke Peninsula (Fig. 1.6). The limestone has a maximum thickness of 125 m in the Troubridge Island bore hole but rapidly thins to zero to the west and north. The thinning is depositional as well as erosional. Onshore units are Oligocene to Early Miocene in age, whereas units in the Troubridge Island bore hole extend from Eocene to Middle Miocene (Stuart, 1970; Cooper, 1985). They unconformably overlie the Eocene Rogue Formation and are unconformably overlain by the Pliocene Hallett Cove Sandstone in the south and by Quaternary sediments in the northern parts of the peninsula (Fig. 3.1-A).

The Port Vincent Limestone has a cool-water skeletal association (cf. bryomol, Nelson et al. 1988a). It is a bryozoan-dominated calcarenite, locally enriched in foraminifers,

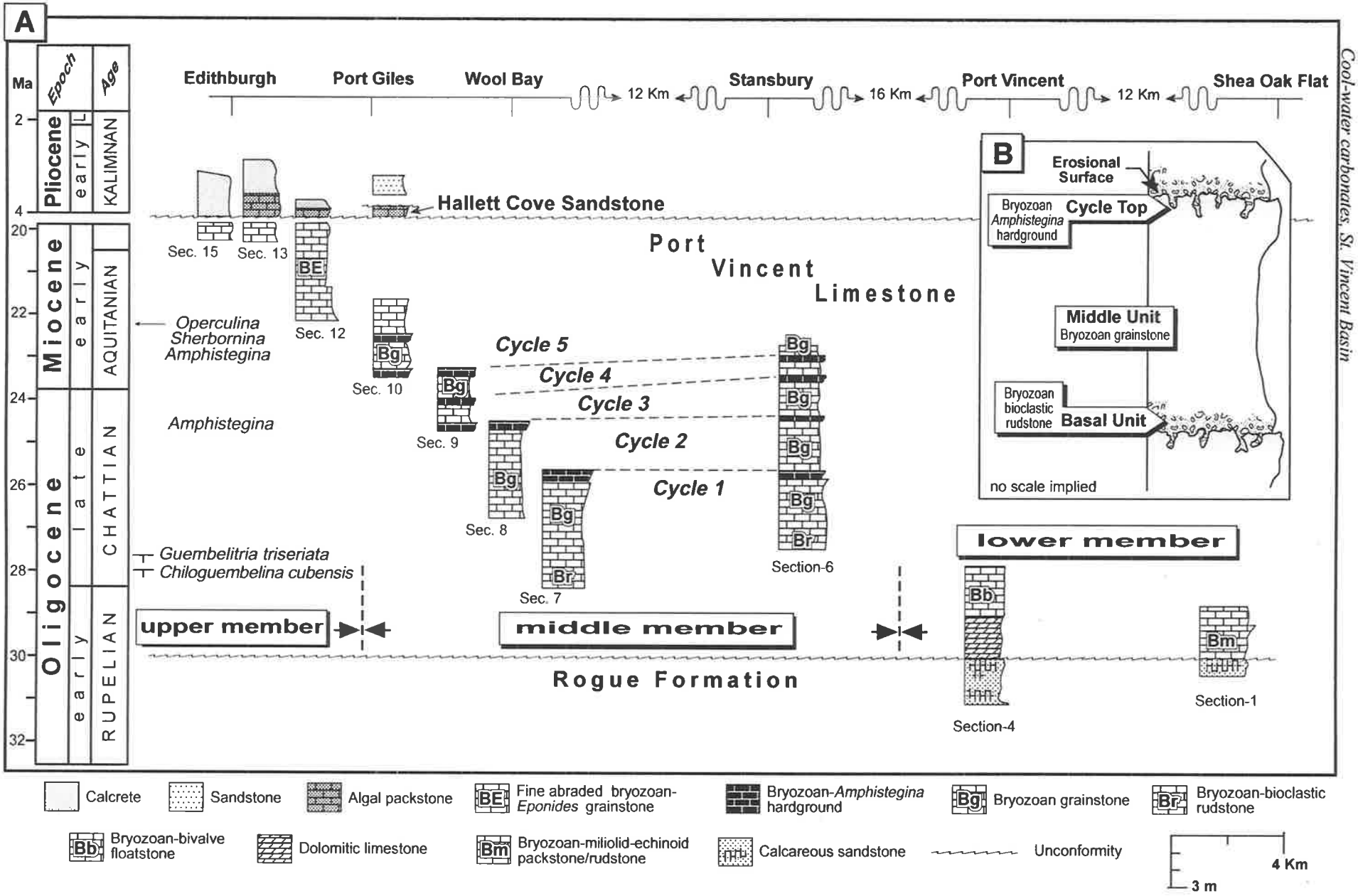
A
Ma
Epoch
Age
Pliocene
early
L
KALIMNAN
Miocene
early
AQUITANIAN
Oligocene
late
CHATTIAN
early
RUPELIAN
2
4
20
22
24
26
28
30
32
Edithburgh
Port Giles
Wool Bay
12 Km
Stansbury
16 Km
Port Vincent
12 Km
Shea Oak Flat
Hallett Cove Sandstone
Port Vincent Limestone
Sec. 15
Sec. 13
Sec. 12
Sec. 10
Sec. 9
Sec. 8
Sec. 7
Section-6
Section-4
Section-1
Operculina
Sherbornina
Amphistegina
Amphistegina
Guembelitria triseriata
Chiloguembelina cubensis
Cycle 5
Cycle 4
Cycle 3
Cycle 2
Cycle 1
upper member
middle member
lower member
Rogue Formation
B
Erosional Surface
Bryozoan Amphistegina hardground
Cycle Top
Middle Unit
Bryozoan grainstone
Bryozoan bioclastic rudstone
Basal Unit
no scale implied
Calcrete
Sandstone
Algal packstone
Fine abraded bryozoan-Eponides grainstone
Bryozoan-Amphistegina hardground
Bryozoan grainstone
Bryozoan-bioclastic rudstone
Bryozoan-bivalve floatstone
Dolomitic limestone
Bryozoan-miliolid-echinoid packstone/rudstone
Calcareous sandstone
Unconformity
4 Km
3 m

Figure 3.1:

A- Stratigraphic section of the Port Vincent Limestone along coastal cliffs, east of Yorke Peninsula. The Port Vincent Limestone is divided into three informal members: The lower member is comprised of two facies, which represent a transgressive phase of deposition; the middle member is comprised of five warming-upward, metre-scale, asymmetric, hardground-bounded, subtidal carbonate cycles; the upper member is comprised of one single facies.

B- An idealised depositional cycle is shown.

echinoids, coralline algae, bivalves, gastropods and brachiopods (plate 3.1-A, C). Several buff coloured, 0.5- to 1-m thick hardgrounds punctuate the sequence (Fig. 3.1-A, plate 3.2). The dominant lithology is a poorly cemented, friable, bryozoan calcarenite. Most bryozoan remains consist of erect rigid delicate branching cyclostomes, erect flexible articulated branching cheilostomes and, less commonly, erect rigid flat robust branching, encrusting and vagrant growth forms (plate 3.3). The hardgrounds are well-cemented and dominated by erect articulated branching cheilostomes, erect flat robust branching, erect delicate branching cyclostomes, encrusting and vagrant bryozoan growth forms (plate 3.4). The majority of constituents were composed of low (LMC) to intermediate Mg-calcite (IMC) and lesser amounts of high Mg-calcite (HMC) originally, but are now all (LMC) (Appendix B-1). The presence of mouldic porosity indicates an aragonitic origin for some constituents, especially molluscs and erect flat robust-branching bryozoans.

In this study, the Port Vincent Limestone is divided into three informal members: lower, middle, and upper. The lower member is comprised of two facies, which represent a transgressive phase of deposition. The middle member is comprised of five warming-upward cycles and shallowing-upward cycles. The upper member is comprised of one single facies.

2.1 LOWER MEMBER

2.1.1 Bryozoan Miliolid Echinoid Packstone/Rudstone Facies:

Description:

Rocks are cream to pale yellow, friable to moderately lithified, poorly sorted, fossiliferous calcarenites and calcirudites. The facies is dominated by bryozoans but contains more benthic foraminifers and echinoids than other facies (plate 3.1-A). Less common skeletal constituents include coralline algae, disarticulated and broken molluscan shells, gastropods, brachiopods, other bioclasts, very rare planktonic foraminifers, peloids and rare silt to sand

size quartz grains. Glaucony grains (cf. Odin and Fullagar, 1988), in the form of granular-habit internal moulds, are common.

Although the facies is bryozoan-dominant, the abundance of total bryozoan fragments is low compared to that in other facies. Many delicate bryozoan colonies are large, unbroken and show little evidence of abrasion. Cheilostome bryozoan fragments are dominant and cover a broad spectrum of sizes, ranging from fine-calcarenite to medium-calcirudite (0.25-16 mm). Identifiable fragments are of articulated branching, flat robust branching, *Adeona*-like, fenestrate and encrusting unilaminar growth forms. Cyclostomes are mostly delicate branching morphotypes. Fine skeletal fragments are volumetrically minor and, although difficult to classify into individual growth forms, are easily recognised as bryozoan fragments. Benthic foraminifers are present as whole well-preserved tests, some with recrystallised walls; others are recognised from their moulds, now composed of glaucony. Tests are dominated by large miliolids, up to 2 mm in diameter. *Spiroloculina, Quinqueloculina,* and *Triloculina* are among the most common genera, whereas *Elphidium*, *Cibicides* and the agglutinated textularids are less abundant. The majority of echinoid tests are complete and upright but freed of spines. Spines are usually nearby in the same outcrop and show little evidence of abrasion. Irregular infaunal echinoids are abundant and represented by at least three genera: *Lovenia*, *Eupatagus*, and *Monostychia*. They are preserved as whole tests, as gravel to pebble size broken plates and as spines. Most echinoid grains are surrounded by large crystals of clear syntaxial calcite cement (plate 3.1-A). Small fragments (< 2 mm) of coralline algae, molluscs and brachiopods are common throughout but never occur as major constituents. They are generally little abraded, and subangularity amongst these grains is high except for coralline algal fragments, which are typically well rounded.

Packstones contain micrite in the form of a grey, patchily distributed matrix. Both internal sediment and internal micrite cement (cf. Reid et al., 1990) are also present and have a fine-

grained peloidal texture that grades into coarser (< 0.1 mm), clear calcite crystals towards void centres.

Interpretation:

Most clasts are medium- to coarse-grained size and only slightly abraded, indicating local production of major constituents, minimal transport, little winnowing and suggesting low-energy levels within the environment of deposition. Delicate and articulated branching growth forms are common in deep waters (> 70 m) as well as in shallower-water modern environments (Nelson et al., 1988b; James et al., 1992; Bone and James, 1993). Flat robust branching, *Adeona*-like sp., other fenestrate and encrusting unilaminar growth forms are all widely distributed on shallow parts of modern continental shelves around southern Australia and New Zealand, and despite being highly adaptable to various environmental factors, they commonly favour either unconsolidated or moderately hard substrates in regions of low sedimentation rates (Nelson et al., 1988b; James et al., 1992; Bone and James, 1993). The relatively low abundance of encrusting coralline algae, most of which are interpreted to be allochthonous, also suggests a soft substrate.

Modern sediments rich in miliolids are characteristic of low-energy, lagoonal or shallow marine shelves, with soft substrates and low rates of sedimentation (Bignot, 1985; Murray, 1991). In modern surficial cool-water sediments from northern Spencer Gulf and Gulf St. Vincent, *Triloculina* is particularly common in shallow subtidal environments in water depths below 10-20 m and seems to be concentrated in protected areas behind sand shoals (Gostin et al., 1988). In the rock record, highly glauconitic layers commonly occur at the base of transgressive sequences (e.g., the global Cenomanian transgression, Odin and Hunziker 1982; Lutetian transgression in the Paris Basin, Odin et al. 1982; Holocene transgression on the Congolese continental shelf, Odin, 1988).

From the foregoing this facies is interpreted as being deposited during a transgressive phase, on a shallow inner ramp (Fig. 3.2), characterised by a soft to moderately hard substrate.

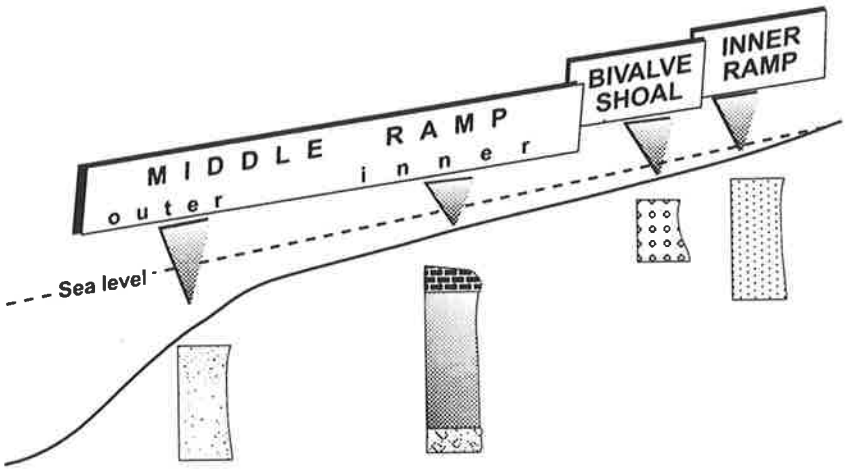

Facies	Constituents
Bryozoan miliolid-echinoid packstone/rudstone	Cheilostome bryozoans are abundant and include articulated branching, flat robust branching, *Adeona*-like, fenestrate, encrusting unilaminar, as well as delicate-branching cyclostomes. Benthic foraminifers *Spiroloculina*, *Quinqueloculina* , and *Triloculina* are common, whereas *Elphedium*, *Cibicides*, and agglutinated textularids are less common. Echinoids *Lovenia*, *Eupatagus*, and *Monostychia* are common. Less common constituents include coralline algae, disarticulated mollusc shells, gastropods, brachiopods, and rare planktonic foraminifers, peloids, silt to sand size quartz and glaucony grains.
Bryozoan bivalve floatstone	Flat robust branching, articulated branching, arborescent, and encrusting bryozoan growth-forms. Delicate-branching forms are common in the lower parts of the facies but decrease upwards. Bivalves are dominated by disarticulated shells of the epifaunal genus *Chlamys*. Benthic foraminifers are also common, and include *Cibicides*, *Elphedium*, and *Bolivina*, as well as rare textularids and miliolids. Planktonic foraminifers are scarce, and represented by the genera *Guembelitria*, *Chiloguembelina*, *Globogerina*, and *Subbotina*. Irregular infaunal echinoid plates and spines of *Lovenia* are common as well as coralline algae.
Bryozoan bioclastic rudstone	Bryozoans are dominated by nodular arborescent, erect rigid flat robust-branching, fenestrate, foliose, and encrusting growth-forms. Articulated branching cheilostomes are common, whereas delicate branching growth-forms are rare to absent. Benthic foraminifers are dominated by epifaunal *Cibicides*, and rare textularids. Planktonic foraminifers, and fragments of coralline algae are rare to absent.
Bryozoan grainstone	Delicate branching cyclostomes and articulated branching cheilostomes are abundant. Other bryozoan fragments include rare arborescent, flat-robust branching, fenestrate, foliose, and encrusting growth-forms. Broken plates and abraded spines of irregular infaunal echinoids are prolific. Small whole tests of *Lovenia*, *Eupatagus*, and *Monostychia* are common. Benthic foraminifers include species of *Cibicides*, *Spirillina*, *Notorotalia*, *Operculina*, and rare *Crespinina*, miliolids and textularids. Planktonic foraminifers *Guembelitria* and *Chiloguembelina* are rare and present only in lower parts. Coralline algae are absent to rare at the bottom, but become common upwards.
Bryozoan *Amphistegina* hardground	Articulated branching cheilostomes and delicate branching cyclostomes, with common flat robust branching, foliose and vagrant growth-forms. There is an increase in the percentage of robust branching growth-forms and a decrease of the delicate branching forms, compared to the underluing bryozoan grainstone facies. The most characteristic feature of this facies is the abundance of large epifaunal benthic foraminifer *Amphistegina*. *Cibicides* are common, whereas miliolids and textularids are rare. Whole and partial tests of echinoderms are common. Fragments of coralline algae and bivalves are common to rare. Planktonic foraminifers are rare.
Fine highly-abraded bryozoan-*Eponides* grainstone	Erect rigid-delicate branching cyclostomes and erect flexible-articulated branching cheilostomes, together with other broken unidentified bryozoan fragments. Benthic foraminifers *Eponides*, and small tests of *Cibicides*, *Sherbornina* are common, miliolids and textularids are rare. Other common constituents include bivalves, echinoids, coralline algae, and calcareous sponge spicules.

Figure 3.2: Idealised sketch and summary of the Port Vincent Limestone facies and their depositional environments in the coastal cliffs on eastern Yorke Peninsula.

Location and extent:

The strata outcrop from approximately 600 m south of Shea Oak Flat for some 200 m southward along the coastal cliffs. It has an average thickness of about 2.5 m (Appendix B-2). The facies is unconformably overlain by the Quaternary clay and sand sediments, and lateral correlation is hindered by an upthrown faulted block 1 km south of Shea Oak Flat.

2.1.2 Bryozoan Bivalve Floatstone Facies:

Description:

Rocks of this facies are present as discontinuous lens-shaped bodies with a low relief geometry (< 2.5 m). They are pale yellow to cream coloured, poorly sorted, friable to moderately-hard calcarenites and coarse calcirudites that are locally stained with orange-brown iron oxides. The base of the facies, at one location only, is variably altered to fine crystalline (< 100 μm), idiotopic, cloudy cored, clear rimmed, sucrosic dolomite (plate 3.1-B). The sequence is interrupted by a diastem, which is capped by a hardground that is compositionally identical to the surrounding rocks but is differentiated by its significant amounts of cement. The limestones are composed mainly of bryozoans, pectinid bivalves, echinoids, benthic and planktonic foraminifers, coralline algae, a few solitary corals and a few glaucony grains (plate 3.1-C).

Bryozoan fragments are abundant, and range in size between 0.25-0.5 mm (fine sand) with a few between 0.5-2 mm. Common growth forms are flat robust branching, articulated branching, arborescent, and encrusting. Delicate branching bryozoans are common in the lower parts of the facies but decrease upwards. Bivalve shells, and to a lesser extent moulds, are abundant. Most bivalve fragments are disarticulated shells of the epifaunal *Chlamys,* ranging in size from 0.5 to 5 cm. Benthic foraminifers are also common, and include *Cibicides*, *Elphidium*, and *Bolivina*, as well as rare textularids and miliolids. Planktonic foraminifers, although rare, are represented by the genera *Guembelitria*, *Chiloguembelina* and

Globigerina. Spines and plates of irregular infaunal echinoids, especially *Lovenia*, are common, as is coralline algae.

Interpretation:

Increasing grain size and decreasing percentage of delicate branching bryozoans towards the top of the facies suggests an overall shallowing-upward phase of deposition. The well-preserved ornamentation and minimal degree of abrasion and breakage of disarticulated pectinid shells imply little transport.

The common occurrence of flat robust branching bryozoa suggests a relatively shallow high-energy environment on soft substrates (Bone and James, 1993), as well as on marine hardgrounds (James et al., 1992). Encrusting bryozoans are one of the common growth forms in shallow-water inner shelf environments with high energy, particularly underneath rocks and other hard surfaces like bivalve shells (Nelson et al., 1988b; Bone and James, 1993). Articulated branching growth forms are found in a wide range of depths from shallow inner shelves to middle shelves up to 250 m deep (Bone and James, 1993). However, their association with other shallow growth forms, including coralline algae, and biogenic components in this facies suggests an overall shallow environment. All benthic foraminifers in this facies commonly live in inner shelf areas. Some of these live on hard substrates (e.g., *Cibicides*), others on soft substrate (e.g., *Elphidium* and *Bolivina*), and the rest are non-specific (Murray, 1991). The appearance of planktonic foraminifers in this facies, however, reflects the increasing influence of the open sea. Furthermore *Guembelitria* and *Chiloguembelina* both indicate open marine and cool-water conditions (McGowran and Beecroft, 1985).

In conclusion these rocks represent local bivalve and bryozoan shoals on an inner ramp. Such shoals provide protected settings behind which relatively low-energy sediments accumulate. The presence of laterally equivalent miliolid-rich facies, which require tranquil conditions, supports such an interpretation.

Plate 3.1:

A- Photomicrograph (plane light) of the bryozoan miliolid echinoid packstone/rudstone facies. Most echinoid grains in this facies are surrounded by large crystals of clear syntaxial calcite cement (c). Sample 3, section 1.

B- Photomicrograph (polarised light) of iron zoned, sucrosic dolomite at the base of the bryozoan bivalve floatstone facies. Sample 6, section 4.

C- Photomicrograph (plane light) of encrusting bryozoa (arrow) in the bryozoan bivalve floatstone facies. Sample 9, section 4.

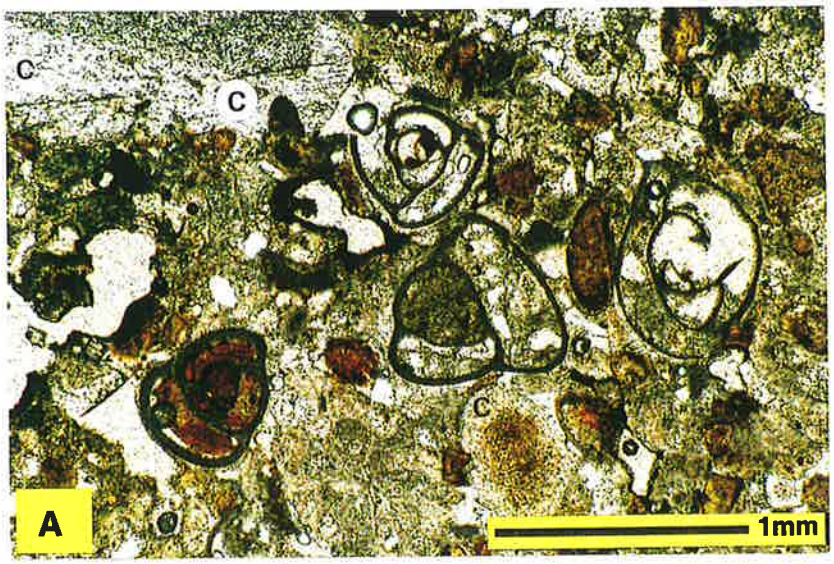
C
C
C
A
1mm

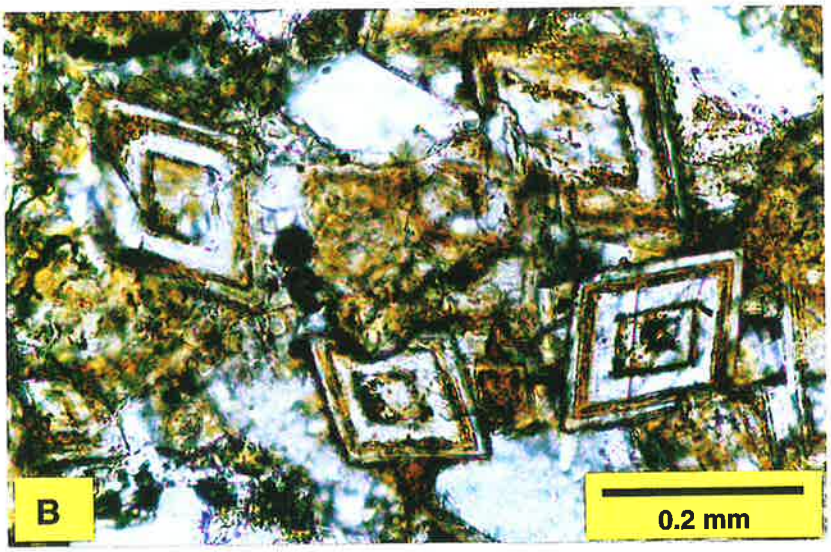
B
0.2 mm

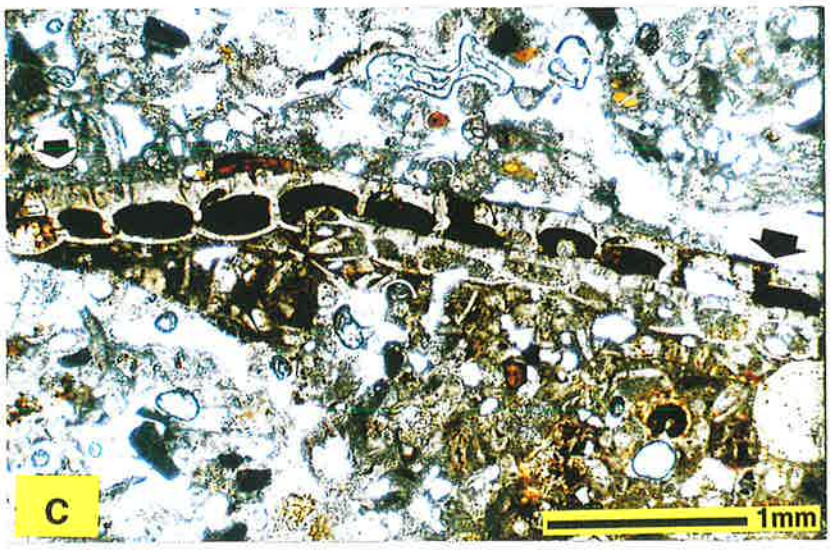
C
1mm

Plate 3.2:

A- Warming-upward cycles of the Port Vincent Limestone middle member. Photo shows alternating friable Bryozoan Grainstone Facies (G) and Bryozoan-*Amphistegina* Hardground Facies (H). Scale at the bottom left corner (arrow) = 1m. Stansbury section no. 6.

B- Warming-upward cycles of the Port Vincent Limestone middle member. Photo shows alternating friable Bryozoan Grainstone Facies (G) and Bryozoan-*Amphistegina* Hardground Facies (H). Wool Bay section no. 10.

C- Erosional surface (arrows) between hardground (H) and overlying bryozoan bioclastic rudstone facies (R). The rudstone facies are rich in nodular arborescent bryozoan growth forms (n) and echinoids. Stansbury section no. 6.

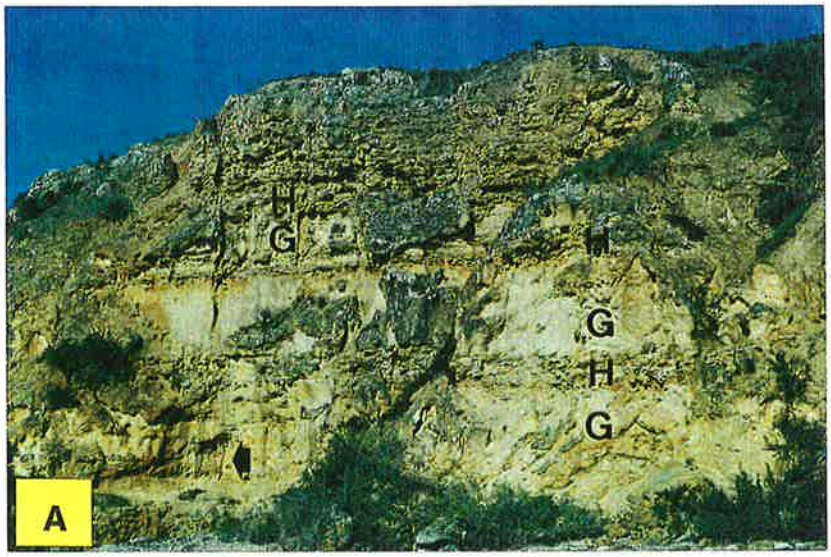
H
G
H
G
H
G
A

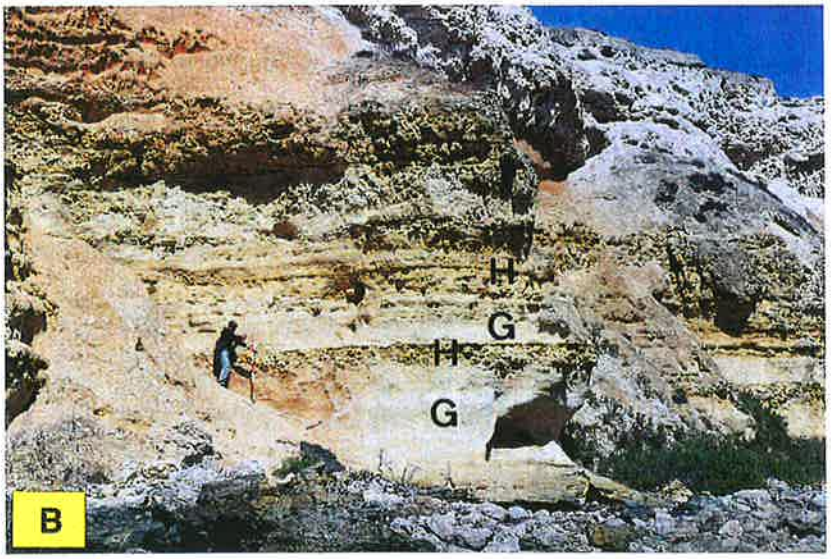
H
G
H
G
B

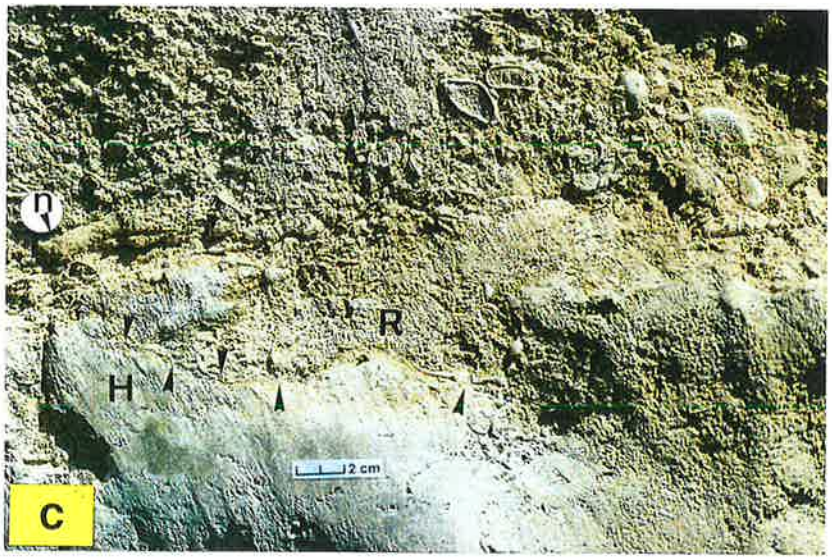
Q
R
H
2 cm
C

Location and extent:

This facies is best represented in the well exposed cliffs approximately 1 km south of Port Vincent township (Appendix B-3). Lenses have an average thickness of 2 m but south of Shea Oak Flat the thickness is less than 40 cm.

2.2 MIDDLE MEMBER

The middle member is the largest in lateral extent and volume, forming 60-70% of the succession. It is built of meter-scale, warming-upward and shallowing-upward, asymmetric, hardground-bounded, subtidal cycles. Like other depositional subtidal carbonate cycles on high-energy distally-steepened ramps or open shelves (e.g., Osleger, 1991; James and Bone, 1994; Boreen and James, 1995), they are characterised by coarsening-upward grain size, lack of intertidal facies, absence of features indicative of subaerial exposure and demonstrate subtle differences between facies.

Warming-Upward Cycles

Five episodic discontinuous depositional events are documented by the multiple appearance of a hardground-bounded depositional cycle. These cycles are exposed for 14 km between Stansbury and Port Giles (Fig. 3.1-A, plate 3.2). Each cycle consists of three facies types (Fig. 3.1-B): (A) bryozoan bioclastic rudstone (the basal unit), (B) bryozoan grainstone (the middle unit), and (C) bryozoan-*Amphistegina* hardground (the cycle top). The middle unit is well-sorted, soft and friable and forms the bulk of the cycle. Its thickness varies between cycles, with the thickest (12 m) in cycle-1, whereas the upper four cycles (2, 3, 4, and 5) range from 1 to 5 m thick. In contrast to the middle unit, cycle tops show less thickness variation, ranging from 0.5 to 1 m thick. The cycle top is capped by an erosional surface featuring truncated grains and cements, bioturbation, and mechanical erosion. Erosional surfaces are stained by a red-brown iron oxide, marking the end of the cycle. Sediments from the overlying cycle fill uppermost intergranular pores and open burrows.

A- Bryozoan Bioclastic Rudstone Facies (basal unit):

Description:

Moderately-sorted, cream-coloured, calcirudite, rich in bryozoans, foraminifers, bivalves, epifaunal echinoids and brachiopods, forms a thin layer (15-25 cm) at the base of each cycle (plate 3.2-C). These units overlie the erosional surface atop the subjacent cycle (Fig. 3.1-B). Early marine syntaxial cementation is common. Most grains are fragmented. Bryozoans are dominated by nodular arborescent, erect rigid flat robust branching, fenestrate, foliose and encrusting growth forms. Articulated branching cheilostomes are common, whereas delicate branching growth forms are rare to absent. Benthic foraminifers are dominated by epifaunal *Cibicides* and rare textularids. Planktonic foraminifers and coralline algae are rare. The basal unit grades upwards into the middle unit.

Interpretation:

The bryozoan growth-form association indicates deposition in relatively shallow-water (60-140 m), high-energy environments, on hard and/or soft substrates, above swell base but below the base of wave abrasion (James et al., 1992; Bone and James, 1993; James and Bone, 1994). Presence of epifaunal macrofossils suggests deposition on hard substrates. Abundance of epifaunal *Cibicides* indicates deposition on relatively deep hard substrates (Murray, 1991). Perhaps one of the most significant indicators for environmental interpretations is the presence of phototrophic organisms, most commonly coralline algae. Absence or rarity of coralline algae in most of the basal units suggests deposition was in the subphotic environment, probably > 70 m deep (Collins, 1988; Nelson et al., 1988a; James et al., 1992).

B- Bryozoan Grainstone Facies (middle unit):

Description:

Calcarenites are cream to pale yellow coloured, well sorted, locally cross-bedded, soft and friable (plate 3.3-A), and coarsen upward. Cementation is generally minimal, usually as syntaxial overgrowths around echinoderm grains. Textures are grain-supported and devoid of carbonate mud. All grains are skeletal.

Bryozoan fragments with sizes mostly < 2 mm dominate the rocks, forming up to 70% of the constituents. They are variably abraded and composed mainly of delicate branching cyclostomes and articulated branching cheilostomes (plates 3.3-B, C). Other bryozoan fragments include flat robust branching, fenestrate, foliose and rare arborescent and encrusting growth forms. Broken plates and abraded spines of irregular infaunal echinoids are prolific. Small whole tests of *Lovenia*, *Eupatagus* and *Monostychia* are common. Benthic foraminifers are also common and show an increase in abundance and diversity towards the top of the facies. They include species of *Cibicides*, *Spirillina, Notorotalia*, *Operculina*, and rare *Crespinina*, miliolids and textularids (plates 3.6-A, 4.10-C). Planktonic foraminifers *Guembelitria* and *Chiloguembelina* are rare and present only in lower parts. Fragments of coralline algae are absent to rare at the bottom but become common upwards.

Interpretation:

The broad thickness variation of this facies between successive cycles reflects variations in the depth of wave base erosion and accumulation space on the seafloor (James and Bone, 1991, 1994). Sediments composed primarily of delicate branching and articulated branching bryozoan growth forms imply a relatively deep shelf setting (e.g., Nelson et al., 1988a; James et al., 1992; Boreen et al., 1993). Volumetrically, they are most abundant in low-energy environments below swell wave base, preferably on unconsolidated substrates (Bone and James, 1993). Shallower occurrences are reported for the New Zealand forms, where they are found commonly in middle to inner shelf areas that have a slightly consolidated

substrate and a low-moderate water energy level (Nelson et al., 1988b). The abundance of bryozoans in the lower parts supports the presence of a soft substrate in this facies. Nevertheless, these depth ranges seem to be too deep for the deposition of the Port Vincent Limestone, especially in the context of an accompanying variety of shallow-water biota.

Increasing abundance, size, and roundness of coralline algal fragments towards the top indicates that initial stages of deposition may have occurred on a seafloor below the photic zone but that later shallowing brought the seafloor into the photic zone. Shallowing upward is also supported by the presence of planktonic foraminifers in the lower parts and the increasing abundance and diversity of benthic foraminifers at the top. *Cibicides*, *Spirillina* and textularids are generally found on hard substrates; miliolids are characteristic of epifaunal shallow inner shelves and hypersaline lagoonal environments (Murray, 1991). Presence of these foraminifers restricts depth estimations and suggests a shallow depositional environment, more likely within the shallower depth ranges of the dominant bryozoan growth forms.

This facies represents part of a shallowing-upward succession, deposited on a middle ramp and more probably the inner parts of the middle ramp. The variably abraded delicate grains and the presence of whole echinoid tests at the base, indicate local production and infrequent transportation. Low diversity bryozoan sediments lacking coralline algae were deposited in deep waters (> 70 m) on a middle ramp. In contrast, sediments with coarser, well-rounded coralline algal fragments and a more diversified fauna accumulated in shallower waters (between 40-70 m deep) on the inner parts of the middle ramp.

Location and extent:

This is the most common facies in the Port Vincent Limestone, and by far means the largest in lateral extent and volume. It extends for a distance of approximately 14 km and can be traced along intermittent coastal cliffs from 1 km north of Stansbury jetty to 1.5 km south of Port Giles jetty (Appendix B-4, B-5).

Plate 3.3:

A- Rock sample (friable calcarenite) of the bryozoan grainstone facies of the Port Vincent Limestone. Sample 1, section 6.

B- Photomicrograph (plane light) of the bryozoan grainstone facies. Viewed are: (d) oblique section of delicate branching growth form (cyclostome bryozoa), (r) longitudinal section of flat robust branching growth form (cheilostome), and (arrows) transverse section of articulated branching growth form (cheilostome). Cementation is minimal and generally by syntaxial overgrowth (c) around echinoderm plates. Sample 1, section 6.

C- Frequency analysis by volume % (grain-bulk, Dunham, 1962) for the bryozoan grainstone facies showing constituents of a whole sample (left), and the dominant bryozoan growth forms (right). Sample 1, section 6; point count values are listed in Appendix B-7.

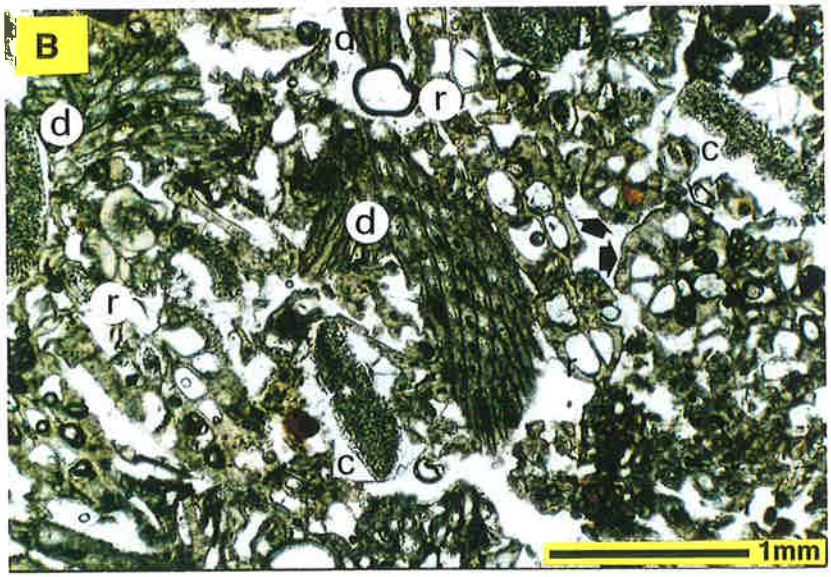

C

Bryozoan grainstone facies

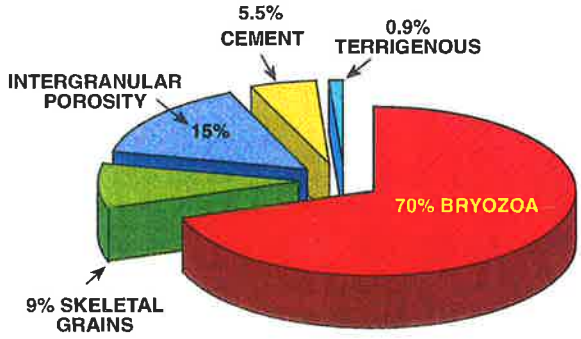

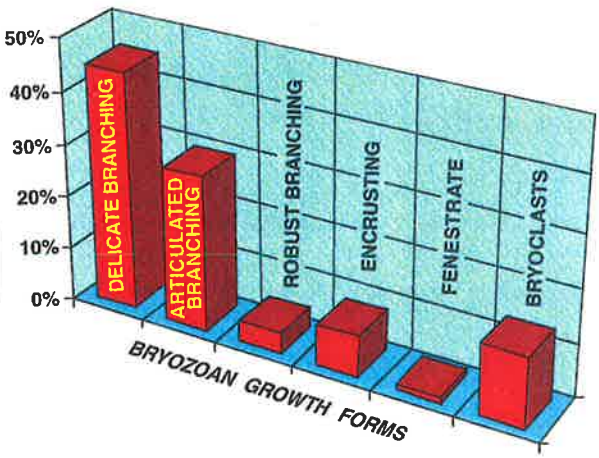

C- Bryozoan-*Amphistegina* Hardground Facies (cycle top):

Description:

Beds are distinctively buff coloured, 0.5-1 m thick, hard, with a gradational base and a sharply cut erosional top (plate 3.4). Erosional surfaces are characterised by truncated grains and cements, abundant irregular decapod crustacean burrows (*Thalassinoides;* plate 3.5-A), and a red-brown iron oxide stain. Rocks are poorly sorted skeletal calcarenite/fine calcirudite (≤ 4 mm) surrounded by internal sediment and internal micrite precipitate. Bryozoan fragments are the dominant grains and comprise a mixture of articulated branching cheilostomes and delicate branching cyclostomes, with common flat robust-branching, foliose and vagrant growth forms. Generally, most bryozoan fragments are large in size (2-4 mm) and show minor evidence of breaking and abrasion. There is an increase in the percentage of robust branching forms and a decrease in the proportion of delicate branching growth forms compared to the underlying bryozoan grainstone facies (plates 3.3-C, 3.4-C).

The most characteristic feature of this facies is the abundance of the large epifaunal benthic foraminifer *Amphistegina* (plate 3.5-B, C). *Amphistegina* increases in abundance, becomes more spherical and develops thicker chamber walls southward and seaward towards Wool Bay and Port Giles. Tests of small benthic foraminifers like *Cibicides* are common, whereas miliolids and textularids are rare. Whole and partial tests of echinoderms are common. Fragments of coralline algae and bivalves are common to rare. Planktonic foraminifers are rare.

Interpretation:

The fine matrix is a post-depositional internal micrite (cf. Reid et al., 1990). Hence the depositional texture of the bryozoan-*Amphistegina* hardground facies is a grainstone. Alteration due to subaerial exposure is absent in these well-lithified layers. The hard layers represent marine hardgrounds that mark the terminations of shallowing upward successions.

This premise is supported by the following lines of evidence. Echinoid fragments and coralline algae are surrounded by a thin isopachous and/or syntaxial cement, which is overlain by the fine microbioclastic matrix. Remnants of many flat robust branching bryozoans (originally aragonite) are present in the form of a thin cortex (IMC) and are now surrounded by a fine microbioclastic matrix (plate 3.1-A, B). This suggests that the thick aragonitic outer periphery (Bone and James, 1993) of these bryozoans was removed by dissolution, probably on the seafloor, prior to deposition of the fine microbioclastic matrix (see also chapter 3).

Today, flat robust branching growth forms are abundant at depths of 90 to 130 m, and common in shallower waters (Bone and James, 1993). Foliose colonies usually grow attached to hard substrates in shallow near-shore environments at < 80 m depth (Bone and James, 1993), preferably on moderate-energy level middle shelves with low sedimentation rates (Nelson et al., 1988b).

Amphistegina is limited geographically by temperature, to tropical/subtropical environments (Cushman, 1950; Betjeman, 1969; Zmiri et al., 1974; Larsen, 1976; Reiss and Hottinger, 1984; Murray, 1991; Betzler and Chaproniere, 1993). Water temperature limits on the distribution of *Amphistegina* in the Pacific region correspond to the present day 20°C mean annual isotherm. It is abundant on the Great Barrier Reef and does not extend south of Sydney Harbour (Hornibrook, 1968). The common association of symbiotic algae with *Amphistegina* implies that light is a main factor determining the depth distribution (Hansen and Buchardt, 1977; Hallock, 1979, 1981; Bignot, 1985; Hallock et al., 1986). The most common occurrences of *Amphistegina* are in shallow waters, ranging from 50 to 130 m (Cushman, 1950; Phleger and Parker, 1951; Drooger and Kaasschieter, 1958; Seiglie, 1968; Betjeman, 1969; Reiss and Hottinger, 1984). The genus is commonly found in coarse sediments, suggesting close relation to high-energy environments (Bandy, 1964). Thicker walls and more robust tests are linked to higher energy levels (Hallock et al., 1986).

Plate 3.4:

A- Rock sample of the bryozoan-*Amphistegina* hardground facies showing depressions of encrusting fauna from the overlying cycle. Sample 12, section 6.

B- Photomicrograph (plane light) of the bryozoan-*Amphistegina* hardground facies. Viewed are: (d) oblique section of delicate branching growth form (cyclostome bryozoa), (r) longitudinal section of flat robust branching growth form (cheilostome), and (ar) transverse section of articulated branching growth form (cheilostome). Internal micrite is abundant (m), filling intergranular and intragranular pores. Sample 12, section 6.

C- Frequency analysis by volume % (grain-bulk, Dunham, 1962) for the bryozoan-*Amphistegina* hardground facies showing constituents of a whole sample (left), and the dominant bryozoan growth forms (right). Sample 12, section 6; point count values are listed in Appendix B-7.

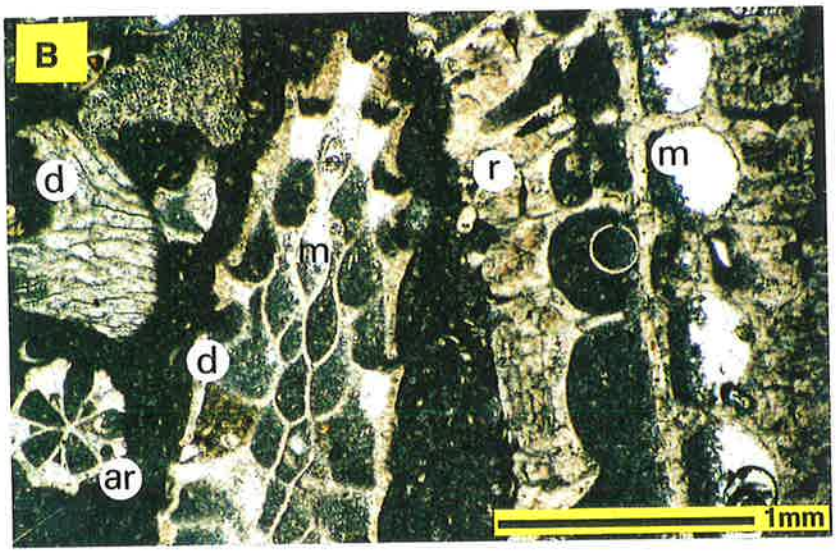

C

Bryozoan-*Amphistegina* hardground facies

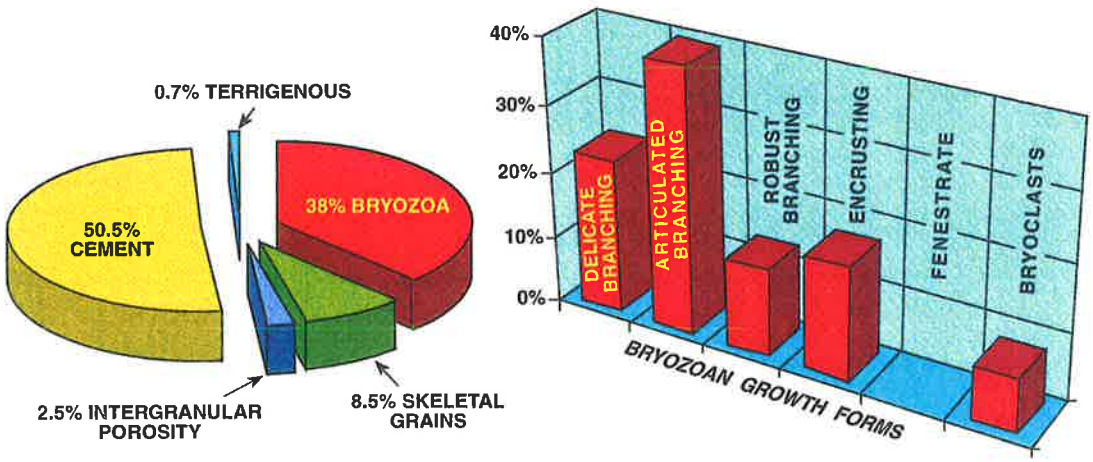

Plate 3.5:

A- Extensive *Thalassinoides* burrows on a bryozoan-*Amphistegina* hardground surface. Section 9, south of Wool Bay.

B- Photomicrograph (plane light) showing abundant *Amphistegina* in the bryozoan-*Amphistegina* hardground facies. Sample 12, section 6.

C- Photomicrograph (plane light) showing abundant *Amphistegina* in the bryozoan-*Amphistegina* hardground facies. Sample 5, section 9.


A

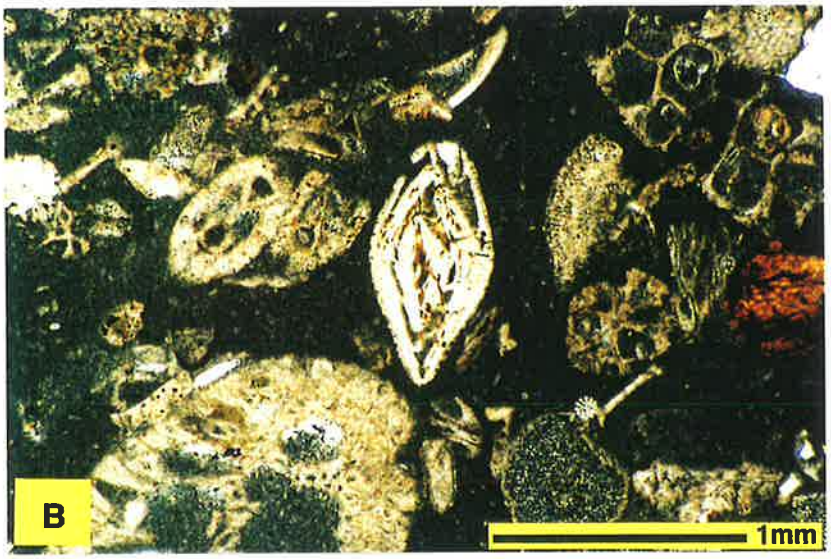
B
1mm


C
1mm

In the stratigraphic record of South Australia, the first appearance of *Amphistegina* is in the middle Janjukian stage (lower *Amphistegina* acme - Lindsay, 1985). This stage represents one of three warm periods that extend through the Miocene and is correlatable with distinct episodic marine transgressions along the southern continental shelf (McGowran and Li, 1994). The *Lepidocyclina* marker zone in the Batesfordian/Balcombian of southern Australia (McGowran, 1979, 1986; McGowran and Li, 1994) and the upper *Amphistegina* acme (Lindsay, 1985) were not found in the Port Vincent Limestone succession. This suggests that the hardgrounds must be older than the Batesfordian/Balcombian, leading to the conclusion that these hardgrounds represent deposition within the Janjukian/Longfordian warm stages.

It is suggested that the bryozoan-*Amphistegina* hardground facies was deposited on a middle ramp, controlled by fluctuating sealevel (a relative fall/rise) with warmer water conditions induced by climatic changes, resulting in sub-tropical incursions of seawater.

Cool-Water Cycles

Cool-water shallowing-upward cycles are less common. Their formation is controlled by eustatic fluctuations on a high-energy distally-steepened ramp (see James and Bone, 1994). The basal and middle units of these cycles are identical to those in the aforementioned warming-upward cycles. The upper unit, however, is a 50 cm thick hardground that contains no *Amphistegina*. Constituents of these hardgrounds are characteristic of high-energy shallow-water deposition. Bryozoan fragments are dominant and composed mainly of flat robust-branching, fenestrate, foliose, encrusting, and rare delicate branching and articulated branching growth forms. Broken echinoid plates and spines are prolific. Benthic foraminifers are abundant and diverse, and are dominated by *Cibicides*, rare miliolids and textularids. Planktonic foraminifers are absent. Well sorted and rounded fragments of coralline algae are abundant.

The hardground atop each cool-water cycle is also interpreted to be marine in origin. It has a gradational base and a sharply-cut erosional top surface featuring truncated grains and marine cements, as well as microboring tubes (plate 3.6-A). Boring tubes extend down from the top surface, cross-cutting grains and their surrounding cements, implying a marine synsedimentary origin for the precipitation of such cements. The sharply-truncated top surface, as well as the microboring tubes, are coated by a red-brown stain. Intraskeletal voids are filled with glaucony pellets. The marine origin is also supported by the absence of subaerially produced features (e.g., calcrete, palaeokarstic features), the absence of inter-tidal fauna and flora in the immediately overlying sediment, and presence of the above mentioned criteria in the hardground, which are indicative of early seafloor lithification (cf. James and Choquette, 1990a).

2.3 UPPER MEMBER

2.3.1 Fine, Highly Abraded Bryozoan-*Eponides* Grainstone Facies:

Description:

This is the youngest exposed facies of the Port Vincent Limestone (plate 3.6-B). Constituents are a mixture of fine (< 0.5 mm) skeletal grains. Rocks are generally white to cream coloured, locally cross-bedded, soft and friable in lower and middle parts grading into hard and moderately cemented in the top 25 cm, where an erosional surface separates the formation from the overlying Pliocene Hallett Cove Sandstone (plate 2.5-A, B). Fine, highly-abraded bryozoan fragments, mainly erect-rigid delicate branching cyclostomes and erect flexible articulated branching cheilostomes, together with unidentifiable, broken bryozoan fragments dominate the grains in this facies (plate 3.6-C). Benthic foraminifers are common and include *Eponides,* small tests of *Cibicides*, *Sherbornina*, rare miliolids and textularids. Other common constituents include bivalves, well-rounded fine (< 0.25 mm) fragments of coralline algae and calcareous sponge spicules (plates 3.6-C, 4.6-C). Echinoids are less common than in the other members and are present as small whole tests and

Plate 3.6:

A- Photomicrograph (plane light) of a hardground showing truncated cements and echinoid plates (arrows), common coralline algae (c), benthic foraminifers *Cibicides* (f), and microboring tubes on the top surface (circle). Sample 6, section 8.

B- Section no. 12 north of Edithburgh showing rocks of the lower member, which are comprised of bryozoan-*Eponides* grainstone facies.

C- Thin section photomicrograph (plane light) showing the fine, highly abraded bryozoan-*Eponides* grainstone facies. Sample 4, section 12.

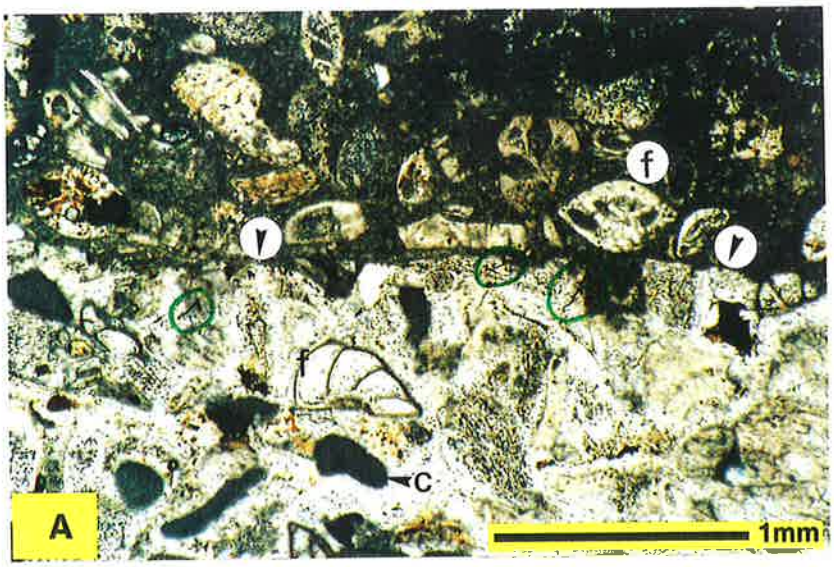
f
f
f
C
A
1mm


B

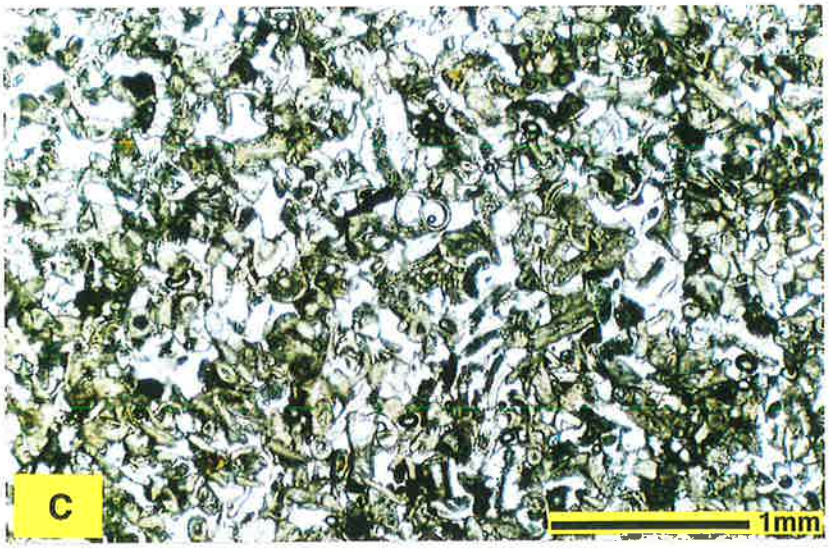
C
1mm

fine to medium sand size plates which are concentrated in isolated shallow pockets.

Interpretation:

Sediments of this facies are similar to the poorly-sorted, slightly muddy, fine sands accumulating today in the deeper subtidal environments in central Gulf St. Vincent and Spencer Gulf (Gostin et al., 1988; Fuller et al., 1994). They also resemble the fine-grained bioclastic sands of the deep shelf on the Otway Platform (Boreen et al., 1993). Skeletal fragments, however, are fine and highly abraded indicating winnowing and abrasion on the seafloor.

Benthic foraminifers are dominated by *Eponides*, which is not seen in any other facies of the Port Vincent Limestone. It is an epifaunal, cold to temperate form living on soft sediments or hard substrates and is most common on outer shelves between depths of 100-200 m, although it may extend into the lower bathyal zone to >2000 m deep (Murray, 1991).

The dominant bryozoan growth forms also suggest a relatively deep-water setting. Delicate branching cyclostomes and articulated branching cheilostomes are common on soft substrates in deeper shelf areas down to 450 m and 250 m respectively (Bone and James, 1993; Nelson et al., 1988b), although they may also occur at shallower depths.

In modern sediments from the Otway Platform, sponges are common in 130- to 180-m deep shelf facies (Boreen et al., 1993). Coralline algae are the least common constituent and are present as very well-rounded, < 0.25 mm fragments that may possibly be allochthonous. It is suggested that the fine, highly abraded bryozoan-*Eponides* grainstone facies was deposited on the deeper parts of the middle ramp (Fig. 3.2).

Location and extent:

Rocks reaching a maximum thickness of 7.5 m in some areas, are intermittently exposed from about 1.5 km south of Point Giles until the beds finally disappear as they dip below sealevel approximately 1 km south of Edithburgh (Appendix B-6).

3. DISCUSSION

3.1 Palaeoenvironment

Port Vincent Limestone facies were interpreted on the basis of modern analogues, most of which are open marine shelves, as well as the modern Spencer and St. Vincent Gulfs. The St. Vincent Basin has been regarded as a confined, intracratonic basin shielded by Kangaroo Island (Stuart, 1969; Cooper, 1985, McGowran and Beecroft, 1986). The presence of marine sediments that are similar to those accumulating today in open marine settings (e.g., Eucla Shelf, Lacepede Shelf) and the lack of evaporites allow these modern areas to be used as depositional analogues, with the caveat that the Cenozoic environments were generally lower energy. Reconstructed palaeoenvironments indicate deposition on a cool-water carbonate ramp, with several incursions of warmer water into the area. Lateral and vertical facies analysis indicate aggradational deposition.

Prior to deposition of the Port Vincent Limestone, the Rogue Formation was exposed on most of the southern parts of Yorke Peninsula. The upper part of the Rogue Formation, just south of Shea Oak Flat, is earliest Oligocene age (Stuart, 1969). The sea advanced over this unconformity surface, depositing the basal units of the Port Vincent Limestone. Today, these units are exposed from a few kilometres south of Shea Oak Flat and extend to south of Port Vincent township. Conditions during Early Oligocene time were shallow-marine, promoting the distribution of a diverse benthic fauna and flora, including coralline algae. Several local, subtidal, bivalve shoals developed on the inner parts of this shallow ramp. These absorbed

much of the wave energy, creating locally protected environments leeward, which allowed the production and accumulation of sediments rich in a shallow restricted benthic fauna (i.e., bryozoan miliolid echinoid packstone/rudstone facies). The sea continued to rise during the Oligocene over the remainder of southeastern Yorke Peninsula. Conditions were cool, open marine, favouring the distribution of deeper bryozoan growth forms and planktonic foraminifers like *Guembelitria.* The seafloor was just below the photic zone but was later within it, thus allowing the growth of coralline algae. Today, the base of the photic zone in similar environments around southern Australia is at a depth of 70 m (Shepherd, 1982; James et al., 1992). Warmer and more shallow regional environments prevailed at the end, late in the Oligocene, facilitating the ingress of subtropical large benthic foraminifers and allowing flat robust branching bryozoans to flourish. Cooler and warmer water environments alternated repeatedly in a cyclic manner, producing distinct alternating cool-water and warmer-water facies on the middle ramp. These are exposed today as bryozoan grainstone and bryozoan-*Amphistegina* hardground facies at Stansbury, Wool Bay and Port Giles. Further south, deeper environments hosted delicate bryozoans, sponges and deep water large benthic foraminifers. Similar fauna are found today on the outer middle ramp (Gostin et al., 1988; Boreen et al., 1993).

3.2 Origin Of Cyclicity:

Subtidal cyclicity on carbonate shelves and ramps has been attributed to allogenic and/or autogenic controls. The prime activator in the allogenic models is short-term fluctuations in eustatic sealevel, which control intrinsic processes such as depth of wave abrasion and accumulation space, thus resulting in the formation of erosional surfaces (e.g., Osleger, 1991; James and Bone, 1991, 1994; Boreen and James, 1995). In autogenic models, the mechanisms proposed for generating metre-scale subtidal cycles include the progradation of tidal flat sediments over the subtidal carbonate factory, and variations in sedimentation-redistribution patterns, which are caused mainly by wave action (e.g., Ginsburg, 1971; Spencer and Demicco, 1989).

Autogenic controls are discarded from being the generating mechanism of the warming-upward, subtidal, carbonate cycles of the Port Vincent Limestone because: 1- tidal flat caps are absent, and 2- variations in sedimentation-redistribution patterns, although contribute significantly to intracycle variations, they can not justify the relatively large lateral and vertical extent of semihomogeneous cycles in the Port Vincent Limestone. Furthermore, wave action and depth of wave abrasion and accumulation space are controlled by external and more general factors. These warming-upward subtidal cycles of the Port Vincent Limestone are interpreted to be caused by episodic fluctuations in sealevel, accompanied by warm-water incursions. It is suggested here that warming was brought about by an overall temperature rise in the environment (stimulated by climatic changes or oceanic currents), acting in concert with a relative fall in sealevel. The latter would result in illuminated shallower and warmer near-shore, but still unconsolidated, depositional surfaces. This would enable a different fauna and flora to become established, replacing the deeper water assemblage, for as long as conditions remained stable. Warmer and shallower environments have a higher ratio of aragonitic to calcitic benthic invertebrates and so are more prone to seafloor cementation. This eventually results in marine cementation at the top of each cycle creating a hard substrate. A very different fauna and flora would colonise this hard substrate.

In the Port Vincent Limestone cycles, the presence of shallow-water, tropical to subtropical *Amphistegina* in the hardgrounds at the top of each cycle indicates warming upward. Temperature changes are fostered by changes in climate and/or sealevel and/or major ocean currents. No evidence is seen to support such a hypothesis that involves the turning on and off of a warm ocean current to explain the episodic nature of the cycles. Certainly, today, we see the half-yearly influx of warm water of the Leeuwin Current into the Southern Ocean allowing the establishment of a warm-water fauna and flora in an otherwise temperate environment (Bone et al., 1994). It has been hypothesised that this current may have switched on during the mid-Tertiary (Li and McGowran, 1994). If this is so, then this episodic paleo-Leeuwin Current could explain both the increase in temperature and the presence of exotic species. Similarly, the opening and closing of the Indonesian Seaway

throughout the Tertiary period has had a major control on warm southward flowing currents (Opdyke and Bird, 1996). In addition to this oceanic current effect, an overall climatic temperature rise is possible. Several episodes of climatic warmth reflected by warm-water deposition are recorded in the southern Australian Miocene biostratigraphy (McGowran, 1986; McGowran and Li, 1994). The same influx of exotic species has not been observed in the Oligo-Miocene Abrakurrie Limestone cycles, although other characteristics are similar (James and Bone, 1991, 1994 - see below), including marine hardgrounds at the top of each cycle. But then, today, the Leeuwin Current does not sweep into the near-shore portion of the Great Australian Bight, but rather hugs the mid shelf and shelf edge, with localised eddies (Y. Bone, pers. obs.).

The less common cool-water cycles of the Port Vincent Limestone were formed by allogenic short term eustatic fluctuations, with no significant temperature change. The forming mechanism of such cycles is summarised in James and Bone (1994).

3.3 Comparison With Other Cool-Water Carbonate Cycles:

Subtidal cycles are common in many Tertiary cool-water carbonate successions in southern Australia. Two well-studied examples are the Abrakurrie Limestone of the Eucla Platform (James and Bone, 1994), and the cross bedded cycles in the Tertiary limestones of the Otway Basin of southeastern Victoria (Boreen and James, 1995). Cycles in both examples are similar in most aspects to those of the Port Vincent Limestone. All cycles are capped by biologically and mechanically eroded hardgrounds that are stained by red-brown iron oxides. The bulk of all cycles (basal and middle units) are formed from largely similar bryozoan facies. Basal units consist of shallow, high-energy bryozoan calcirudite associated with epifaunal organisms, all characteristic of hard substrates. Middle units are mainly well-sorted bryozoan grainstones dominated by delicate branching cyclostomes and articulated branching cheilostomes. Dissimilarities exist in the upper unit of the warming-upward cycles, where the bryozoan-*Amphistegina* hardground facies has not been reported in the other two studies.

4. SEQUENCE STRATIGRAPHY

4.1 Concepts and Definitions:

Derived from seismic stratigraphy, sequence stratigraphic analyses define and subdivide stratigraphic sequences on the basis of their bounding discontinuities, which represent geological time planes. Most discontinuities form as a result of fluctuations in relative sealevel, which are in turn determined by rates of eustasy and tectonic subsidence (Schlager, 1981; Tucker, 1991). Certain environmental changes like drowning unconformities may also form discontinuities (Schlager, 1991). The basic element of sequence stratigraphy is the sequence, which is defined as being a relatively conformable succession of genetically-related strata bounded at its top and base by unconformities and their correlative conformities (Van Wagoner et al., 1988, 1990; Posamentier et al., 1988). Most sequences are the result of third-order relative sealevel changes (1 - 10 million years), and may contain thinner stratigraphic units termed parasequences. Parasequences are formed as a result of higher frequency, fourth- and/or fifth-order relative sealevel fluctuations ($10^5/10^4$ years) that are superimposed on the third-order change (Tucker, 1991), and may be related to Milankovitch orbital forcing (Vail et. al., 1991). A sequence can be subdivided into a succession of systems tracts (lowstand, transgressive, and highstand), depending on the position of the sealevel. Systems tracts are defined as a linkage of contemporaneous depositional systems (Posamentier et al., 1988). Systems tract however, are descriptive entities, though commonly interpreted in terms of eustatic fluctuations (Christie-Blick, 1991). While facies analyses described earlier in this chapter helped unravel and interpret the palaeoenvironments of the Port Vincent Limestone, they did not address how the carbonate factory and platform responded to external controls through time - particularly eustatic sealevel fluctuations and tectonics. This is because facies analyses provide a representation of the types of deposits on a platform during one short period of time. Cyclicity focused on events in the platform centre, thus only partially addressing sealevel effects. To describe and interpret the depositional and erosional history of a platform (margins as well as centre), and to track the

migration of facies caused by relative sealevel fluctuations, three main schemes are now increasingly being employed:

1- Allostratigraphy: "...subdivision of the stratigraphic record into mappable rock bodies, defined and identified on the basis of their bounding discontinuities" (see review in Walker, 1992).

2- Sequence stratigraphy: "...the study of rock relationships within a chronostratigraphic framework wherein the succession of rocks is cyclic and is composed of genetically related stratal units (sequences and systems tracts)" (Vail et al., 1977; Haq et al., 1987; Posamentier et al., 1988; Posamentier and Vail, 1988; Van Wagoner et al., 1988, 1990).

3- Genetic stratigraphic sequence: "...the sedimentary product of a depositional episode, where a depositional episode is bounded by stratal surfaces that reflects major reorganisations in basin palaeogeographic framework" (Galloway, 1989).

These lithostratigraphic disciplines evolved from studies on siliciclastic depositional systems and are similar in most of their general concepts and objectives, but differ from one another in their type of sequence boundary. Allostratigraphy is the most flexible of all, since it utilises a diverse variety of bounding discontinuities to serve as sequence boundaries. Bounding discontinuities in allostratigraphy may be erosional including both angular unconformities and subtle erosional surfaces, or nonerosional resulting from changes in depositional conditions (e.g., flooding surface, condensed horizons, glaucony-rich or organic-rich horizons and hardgrounds). Sequence stratigraphy (the Exxon Production Research model) uses unconformities as sequence boundaries whereas Galloway's genetic sequence analysis uses maximum marine flooding surfaces as sequence boundaries.

Carbonate systems, owing to vast dissimilarities between them and their siliciclastic counterparts (see James and Kendall, 1992), respond to sealevel fluctuations in a different manner from that followed by siliciclastic systems. In siliciclastic systems, sealevel

fluctuations control the accumulation space and hence relocate sedimentation sites across the platform, whereas in carbonate systems such changes determine the health and existence of the carbonate factory (James and Kendall, 1992). Such differences dictate that the application of these silisiclastic-based schemes to carbonate systems be modified. This has led to the development of separate carbonate sequence and systems tract models. These have been reviewed in Sarg (1988), Tucker (1991), James and Kendall (1992), Schlager (1992), Handford and Loucks (1993). Furthermore, the fundamental differences between tropical and cool-water carbonate environments, which govern the types of facies and diagenetic pathways, influence the mechanisms of sediment ordering into stratigraphic packages. The principle concepts of sequence stratigraphy that apply to cool-water carbonate settings are discussed in Boreen and James (1995), and are briefly outlined below:

1- Condensed sections, grain abrasion, and nondeposition are produced during shallowest relative sealevel in highest energy nearshore (0 - 50 m) settings. Hardgrounds capping subtidal cycles, abrupt contacts between open marine and nearshore sediments, and complex lowstand and flooding surfaces are typical results.

2- Large scale platform progradation is common in cool-water bioclastic carbonate systems, due to the potential of these systems to maintain sediment production and accumulation during various phases of the sealevel cycle. Boreen and James (1995) note that this can produce highly variable systems tract responses depending upon the rate of relative sealevel fluctuation.

3- Cool-water carbonate sediments are dominantly calcitic and thus have a low diagenetic potential. This renders the rocks less vulnerable to dissolution and cementation than the aragonite-dominated tropical carbonates, and as a result the dominantly friable sediments are easily eroded and reworked and lowstand exposure surfaces become difficult to recognise.

4- Cross-bedded grainstone facies are more likely to be deposited in open shelf depths (50 - 130 m), away from the shoreline.

Cool-water carbonates develop mainly on high energy ramps and unrimmed shelves (Nelson, 1988; James et al., 1992; James and Kendall, 1992; Boreen and James, 1995; Li et al., 1996). Sequences deposited on homoclinal ramps are generally simple, being dominated by transgressive (TST) and highstand systems tract (HST) deposits. Distally-steepened ramps resemble rimmed shelves in that they have the potential for resedimentation, and thus a lowstand fan or wedge could form during substantial sealevel fall (Tucker, 1991). However, facies of the Port Vincent Limestone were deposited in shallow inner to mid-ramp environment, and thus would be expected to contain a series of systems tracts similar to those developed on the shallow parts of a homoclinal ramp.

4.2 Port Vincent Limestone Sequence and Systems Tract:

Outcrop exposure of the Port Vincent Limestone is discontinuous between Shea Oak Flat and Edithburgh and is further obscured by several covered intervals and faults, thus rendering stratigraphic correlation impossible in the absence of tight biostratigraphic control. Therefore, sequence stratigraphic analysis is carried out on outcrops of the middle member, where exposures between Stansbury and Port Giles are semicontinuous and easily correlated over a distance of 14 km. The middle member comprises most of the Port Vincent Limestone. It is built of five warming-upward, metre-scale, asymmetric, hardground bounded, subtidal, carbonate cycles. Rocks of the middle member contain *Guembelitria triseriata* and *Chiloguembelina cubensis* in the lower part, *Amphistegina* rich hardgrounds throughout, and *Operculina* at the top above the last *Amphistegina* hardground. The middle member package therefore occurs within the Janjukian stage (Late Oligocene-Early Miocene) of the southern Australian biostratigraphic succession (McGowran et al., 1996). During much of this time, eustatic sealevel fluctuations were of relatively short duration and low amplitude (Kennett and Barker, 1990).

Based on vertical facies stacking relationships in each hardground-bounded cycle, sequence stratigraphic analyses reveal the relative position of sealevel throughout the depositional history of the middle member. These warming-upward carbonate cycles represent fourth-

order parasequences that developed during high frequency fourth-order sealevel fluctuations and are superimposed on the longer term third-order cycle. Each parasequence resembles a mini third-order cycle in its systems tract components. The three building units (facies) of each warming-upward cycle represent three distinctive systems tract.

Transgressive Systems Tract (TST):-

Transgression is generally typified by carbonate production, ravinement, embayment filling, condensed sedimentation, glaucony-rich sediments, mollusc coquinas, and facies backstepping (Ginsburg and James, 1975; Boreen, 1993). Transgression in the middle member cycles is indicated by a facies change from relatively shallow-water high-energy rudstone (basal unit of each depositional cycle) to deeper water grainstone (middle unit) (plates 3.2-C, 3.3-B). The shallow-water, high-energy facies is composed of moderately sorted bryozoan bioclastic rudstone rich in benthic foraminifers, epifaunal echinoids, bivalves and brachiopods. Most grains are fragmented. The nature of the bryozoan growth-form association, dominated mainly by nodular arborescent forms, is characteristic of shallow environments. Overlying these shallow sediments lie well sorted, bryozoan grainstone facies (middle unit) which reflect deposition in deeper water environments. This facies relationship indicates that the basal unit of each cycle represents a transgressive system tract that was deposited during a short and rapid relative sealevel rise, which covered the subjacent omission surface atop the underlying cycle. The presence of deeper water sediments overlying the thin basal unit facies and the absence of wackestone-dominated textures, suggests deposition took place during a rapid and short lived sealevel rise. The geometry of the package reflects a lateral offshore transition from shallow water high energy rudstones, to deeper and lower energy bryozoan grainstone facies (HST).

Highstand Systems Tract (HST):-

Flooding is indicated by a gradational vertical change in facies from shallow-water, high-energy rudstone of the transgressive system tract (TST), to well sorted, locally cross-bedded,

soft and friable bryozoan grainstone facies deposited on the inner middle-ramp. These grainstones are dominated by deep water bryozoans, associated with other fossils including planktonic foraminifers. Facies components and vertical relationships between the basal and middle units of each cycle indicate a gradual deepening caused by relative sealevel rise or highstand. These HST deposits are relatively homogeneous throughout their thickness, with no marker from which one can locate the maximum flooding surface and subsequent sealevel fall. Furthermore, thickness variations between basal, middle and top units of each cycle suggests that the sealevel rise/fall was asymmetric. This further obscures evidence of the maximum flooding surface (MFS).

Lowstand Systems Tract (LST):-

Lowstand events produced a series of depositional-diagenetic cycles that are capped by hardgrounds with erosional surfaces. Deposits of the highstand system tract (bryozoan grainstone facies) are overlain by deposits of shallower and warmer environments (bryozoan *Amphistegina* hardground). As interpreted earlier (chapter 2), shallowing upward and warming upward is indicated by the presence of large benthic foraminifers (e.g., *Amphistegina*) and an increase in the abundance of flat robust branching bryozoans compared to the underlying HST deposits (plates 3.3-C, 3.4-C, 3.5-B, C). These hardgrounds were formed in subtidal, high-energy, shallow-marine environments. Early marine dissolution of aragonitic shells and seafloor cementation in these hardgrounds are products of shallow-water, cyclic, diagenetic processes. The hardground has a burrowed, irregular erosion surface, featuring truncated grains and cements. Offshore geometry of these erosional discontinuities is not clearly defined, as their gently dipping exposures disappear below the surface just south of Port Giles. This enrichment in shallow-water components, gradational superposition of nearshore facies over offshore facies, subtidal erosion, and formation of hardgrounds in carbonate ramp settings, are diagnostic of relative lowstand (Collins, 1988; James and Bone, 1991; Boreen, 1993; Boreen et al., 1993).

4.3 Correlation with the Global Sealevel Curve and Australian Sequences:

The eustatic sealevel curve of Haq et al. (1987, 1988) has been widely used for correlating sealevel histories in sedimentary sequences. The middle member package, bounded by *Guembelitria triseriata* and *Chiloguembelina cubensis* in the lower part and *Operculina* at the top, is interpreted to have been deposited during the time interval which spans zones TB 1.1 to TB 1.4 in the Haq et al. sealevel curve (Fig. 3.3). The Late Oligocene is a time of major transgression, with a regression occurring at the Oligocene/Miocene boundary at 25.5Ma. This regression is marked by a type 2 sequence boundary which was not recognised in this study, but would be expected below the *Operculina* horizon at Port Giles.

When compared with the southern Australian time scale, the middle member package fits in the Janjukian stage (McGowran et al., 1996).

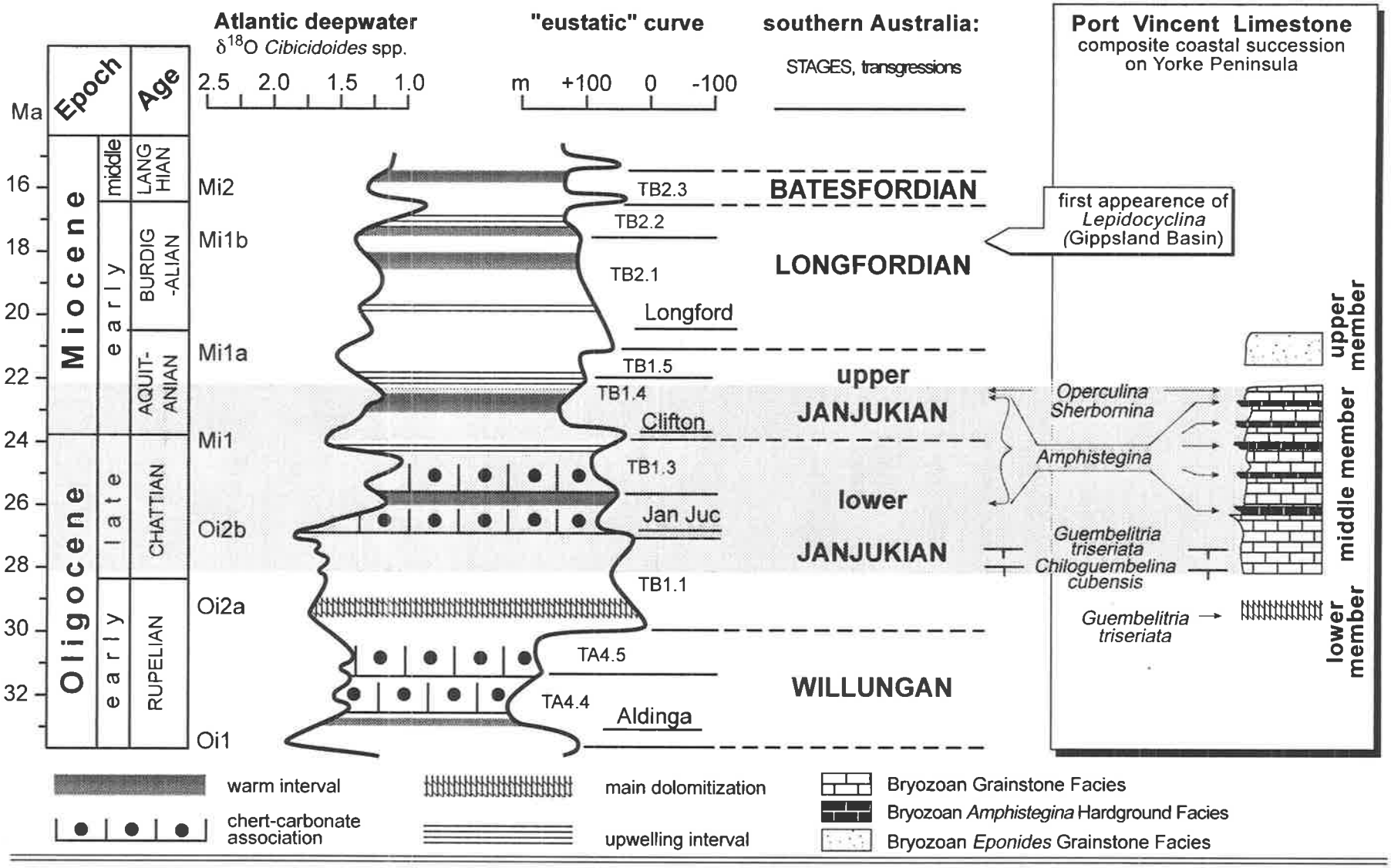

Figure 3.3: Correlation of the Port Vincent Limestone middle member parasequences with the global eustatic curve (Haq et al., 1988) and the southern Australian Oligocene/Miocene depositional sequences (McGowran et al., 1996).

Chapter 4

DIAGENESIS

INTRODUCTION

Unravelling the products and understanding the processes and evolution of carbonate diagenesis is essential to facies analysis, palaeoenvironmental studies, and exploration for hydrocarbons and ore deposits. Diagenesis encompasses all the chemical, biological and physical alterations which occur in the character and composition of sediments, beginning from the moment of deposition, and lasting until the resulting materials (rocks) are moved into the realm of metamorphism (Larsen and Chilingar, 1979). Carbonate sediments and rocks are easily susceptible to diagenesis, and may often undergo multiple stages of diagenesis. In most cases, depositional constituents of carbonate sediments differ chemically, texturally and structurally. As a result of this heterogeneity, the sediments will variably respond to the acting diagenetic processes and will induce a series of ongoing diagenetic processes until a state of equilibrium is approached between the sediments and the chemical and physical conditions in the micro- and macro-environment. Accurate identification of these diagenetic sequences helps identify the type of diagenetic environments that hosted the sediments. Carbonate diagenesis operates in three major diagenetic environments, the seafloor, meteoric, and burial. Each diagenetic environment is governed by assemblages of characteristics that stimulate a multitude of processes, each with an exclusive product. Seafloor diagenesis take place on and just below the seafloor, as well as at the strandline (James and Choquette, 1990a). Seafloor processes are commonly synsedimentary and often times may variably influence the ongoing depositional cycle by modifying the substrate. Meteoric diagenesis is brought about by percolating freshwater through subaerially exposed sediments. Freshwater may nonselectively affect the bulk rock, resulting in water-controlled meteoric diagenesis, or may selectively affect different mineralogies, resulting in mineral-controlled meteoric diagenesis (James and Choquette, 1990b). Burial diagenesis encompasses any change or collection of changes that take place below the zone of near-surface diagenesis and above the realm of low-grade metamorphism (Choquette and James, 1990). These changes are induced by overburden produced from

progressive sediment accumulation. Burial diagenetic processes may begin in depths as shallow as one metre below the seafloor or a few metres below subaerial surfaces, yet still beyond the reach of surface related processes (Choquette and Pray, 1970). The intensity of alteration endured by any sediment or rock is related to the duration of exposure to the hosting diagenetic environment (Purday, 1968). In this respect, diagenetic processes are variables in time and space.

Most of our knowledge of carbonate diagenesis is derived from classical low latitude tropical models, where sediments are generally more affected by constructive diagenetic processes (carbonate aggradation) than by destructive processes. In particular, marine cementation and preservation of metastable carbonate phases dominate (Bathurst, 1975; Larsen and Chilinger, 1979; Longman, 1980; Flügel, 1982; James and Choquette, 1990a, 1990b). On high-latitude cool-water carbonate shelves bottom waters are below 20°C in temperature, higher in CO_2 content, salinity is normal, circulation is mainly open, sedimentation rates are low and the carbonate content may decline to 50% (Brookfield, 1988; Nelson, 1988). Accordingly, earlier workers suggested that the direction of carbonate flux is considerably reversed to the seawater from sediments (by dissolution/breakdown). Destructive diagenetic processes (carbonate degradation) prevailed over constructive diagenesis, producing much of the carbonate mud by skeletal abrasion, bioerosion, and maceration (Alexandersson, 1978, 1979; Nelson et al., 1982, 1988c). More recently, however, direct precipitation of marine inorganic low-Mg calcite (LMC) cement has been reported from Tasmania and New Zealand (Rao, 1981b; Nelson et al., 1988c); nevertheless, this process still remains limited and rather selective. Chemical heterogeneity between constituents is minor in cool-water carbonates. Constituents are more often calcitic, LMC or intermediate-Mg calcite (IMC), as well as aragonite and/or high-Mg calcite (HMC), with the latter being more restricted to specific environments. Accordingly, little mouldic porosity is created and minimal cement is produced and the rocks remain friable and highly porous (Reeckmann, 1988; James and Bone, 1989, 1992). Therefore, cool-water carbonates have less diagenetic potential (Schlanger and Douglas, 1974) than their warm-water counterparts, rendering them less

vulnerable to grain dissolution and elemental changes (Brand and Veizer, 1980).

THE PORT VINCENT LIMESTONE

Outcropping units of the Port Vincent Limestone are dominated by friable, slightly cemented bryozoan calcarenite, with several sharp and distinctively well-cemented hardgrounds punctuating the sequence (plate 3.2). The nature of these depositional sub-tidal cycles strongly influenced the subsequent diagenetic sequence. Evidence indicates that diagenesis operated in two distinct, but ultimately related, depositional-diagenetic phases. The first phase is synsedimentary, operating during the deposition of each depositional cycle independently, and can be seen in each of the successive cycles. The second phase is broader and relatively later, affecting all depositional cycles together: i.e. the whole package including its synsedimentary diagenetic products. This chapter concentrates on the diagenetic processes, products, and their chronological order. Dolomite is dealt with in a separate chapter.

1. DISSOLUTION

Carbonate sediments, rocks, and cements may undergo dissolution when exposed to pore waters that are under saturated with respect to the host carbonate mineralogy. Much dissolution takes place in meteoric and marine environments, whereas stress-induced dissolution is common under burial (Bathurst, 1975; Alexandersson, 1978, 1979; Longman, 1980; Flügel, 1982; Tucker and Wright, 1990). The whole process is governed by a number of inter-related physicochemical conditions (the intrinsic and extrinsic factors of James and Choquette, 1990a & 1990b). Among the most important of these is the amount of dissolved CO_2 in water (referred to as P_{CO_2}), which in turn is a function of temperature and pressure (Friedman, 1964). Other factors include the initial composition and mineralogy of the sediments, their grain size and texture, porosity and permeability, climate, and time (James and Choquette, 1990a, 1990b).

Dissolution of the Port Vincent Limestone is interpreted to have taken place mainly in the marine and meteoric environments. Burial dissolution due to chemical compaction is of minor importance. Results show that the intensity of dissolution of various skeletal components can be placed according to their relative solubility from most soluble to least in the following order: flat robust branching bryozoa > aragonitic bivalve shells > benthic foraminifers > echinoids > coralline algae > planktonic foraminifers > calcitic bryozoans > brachiopods.

1.1 Dissolution In The Marine Environment:

Small scale dissolution of skeletal carbonates exposed on the seafloor in cool-water environments has been documented, and is accelerated if the sediments are already macerated or disintegrated (Alexandersson, 1978, 1979; Nelson et al., 1988a). However, SEM examination indicates little abrasion and maceration of skeletal fragments from the Port Vincent Limestone (plate 5.4-A, B, C). Instead, moulds of flat robust branching bryozoans and many aragonitic bivalve shells are common in the Port Vincent Limestone, particularly in the bryozoan-*Amphistegina* hardground facies (plate 4.1). Only the thin axial core of this particular bryozoan growth form is preserved, indicating removal of the thicker outer part by dissolution. A subsequent marine internal-micrite (this chapter, section 2.1.4) envelopes the core and therefore fills moulds of the thicker outer part, as well as many bivalve moulds (plate 4.1). Modern flat robust branching bryozoans are bimineralic. Their axial core is mainly lMC, whereas their thicker outer parts are made of aragonite (Bone and James, 1993). Up to 30% of their skeleton consists of Mg-calcite, and x-ray analysis show this to be between 2.0 and 10.0 mole % $MgCO_3$.

There is no evidence of subaerial exposure or a stage of meteoric cementation between the dissolved grains and the internal micrite. These observations indicate that mineral-controlled dissolution of these particular bryozoan growth forms must have taken place on the seafloor. Furthermore, it indicates that marine dissolution in cool-water carbonate settings is a significant early diagenetic process. However, not all metastable grains were dissolved by

marine carbonate-undersaturated water. Some remained unaffected until exposed to the meteoric environment.

1.2 Dissolution In The Meteoric Environment:

Carbonate rocks exposed to freshwater may with extended time suffer extensive water-controlled (congruent) and mineral-controlled (incongruent) dissolution. As a result, a wide array of surface and subsurface karst features as well as secondary macro- and micropores are produced (Jennings, 1985; James and Choquette, 1988). Cool-water carbonates are largely aragonite-poor and are therefore only slightly affected by these processes in the meteoric realm (Reeckmann, 1988; James and Bone, 1989, 1992).

1.2.1 *Mineral-controlled meteoric dissolution:*

Crescent and other fossil-shaped mouldic pores are locally abundant in otherwise unaffected parts within lithified hardgrounds. Brachiopods, calcitic bryozoans, echinoids, and other benthic and planktonic foraminifers remain undissolved or only partially affected.

These mouldic pores are interpreted to have been created by selective meteoric dissolution (leaching) of metastable aragonitic and HMC molluscan shells, and benthic foraminifers like miliolids. This interpretation is based on several lines of evidence, particularly on the textural relationships between cements. The early marine cements stop growing at pore boundaries and do not fill or extend into the mould, reflecting the presence of the original shell during marine dissolution and cementation. Subsequent subaerial exposure promoted a phase of meteoric dissolution and cementation. Meteoric cements now grow into these mouldic pores filling them partially or completely (plate 4.2-A, B).

Marine dissolution is further ruled out by the presence of well preserved casts, moulds and steinkerns of various fossils. The fossil cavities were filled by marine microbioclastic internal-micrite prior to dissolution of the original shells. Pore walls are sharply defined within the micrite, and most times bear ornamentation reflecting surface structures of the

Plate 4.1:

A, B- Flat robust branching bryozoan growth forms (r) in the bryozoan-*Amphistegina* hardground facies. The now thin LMC axial core of many of these bimineralic bryozoan growth forms are surrounded by internal micrite precipitate which fills partial moulds after removal by dissolution of the outer thicker aragonite periphery. Photomicrograph under plane light. A- sample 8, section 8. B- sample 1, section 10.

C- Crescent shaped mould now filled with internal micrite. Transverse section through an articulated branching cheilostome bryozoan growth form (ar). Sample 2, section 8.

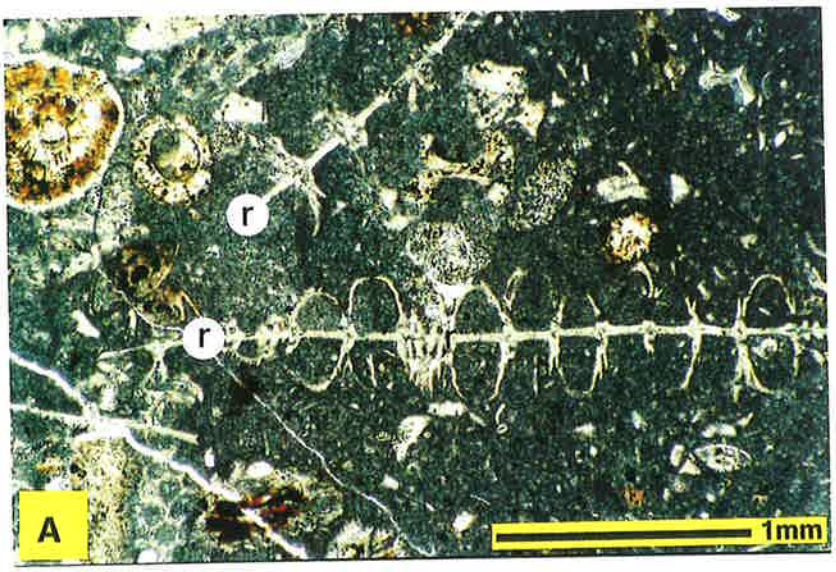
r
r
A
1mm

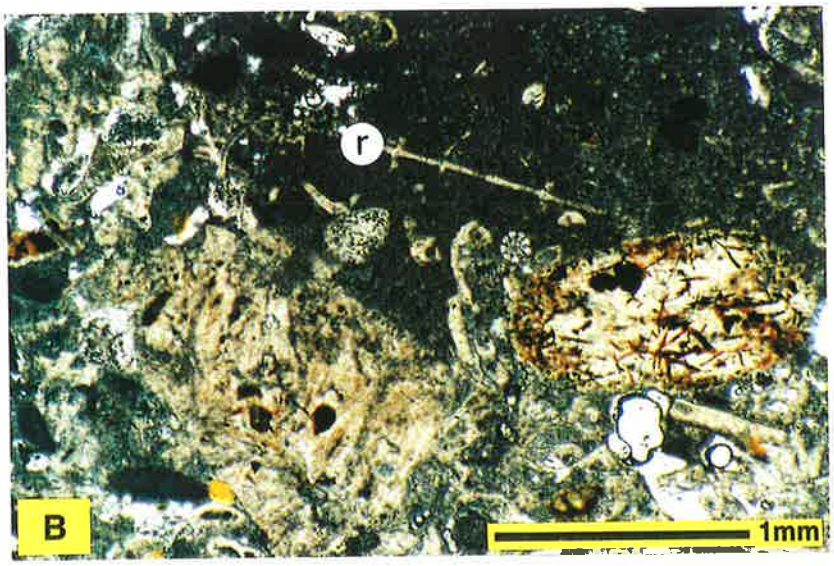
r
B
1mm


ar
C
0.5 mm

Plate 4.2:

Thin section photomicrograph under polarised light **(A)** and CL **(B)** showing meteoric cements (arrows) growing into meteorically formed mouldic pores. The early marine cements stop growing at pore boundaries and do not fill or extend into the mould suggesting that the mould was formed after subaerial exposure, which then allowed the precipitation of meteoric cement in these moulds. Sample 4X, section 2.

C- Mineral-controlled meteoric dissolution created secondary mouldic porosity in many facies of the Port Vincent Limestone, and can be seen clearly in marine hardgrounds rather than in friable calcarenites as these unconsolidated sediments collapse easily or filter into the mould. Section 4.

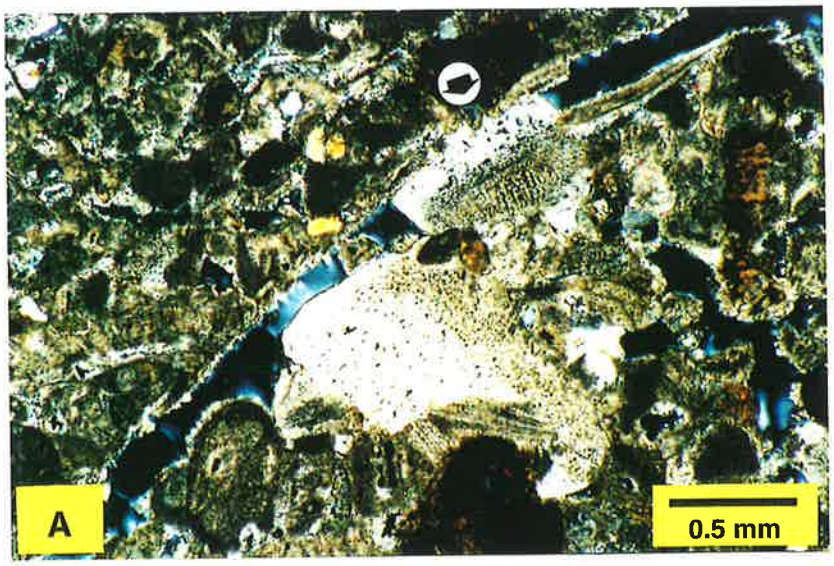
A
0.5 mm

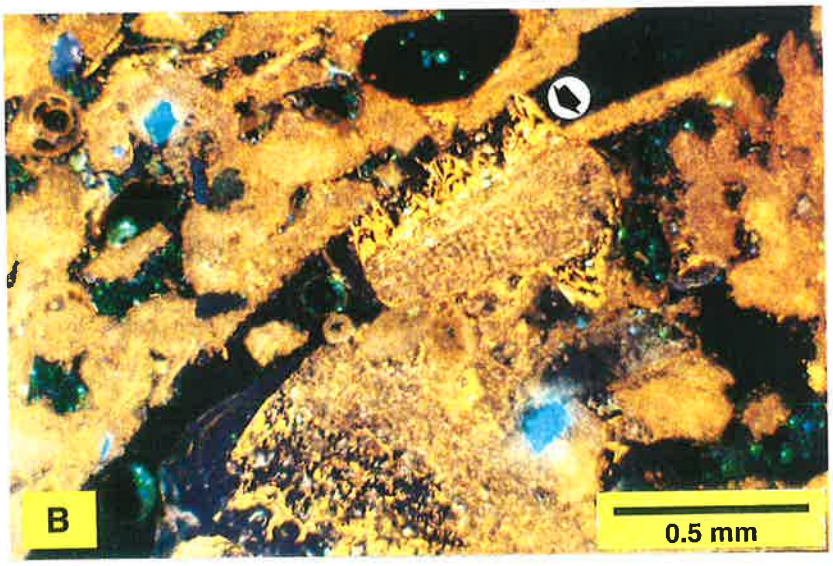
B
0.5 mm

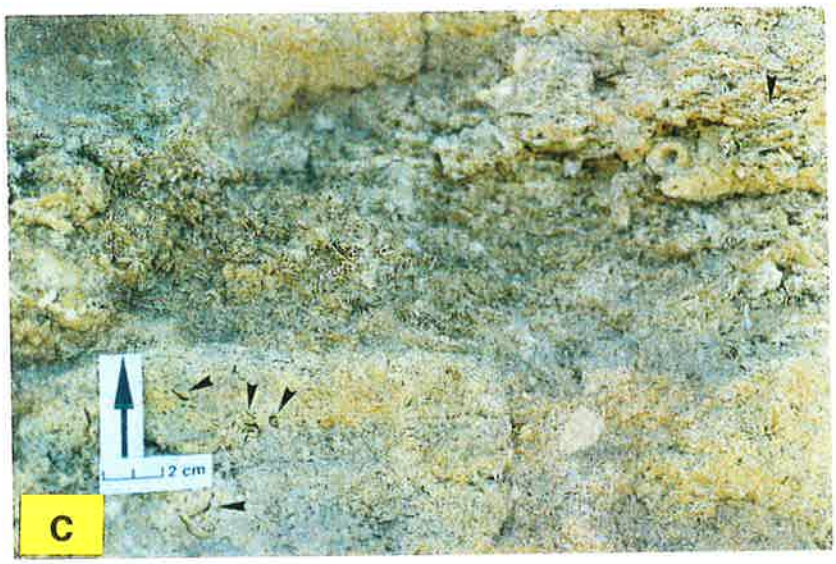
2 cm
C

Plate 4.3:

A- Palaeokarst surface above Miocene beds of the Port Vincent Limestone at section no. 15, south of Edithburgh (arrows). Beds above the palaeokarst surface are Pliocene Hallett Cove Sandstone and Quaternary calcrete. Exposure of the Port Vincent Limestone sequence ends at this section.

B, C- Palaekarst features on Miocene beds of the Port Vincent Limestone at section no. 14, south of Edithburgh. (scale rod in B = 1 m, hammer in C = 32 cm long)


A


B


C

Plate 4.4:

Dolines and caves are common in the Port Vincent Limestone exposures between Stansbury and Port Giles. Dolines have a cylindrical form, less than 2 metres in diameter and extend vertically from the top of the cliffs, cutting across bedding plains, to depths up to 15 metres. Most of these dissolution features are now filled with soil and clay, which infiltrated from the surface (arrows). These dolines are interpreted to be products of water-controlled dissolution in the meteoric environment. (scale rod = 1 m).


A


B


C

former shell (e.g., ridges and grooves). This suggests that the internal micrite filled and surrounded these shells on the seafloor soon after the animal's death. Later, when the rocks were exposed to the meteoric environment, original shells were dissolved creating mouldic pores (plate 4.2-C).

Mineral-controlled meteoric dissolution appears to be more effective than marine dissolution. The metastable grains that escaped marine dissolution were partially or completely removed upon exposure to freshwater. However, some tests of foraminifera appear to have resisted complete dissolution and maintained a neomorphosed shell. This is possibly due to abnormal morphochemical diagenesis, which allows mineral stabilisation without major textural alteration or complete dissolution of the shell wall (Budd, 1992; Budd and Hiatt, 1993).

1.2.2 *Water-controlled meteoric dissolution:*

The top of the Port Vincent Limestone at Edithburgh is a small-scale surface karst overlain by the Pliocene Hallett Cove Sandstone (plate 4.3-A, B, C). This clearly indicates that meteoric dissolution must have begun after subaerial exposure, some time during the late Middle Miocene. Ludbrook (1967) and Lindsay (1969) recognised a regional stratigraphic break, representing Middle Miocene-Early Pliocene time, in the St. Vincent Basin and adjacent southern Australian basins. They further indicated that this major break is possibly due to non-deposition or erosion following subaerial exposure.

Younger, probably Pliestocene, surface and subsurface karst features in the form of dolines and caves are common in cliffs between Stansbury and Port Giles (plate 4.4). Dolines have a cylindrical form, less than 2 metres in diameter and extend vertically from the top of the cliffs, cutting across bedding planes, to depths up to 15 metres. Most of these dissolution features are now filled with soil and clay, which infiltrated from the surface. The limestone walls in these vertical solution shafts are unaltered, except for patchy iron stains brought about by soil infiltration. These dolines are interpreted to be produced by gravity-controlled vadose diffuse-flow (cf. James and Choquette, 1990b). A few dome-shaped isolated caves are also present in these coastal cliffs. They are relatively small, with diameters ranging from

1 to 4 metres. Their roofs, which are either partially collapsed hardgrounds or friable calcarenite, are 1-6 metres high. The limestone surface in most caves is weathered and often times coated with a thin translucent recent carbonate cement. These coastal caves are also interpreted to have been formed by meteoric water. Shallow caves situated within the reach of high tide level were later enlarged by mechanical action of sea waves and subsequent collapses.

1.3 Dissolution Under Burial:

Unlike the other two environments, burial dissolution reduces porosity through chemical compaction. Flat surface contacts between grains and intergranular penetration are common among various grain types. Dissolution under burial is regarded here as minor, and produced little $CaCO_3$ for cementation. Burial diagenesis is further discussed later in this chapter under section 3 - compaction.

2. CEMENTATION

Cement includes all passively precipitated space-filling carbonate crystals which grow attached to a free surface (Bathurst, 1975). Commonly, the process involves a series of dissolution and subsequent re-precipitation phases, leading to lithification and reduction in porosity of the original sediments. An efficient fluid flow mechanism, together with an adequate source for the cement phase and the absence of kinetic inhibitors are required for carbonate sediment lithification.

Cementation in the Port Vincent Limestone was minor overall, and much of the rock remains friable and highly porous (30 - 40 % porosity). Skeletons of modern bryozoans, similar to those comprising the Port Vincent Limestone, are mainly made of LMC or IMC, and less commonly completely or partially aragonite (Bone and James, 1993). Therefore, little cement is produced from such skeletons and the sediments remain largely loose and friable (Reeckman, 1988; James and Bone, 1989). Cements are now entirely LMC (1 - 3 mole %)

as confirmed by microprobe and x-ray diffraction analyses. They stain pink with Alizarin Red-s and potassium ferricyanide solutions (Dickson, 1966) indicating a low iron content (< 700 ppm). Cathodoluminescent (CL) petrography was used in this study for recognising and interpreting the types of cement fabrics, their textural relationships, and sequential order of precipitation. All polished thin sections were investigated under the same CL conditions, with a setting of 12 kv and 200 uA. The criteria and interpretations revealed by this technique are briefly outlined in Appendix A-2.

2.1 Cement Fabrics:

Four common cement fabrics are distinguished: Scalenohedral, syntaxial calcite rim, blocky calcite, and internal micrite. Syntaxial and scalenohedral cements predominate largely over other fabrics. A list of similar cement fabrics and their diagenetic environments as interpreted by various authors are presented in Table - 4.1.

Cement fabric	Diagenetic environment	Pore water	Author
Scalenohedral *(dentate)*	meteoric	freshwater	James and Bone, 1989
	marine	marine	Kerans et al., 1986; Nicolaides, 1995
Syntaxial	meteoric	freshwater	Meyers, 1978; Walkden and Berry, 1984
	marine	marine	Görür, 1979
	burial	marine	Nelson et al., 1988c, Tucker&Wright, 1990
Blocky	meteoric	freshwater	Mohamad&Tucker,1992
	burial	freshwater	Dorobek, 1987
Internal micrite	meteoric	fresh water	Reeckmann, 1988
	marine	marine	Reid et al., 1990

Table - 4.1: Common cement types and their diagenetic environments.

2.1.1 *Scalenohedral spar:*

This cement forms thin, almost isopachous, rinds surrounding grains or lining intragranular pores, and appears white coloured with a light brownish stain. The cement comprises around 20% of the total cement content in the studied rocks. It also occurs as a few crystals grouped in clusters scattered throughout the limestone succession. The cement is most commonly intergranular in the upper 10-30 cm of hardgrounds, whereas in the friable calcarenite it is more commonly intrabryozoan than intergranular. Crystals are euhedral, inclusion-rich, 10 to < 50 μm long, and decrease in width from 20 to 7 μm towards their distal end. They grow perpendicular or slightly inclined on their substrate, and have prismatic terminations (plate 4.5-A, B).

Scalenohedral cements stain very pale pink with potassium ferricyanide and appear non-luminescent (black) in hardgrounds, but non-luminescent with a thin jagged bright yellow rim in the friable calcarenites. They are slightly ferroan (0 - 100 ppm Fe), and show a progressive increase in Mn, Sr, Al, and Na ions towards crystal terminations (Fig. 4.1). This relates directly to the element's ratio in the remaining fluid (Bathurst, 1975). X-ray maps and traverses across the non-luminescent scalenohedral cements show them containing a higher Mg content (3 mole %) than the adjacent grains and subsequent internal micrite precipitate (Figs. 4.2, 4.3).

The cement predates microboring, physical and chemical compaction, and a phase of intergranular and intragranular microbioclastic internal micrite precipitate.

Similar LMC cement fabrics in other cool-water carbonates (both ancient and modern) from southern Australia, New Zealand, and England have been interpreted as marine precipitates. Their source is believed to be derived from stabilisation of metastable minerals, or even a possible direct marine contribution (Al-Hashimi, 1977; Rao, 1981a; Nelson et al., 1988c; Nicolaides, 1995). They are also commonly associated with unconformities and hardgrounds (Rao, 1981b).

Plate 4.5:

A- Thin section photomicrograph under plane light showing scalenohedral cement stained very pale pink with potassium ferricyanide. Sample 2, section 8.

B- SEM photomicrograph showing scalenohedral cement crystals; note how crystals grow perpendicular on the grain surface (g) and more abundantly into the intrabryozoan pores. Trace element composition of the large crystal (X) is shown in Fig. 4.1. Sample 6, section 8.

C- Large clear crystals of syntaxial rim cement grow abundantly around, but more commonly beneath, echinoid fragments. In these limestones the cement is non-neomorphic, since it is unevenly developed around the grain. Cements that grow thicker beneath the grains, due to gravitational-controlled precipitation, are characteristic of precipitation in the meteoric environment (Bathurst, 1975), and can also occur in the marine environment (Görür, 1979). Thin section photomicrograph under polarised light. Sample 5, section 6.

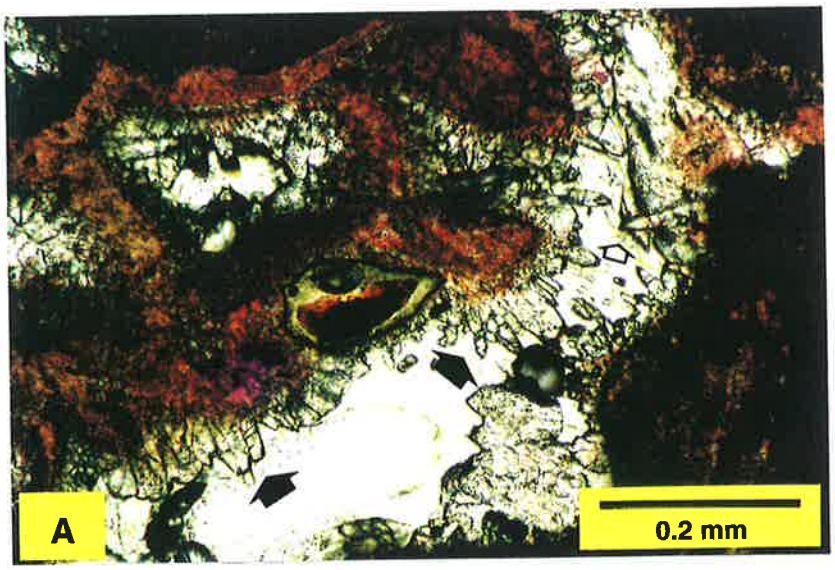
A
0.2 mm

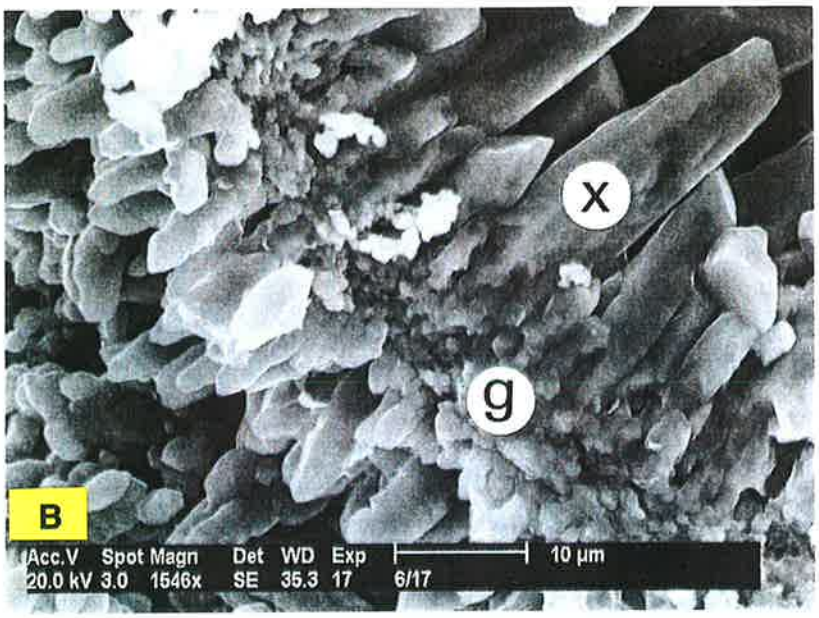
X
g
B
Acc.V Spot Magn Det WD Exp
20.0 kV 3.0 1546x SE 35.3 17 6/17
10 µm

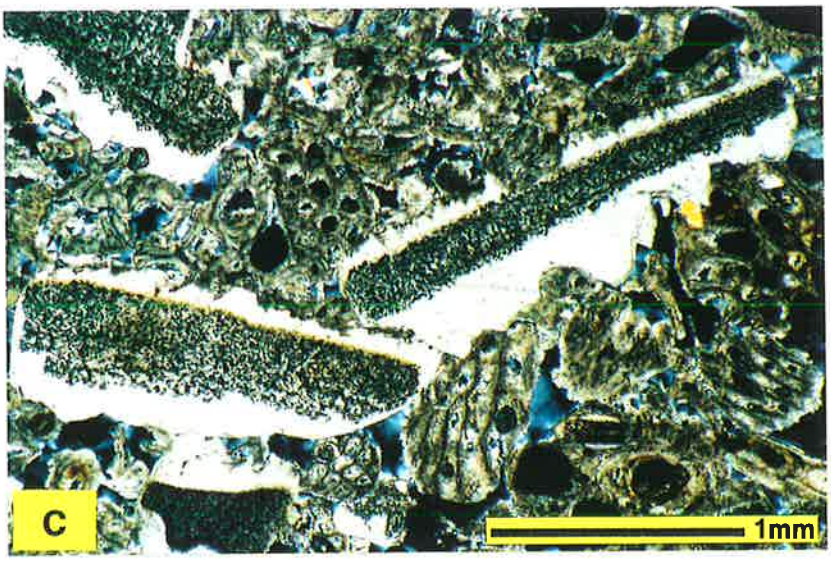
C
1mm

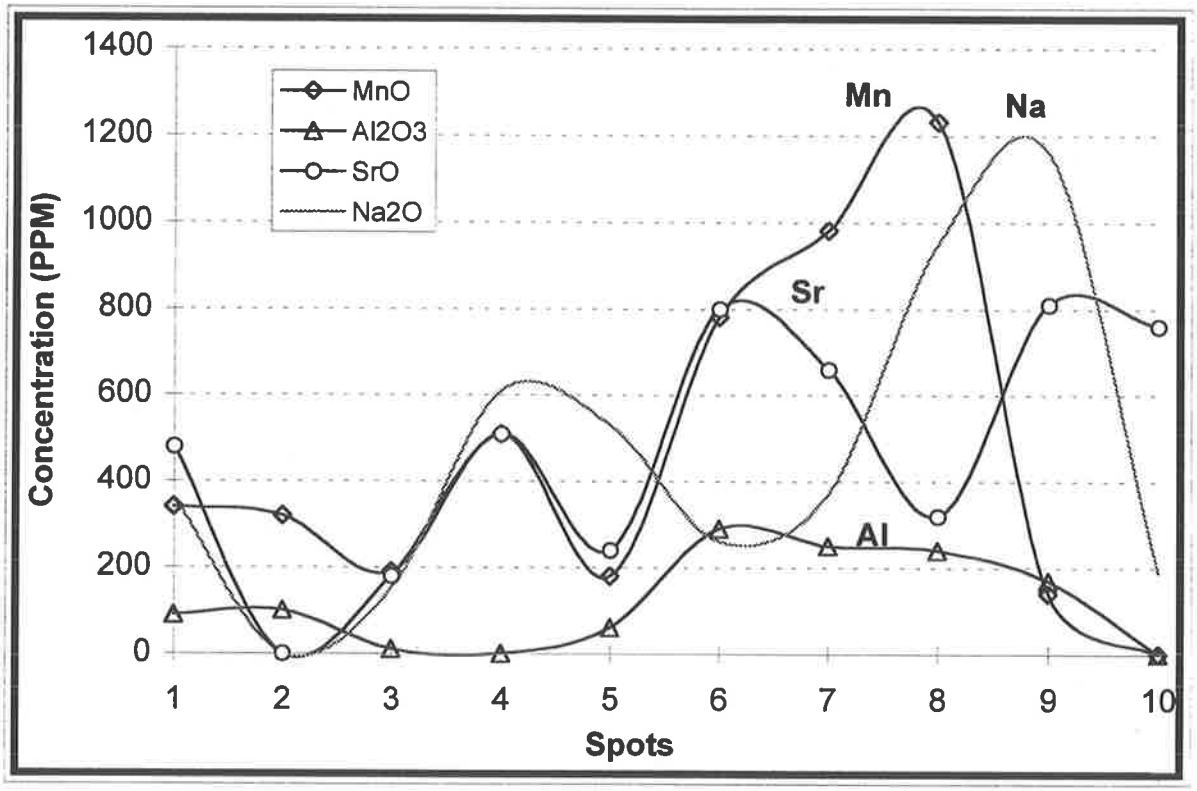

Figure 4.1: Trace element distribution along the scalenohedral cement crystal marked X in plate 4.5-B. Notice the increasing percentage of elements towards crystal terminations.

Moulds are rare to absent in the rocks immediately surrounding these cements, and carbonate dissolution by intergranular pressure solution is minor, or has not yet commenced in these rocks. These two forms of dissolution seem insufficient to account as a source for all the scalenohedral cement present in the Port Vincent Limestone, suggesting an additional potential source for cement, most likely seawater.

From the foregoing, the non-luminescent scalenohedral cement is interpreted to represent an early cement generation. It precipitated in the seafloor environment from oxidising marine pore water, and is now LMC (< 4 mole %). A genuine marine origin together with early carbonate dissolution is suggested as a source for the non-luminescent, intergranular cements in hardgrounds. The essential requirements for the precipitation of this marine cement are provided by the hardgrounds in the form of prolonged non-deposition in an active marine environment (Rao, 1981b). The other version of non-luminescent scalenohedral crystals with a yellow bright-luminescent rim, reflects changes in the pore water chemistry during an environmental transition. Pore water was initially oxidising marine but altered later to reducing conditions during shallow burial.

2.1.2 *Syntaxial rim spar:*

Cement crystals in optical continuity with monocrystalline particles (Bathurst, 1975; Reijers and Hsü, 1986) are the most frequent form of cement in the Port Vincent Limestone (40-50%). In these limestones the cement is non-neomorphic (Bathurst, 1975), since it is unevenly developed around the grain, and where space is available, large clear crystals (up to 0.7 mm) grow abundantly around and more commonly beneath echinoid fragments. They are 4 - 5 times thicker below grain surfaces than above (plates 4.5-C, 4.6-A, B). A few syntaxial rims are also found surrounding calcareous sponge spicules, but are volumetrically insignificant (plate 4.6-C). The cement stains pale pink with potassium ferricyanide, and is generally iron poor LMC. Generally, syntaxial cements are advantageous since a large single crystal may often bear many generations of cement overgrowth, which were formed during

Plate 4.6:

A, B- Thin section photomicrograph (A plane light, B under CL) showing inner non-luminescent (marine) and bright-luminescent (shallow-burial) syntaxial rim cement around an echinoid fragment. The non-luminescent cement is mostly uniform in its thickness around the grains when pore space is available, particularly in the pores of the friable bryozoan calcarenite (arrows). In the absence of space large clear crystals grow abundantly around but more commonly 4 to 5 times thicker beneath echinoid fragments. Sample 5, section 6.

C- Thin section photomicrograph (plane light) of syntaxial rim cement around a calcareous sponge spicule in the fine highly abraded bryozoan-*Eponides* grainstone facies. Sample 3, section 15.

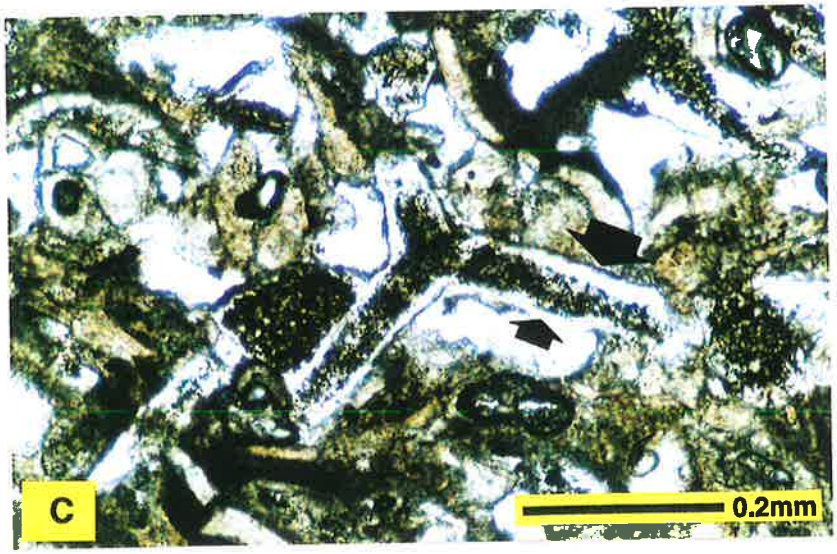

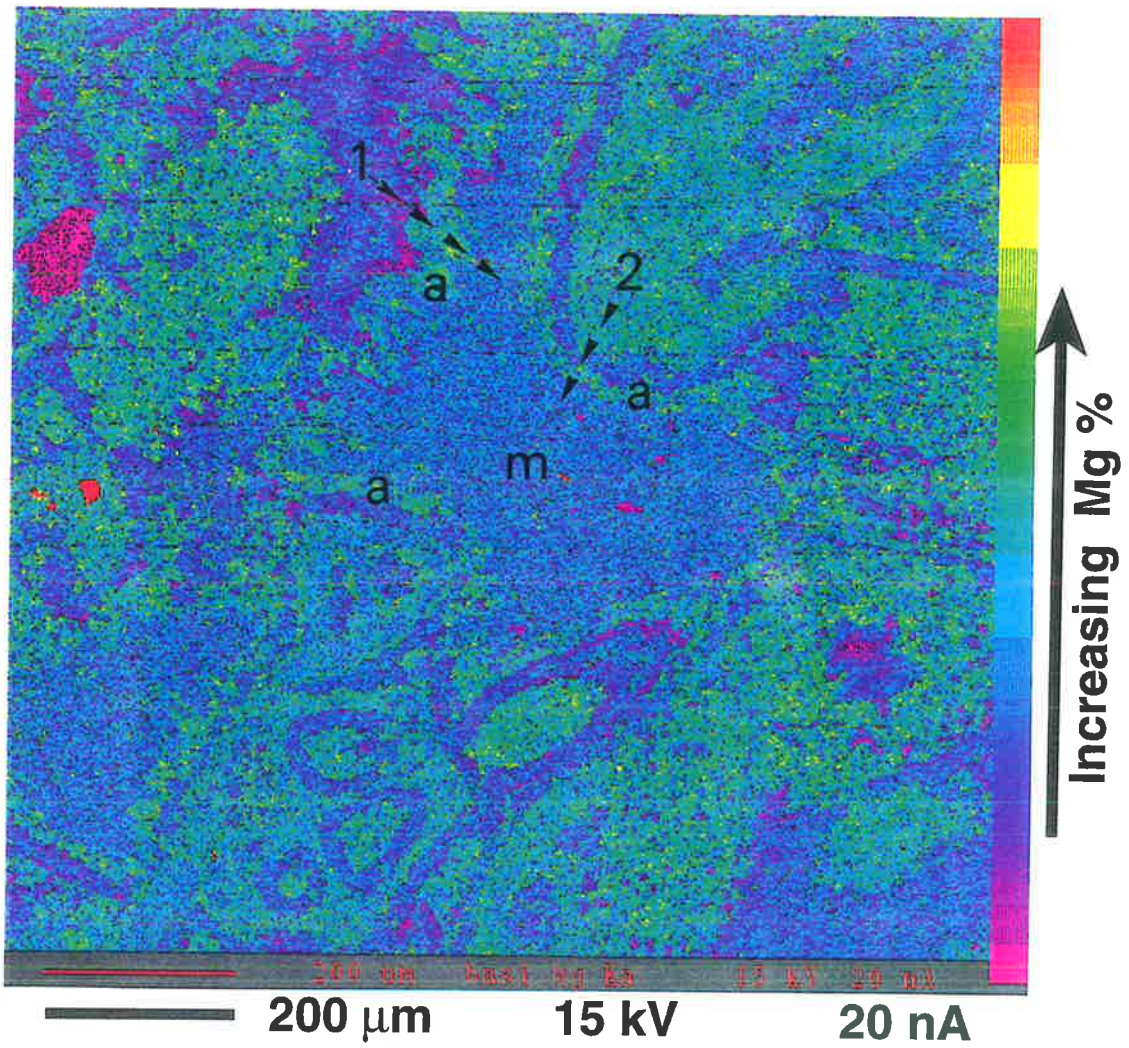

Figure 4.2: X-ray map showing Mg concentration in cements from hardgrounds of the Port Vincent Limestone. Traverses 1 and 2 cut across the non-luminescent synsedimentary cement (a). These cements are higher in Mg content than the surrounding grains and internal micrite precipitate (m), see figure 4.3, Appendix C-1a, Appendix C-1b, and plate 4.8-A. Sample 6, section 8.

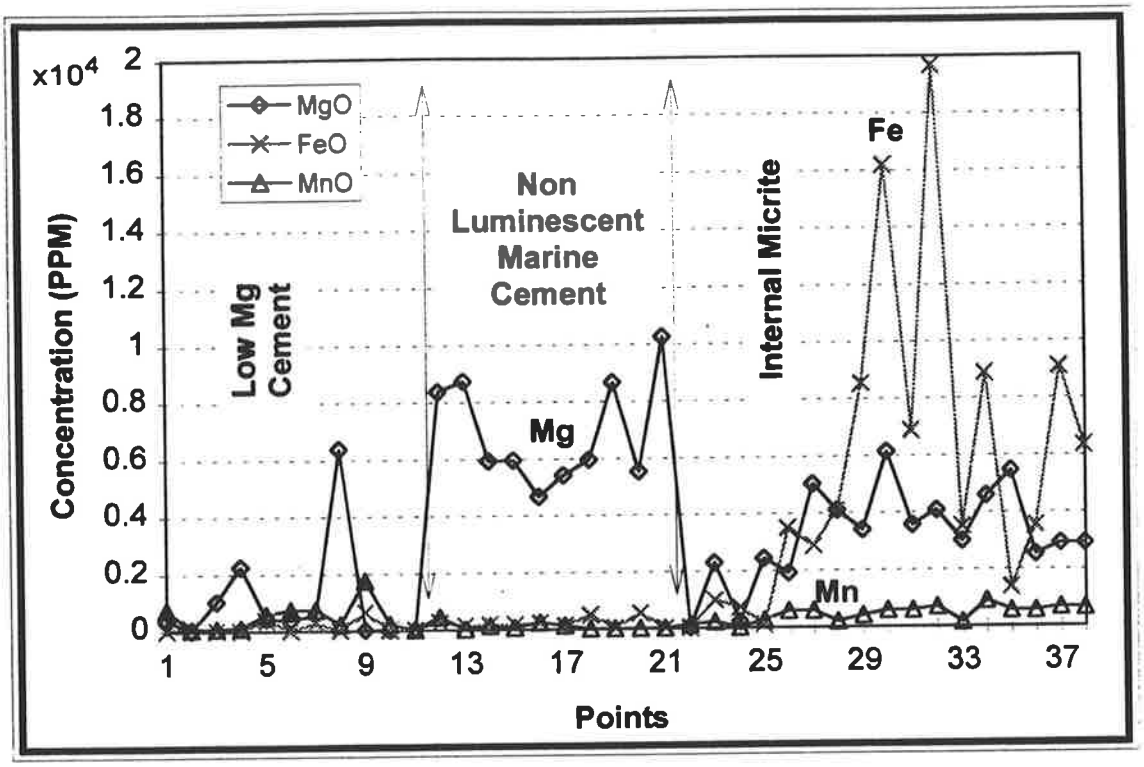

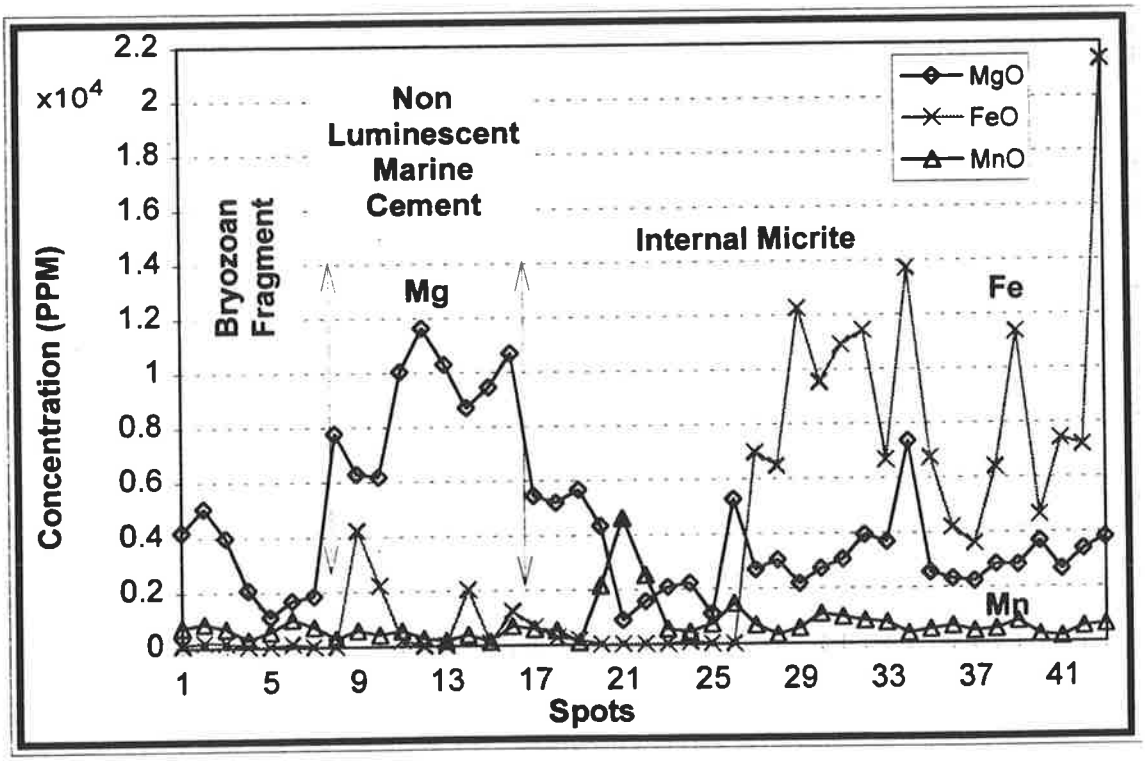

Figure 4.3: Microprobe analysis showing Mg, Mn, and Fe concentration across various grains, non-luminescent marine cement, and internal micrite precipitate. In figure 4.2, the marine synsedimentary cement (a) is higher in Mg content than the surrounding grains and the internal micrite precipitate. Quantitative analyses for traverses 1 and 2 in Fig. 4.2, are listed in Appendix C-1a, and Appendix C-1b respectively.

various diagenetic sequences. Progressive syntaxial overgrowths in the studied limestones are clearly revealed by their CL characteristics, and reflect precipitation from compositionally variable pore waters (Machel, 1985; Appendix A-2). Crystals with complete cement sequences comprise three successive zones (plate 4.7-A, B):-

Zone-1: an inner non-luminescent zone equally surrounding the echinoid fragment.

Zone-2: an intermediate bright-luminescent yellow zone.

Zone-3: a thick outer non-luminescent zone with several thin dull to bright-luminescent zones. All zones can be seen beneath most echinoid fragments in friable calcarenites. The high primary, and enhanced secondary, porosity in these lithologies provides sufficient space for cement precipitation (plate 4.6). In hardgrounds, only a thin rim of the inner non-luminescent zone (zone-1) has developed around 15-20% of the echinoid grains, whereas the remaining grains are surrounded by internal micrite precipitate (plate 4.7-C).

Environments of precipitation:

Syntaxial cement may precipitate in the meteoric, seafloor, or burial diagenetic environments (Table-4.1). Due to it's preferential growth over other cement fabrics (Lucia, 1962; Evamy and Shearman, 1965, 1969; Longman, 1980), syntaxial rim spar will rapidly occupy all or most of the pore space and thus restrict the growth of other fabrics. This fact equally applies to syntaxial cements precipitated in cool-water carbonate settings (plates 4.5-C; 4.6-A, B; 4.7-A, B). Textural relationships and geochemical data reveal that the three CL zones reflect three distinctive generations of syntaxial overgrowth and represent precipitation from various diagenetic environments:

a- Marine:- The inner non-luminescent zone reflects minimal incorporation of manganese in an oxygenated environment. The zone is mostly uniform in its thickness around the grain (plate 4.7-C). It is higher in Mg concentration (now up to 3 mole %) than that in the surroundings (< 2.5 mole %; Fig. 4.3), but has lower contents of Mn (0 - 310 ppm) and Fe

(0 - 350 ppm). The zone predates precipitation of the marine internal micrite in all hardgrounds (plates 4.7-C). A meteoric origin for the precipitation of this zone is unlikely because of its relatively higher Mg concentration (3 mole %). Other supporting evidence for a meteoric origin, like solution coronas (cf. Walkden and Berry, 1984), presence of birds eye structures, meniscus and early gravitational cement fabrics, are absent. Precipitation under shallow subsurface burial conditions from marine derived pore water (above the oxidation/reduction boundary, cf. Nelson et al. 1988c) is also ruled out since the zone clearly predates mild chemical compaction and grain breakage (plate 4.8-C). There is also no significant concentration of cement adjacent to grain contacts, similar to that which would be expected around compacted grains.

From the foregoing arguments, initial development of syntaxial rim cement in the Port Vincent Limestone is interpreted to be an early synsedimentary generation, which precipitated from oxidising marine pore fluids.

b- Shallow burial:- A second stage of syntaxial overgrowth is marked by a zone of yellow bright-luminescent cement. The zone is rich in manganese (1330 - 18,680 ppm) but poor in iron (0 - 670 ppm). It encloses the inner non-luminescent zone when free pore space is available, but most importantly, it postdates a younger phase of mild mechanical and chemical compaction. This is clearly evident in younger fractures that cut across pre-cemented echinoid fragments. Here, the inner non-luminescent cement is absent and the second stage bright-luminescent yellow cement grows immediately on the fresh fractured surfaces (plate 4.8-C). These textural relations suggests that this zone precipitated from reducing pore waters under shallow burial (< 100 m).

c- Meteoric:- The outer non-luminescent zone (0 - 160 ppm Mn, and 0 - 430 ppm Fe) is the thickest and comprises several thin dull to bright-luminescent zones (200 - 560 ppm Mn, 0 - 490 ppm Fe). This zone postdates meteoric dissolution by growing into moulds of aragonitic bivalves and other secondary developed porosity (plate 4.2-A, B). A meteoric origin is suggested for the outer non-luminescent zone. The enclosed dull to bright-luminescent zones

Plate 4.7:

A- Thin section photomicrograph (polarised light) of syntaxial cement surrounding an echinoid fragment in the bryozoan grainstone facies. Sample 1, section 6.

B- Enlargement of the cement crystal in photo A shows three generations of syntaxial cement overgrowth when examined under CL. These progressive syntaxial overgrowths reflect precipitation from compositionally variable pore waters in different environments as revealed by microprobe analysis. Sample 1, section 6.

a- The inner non-luminescent zone reflects minimal incorporation of manganese in an oxygenated marine environment. The zone is commonly uniform in its thickness around most grains, and is higher in Mg concentration (now up to 3 mole %) than the surrounding grains and cements (< 2.5 mole %).

b- The second stage of syntaxial overgrowth is marked by a zone of yellow bright-luminescent cement. The zone is rich in manganese (1330 - 18,680 ppm) but poor in iron (0 - 670 ppm). It encloses the inner non-luminescent zone when free pore space is available but most importantly it postdates a younger phase of mild mechanical and chemical compaction (see plate 4.8-C).

c- The third stage is indicated by an outer non-luminescent zone, which comprises several thin dull to bright-luminescent zones. This zone postdates meteoric dissolution by growing into moulds of aragonitic bivalves and other secondary porosity.

C- Thin section photomicrograph (under CL) showing syntaxial rim cement in the bryozoan *Amphistegina* hardground facies. In this example, a thin rim of the inner non-luminescent marine zone has developed around 15-20% of the echinoid grains, predating the deposition of internal micrite precipitate. Sample 17, section 6.

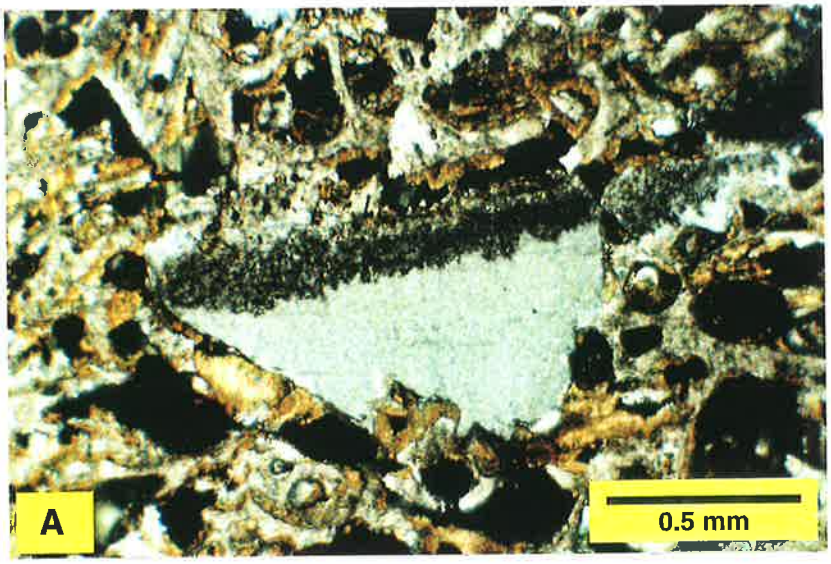
A
0.5 mm

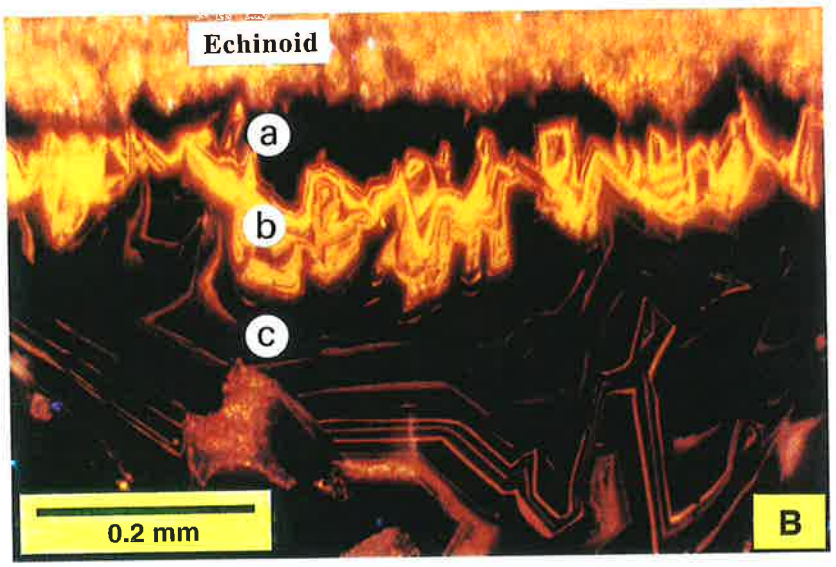
Echinoid
a
b
c
0.2 mm
B

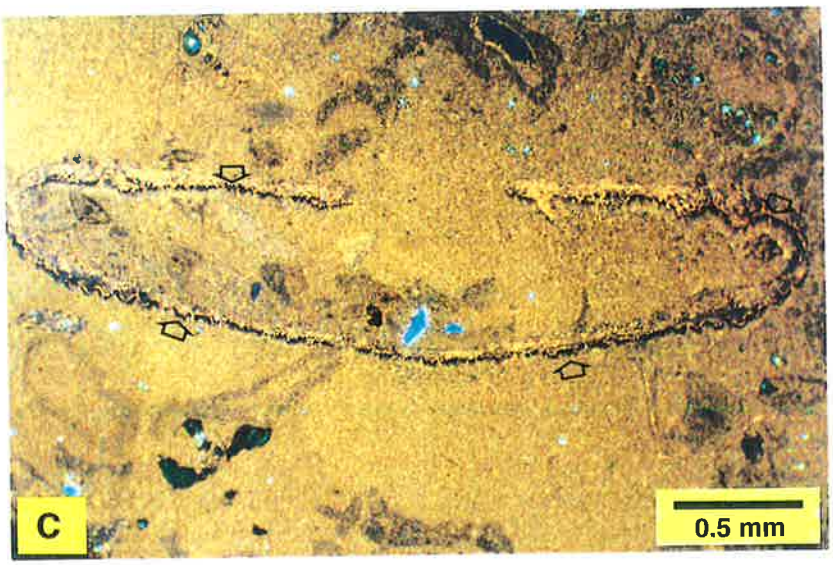
C
0.5 mm

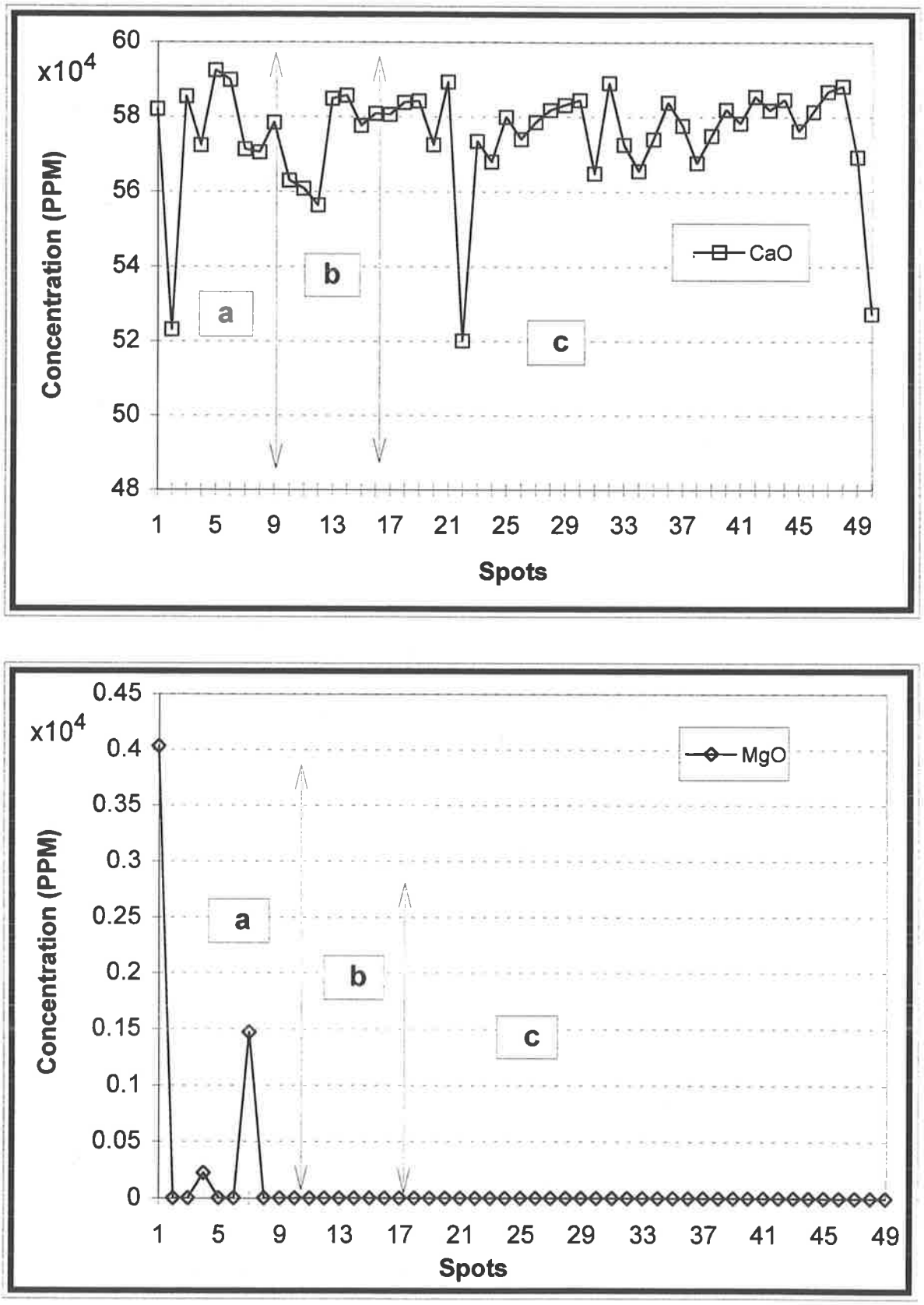

Figure 4.4: Microprobe analyses showing Ca and Mg concentration in the three generations of syntaxial cement shown in plate 4.7-B. Microprobe quantitative analyses for the traverse along a, b, c in plate 4.7-B are listed in Appendix C-2.

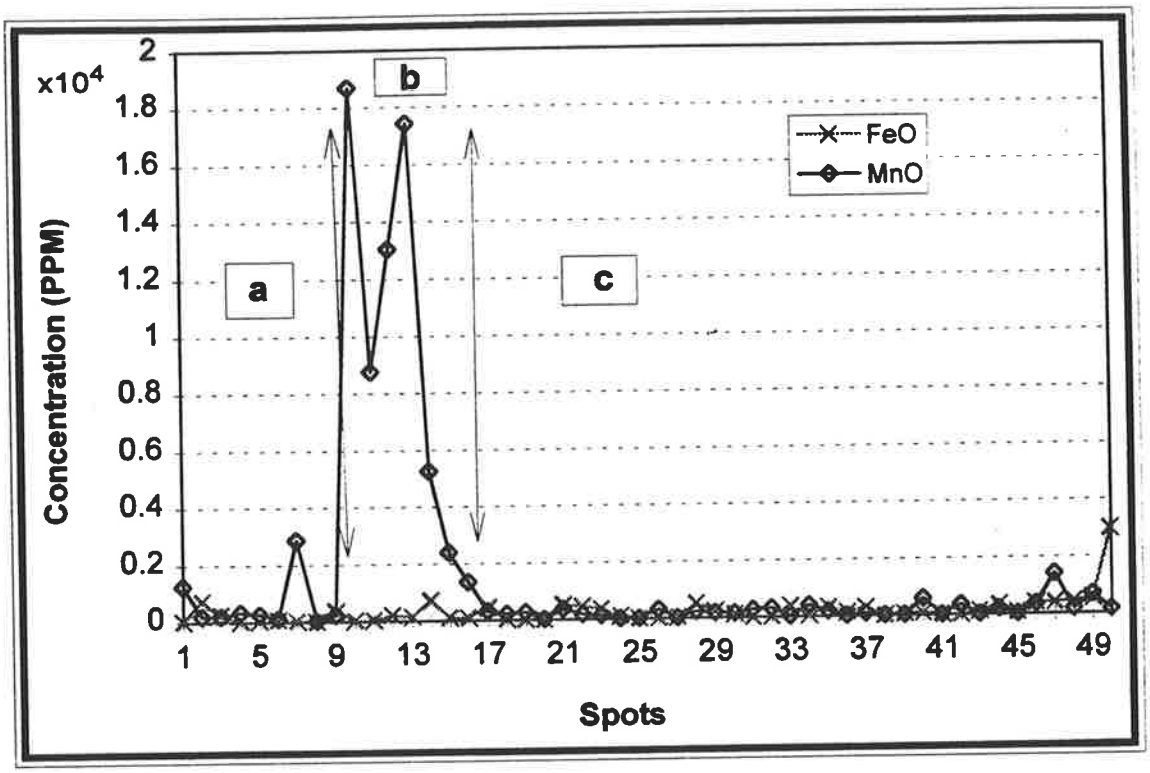

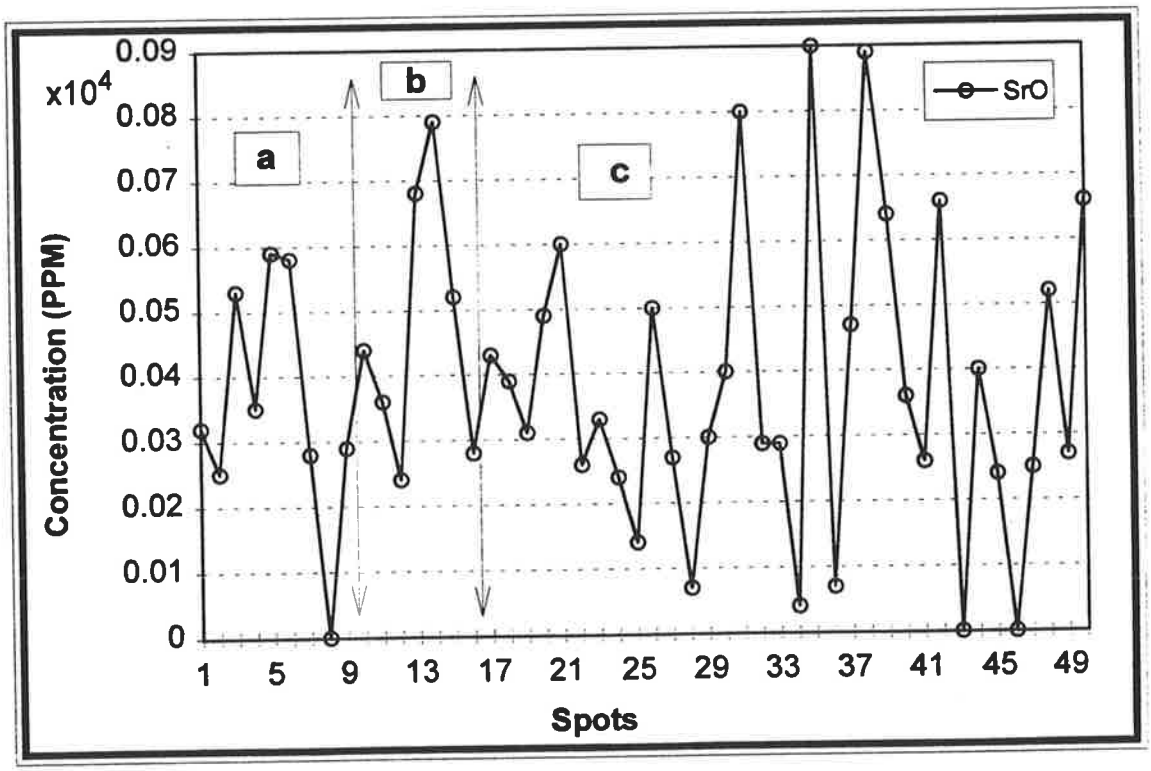

Figure 4.5: Microprobe analyses showing Mn, Fe, and Sr concentration in the three generations of syntaxial cement shown in plate 4.7-B. Microprobe analyses for the traverse a, b, c in plate 4.7-B are listed in Appendix C-2.

Plate 4.8:

A- Non-luminescent marine cements in hardgrounds. The cement is mostly uniform in its thickness around grains, but slightly thicker when syntaxially growing around echinoid fragments (arrow) because of their preferential growth over other cement fabrics. Textural relationships show that the cement predates precipitation of the marine internal micrite in all hardgrounds, and is higher in Mg content than the surrounding grains and cements (see figures 4.2, 4.3). Sample 6, section 8.

B- Non-luminescent marine cement around an echinoid fragment, whereas the other grains have little or no cement reflecting the preferential growth of cements around echinoids. Sample 5, section 6.

Thin section photomicrographs under plane light (left) and CL (right).

C- Yellow bright-luminescent syntaxial cement postdating a phase of mild mechanical and chemical compaction. The cement grows in fractures that cut across precemented echinoid fragments (arrow). The inner non-luminescent earlier marine cement is absent in these fractures and the second stage bright-luminescent Mn-rich cement grows immediately on the fresh fractured surfaces (see enlargement on the right). Sample 5, section 6.

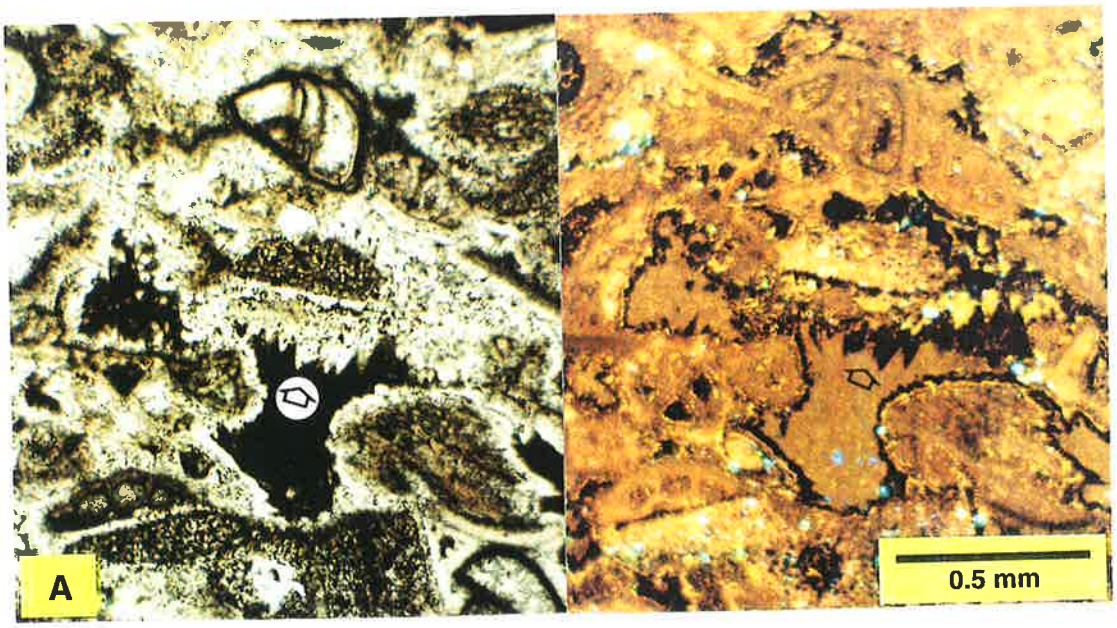
A
0.5 mm

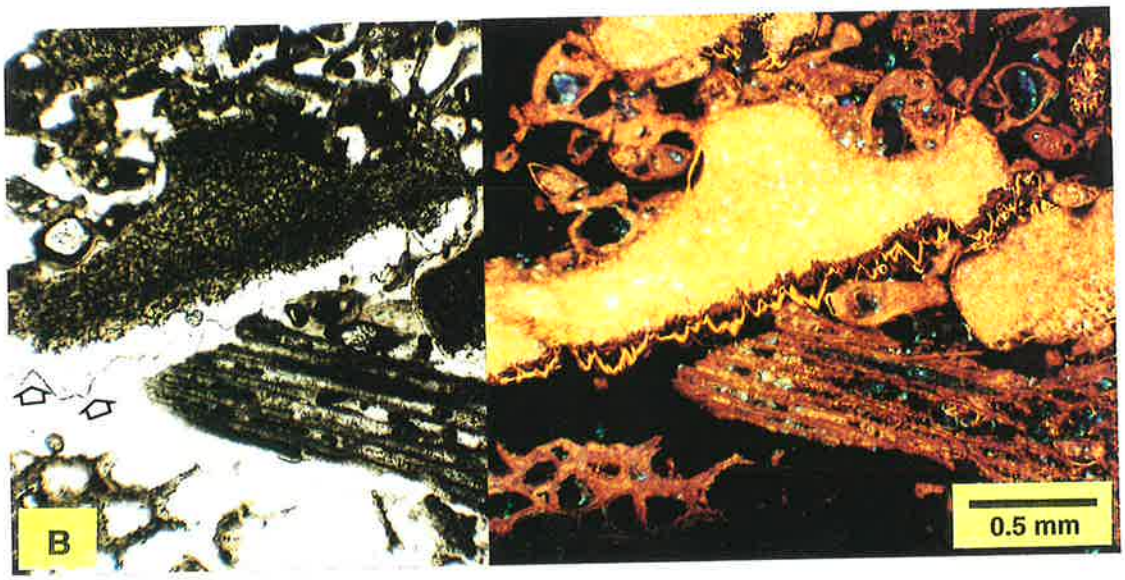
B
0.5 mm

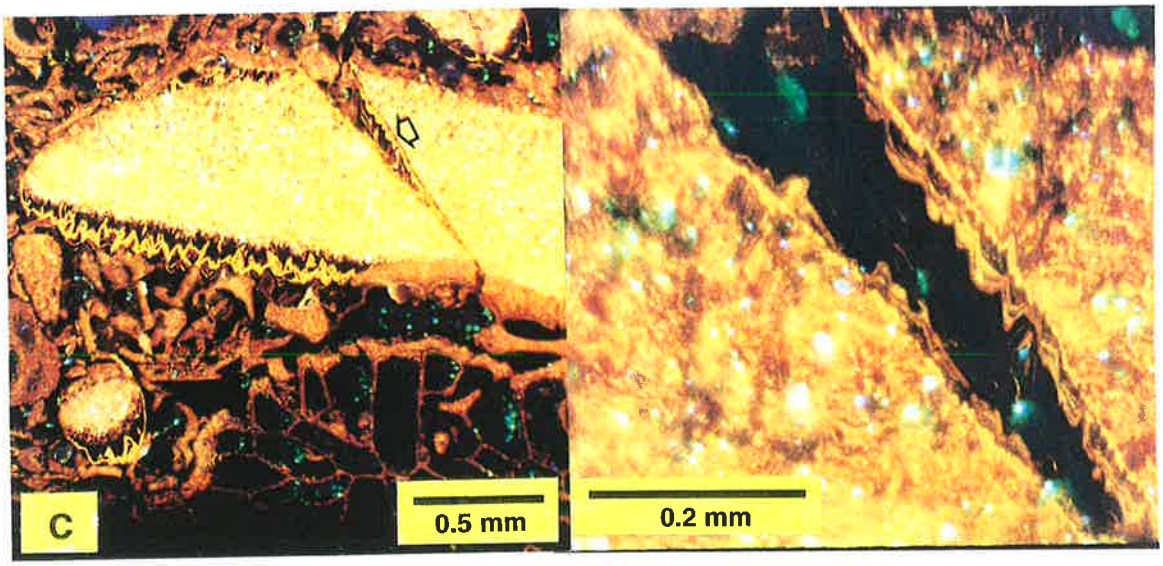
C
0.5 mm
0.2 mm

reflect precipitation during short periods of diminished fresh water supply, and precipitation of Mn^{2+} bearing cement. Such subzones may be induced by climatic fluctuations (Ogden, 1984).

2.1.3 *Blocky spar:*

Blocky calcite cement constitutes the least common form of cement fabric (< 10%) in the Port Vincent Limestone, and appears to be the youngest phase of cementation. It is locally distributed near the top of the formation, especially where the rocks become increasingly neomorphosed. These cements have the characteristic features of orthosparite (Bathurst, 1975) because:

a- They are devoid of relict structures.

b- Crystals are optically clear, euhedral equant calcite and are up to 0.8 mm long and 0.4 mm across.

c- They have sharp straight to slightly curved intercrystalline boundaries.

d- Enfacial junctions and compromise boundaries are common.

e- Boundaries between these cements and their depositional substrates are also sharp and well defined.

f- Initial crystallites grow with their *C* axis oriented normal to the host substrate, producing a bladed calcite rim, whereas others nucleate syntaxially when growing inside echinoid cavities (plate 4.9-A, B).

The morphology and textural relationships of these blocky cements and their host rocks allows distinction of two types of mosaics, both filling intragranular and intergranular pores:

1- Non-equicrystalline mosaic: this form often occupies the remaining pore space in geopetal structures. The crystals coarsen in size towards pore centres. They are non-luminescent (Mn

= 0 ppm, Fe = 0 - 180 ppm), with thin dull to bright-luminescent intercrystalline boundaries (Mn = 100 - 560 ppm, Fe = 40 - 430 ppm) (plate 4.9-A).

2- Equicrystalline mosaic: this form is rare and characterised by crystals showing no significant change in size towards any preferred orientation. They are non-luminescent (Mn = 0 - 80 ppm, Fe = 0 - 200 ppm), with thin bright luminescent orange intercrystalline boundaries (Mn = 80 - 490 ppm, Fe = 0 - 490 ppm) (plate 4.9-B).

Blocky calcite cement may precipitate in the meteoric phreatic or burial diagenetic environments, and on very cold seafloors (Longman, 1980; Flügel, 1982; James and Choquette, 1990a). A burial origin is excluded since the rocks containing these blocky cement fabrics were never buried under more than 50 metres of sediments, and cements are not found filling any fractures or compacted pore spaces. The cement postdates internal micrite precipitate in many intragranular pores indicating a late phase of precipitation (plate 4.9-A). Crystals equally fill intragranular pores suggesting that the pores were filled with water (Halley and Harris, 1979; Longman, 1980; Pierson and Shinn, 1985). The association of blocky cement with extensively neomorphosed horizons, together with the absence of relict structures of the replaced grains suggests a dissolution-reprecipitation phase in an active meteoric phreatic zone (Longman, 1980).

Elemental composition of these cements further supports a meteoric origin. There is a decrease in Mg, Al, Fe, and Mn concentrations, whereas Ca ions increase compared to the underlying (geopetal) internal micrite (Figs. 4.6, 4.7, 4.8, 4.9). This is expected, because elemental exchange between the depositional constituents and pore water is efficient in highly porous grainstones (Pingitore Jr., 1982). Yet Sr^{2+} ions in these blocky cements show negligible difference when compared with original constituents (Fig. 4.7). This may be attributed to two combined factors. The first comes from the fact that cool-water carbonate constituents originally have low strontium concentrations (700-2700 ppm; Rao and Jayawardane, 1994). Based on elemental analysis carried out on modern cool-water shelf

Plate 4.9:

A- Blocky non-equicrystalline mosaic cement overlying an earlier internal micrite precipitate (m) in an intrabryozoan pore. The cements are non-luminescent, with thin dull to bright-luminescent intercrystalline boundaries (photo on right). Crystals coarsen in size towards pore centres. This cement is interpreted to have been precipitated within an active fresh water phreatic zone. The elemental composition of the internal micrite and the blocky cement crystals (along traverse shown in the left photo) is illustrated in figures 4.6 and 4.7. Sample 17, section 6.

B- Blocky equicrystalline non-luminescent cement nucleating syntaxially inside an echinoid cavity. This cement is interpreted to have been precipitated within a relatively stagnant fresh water phreatic zone. Intercrystalline boundaries are thin bright-luminescent orange, reflecting chemical variations in microenvironmental conditions, caused by periods of water stagnation, possibly due to climatic changes. The elemental composition of the echinoid fragment and the blocky cement (along traverse shown in the right photo) is illustrated in figures 4.8 and 4.9. Sample 10, section 4.

Thin section photomicrographs under polarised light (left) and CL (right).

C- Internal micrite cement partially filling intragranular pore space forming geopetal structures. The cement has a fine grained peloidal texture that grades into coarser (< 0.1 mm) clear calcite crystals towards void centres. Thin section photomicrograph under plane light. Sample 8, section 8.

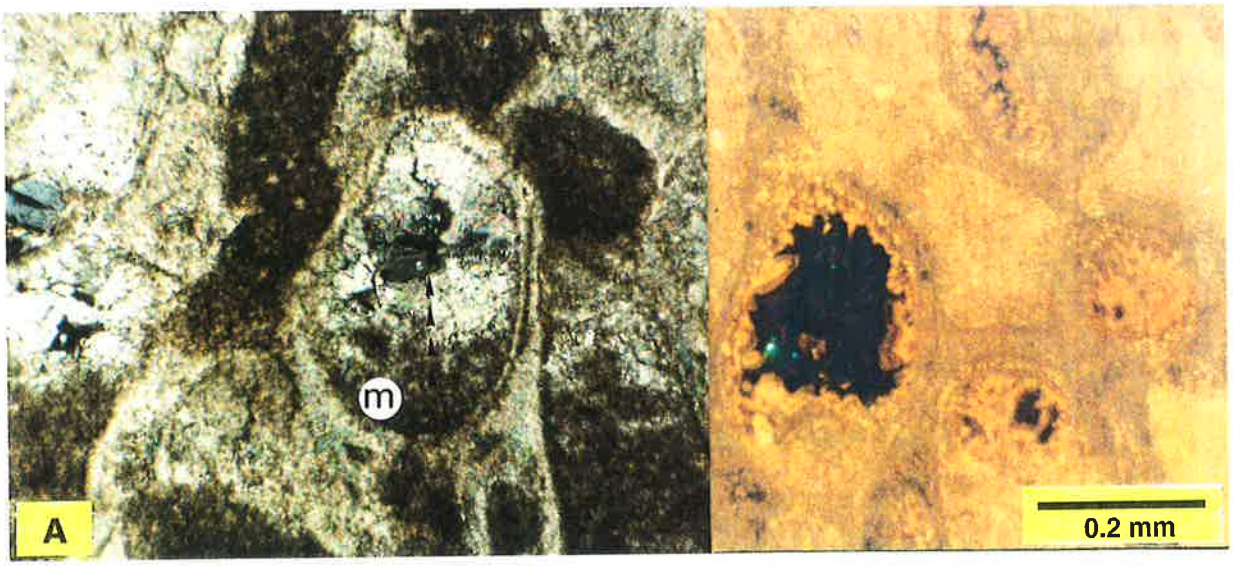
m
A
0.2 mm

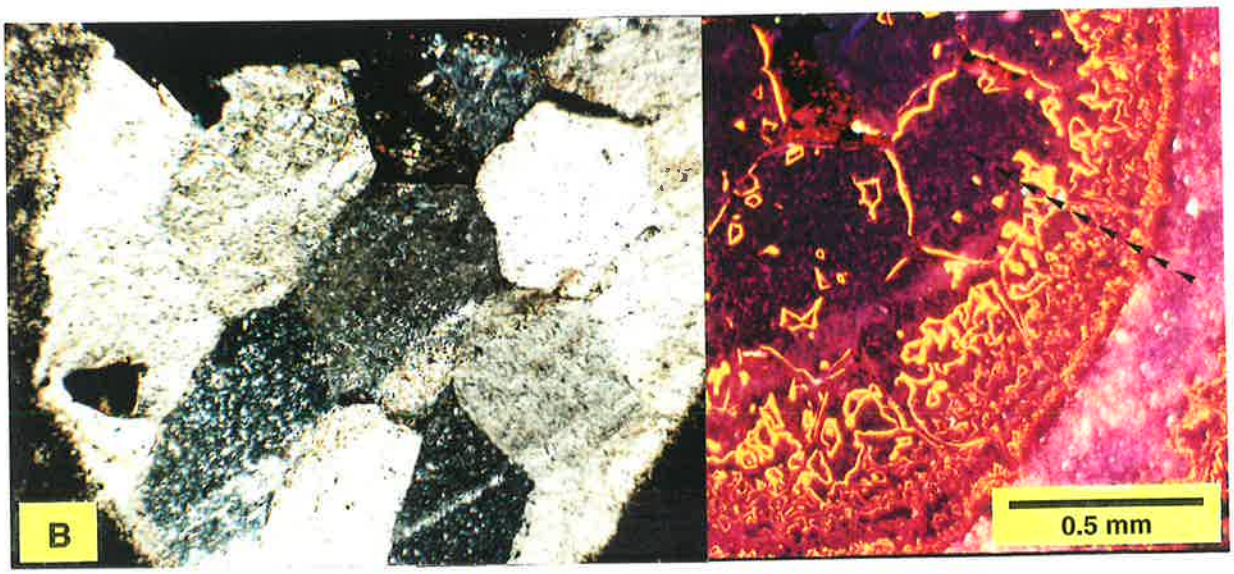
B
0.5 mm


C
0.2mm

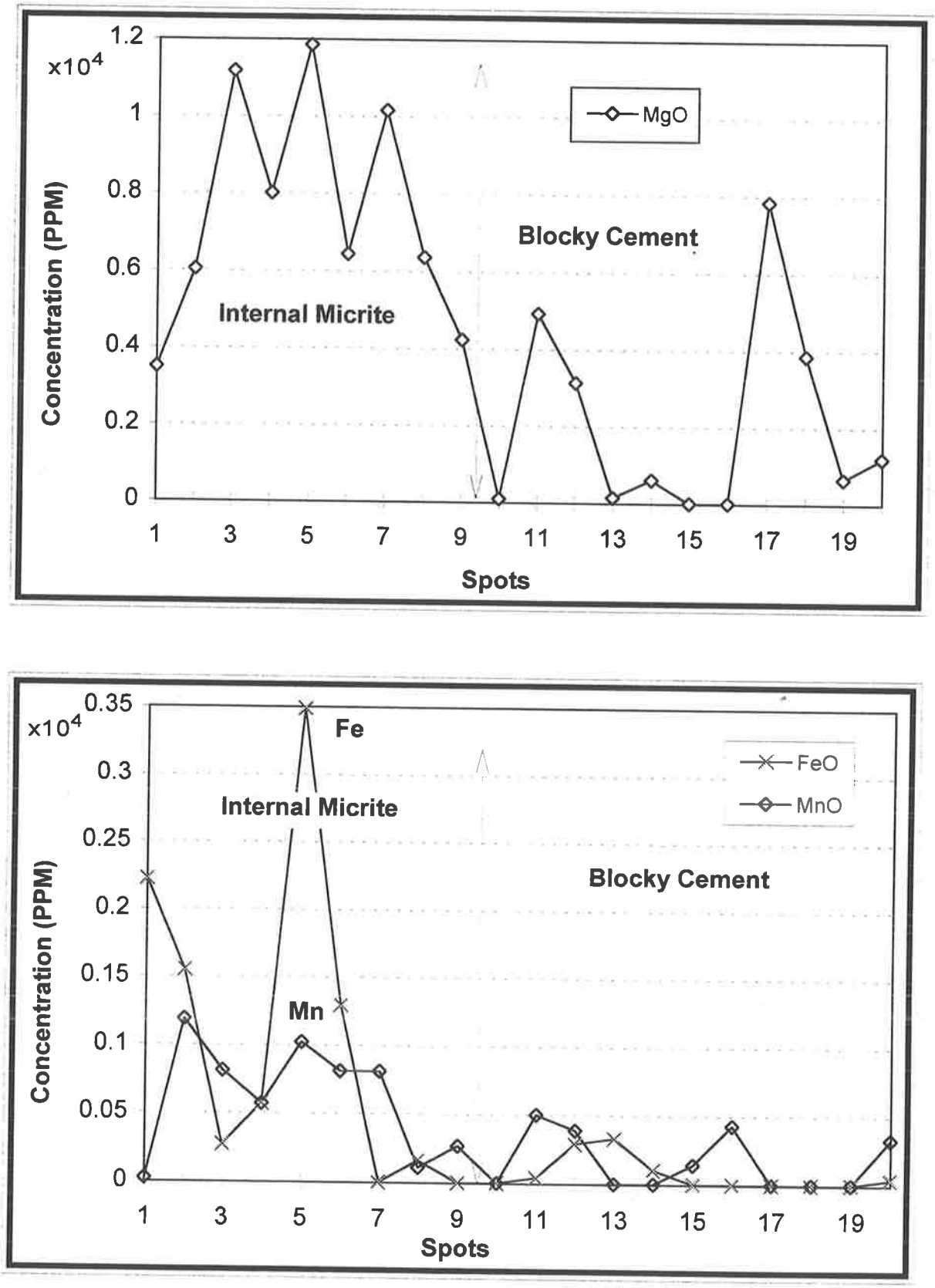

Figure 4.6: Microprobe analysis across the internal micrite and blocky calcite cement shown in plate 4.9-A. Spots 13 and 14 are for the centre of the blocky crystal.

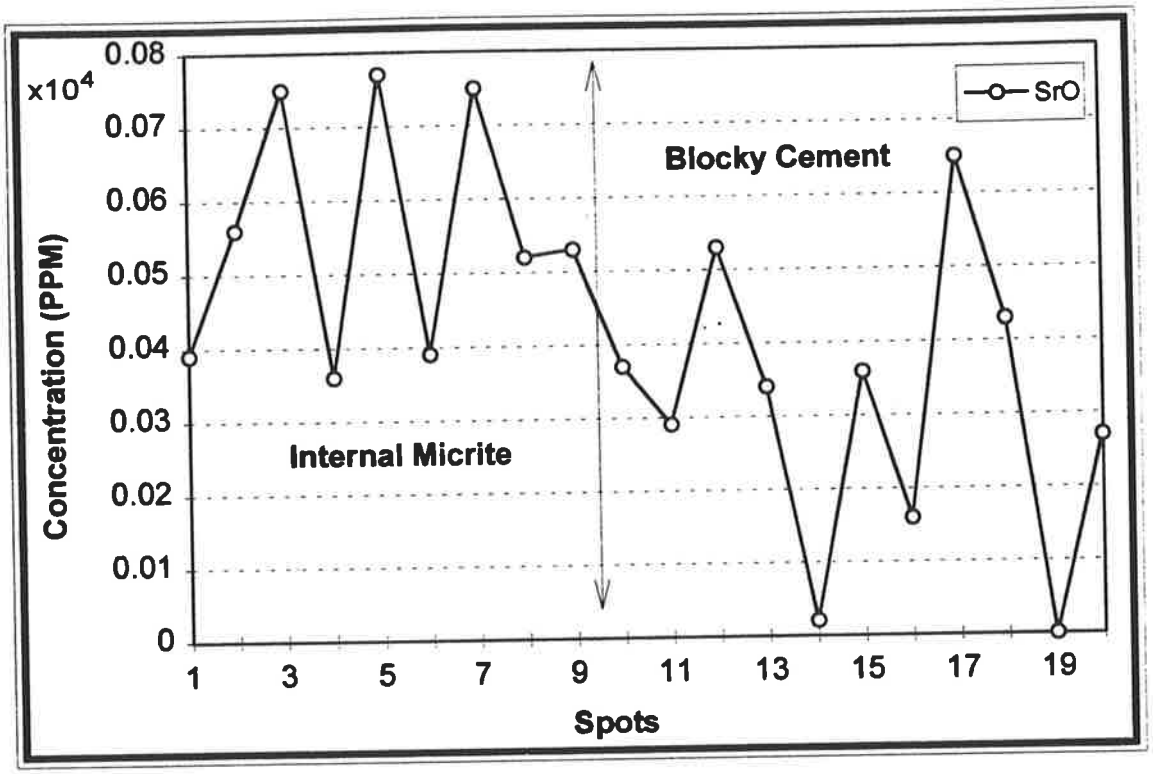

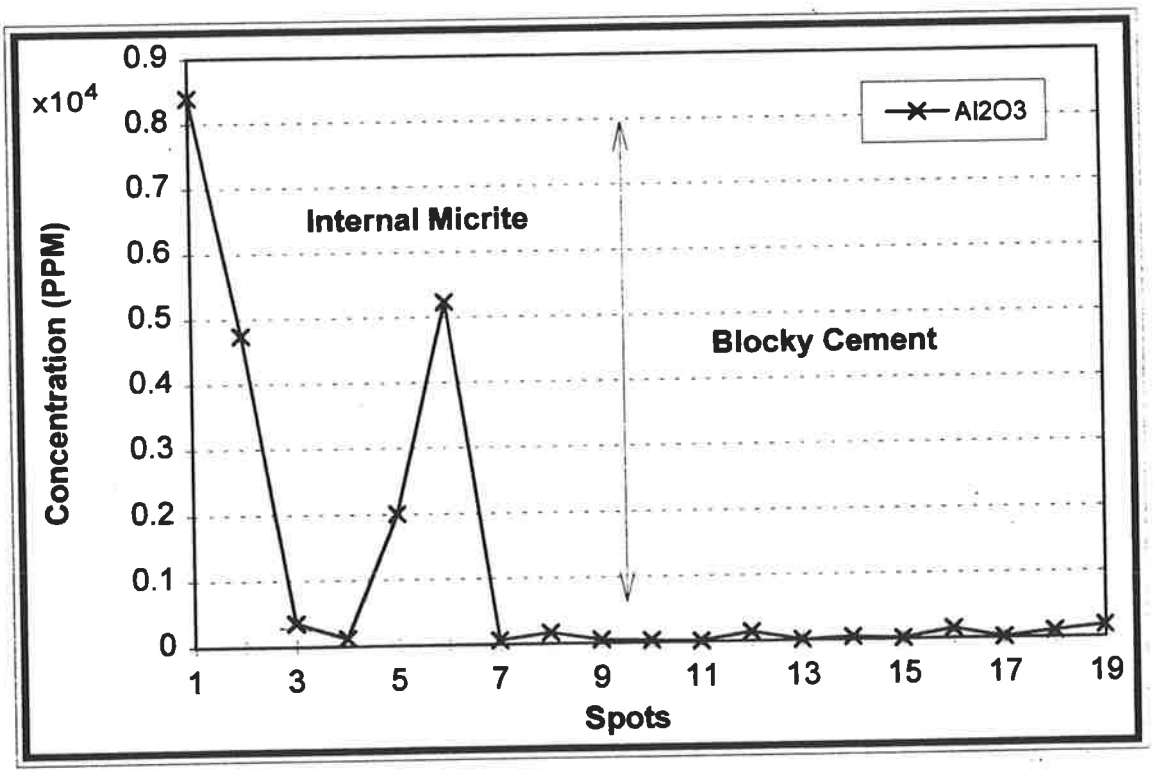

Figure 4.7: Microprobe analysis across the internal micrite and blocky calcite cement show in plate 4.9-A. Spots 13 and 14 are for the centre of the blocky crystal.

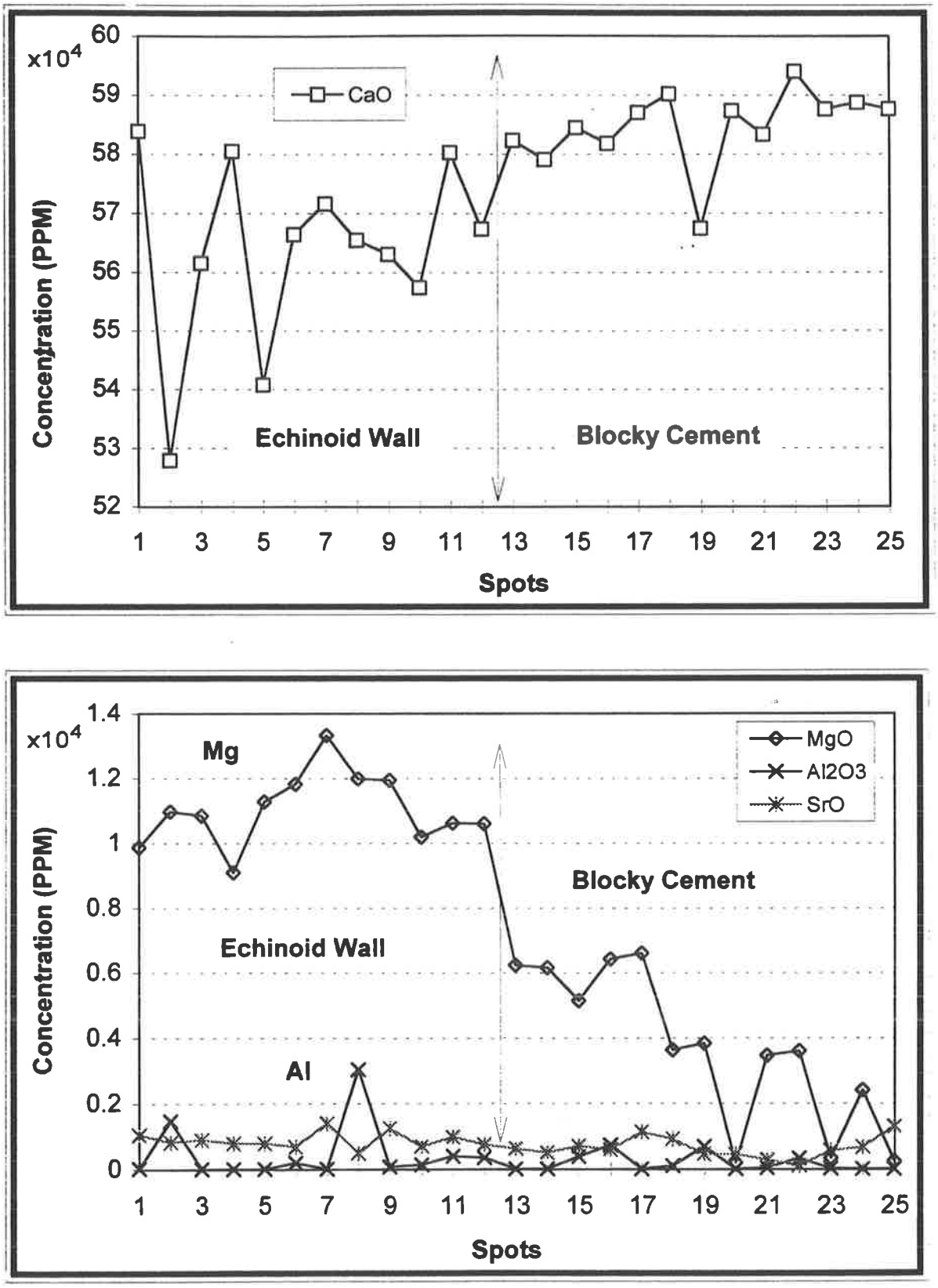

Figure 4.8: Microprobe analysis across the echinoid wall and intragranular blocky calcite cement shown in plate 4.9-B.

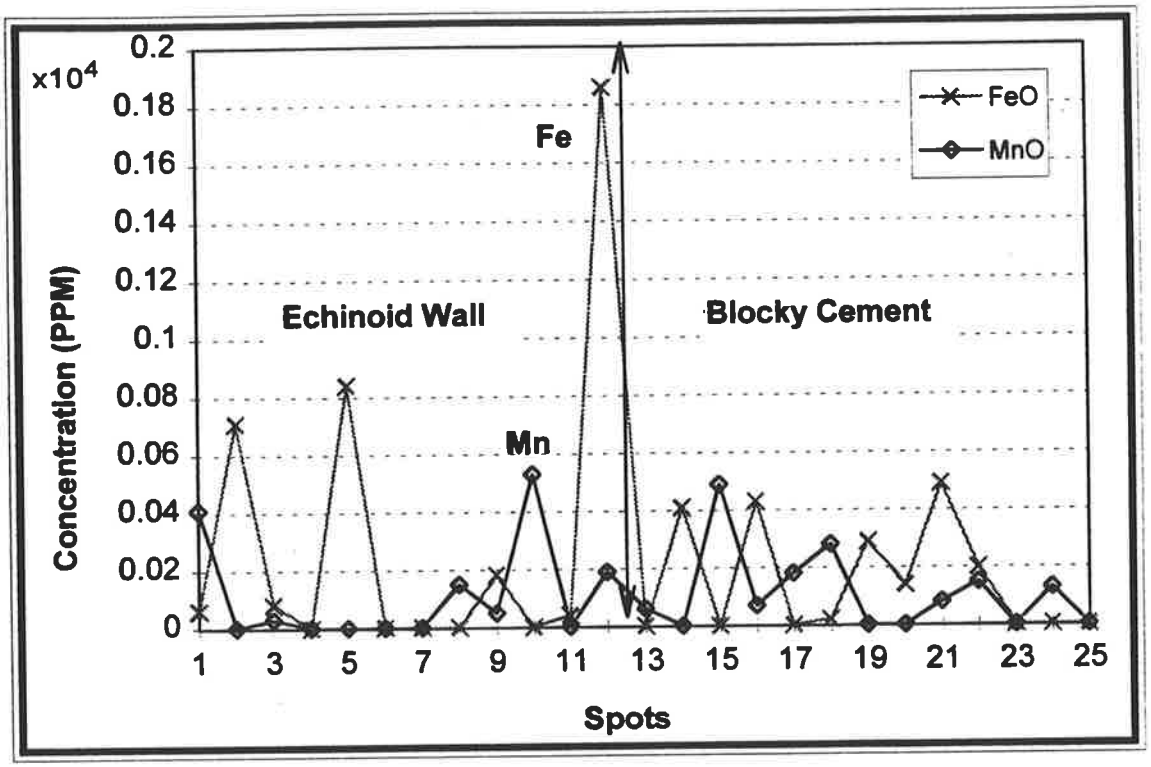

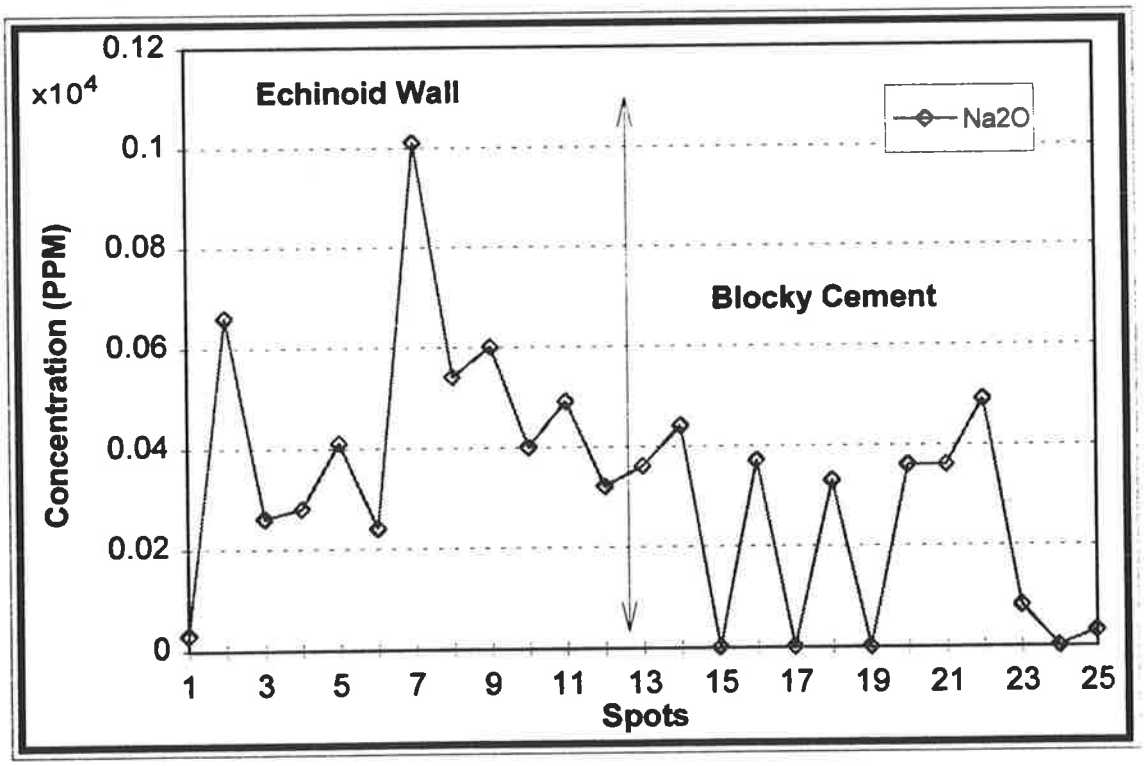

Figure 4.9: Microprobe analysis across the echinoid wall and intragranular blocky calcite cement shown in plate 4.9-B.

carbonates from Eastern Tasmania, Rao and Jayawardane (1994) conclude that Sr concentrations range between 700 - 2700 ppm, and that these concentrations decrease with increasing Ca concentrations. The second factor relates to the nature of chemical reactions occurring at the rock/water interface. Pingitore (1982) notes that because of strontium's effective diffusion, it would easily be removed from the reaction sites, and if early cements are produced, then they are expected to have relatively low strontium concentrations. But as diffusion progresses, Sr concentrations build up in pore waters and Sr enriched cements are then produced. These conclusions seem to be in accord with a meteoric interpretation.

The relatively significant iron content (up to 400 ppm) appears to be common in many meteoric cements. Ferroan calcite cements are regarded as characteristic meteoric phreatic precipitates (Richter and Füchtbauer, 1978) and may encompass up to 3.2 mole % $FeCO_3$ (Mohamad and Tucker, 1992). Fe content in modern marine pore fluids in the Atlantic and off north west Africa is very low (Fe:Ca ratio = 0.001 mole %), rendering marine waters unfavourable producers of ferroan calcite cement (Manheim and Bischoff, 1969; Hartmann et al., 1976).

In conclusion blocky non-equicrystalline mosaic cement is interpreted to have been precipitated within an active fresh water phreatic zone. Their characteristic crystal size enlargement towards pore centres reflects high original crystal nucleation. Blocky equicrystalline mosaic cement, on the other hand, precipitated within a relatively stagnant fresh water phreatic zone. A low nucleation rate is expected at this late stage, as pore waters become continuously depleted in $CaCO_3$. These interpretations are in close accord with those discussed by Longman (1980). The thin dull to bright-luminescent intercrystalline boundaries in both mosaics reflect chemical variations in microenvironmental conditions. Most likely, these contrasting zones indicate periods of water stagnation possibly due to climatic changes (Ogden, 1984). The iron is most likely derived from the clay and iron-rich internal micrite that commonly fills nearby void space, or from the overlying Plio-Pleistocene ferruginous Ardrossan Clay and Sandrock.

2.1.4 *Internal micrite precipitate:*

Cool-water carbonate environments are regions where inorganic carbonate precipitation does not apparently occur (Milliman, 1974; Alexandersson, 1978, 1979; Blom and Alsop, 1988; Nelson, 1988). They are almost entirely biogenic and composed of more calcite components, that contain variable amounts of magnesium, than of aragonite components. Therefore awareness of possible diagenetic overprint is required before carrying out facies interpretations on an apparently mud-supported facies in cool-water carbonate settings.

Microcrystalline calcite precipitate (micrite) is genetically subdivided into internal micrite precipitate and seafloor micrite (Reid et al., 1990; Fig. 4.10). Internal micrite precipitate is post depositional (diagenetic) and is a product of bioerosion, accumulation of nannofossils, or direct precipitation. This micrite precipitate accumulates as an internal sediment and/or a marine cement in high energy environments, as opposed to the depositional seafloor micrite which accumulates in low energy environments through disintegration of calcareous green algae. Micrite is common in the Port Vincent Limestone, particularly in the bryozoan-*Amphistegina* hardground facies. In these hardgrounds the fine micrite matrix commonly overlies early scalenohedral and syntaxial cements (plates 4.7-C, 4.8-A). Skeletal grains are marginally bored, and microboring tubes do not cut across intergranular and intragranular cements, indicating that biological activity was prior to cementation (i.e. initial sedimentation was matrix-free) (plate 3.6-A). The micrite also fills partial moulds of many flat-robust branching bryozoan fragments and bivalves after they had been removed by marine dissolution (see section 1.1 in this chapter and plate 4.1). Furthermore, there is no evidence of near-surface alteration due to subaerial exposure in these well-lithified layers. From the above evidence, the fine micrite matrix present in the bryozoan-*Amphistegina* hardgrounds is interpreted to be a post-depositional internal micrite precipitate. This internal micrite precipitate can be further subdivided into two forms:

1- Internal sediment: this form fills intragranular and intergranular pore space within hardgrounds. It contains floating fine skeletal debris, which indicate a marine origin for

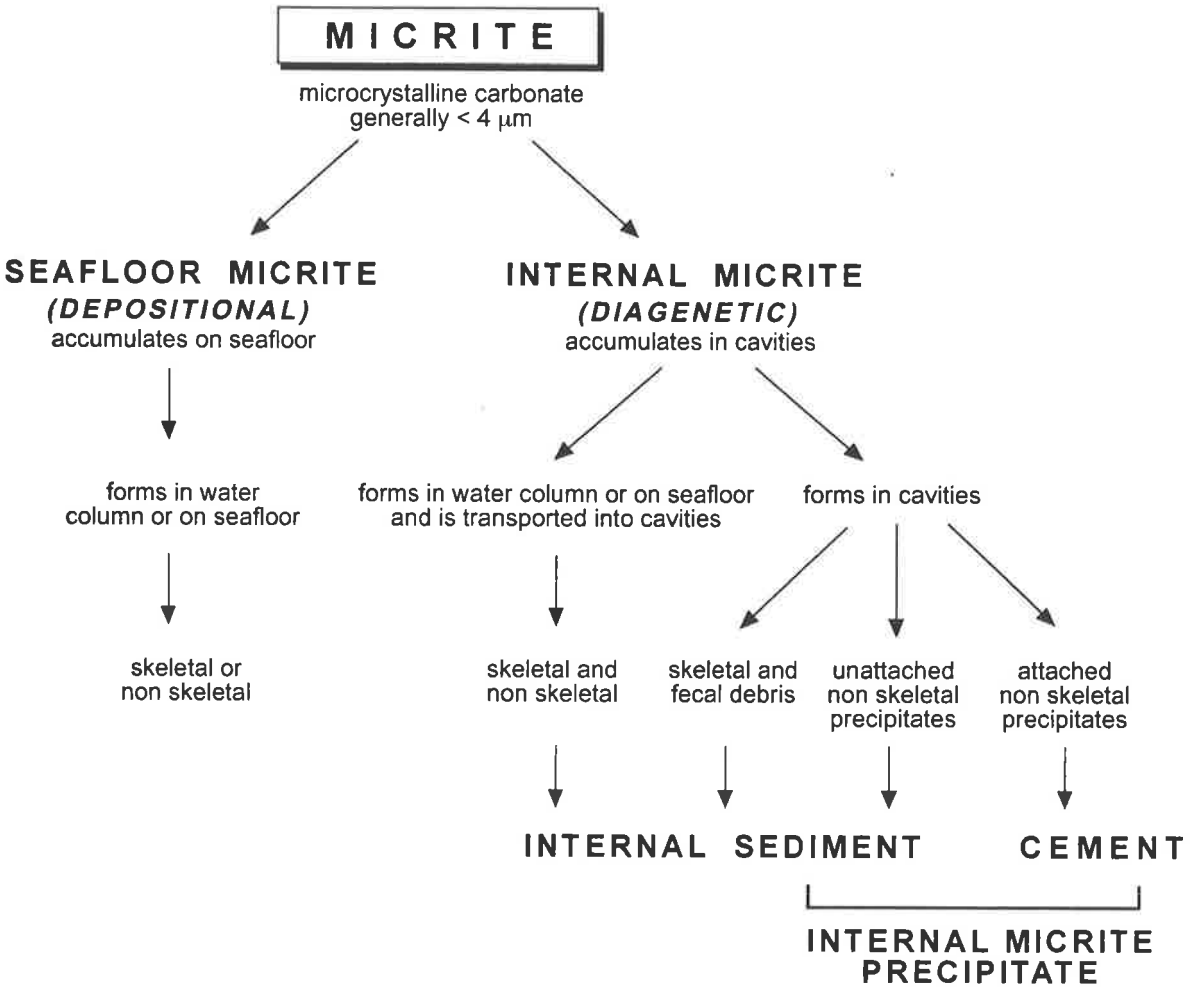

Figure 4.10: Genetic classification of microcrystalline carbonate matrix based on sites of accumulation. From Reid et al., 1990.

In most classical tropical carbonate classification schemes (e.g., Folk, 1959, and Dunham, 1962), depositional textures like grainstones and wackestones reflect energy levels within the environment of deposition. This in turn is evaluated by the amount of microcrystalline carbonate present in the rocks, and traditionally mud-supported textures indicate low energy environments. In contrast, microcrystalline carbonate matrix may also accumulate internally, in high energy environments between already deposited grains or within intragranular voids below the seafloor (i.e. diagenetic). In such cases it occurs as an internal sediment or a marine cement termed by Reid et al. (1990) as "internal micrite".

Element / Form	Al (ppm)	Sr (ppm)	Mn (ppm)	Fe (ppm)
Internal sediment	0 - 8390	20 - 770	20 - 1800	0 - 4730
Internal micrite cement	-	0 - 210	0 - 580	0 - 760

Table - 4.2: Elemental concentrations of internal sediment and internal micrite in the Port Vincent Limestone.

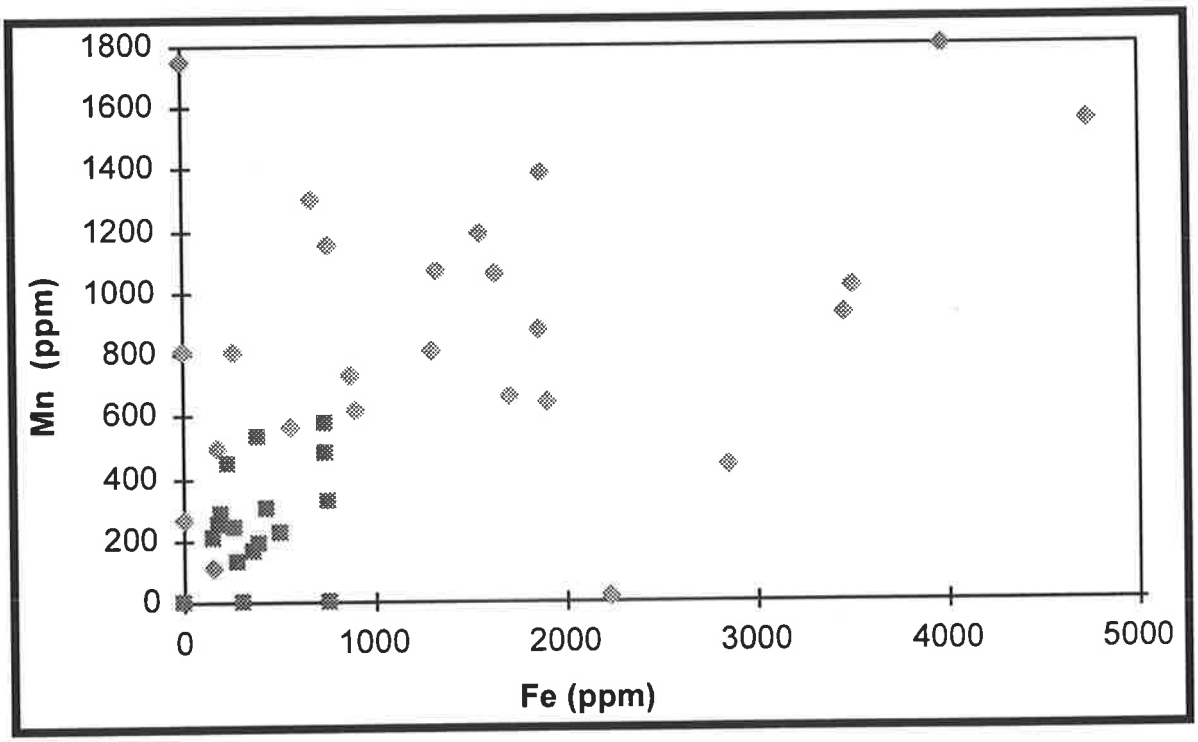

Figure 4.11: Concentration of Mn and Fe ions in the internal sediment and internal micrite cement, Port Vincent Limestone.

accumulation (plate 3.4-B). It is rich in clay content as reflected by its relatively high Al concentration.

2- Internal micrite cement: this form is rare, and is found partially filling intragranular pore space forming geopetal structures (plate 4.9-C). The cement has a fine grained peloidal texture that grades into coarser (< 0.1 mm) clear calcite crystals towards void centres.

Under plain light, internal micrite sediment and cement appear dark grey with patches of variable brown iron oxide stain, and speckled dull to bright-luminescent yellow under CL (plate 4.7-C). Both forms are partially to completely recrystallised and have a magnesium content of < 3 mole%. Elemental concentrations of these two forms are rather contrasting, with the internal sediment being more heterogeneous (Table - 4.2; Fig. 4.11).

This suggests that internal sediment was derived, by winnowing and abrasion on the seafloor, from a diverse mixture of sources. In contrast, internal micrite cement reflects precipitation from less heterogeneous sources, most likely by abrasion of skeletal grains with similar mineralogies.

The hardness and induration of the hardgrounds in the Port Vincent Limestone is a result of cementation by scalenohedral cement and the associated internal micrite, whereas cementation by other cement fabrics is less significant in these hardgrounds. Rock samples from units other than hardgrounds are friable and highly porous. They lack internal micrite precipitate, and are commonly only slightly cemented by scalenohedral, syntaxial, or blocky cement fabrics.

2.1.5 *Neomorphic blocky cement (pseudospar):*

Mosaics with irregular crystal boundaries, undulose extinction, diffuse contacts with the surrounding grains and internal micrite are rare (plate 4.10-A). They appear as irregular patches associated with extensively neomorphosed horizons near hardground surfaces. They

are produced by recrystallisation of internal micrite and other components by freshwater following subaerial exposure (Bathurst, 1975).

2.2 Sources Of $CaCO_3$ For Cementation:

Sediments mainly made of calcite and LMC have low diagenetic potential compared to those made of aragonite and HMC (Schlanger and Douglas, 1974). As a consequence cool-water carbonate sediments have low diagenetic potential and will yield little $CaCO_3$ (through mineral-controlled alteration) for cementation. Their high porosities permit rapid flow of fresh water through the sediments before becoming saturated with $CaCO_3$. Two possible origins are listed here to account for the supplied calcium carbonate for the precipitation of cement in the Port Vincent Limestone:

1- Little cement is produced by mild intergranular pressure solution as evident from slightly to non-sutured grain contacts. This paucity is expected since the rocks have only undergone shallow burial. In addition pressure solution decreases with increasing pore water pressure and increasing calcitic mineralogy of the constituents (Choquette and James, 1990) (section 3, this chapter).

2- Marine and meteoric dissolution are additional sources for cement, as evident from numerous moulds of aragonitic bivalves and flat robust branching bryozoans in the rocks.

2.3 Cement Paragenesis:

Cement is limited and precipitated in three diagenetic environments: the seafloor, shallow-burial, and meteoric. Seafloor cementation was synsedimentary, affecting each depositional cycle separately (phase-1) whereas later shallow-burial and meteoric cementation affected the entire succession (phase-2).

Phase-1: Synsedimentary cement precipitated as thin rinds of isopachous spar around echinoid grains (syntaxial), and around calcareous algae and other constituents

(scalenohedral) (plates 4.7-B, 4.8-A). These cements are non-luminescent, iron-poor, and are now LMC. They reflect precipitation from oxidising marine water on or just below the seafloor. At the top of each depositional-cycle, microbioclastic internal micrite partially infills intergranular and intragranular pores, and also overlies the aforementioned cement. This diagenetic sequence is seen in each successive depositional cycle.

Phase-2: After shallow burial, a zoned bright-luminescent syntaxial cement precipitated in available pore space around the synsedimentary cement. This cement heals fractures that cut across pre-cemented echinoid fragments (plate 4.8-C). It indicates precipitation from reducing pore water under shallow burial.

Later, the rocks were exposed to the meteoric realm, where they underwent minor dissolution and the formation of two cement fabrics, both of which occur in rare amounts. The first is a non-luminescent syntaxial overgrowth, consisting of several thin dull to bright-luminescent zones (plates 4.7-A, B). The thin dull to bright-luminescent zones reflect precipitation during short periods of diminished freshwater supply, possibly induced by climatic fluctuations. The second is a blocky (nonequicrystalline and equicrystalline) non to dull-luminescent mosaic, with thin bright to dull-luminescent intercrystalline boundaries (plate 4.9-A, B).

3. COMPACTION

The Port Vincent Limestone has never been buried under more than 100 metres of sediments, thus only minor pressure solution occurred. In hardgrounds, compaction is reduced by early cementation in the form of synsedimentary marine cement and internal micrite precipitate.

Compaction postdates early synsedimentary non-luminescent cements, but newly fractured grains are filled with later luminescent shallow burial cements (plate 4.8-C). Compaction is manifest in the form of grain breakage, plastic deformation and contact relations between depositional grains and surrounding cements (plate 4.10-B, C). However, due to shallow burial neither extensive grain breakage, nor intensive stylolites and microstylolites are

present.

The response of porous rocks to chemical and physical compaction strongly relates to a number of varying extrinsic and intrinsic factors (Flügel, 1982; Choquette and James, 1990). Among the most influential of these are the amount of overburden, pore water pressure and chemistry, temperature of the environment, mineralogy of constituents, clay content, grain size, rock texture and early diagenesis. As a consequence overburden stress is sufficient to produce mild intergranular chemical compaction (< 100 m - James and Bone, 1989) but not stylolites (plate 4.10-C). Stylolitisation is rare in similar cool-water carbonates even up to depths of 600 m (Nelson et al., 1988c). Temperature, pore water pressure and chemistry are less significant, since the limestones are not extensively buried, highly porous, and form an unconfined aquifer. Intrinsic factors appear to further inhibit compaction. In particular the calcitic mineralogy of the constituents, due to its low diagenetic potential, places constraints on compaction. No insoluble residues concentrated along solution fronts, indicating that the limestones are pure, they lack clay and organic matter, and hence are less susceptible to compactional stresses (Dewers and Ortoleva, 1994). Coarse grain sizes and grain-supported carbonates are less susceptible to compaction than finer grained mud-supported textures (Tucker and Wright, 1990).

In conclusion, the Port Vincent Limestone was effected by only mild compaction under shallow burial (< 100 m).

Plate 4.10:

A- Thin section photomicrograph (polarised light) showing neomorphic blocky cement (pseudospar) with irregular crystal boundaries, undulose extinction, and diffuse contacts with the surrounding grains and internal micrite. Sample 17, section 6.

B- Thin section photomicrograph (plain light) showing plastic deformation and grain penetration due to compaction (arrows). Sample 17, section 6.

C- Cementation by mild intergranular chemical compaction between benthic foraminifer *Crespinina* (f) and an articulated branching bryozoan fragment (ar). Thin section photomicrograph under polarised light and gypsum plate. Sample 1, section 6.

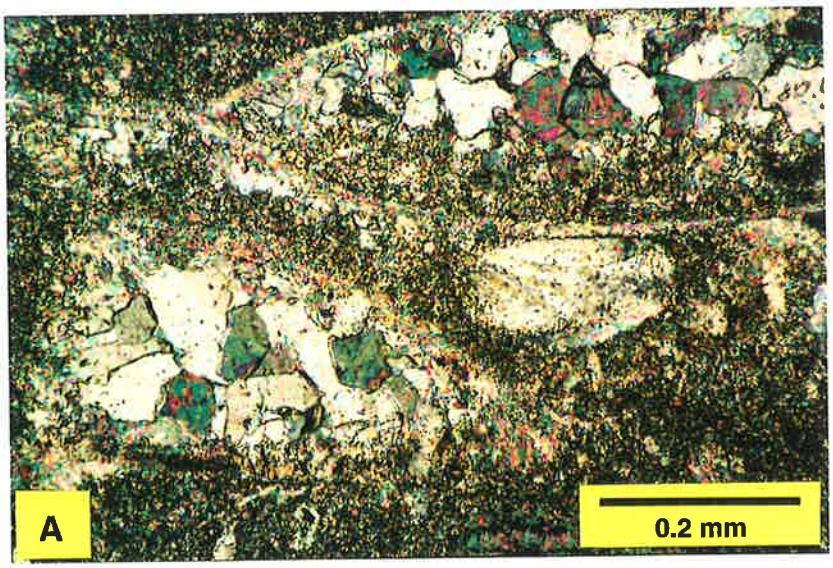
A
0.2 mm

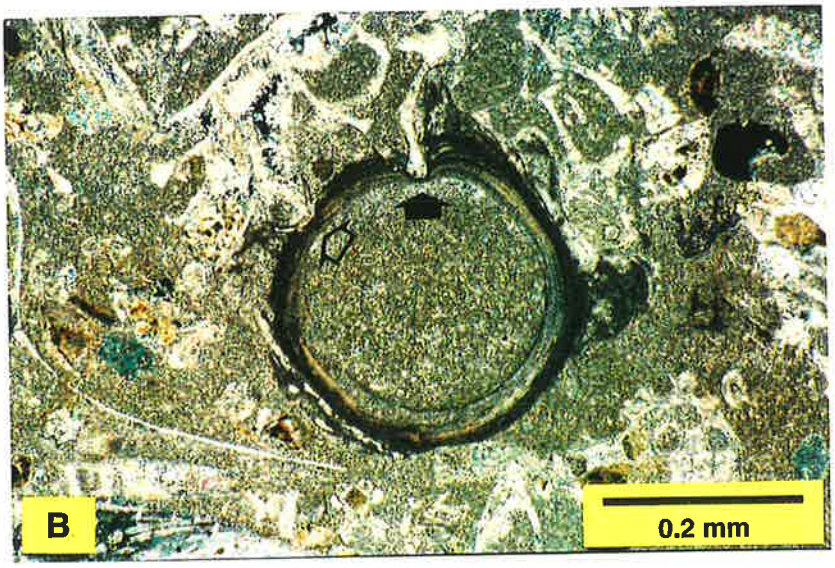
B
0.2 mm

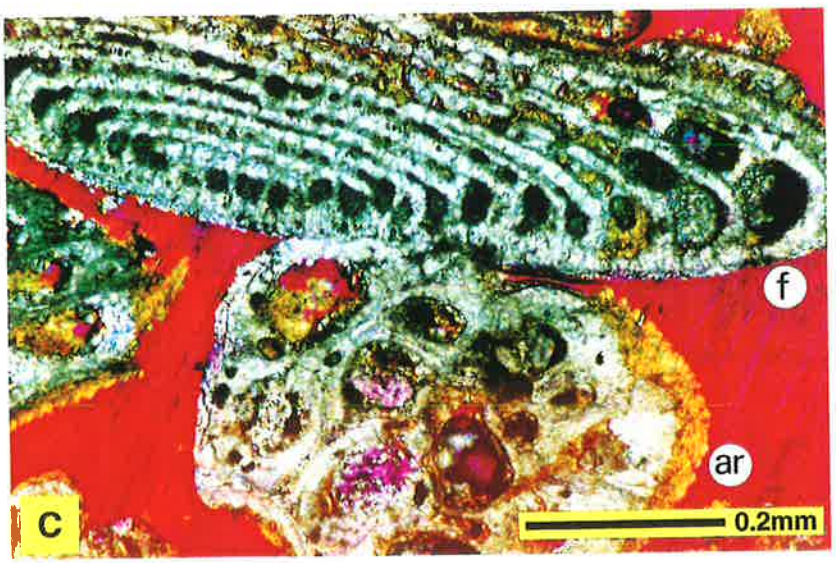
f
ar
C
0.2mm

Chapter 5

DOLOMITE

DOLOMITE

1. DESCRIPTION

Dolomitisation is local, replacing only a small volume of the Port Vincent Limestone at the base of the bryozoan bivalve floatstone facies. The lensoid shaped dolomite body is exposed approximately 1200 m south of the township of Port Vincent (Fig. 1.6, Appendix B-3). The dolomitised beds are approximately 3 m thick, 20 m wide, and extend for 250 m in a north-south direction with a low westerly dip. Overlying these beds is a 3 m thick bed of the Port Vincent Limestone and a calcrete cap < 1 m thick (plate 5.1-A, B). It is not known how far the dolomite body extends beyond these limits, since there are no nearby offshore or onshore bore holes, and other outcrops elsewhere in the study area appear devoid of dolomite. Dolomitisation cuts across beds, and the dolostone - limestone contact is gradational. The intensity of dolomitisation varies laterally (east-west) from a hard rusty yellowish brown dolostone at the modern strandline (< 50 cm thick), to a friable pale yellow dolomitic limestone and scattered rhombs within the limestone in the adjacent cliffs (2.5 m thick). The dolomite is non-pseudomorphic, has a planar-e texture (cf. Sibley and Gregg, 1987), and forms an idiotopic sucrosic mosaic with an estimated intercrystalline and intracrystalline porosity reaching 40%. Individual crystals range in size from 50-100 μm. They are euhedral in dolomitic limestones and euhedral to subhedral in dolostones. Almost all crystals are distinctly zoned and generally contain one, or sometimes two, incomplete rhomb-shaped thin iron-rich bands with up to 17.2 % Fe (Figs. 5.1, 5.3; plates 5.1-C, 5.2). The majority of crystals appear to have inclusion-rich cloudy cores and clear rims, while others are not so clearly distinct (Fig. 5.1). Crystals larger than 100 μm are rare, and have clear cores which display non-uniform extinction when examined under polarised light (plate 5.3-A). Crystal faces are slightly etched and, despite intracrystalline compositional variations, appear straight (plate 5.4-A, B, C, D). Dolomite cuts across fabrics replacing all the original matrix and most grains. Relict textures of the original limestone are absent in dolostones. The only unreplaced constituent is widespread oxidised glaucony grains that infilled various fossil

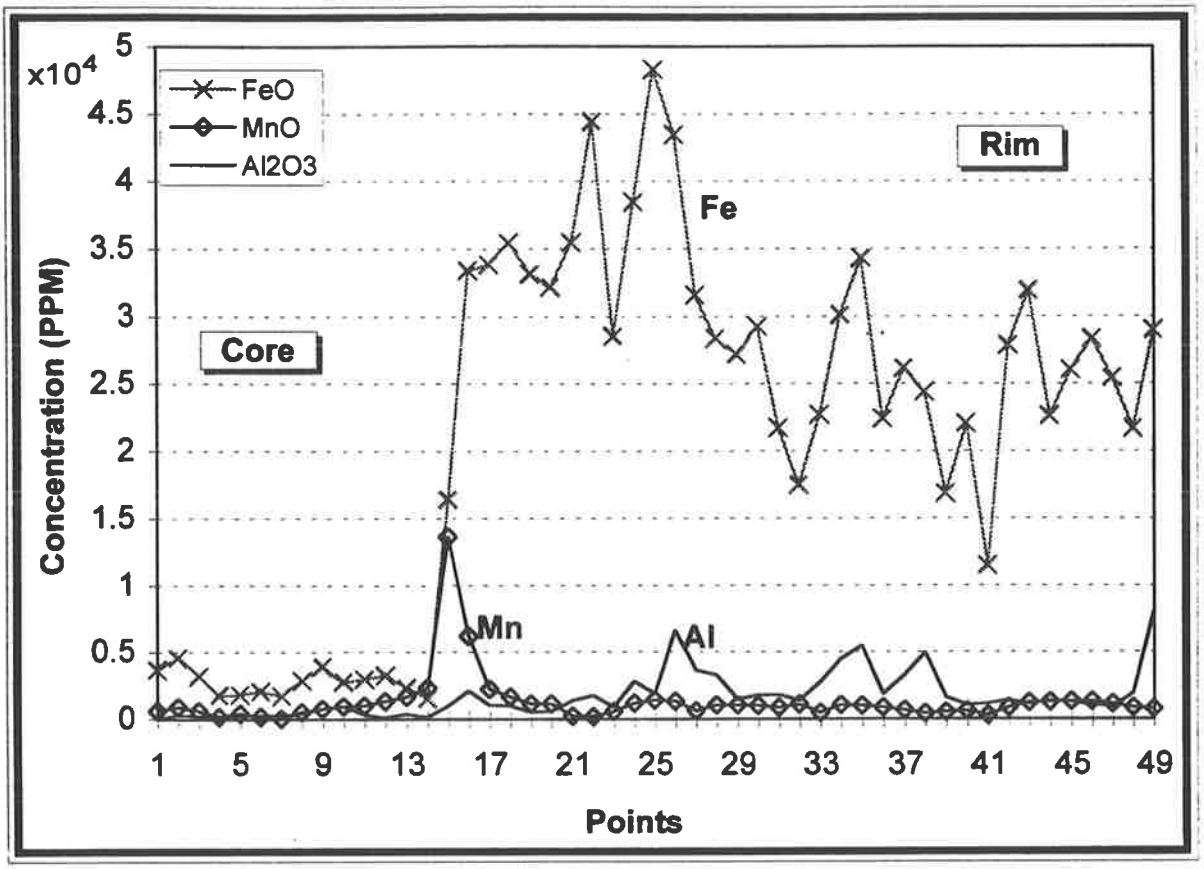
x10^4
5
4.5
4
3.5
3
2.5
2
1.5
1
0.5
0
FeO
MnO
Al2O3
Rim
Core
Fe
Mn
Al
Concentration (PPM)
1
5
9
13
17
21
25
29
33
37
41
45
49
Points

A

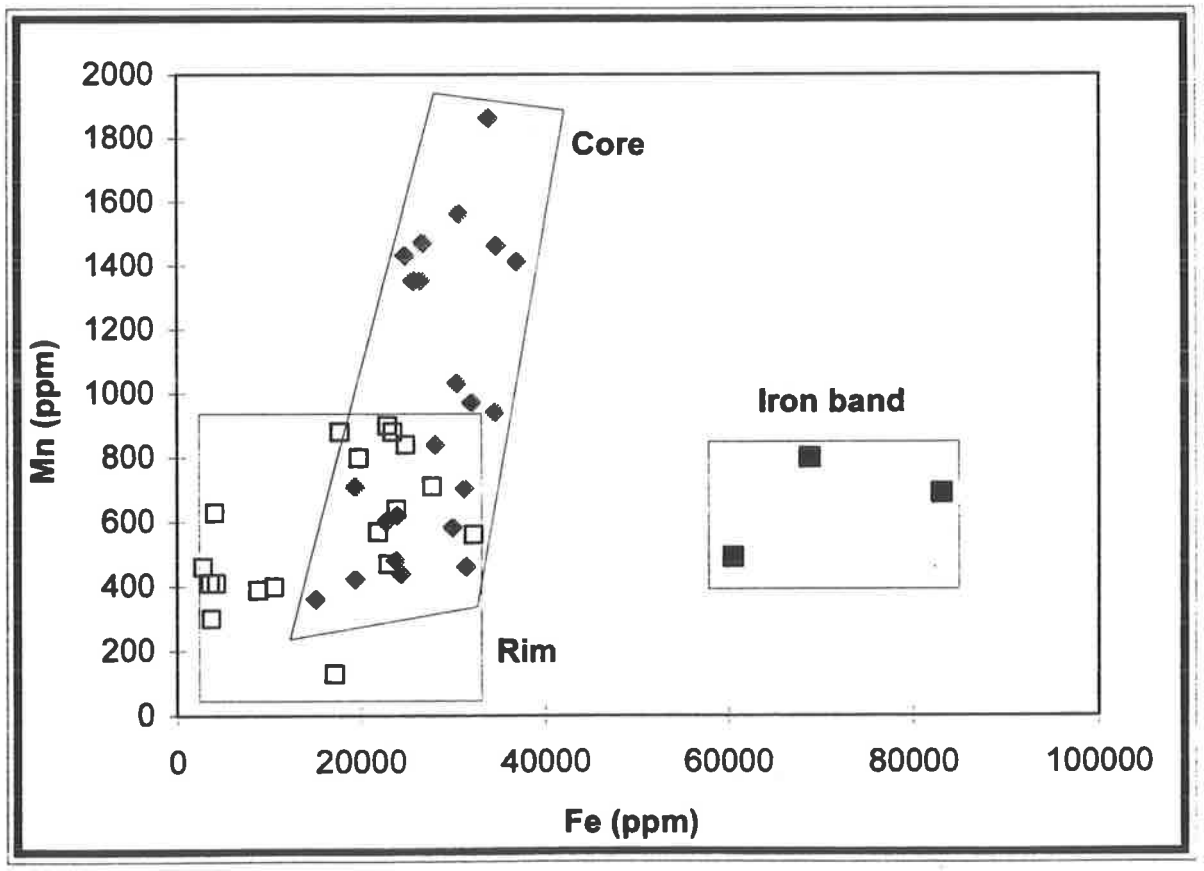
2000
1800
1600
1400
1200
1000
800
600
400
200
0
Core
Iron band
Rim
Mn (ppm)
0
20000
40000
60000
80000
100000
Fe (ppm)

B

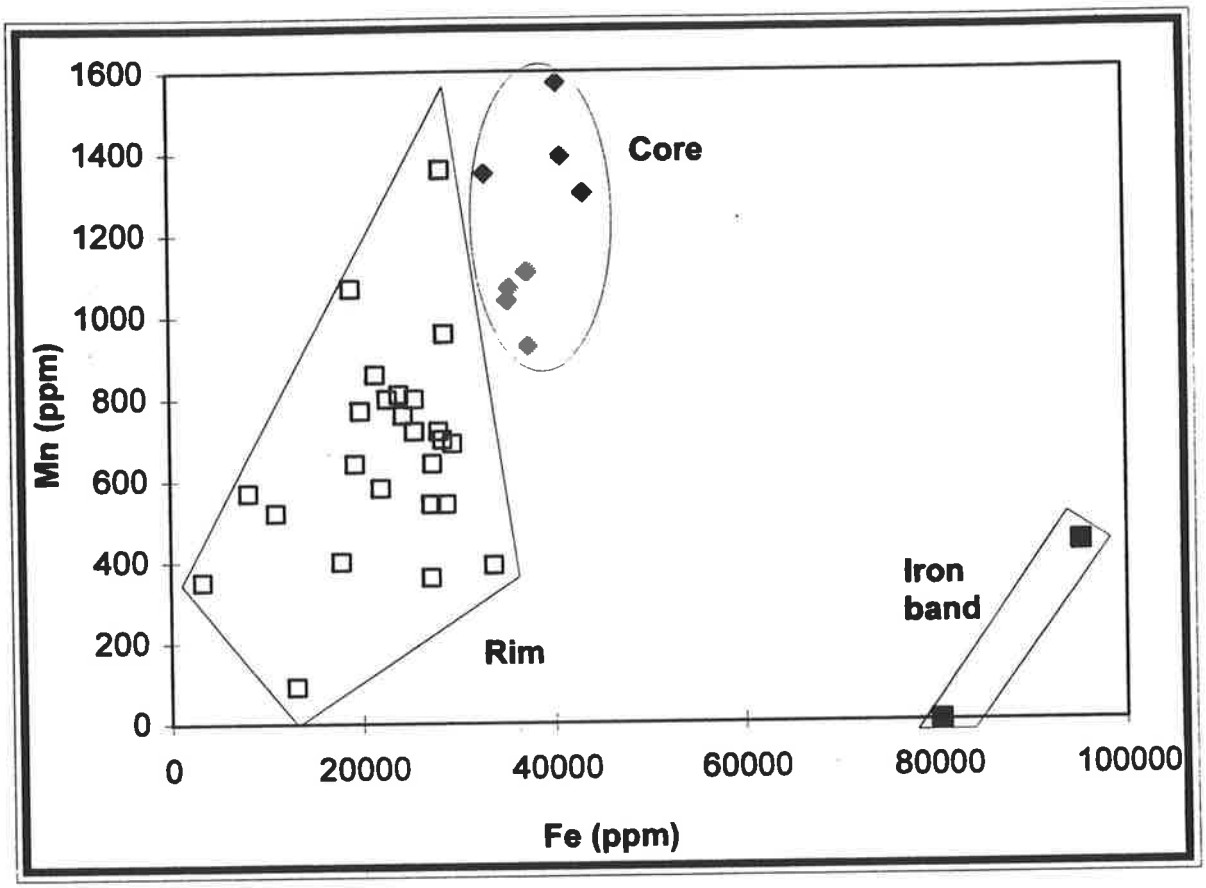

C

Figure 5.1: Variations in Fe and Mn distribution within various dolomite crystals from the Port Vincent Limestone. Compositional zoning is due to slight variations in Mn^{2+} and Fe^{2+} concentrations during crystal growth. Dolomite crystals commonly have an *Fe-poor core*, an *Fe-rich rim*, and a thin *intracrystalline Fe-rich band*. The Al concentrations are proportionally related to Fe concentrations across these dolomite crystal. However, some dolomite crystals may have a Fe-rich core (Figs. B and C) but these are generally rare (< 2%).

Plate 5.1:

A- Lensoid shaped dolomite body (D) in the Port Vincent Limestone (L), appearing in coastal cliffs approximately 1200 m south of Port Vincent township (section 4). The dolomitised beds are approximately 3 m thick, 20 m wide, and extend for 250 m long in a north-south direction with a low westerly dip (plate-B below). See Appendix B-3 for locality.

B- Exposed dolostones during low tide in the modern intertidal zone, south of Port Vincent township (section 4). These beds are an extension of the dolomite body appearing in plate 5.1-A above.

C- Idiotopic, planar-e texture, sucrosic dolomite mosaic with an estimated intercrystalline and intracrystalline porosity reaching 40%. Individual crystals range in size from 50-100 μm. Crystals are distinctly zoned and generally contain one or two, incomplete rhomb-shaped thin iron-rich bands with up to 17.2 % Fe. Thin section photomicrograph under polarised light. Sample 1, section 4.


L
D
A


B

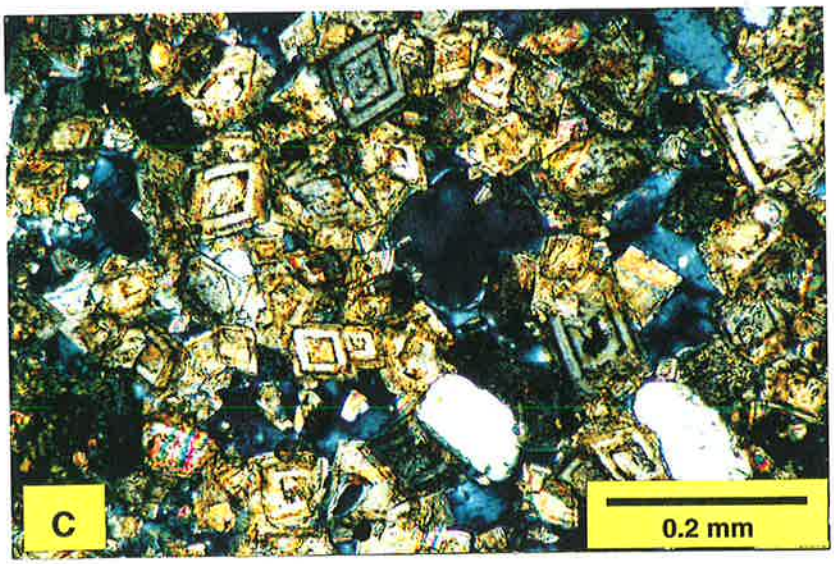
C
0.2 mm

chambers before dolomite was formed (plate 5.5-A). The partially dolomitised limestone reveals clear textural relationships and evidence regarding precursor constituents. The fine microbioclastic constituents were the first to be dolomitised, foraminifers and molluscs followed, and echinoids, delicate branching cyclostome and articulated branching cheilostome bryozoans were the last to be replaced (plates 5.4, 5.5, 5.6).

2. GEOCHEMISTRY

Dolomite forms in a variety of environments under various chemical conditions. Several models have been presented to interpret its genesis (e.g., Adams and Rhodes, 1960; Illing et al., 1965; Shinn et al., 1965; Hanshaw et al., 1971; Badiozamani, 1973; Land, 1985; Bone et al., 1992; James et al., 1993). Geochemical analyses provide evidence about the processes which formed the dolomite. When multiple geochemical techniques are integrated with the sedimentological and petrological context of the dolomite, a realistic and more comprehensive interpretation on the approximate timing of dolomitisation, chemistry of the dolomitising fluid, and the dolomitisation model is possible (e.g., Veizer et al., 1978; Veizer, 1983). Trace element concentration in a dolomite is influenced by the element's distribution coefficient, and its abundance in the dolomitising fluid and precursor carbonate. Such elements are incorporated into carbonates in many ways (McIntire, 1963; Veizer, 1983; Banner, 1995):

1- substitution for Ca^{2+} and to a lesser extent Mg^{+} in the carbonate lattice.

2- occupy lattice positions which are free due to defects in the structure.

3- occupy interstitial positions between lattice planes.

4- present in non-carbonate impurities such as fluid or mineral inclusions.

5- adsorption onto growing crystal surfaces.

The most common of all is by solid solution substitution for a major element of the lattice component, namely Ca^{2+} and Mg^{+}. Mn which has a closer ionic radius (0.83A°) to calcium (1.00A°) and Fe which is smaller (0.78A°) are more easily incorporated into Ca sites than Sr (1.13A°). For the same reason Mn and Fe substitute for Mg (0.72A°) but not Sr. In general, the replacement of a precursor carbonate by dolomite involves an increase in Mg, Fe, Mn ions, and a depletion in ^{18}O isotope content as well as Sr and Na ions (Land, 1980; Allan and Wiggins, 1993).

Dolomites of the Port Vincent Limestone are ferroan and non-stoichiometric (calcian). Microprobe (Fig. 5.2) and X-ray analysis for whole dolostone samples shows that they contain on average $Ca_{(53\ mole\%)}\ Mg_{(41.6)}\ Fe_{(5.4)}\ (CO_3)_2$ (Appendix D-1).

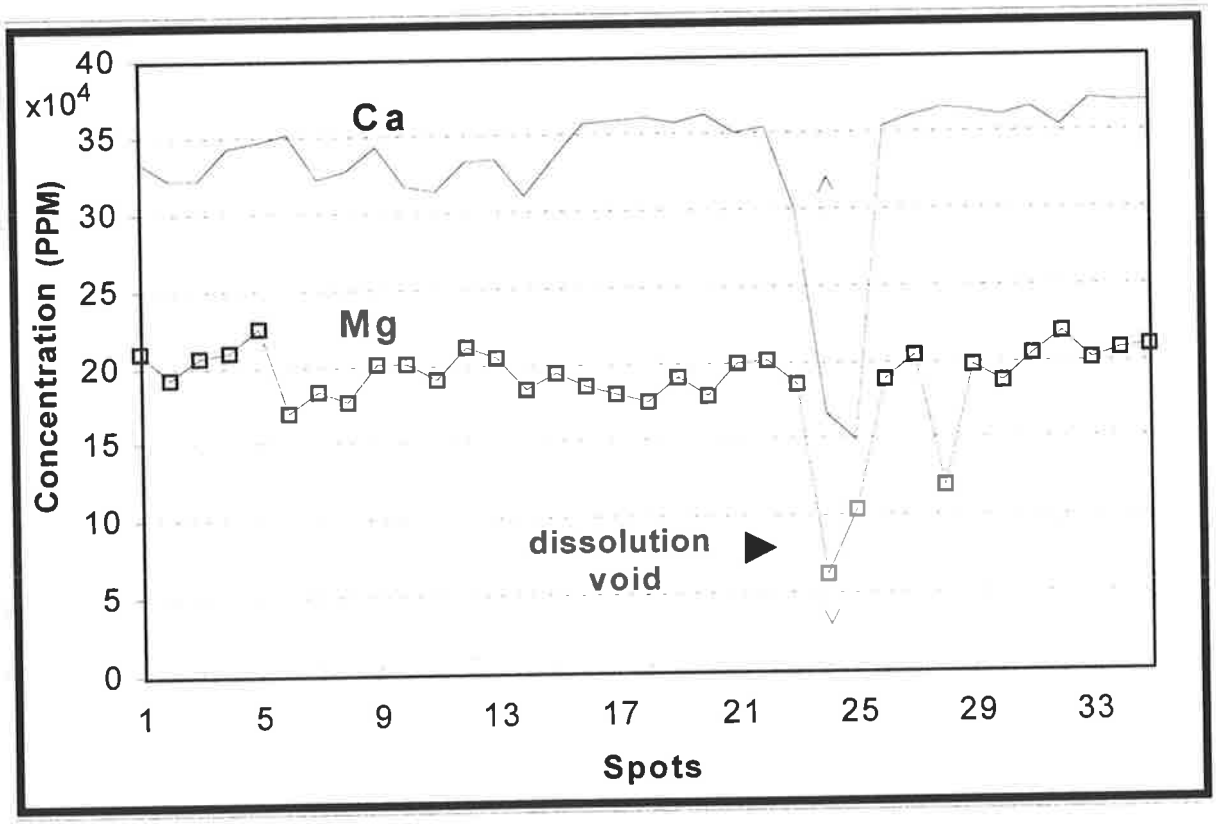

Figure 5.2: Microprobe analysis showing Mg and Ca concentrations across a dolomite crystal, from core to margin. Sample 1, section 4.

2.1 Iron and Manganese:

Intracrystalline variations in chemical composition are clearly revealed under CL microscopy. The dolomite crystals show several alternating non-luminescent and deep red dull-luminescent concentric zones. A thin (< 5 μm) red bright-luminescent concentric zone defines the crystal margins, and may also appear within the crystal near its core. Boundaries between adjacent CL concentric zones are distinctively straight and sharp, and sectoral zonations (Reeder and Prosky, 1986; Reeder and Paquette, 1989) are absent (plates 5.2-B; 5.3-B; 5.6-C). The zoning pattern is symmetrical and coincides with compositional variations across growth surfaces. A typical dolomite crystal comprises up to seven concentric zones (Figs. 5.3, 5.4, 5.5; plate 5.2-B, C, D). They are confirmed by electron microprobe analysis to represent slight variations in Fe and to a lesser degree Mn concentrations during crystal growth (Table - 5.1; Appendix D-2).

Dolomite	Fe (ppm)	Mn (ppm)	Sr (ppm)	Na (ppm)
Core				
Zone-1	3,250 - 3,980	210 - 8,016	130 - 620	360 - 740
Zone-2	14,310 - 23,810	760 - 980	160 - 640	300 - 1150
Zone-3	11,600 - 36,570	0 - 170	420 - 550	660 - 900
Zone-4	30,910 - 36, 940	780 - 1,460	290 - 570	150 - 500
Zone-5	11,840 - 39,630	410 - 2,270	0 - 550	700 - 2290
Zone-6	28,980 - 34,860	760 - 1,850	0 - 710	280 - 570
Zone-7	1,320 - 2,440	0 - 130	680 - 1100	310 - 910
outer rim				

Table - 5.1: Concentration of trace elements in the dolomite crystal illustrated in plate 5.2 and figures 5.3, 5.5. These values do not include Fe and Mn concentrations in dissolution voids appearing in plate 5.2-D and figures 5.3 and 5.5.

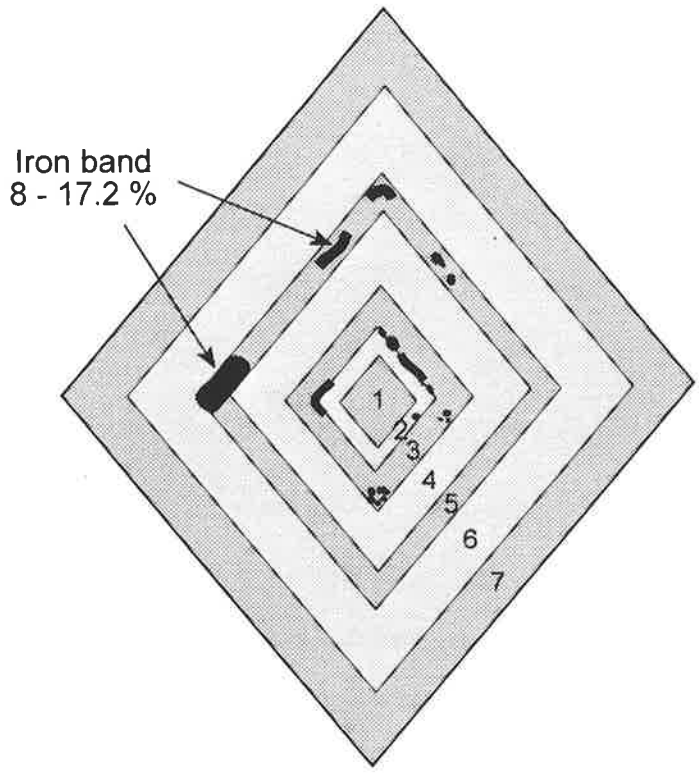

Figure 5.3: Schematic diagram for the dolomite crystal illustrated in plate 5.2, showing compositional variations in Fe and Mn ions. Values are listed in Table - 5.1.

Manganese concentrations in all studied crystals are commonly less than 2000 ppm, with high values (up to 55,300 ppm) corresponding to the thin bright-luminescent zones. The elemental distribution across cores and outer rims of numerous crystals is relatively homogeneous, with the exception of the bright-luminescent zones (plate 5.2; Figs. 5.4, 5.5).

Iron distribution slightly varies within a single dolomite crystal. Cores (dull to non-luminescent red) have distinctly lower iron concentrations (1500 - 4560 ppm) than the rest of the same crystal (up to 4.8 wt %). Fe-rich bands (12.223 - 17.199 wt %) form incomplete or complete intracrystalline rhomb shaped zones (Figs. 5.3, 5.5; plates 5.1-C, 5.2).

Plate 5.2:

Thin section photomicrographs (sample 7, section 4) showing dolomite crystals partially replacing the shell of a benthic foraminifer (marked f in photo B). A- under polarised light and gypsum plate, B- under CL, C- backscattered image, D- microprobe analysis.

Under CL (photo B) the dolomite crystals show several alternating non-luminescent and deep red dull-luminescent concentric zones. A thin (< 5 μm) red bright-luminescent concentric zone appears near the crystal margin, a second zone appears within the crystal near its core. Boundaries between adjacent CL concentric zones are distinctively straight and sharp, and sectoral zonations are absent. Echinoid fragments (e) and bryozoans (b) were the last components of the Port Vincent Limestone to be dolomitised. Oxidised glaucony grains filling chambers of the foraminifer appear black-coloured (see also Fig. 5.5).

Dolomite crystals commonly comprise up to seven concentric zones. The zoning pattern is symmetrical and coincides with compositional variations in Fe, and to a lesser degree Mn, concentrations during crystal growth as revealed by backscattered images (photo C) and microprobe analysis (D). The dark grey-coloured zones in the dolomite crystal (photo C) contain less iron concentration than the lighter grey zones (see also Figs. 5.3, 5.4; and Table-5.1). Figure D also shows one iron-rich band (172,000 ppm Fe) in zone-5, and an Mn rich band (55,300 ppm) in zone-2, both of which precipitated in dissolution voids, i.e. following dolomite dissolution (section 5, this chapter).

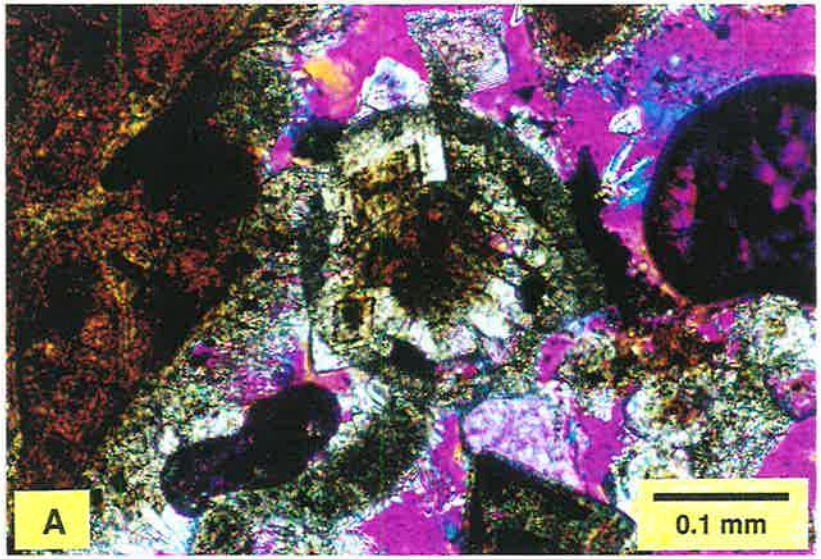
A
0.1 mm

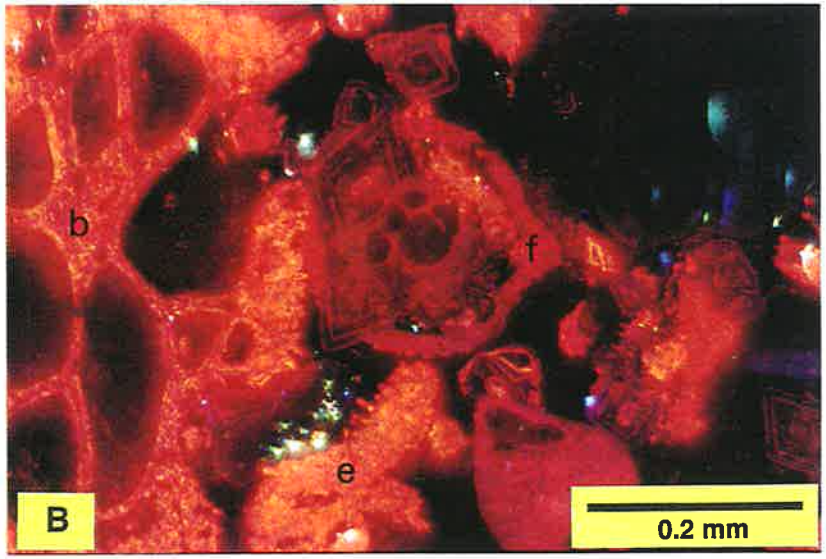
b
f
e
B
0.2 mm

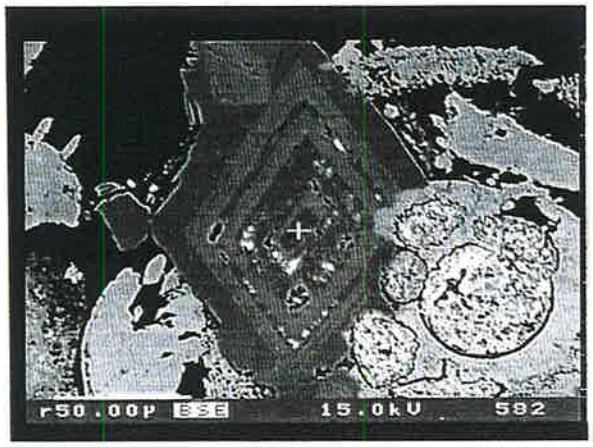
r50.00p BSE 15.0kV 582

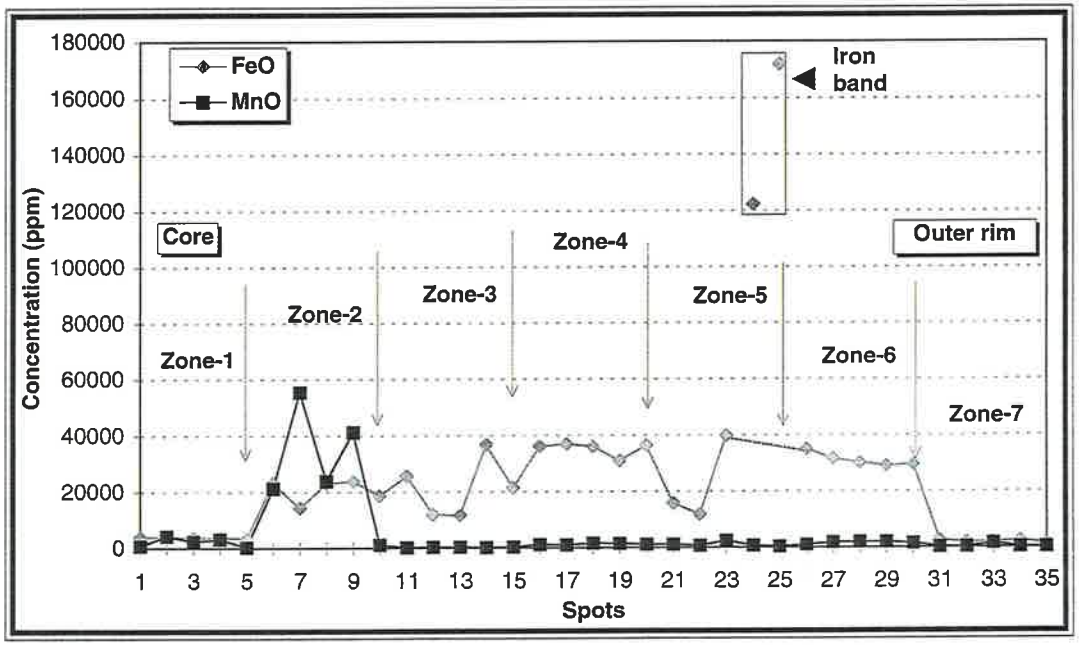
FeO
MnO
Iron band
Core
Outer rim
Zone-1
Zone-2
Zone-3
Zone-4
Zone-5
Zone-6
Zone-7
Concentration (ppm)
180000
160000
140000
120000
100000
80000
60000
40000
20000
0
1 3 5 7 9 11 13 15 17 19 21 23 25 27 29 31 33 35
Spots

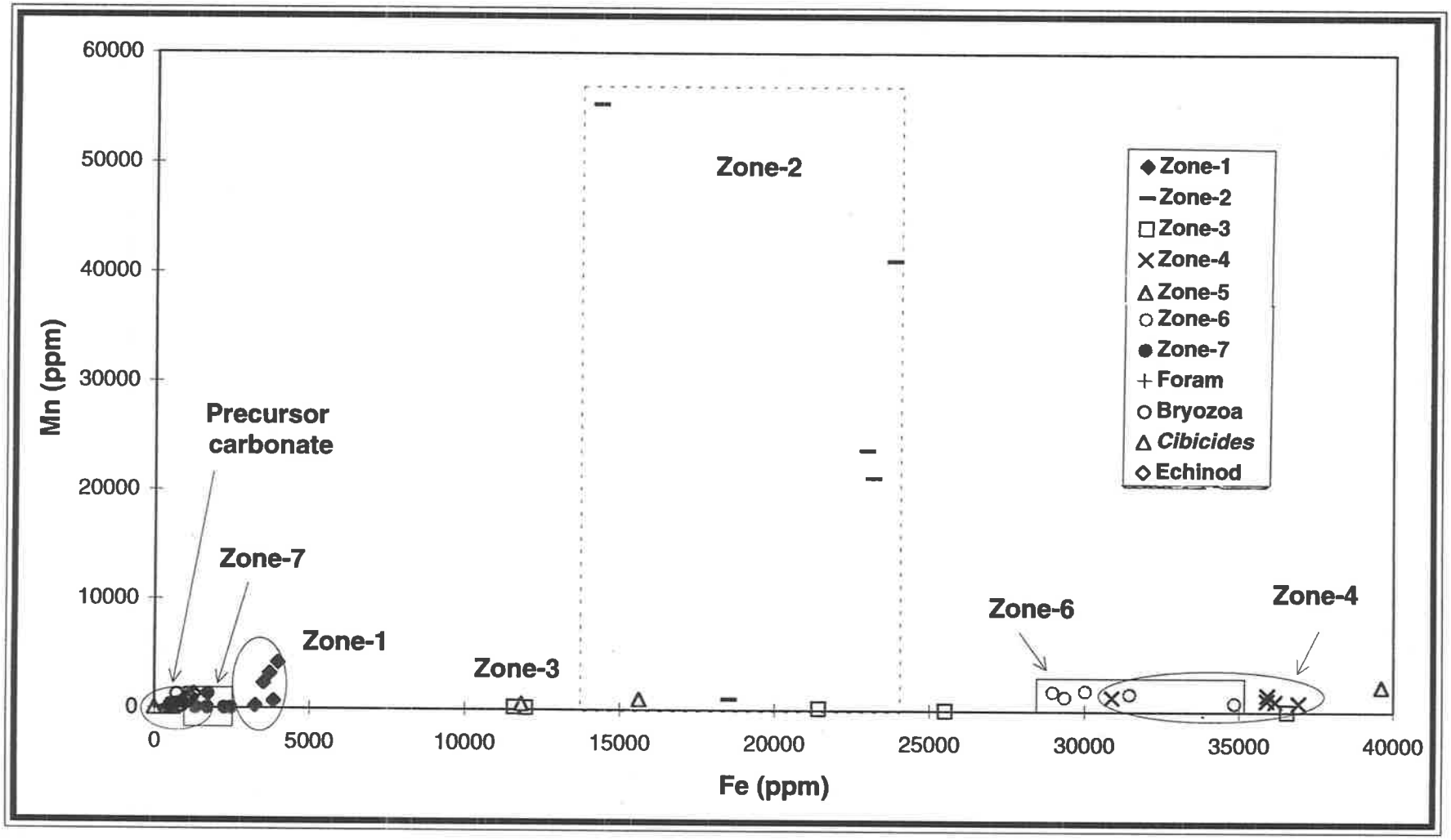

Figure 5.4: Scattered Fe/Mn diagram showing compositional zoning in the dolomite crystal appearing in Fig. 5.3 and plate 5.2. Values for the precursor carbonate are included for comparison.

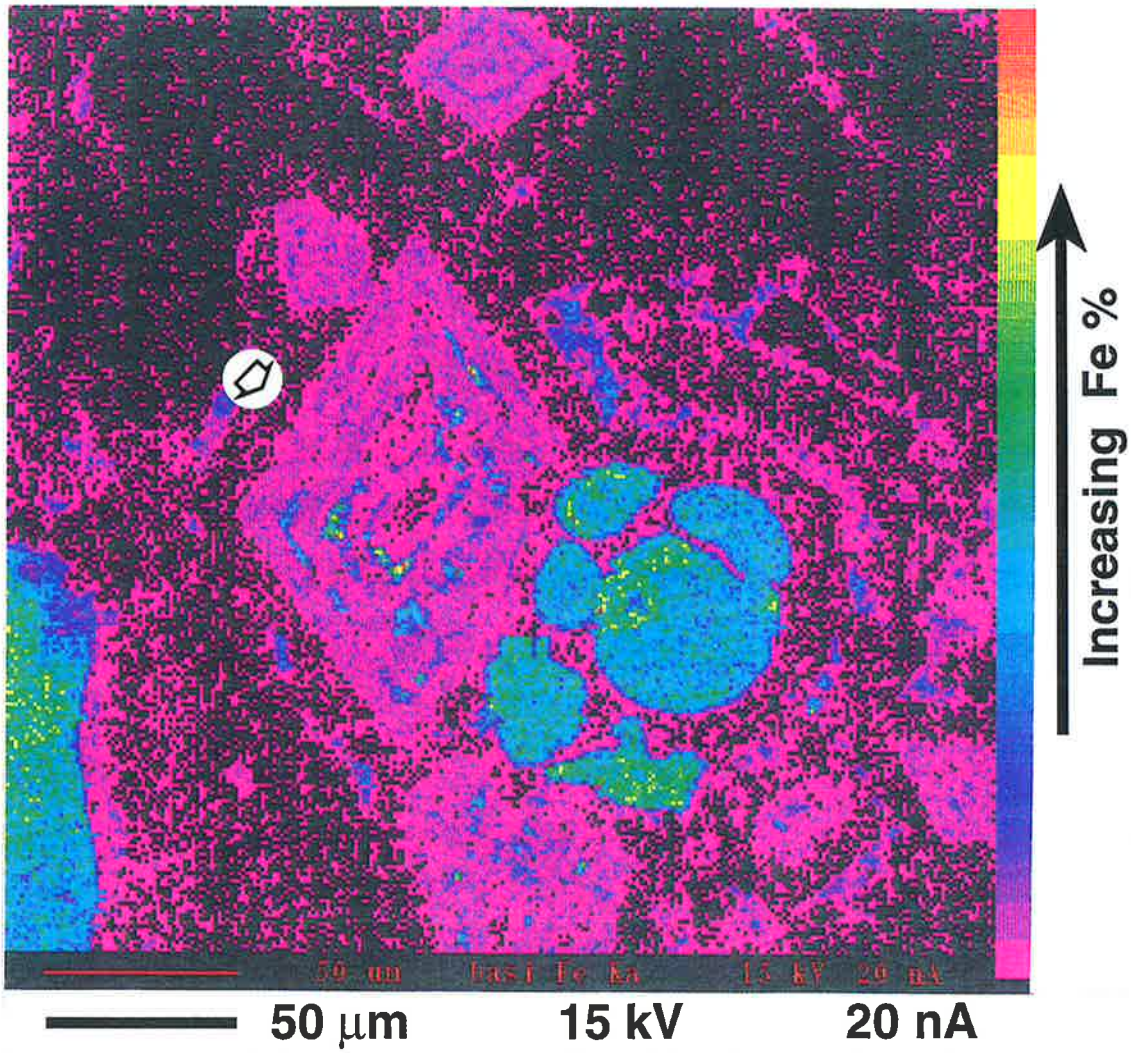

Figure 5.5: X-ray map for the dolomite crystal viewed in plate 5.2 showing the distribution of Fe concentrations and zoning (arrow). The lowest Fe content in the dolomite crystal is represented by magenta-coloured zones, higher Fe content is represented by blue-green-coloured zones, and the yellow-coloured patches within the crystal are the iron filled dissolution voids (values are listed in Table 5.1). The blue-green-yellow-coloured rounded patches (right side of the rhomb) are oxidised glaucony grains filling the chambers of a foraminifer. Sample 7, section 4.

Plate 5.3:

Dolomite crystals larger than 100 μm are rare and have clear cores which display non-uniform extinction when examined under polarised light (A). The cores are bright-luminescent (B). Backscattered images (C) and microprobe analysis (D) show a low iron content in these cores, whereas dissolution voids contain high iron contents. Sample 1, section 4.

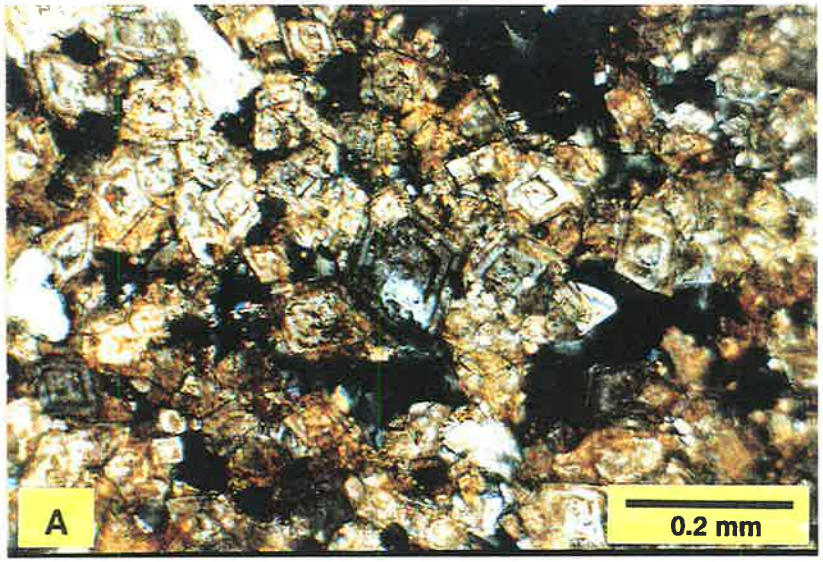
A
0.2 mm

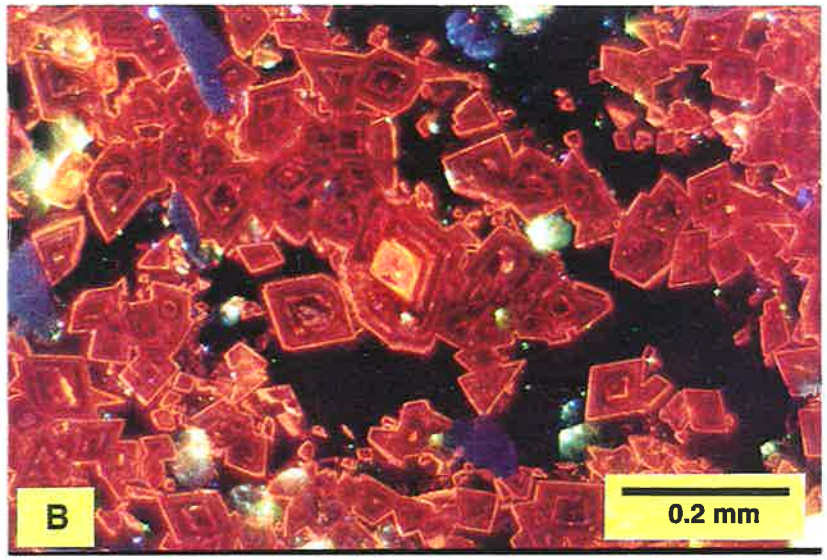
B
0.2 mm

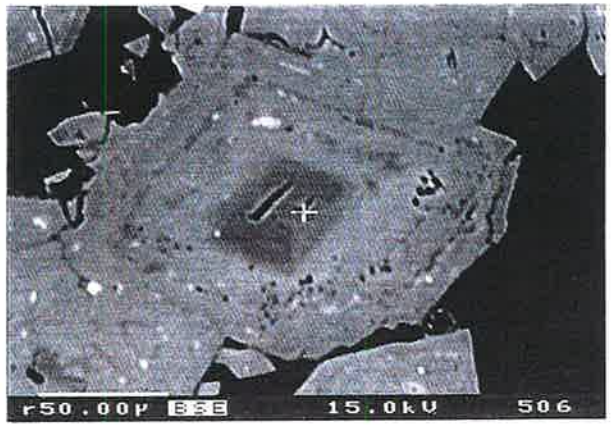
r50.00µ BSE 15.0kV 506

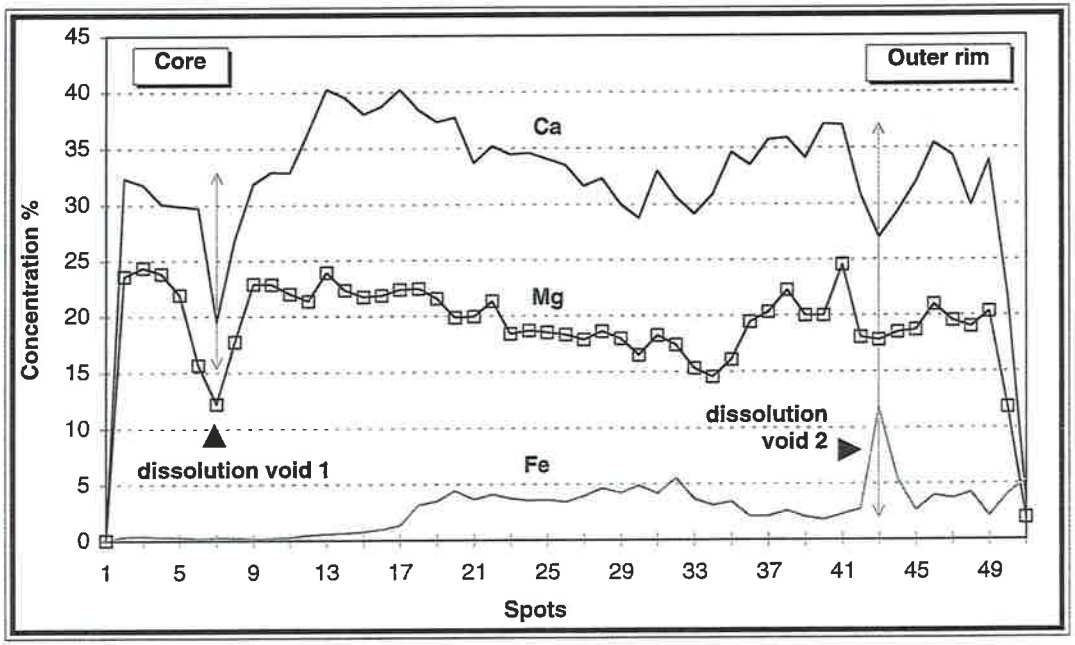
Core
Outer rim
Ca
Mg
Fe
dissolution void 1
dissolution void 2
Concentration %
Spots
0
5
10
15
20
25
30
35
40
45
1
5
9
13
17
21
25
29
33
37
41
45
49

Plate 5.4:

SEM photomicrograph showing dolomite replacing various skeletal components. Crystal faces are slightly etched, and despite intracrystalline compositional variations, they are straight and not distorted (A, B, C, D). The majority of the replaced skeletal fragments show little evidence of abrasion and maceration.

Amongst the skeletal components, foraminifers are the first to be replaced (F), followed by other grains like molluscs, and bryozoans are among the least effected {e.g., foliose (A, B, C) and delicate branching (E) growth forms}.

Photos A, B, C, and D = sample 6, section 4.
Photos E and F = sample 1, section 4.

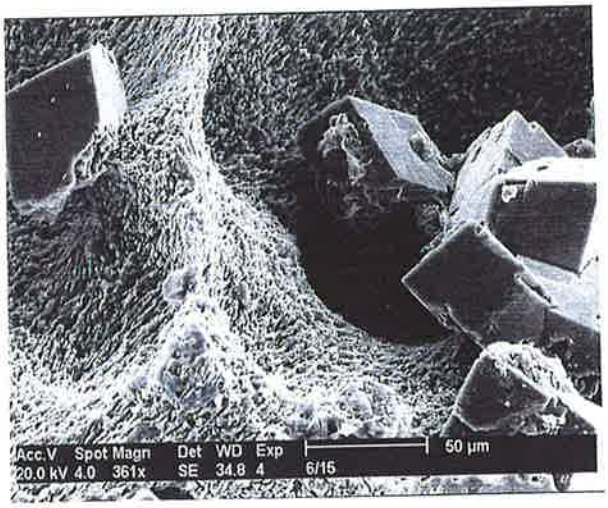
Acc.V Spot Magn Det WD Exp
20.0 kV 4.0 361x SE 34.8 4 6/15
50 µm

A

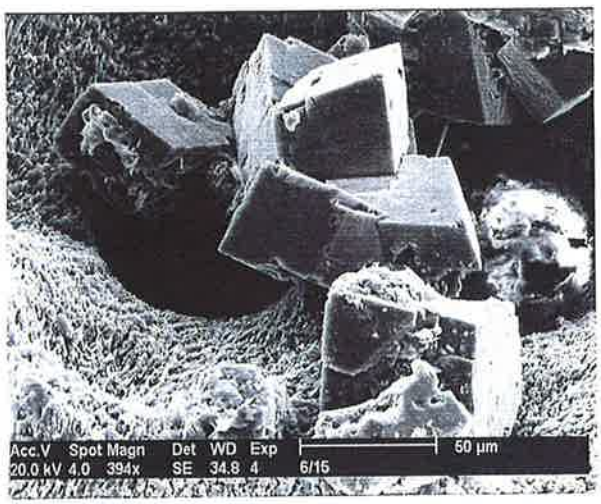
Acc.V Spot Magn Det WD Exp
20.0 kV 4.0 394x SE 34.8 4 6/15
50 µm

B

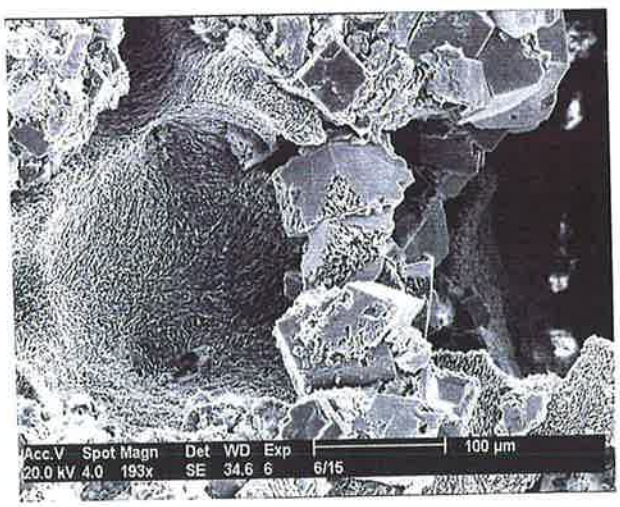
Acc.V Spot Magn Det WD Exp
20.0 kV 4.0 193x SE 34.6 6 6/15
100 µm

C

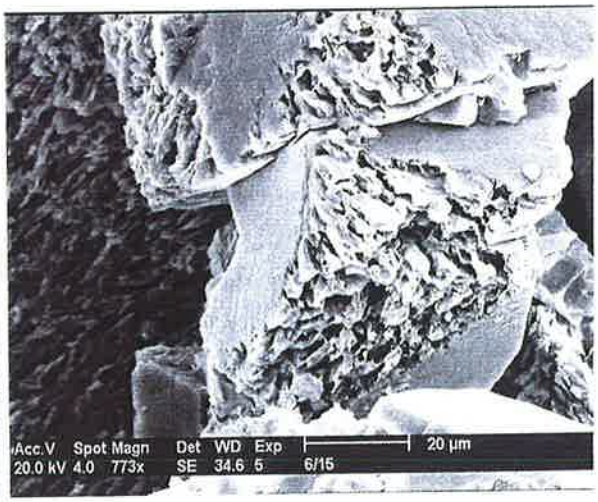
Acc.V Spot Magn Det WD Exp
20.0 kV 4.0 773x SE 34.6 5 6/15
20 µm

D

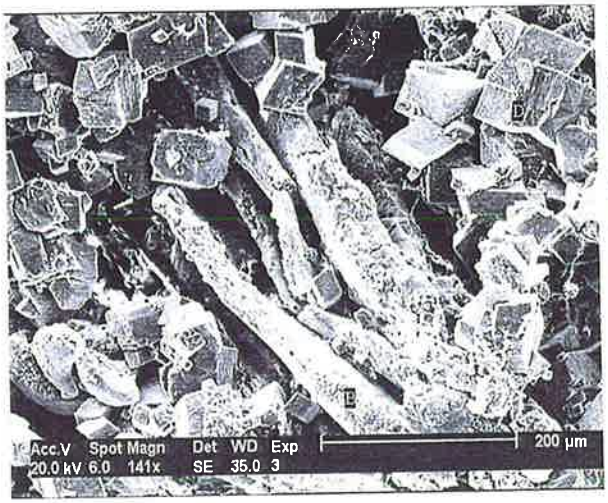
Acc.V Spot Magn Det WD Exp
20.0 kV 6.0 141x SE 35.0 3
200 µm

E

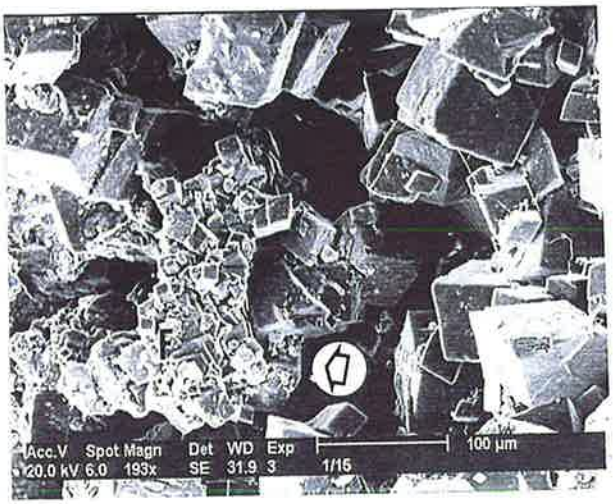
Acc.V Spot Magn Det WD Exp
20.0 kV 6.0 193x SE 31.9 3 1/15
100 µm

F

Plate 5.5:

A- Dolomite cuts across fabrics replacing all the original matrix and most grains. Relict textures of the original limestone are absent in dolostones, except for widespread oxidised glaucony grains that infilled various fossil chambers before dolomite was formed. In this example the mould of a flat robust branching bryozoan growth form (r) is filled with glaucony. Thin section photomicrograph under plain light. Sample 1, section 4.

B- The partially dolomitised limestone reveals clear textural relationships and evidence regarding precursor constituents. In this example, a partially dolomitised fragment of a delicate branching bryozoan growth form is shown (d). Thin section photomicrograph under plain light. Sample 6, section 4.

C- Dolomitisation is postdepositional and occurred after a stage of meteoric diagenesis. The presence of a few preserved echinoid fragments (e) and their surrounding syntaxial cement (c) within the dolostones suggests that the limestones were effected by fresh water dissolution and underwent some stabilisation to LMC prior to dolomitisation (d). Thin section photomicrograph under plain light. Sample 7, section 4.

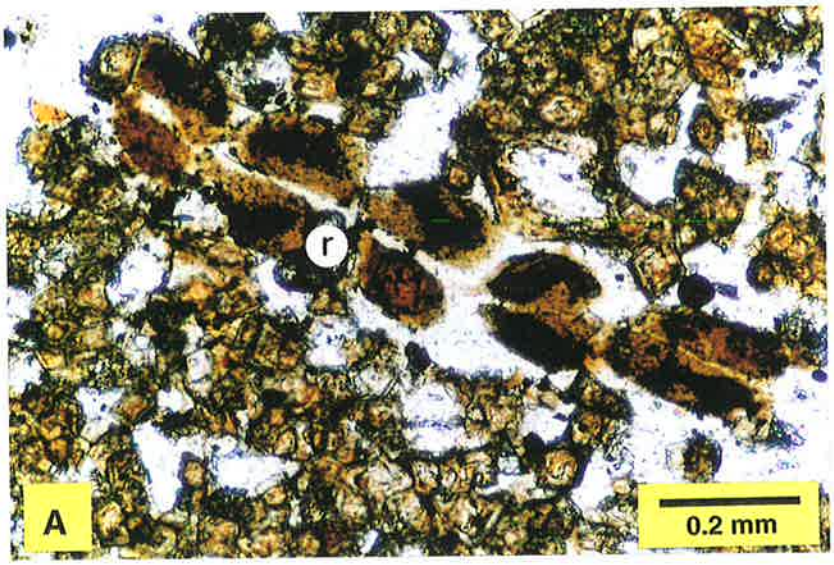
r
A
0.2 mm

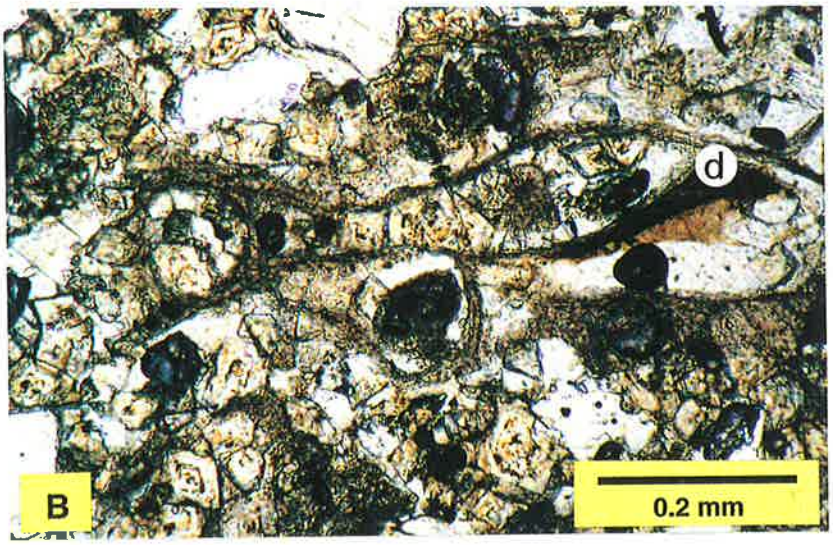
d
B
0.2 mm

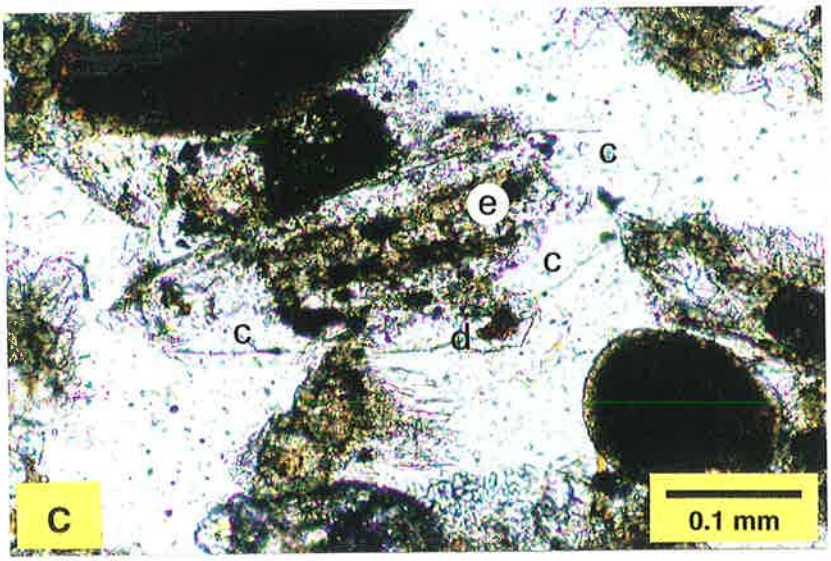
c
e
c
c
d
C
0.1 mm

Plate 5.6:

A- Preserved *Chiloguembelina* in the dolomitised Port Vincent Limestone. This planktonic foraminifer occurs below the Oligocene/Miocene boundary and is regarded as a cool-water indicator (McGowran and Beecroft, 1985). Thin section photomicrograph under plain light. Sample 6, section 4.

B- Dolomitic limestone showing dolomite crystals (arrows) with several alternating non-luminescent to deep red dull-luminescent concentric zones. Brachiopod shell fragment (br) and echinoid fragment (e) surrounded by syntaxial cement are well preserved in most dolomitic limestone samples from the Port Vincent Limestone. Thin section photomicrograph under CL. Sample 6, section 4.

C- Dolomitic limestone showing various preserved skeletal fragments. (b) robust branching bryozoa, (e) echinoid fragments surrounded by syntaxial cement. Dolomite crystals show several alternating non-luminescent to deep red dull-luminescent concentric zones, and a thin red bright-luminescent concentric zone on crystal margins and within the crystal midway between the core and margin. Boundaries between adjacent CL concentric zones are distinctively straight and sharp, and sectoral zonations are absent. Thin section photomicrograph under CL. Sample 6, section 4.

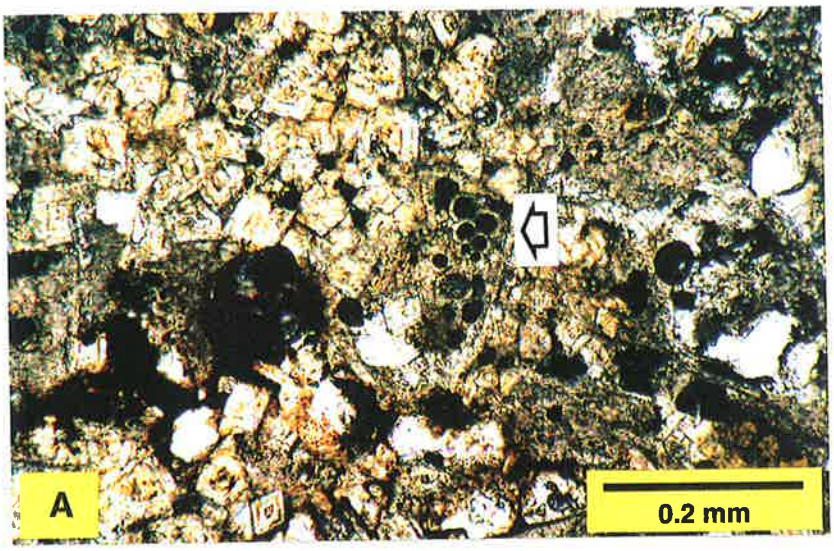
A
0.2 mm

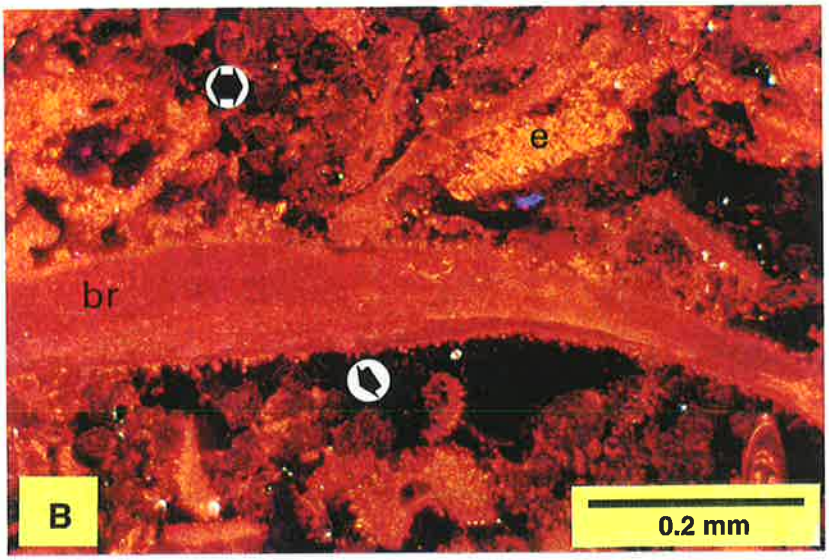
e
br
B
0.2 mm

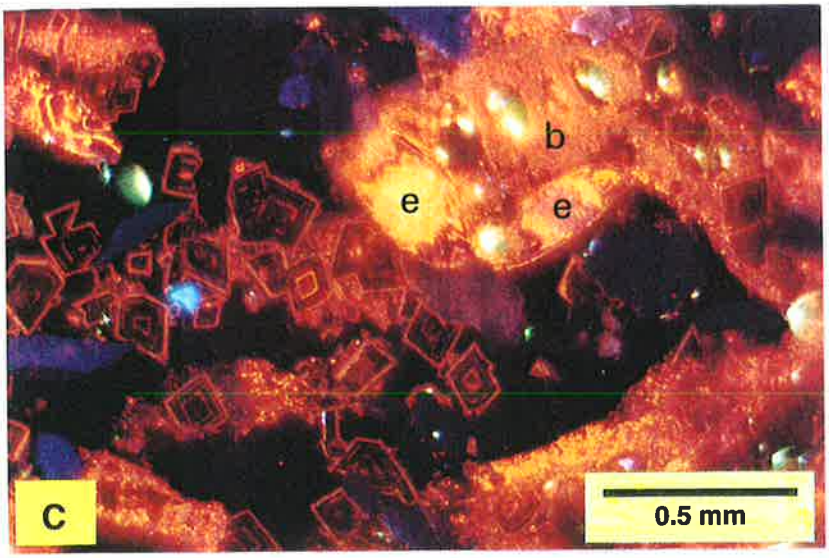
b
e
e
C
0.5 mm

2.2 Strontium:

Strontium is one of the most useful trace elements in limestones and dolomites, and its occurrence in carbonates has been the focus of many recent studies (e.g., Al-Hashimi, 1976; Land, 1980, 1985; M'Rabet, 1981; Veizer, 1983; Banner, 1995). A brief background is introduced herein for purposes of comparison and interpretation of the dolomite in the Port Vincent Limestone.

Synthetic precipitation of calcite from seawater at 25°C shows it to have a strontium distribution coefficient ($K^{Sr}_{calcite}$) value of 0.14, and by further calculations using the Sr/Ca molar ratio in seawater, calcites in equilibrium with seawater are expected to contain around 1375 ppm Sr (Kinsman, 1969; Kinsman and Holland, 1969). Because of relative ionic sizes, strontium in dolomite largely substitutes for Ca ions rather than Mg in the dolomite lattice (Behrens and Land, 1972; Kretz 1982). Therefore, from a theoretical point of view, the distribution coefficient of strontium in dolomite ($K^{Sr}_{dolomite}$) is expected to be approximately half of that for calcite, and thus the strontium content of dolomite should be around 600 ppm (Behrens and Land, 1972; Kretz 1982). Such predictions are close to results obtained from experimental studies on dolomites (at high temperatures of 250-300°C), which give $K^{Sr}_{dolomite}$ values of 0.025 (Katz and Matthews, 1977) and 0.07 (Jacobson and Usdowski, 1976). Analysis of continental waters show them to have a lower Sr concentration than seawater (Kinsman, 1969).

The mineralogy of the precursor carbonate and the timing of dolomitisation are two important inter-related factors that highly influence the chemical composition of the replacement dolomite. Carbonate rocks that are dominated by skeletal grains have a higher Sr content than those dominated by non-skeletal grains, because of the rapid precipitation rates associated with shell accretion in marine organisms (Carpenter and Lohmann, 1992), and may be reflected in the replaced dolomite. Dolomite replacing aragonite is reported to contain a marine type Sr content of 500 - 600 ppm, since aragonite has a Sr/Ca ratio similar to seawater

(Kinsman, 1969; Veizer, 1983). Dolomite replacing LMC and HMC, with around 1000 - 2000 ppm Sr, will contain several hundred ppm Sr. Where calcite is being dolomitised, then a strontium depleted dolomite is formed (Tucker and Wright, 1990). Early formed dolomites (penecontemporaneous) are enriched in Sr compared to late dolomites (Veizer et al., 1978; Land, 1985). As limestones and dolomites undergo successive diagenetic alterations their Sr content will progressively decrease (Shirmohammadi and Shearman, 1966; Kinsman, 1969). Therefore Sr-depleted dolomite would be expected to form, if dolomitisation succeeded stabilisation of the precursor carbonate to a diagenetic LMC (Tucker and Wright, 1990).

In contrast to the distinctively sharp zoning of Mn and Fe, strontium is distributed more homogeneously in the dolomite, with a slight increase noticeable on crystal margins (Fig. 5.6). Sr concentrations are relatively high reaching up to 1100 ppm (Table - 5.1), but are generally lower than Sr values measured from skeletal constituents overlying and surrounding the dolomite (360 - 2280 ppm, Table - 5.2).

Limestone	Fe (ppm)	Mn (ppm)	Sr (ppm)	Na (ppm)
Foram	390 - 750	0 - 270	510 - 810	110 - 440
Bryozoa	490 - 1080	160 - 940	360 - 1000	0 - 490
Cibicides	410 - 750	0 - 290	1060 - 2280	700 - 1050
Echinoid	920 - 1270	550 - 1250	740 - 1110	110 - 330
Crespenina	200 - 1380	140 - 290	610 - 1380	360 - 1510

Table - 5.2: Concentration of trace elements in various constituents of the Port Vincent Limestone.

2.3 Sodium and Aluminium:

Sodium is present as brine in fluid inclusions, as intercrystalline solid inclusions (NaCl) and as Na ions in the dolomite crystal lattice. Like other detected trace elements, Na concentrations are relatively high and range between 20-2290 ppm. The highest values correspond to dissolution voids, which are most likely influenced by the presence of solid NaCl within these voids (Fig. 5.6).

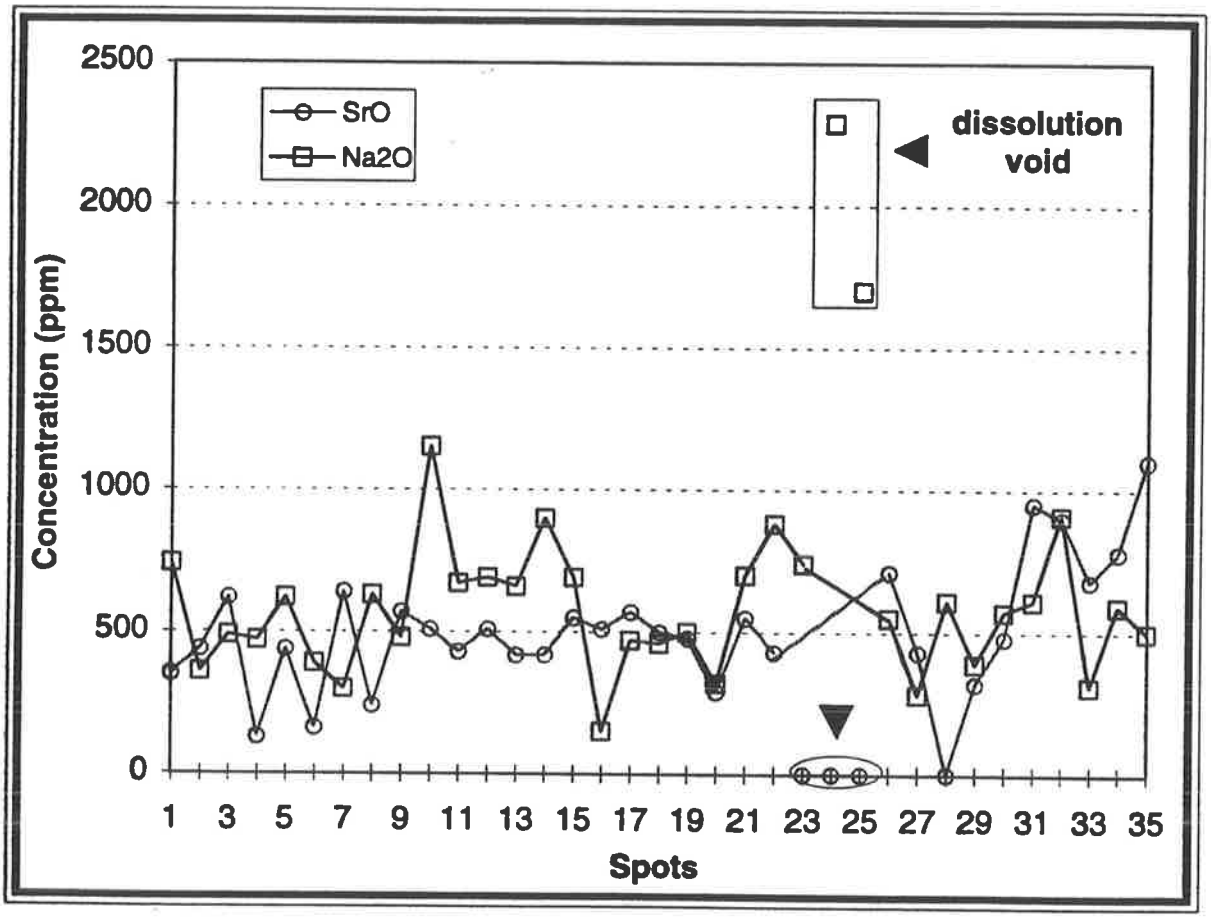

Figure 5.6: Concentration and distribution of Sr^{2+} and Na^{+} across a dolomite crystal, from core to outer rim. Sr^{2+} concentration is relatively homogeneous across the crystal but slightly increases at the margin. Na^{+} concentration is also homogeneous, except were dissolution voids are present (arrows) and contain NaCl.

Aluminium is rare to absent in the dolomite structure, but generally high concentrations are present around the crystal and in dissolution voids. Al concentration appears to relate proportionally to iron concentration in many dolomite crystals (Figs. 5.1A, 5.7).

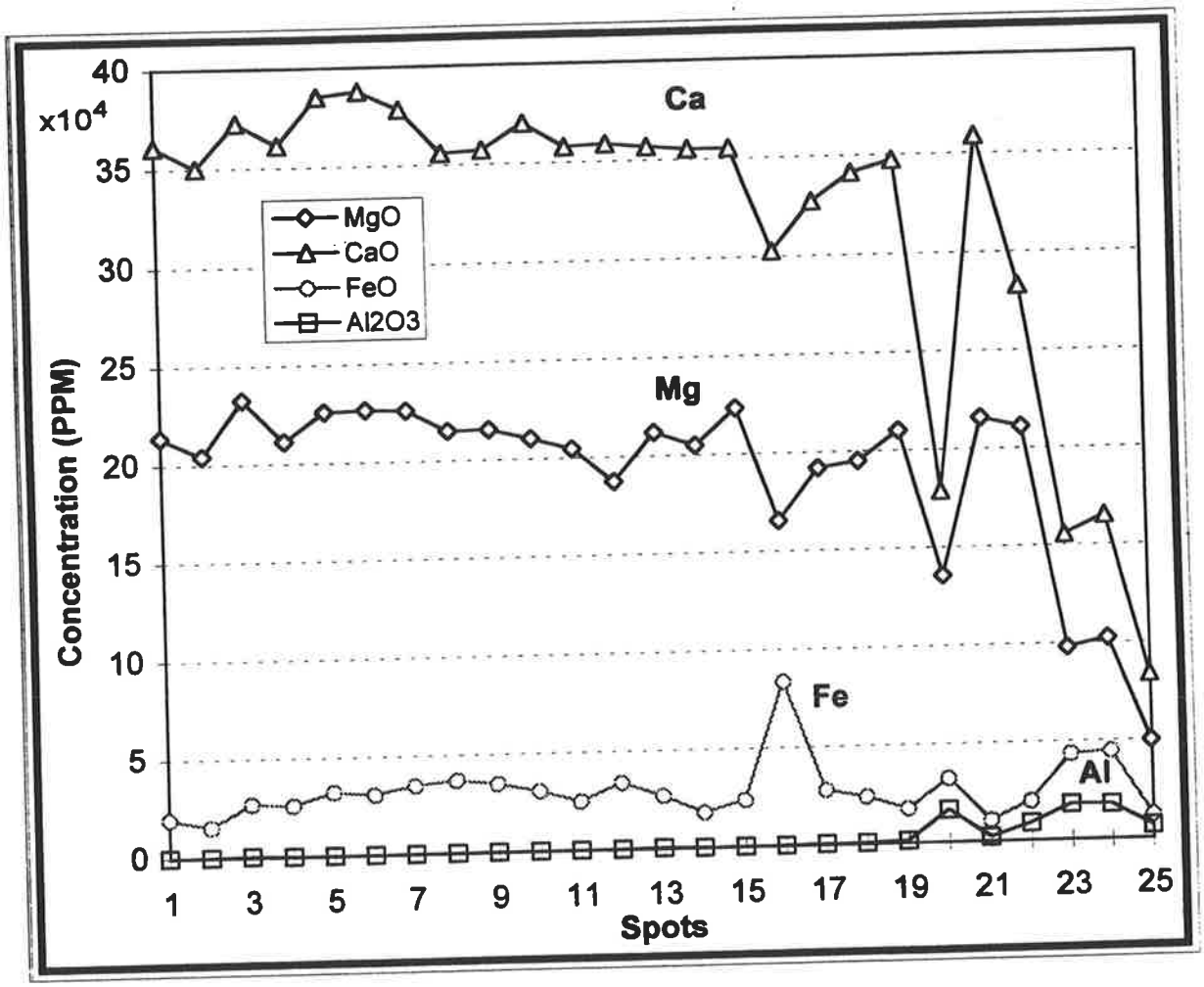

Figure 5.7: Trace element distribution across a dolomite crystal. Aluminium concentration increases with increasing iron concentration in many dolomite crystals.

2.4 Isotopes:

Oxygen and Carbon isotopes: Dolomite is enriched in $\delta^{18}O$ but depleted in $\delta^{13}C$ (Fig. 5.8). $\delta^{18}O$ values range between 0.66 to 2.212, whereas $\delta^{13}C$ values range between -2.56 to -3.32 (Table - 5.3). The isotopic composition of various constituents from samples surrounding the dolomite are plotted in figure 5.8. Oxygen values are similar to those of the Cenozoic Gambier dolomite of southern Australia (James et al., 1993), but $\delta^{13}C$ values contrast significantly.

Strontium isotopes: The $^{87}Sr/^{86}Sr$ ratios of dolomite have a narrow range (Table - 5.3). When compared with the $^{87}Sr/^{86}Sr$ ratios of seawater during the Oligocene/Miocene (Veizer and Compston, 1974; Burke et al., 1982), they are considerably higher.

3. DISCUSSION

The elemental composition of the dolomite is expected to have been inherited from the precursor limestone and/or the dolomitising fluid. The concentrations of these elements are further related to the timing of dolomitisation in respect to any earlier diagenetic alterations (i.e. before or after stabilisation of the limestone).

3.1 Timing of Dolomitisation:

The dolomite occurs within Early Oligocene beds. No dolomite was observed in Miocene or younger deposits. This is supported biostratigraphically by the presence of unaltered planktonic foraminifers *Chiloguembelina* (Plate 5.6-A), which is placed by McGowran and Beecroft (1985) below the Oligocene/Miocene boundary.

The $^{87}Sr/^{86}Sr$ ratios measured for the dolomite depart from that of other Oligocene and Miocene marine carbonates that are plotted in the strontium isotope age-reference curve of Burke et al. (1982). They are also higher than other similar age carbonate rocks (e.g., Gambier dolomite, James et al., 1993). This elevated Sr isotopic composition is undoubtedly

	$\delta^{13}C$‰ PDB	$\delta^{18}O$‰ PDB	$^{87}Sr/^{86}Sr$
dolostone	-2.56 to -3.32	0.66 to 2.212	0.710110
dolomitic limestone	-2.56	+1.32	0.710665

Table - 5.3: Isotope data for pure dolostone and dolomitic limestone samples of the Port Vincent Limestone.

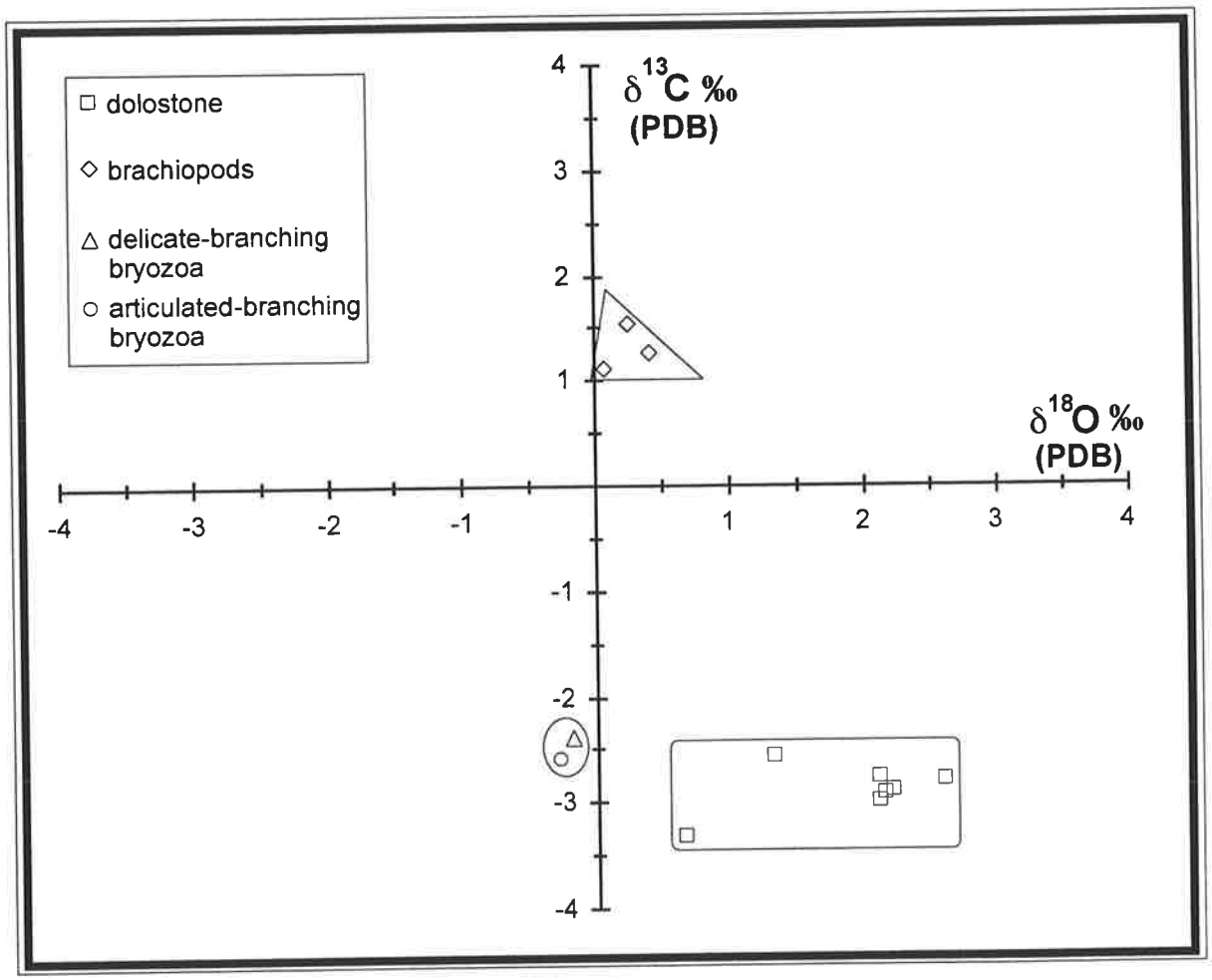

Figure 5.8: $\delta^{18}O$ and $\delta^{13}C$ isotope ratios in the dolomite and other constituents of the Port Vincent Limestone. Brachiopods ~ 0 mole % $MgCO_3$, delicate branching bryozoa = 1.5 mole % $MgCO_3$, articulated branching bryozoa = 2 mole % $MgCO_3$. X-ray analyses are shown in Appendices B-1 and D-3.

allochthonous. It must have been derived from the interaction of seawater with weathered Precambrian/Cambrian, intrusive igneous, and metamorphic rocks which all immediately underlie the Tertiary sediments in the near by vicinity. Such radiogenic rocks are exposed along coastal cliffs and on the strandline during low tide for 3 kms just north and south of Pine Point. They are composed of aplite, strongly altered hornblende-rich rocks, and feldspathic gneisses (Crawford, 1965).

Petrographic evidence further indicates that dolomitisation is postdepositional and occurred after a stage of meteoric diagenesis. The presence of a few preserved echinoid fragments and their surrounding syntaxial cement, as well as a few bryozoan and bivalve mouldic pores within the dolostones suggests that the limestones were affected by fresh water dissolution and underwent some stabilisation to LMC prior to dolomitisation (plate 5.5-C).

The uniformity of the dolomite texture, and the similarity of cathodoluminescent and elemental zoning among almost all crystals (CL stratigraphy and chemostratigraphy), indicate that the dolomite formed during a single event. The straight and sharp intracrystalline boundaries between adjacent zones (plates 5.2-B, C; 5.3-B, C; 5.6-C) indicate that this event was continuous, with no dissolution taking place during crystal growth.

3.2 Trace Elements:

Compositional variations between zones are narrow and most times subtle (e.g., zone 4 and 6 in Fig. 5.4), indicating repeated influxes of pore fluids with slightly varying chemical compositions during crystal growth, possibly on the microenvironment scale.

Despite this minor compositional variation, Mn and Fe zoning is distinct. The concentrations of these elements vary independently between zones (Figs. 5.4; plate 5.2-D; Table - 5.1), indicating that compositional zonation is due to changes in redox conditions of the pore fluid during crystal growth and not the result of variations in precipitation rate or temperature (Frank et al., 1982; Machel, 1985; Fraser et al., 1989; Dromgoole and Walter, 1990). Overall Mn and Fe concentrations are generally high, and the origin of such high

concentrations may well be inherited from the precursor carbonate. However, although dolomite formation generally involves an increase in Mn and Fe concentrations compared to their precursor carbonates (Land, 1980), the values recorded from these dolomites are much higher than those of the precursor carbonate (compare Tables 5.1 and 5.2). The iron is believed to be supplied from nearby iron oxides and glaucony grains. In addition, an iron crust underlies Tertiary sediments, and appears in scattered coastal areas on Yorke Peninsula, and may also contribute to the high Fe ion concentration. Glaucony grains are abundant in the precursor carbonates, and have been partially to completely oxidised prior to the formation of dolomite (plates 5.2-C; 5.5-A, B). The dominantly dull to non-luminescent character of the dolomite crystals is caused by the elevated Fe concentration which quenches the luminescent activator effect of Mn.

Unlike Mn and Fe, strontium is uninfluenced by changes in redox conditions (Fraser et al., 1989). The source of Sr can either come from the precursor limestone or the dolomitising fluid. Limestone facies surrounding the dolomite and those replaced by dolomite are interpreted to be skeletal cool-water carbonate deposits with an initial low to high-Mg calcite mineralogy (Shubber et. al., 1995, 1996). Such sediments would have high strontium values similar to modern cool-water calcitic limestones of eastern Tasmania which contain between 700 - 2700 ppm Sr (Rao and Jayawardane, 1994). In terms of the general concepts discussed earlier in this chapter (section 2.2), these values will drop after stabilisation. The strontium content in the Port Vincent Limestone dolomite is reasonably lower than the strontium values of the stabilised limestones (compare Tables 5.1 and 5.2). This further supports the earlier interpretation regarding the timing of dolomitisation being post meteoric alteration. This strontium content is higher than what would be expected for a fresh water involvement (mixing-zone dolomitisation). They are also above the theoretically estimated values ($K^{Sr}_{dolomite} = 1/2\ K^{Sr}_{calcite}$, section 2.2 this chapter), implying an additional source. Highest Sr concentrations are present in crystal margins, zone-7 (Fig. 5.6), which may suggest prolonged interaction with seawater. This enrichment is attributed to the Precambrian/Cambrian, intrusive igneous, and metamorphic rocks which underlie the

Tertiary sediments in the St. Vincent Basin.

The dominantly LMC and HMC mineralogy of the original carbonate sediment excludes the possibility of these sediments being the source for Mg ions. The nearby volcanics may be a possible source for Mg with either continental or marine waters acting as a transporting agent. Continental water is unlikely to be the transporting agent, since continuous dilution will lower Mg concentration in these waters below dolomitisation requirements. Thus the large amount of extraformational Mg ions is most likely supplied by seawater.

Sodium concentration is also higher than that in the precursor limestones (Tables-5.1, 5.2; Fig. 5.6). The high extreme value is attributed to the presence of halite and brine in fluid inclusions. The amount of Na in low-Mg calcite is around 270 ppm (Veizer, 1983; Rao and Adabi, 1992), and in open marine carbonates between 100 and 300 ppm (Badiozamani, 1973). The most likely source of Na is seawater. Sodium is abundant in seawater (10,565 ppm - Pytkowicz, 1983), and its concentration in sediments has been utilised as a palaeosalinity indicator (Land and Hoops, 1973; Veizer et al., 1977, 1978). Normal marine and hypersaline environments are separated by a 230 ppm Na content (Veizer et al., 1977). However, Veizer et al. (1977) also note that this boundary may be diffused due to variations in facies and post depositional alterations.

3.3 Water Composition:

The size and geometry of the dolomite body indicates that dolomitisation was not a widespread replacement process, which further implies that conditions for dolomitisation were fulfilled only locally. This localisation of the dolomite within the lower part of the Port Vincent Limestone may be the result of a palaeohydrological feature associated with permeability, stratification within the aquifer, or position of the water table. The similarity in texture, crystal form, and distribution of the dolomite crystals reflects precipitation from fluid filled pores. The dominantly dull to non-luminescent character indicates precipitation from either oxidising or reducing pore fluids (Meyers, 1978; Frank et al., 1982; Machel, 1985;

Amieux et al., 1989). Precipitation from oxidising pore fluids is ruled out because both Mn and Fe concentrations in all studied crystals are higher than those expected for precipitation from oxidising pore fluids (James and Choquette, 1990b): i.e. reducing conditions are required to mobilise large concentrations of Mn^{2+} and Fe^{2+} (Frank et al., 1982).

The dolomitised rocks were not buried under more than 20 m (plate 5.1-A). Pyrite is present but in rare amounts as revealed by X-ray. The planar-e texture of these dolomites suggests formation at relatively low temperatures (Sibley and Gregg, 1987). The isotopic composition is tested by comparison with other values measured from other dolomites (eg., Allan and Wiggins, 1993; James et al., 1993) (Figs. 5.9, 5.10). The positive oxygen isotopic composition (Fig. 5.8) is consistent with precipitation from seawater (Land, 1991), and further reflects precipitation at low temperatures ranging between 15 - 18°C (Allan and Wiggins, 1993). However, the low $\delta^{18}O$ positive value (0.66 PDB) further indicates that this seawater was slightly modified by fresh water input. These values are higher than those reflecting brackish waters and too low to reflect any Coorong-like hypersaline waters (Rosen et al., 1989), which might have been generated due to evaporation of the Gulf waters. The depleted carbon isotopic composition reflects subsequent addition of organically derived HCO_3 to the microenvironment (Woodruff and Savin, 1985). Such source is provided by rain forests and wet conditions which prevailed in southern and southeastern Australia during Late Oligocene-Middle Miocene (Alley and Lindsay, 1995), and persisted into the Late Miocene in southeastern Australia (Kemp, 1978) but retreated from the eastern Murray Basin some time during the Late Miocene (Martin, 1991).

4. CONCLUDING INTERPRETATION

1- From the foregoing it is concluded that the Port Vincent Dolomite precipitated from moderately reducing pore fluids, such as that present in shallow burial environments below the sediment-seawater interface.

2- Dolomitisation occurred shortly after deposition as indicated by petrography and isotopes.

3- All original components in dolostones were dolomitised regardless of their mineralogy (mainly LMC to HMC), suggesting a high saturation state of the dolomitising fluid.

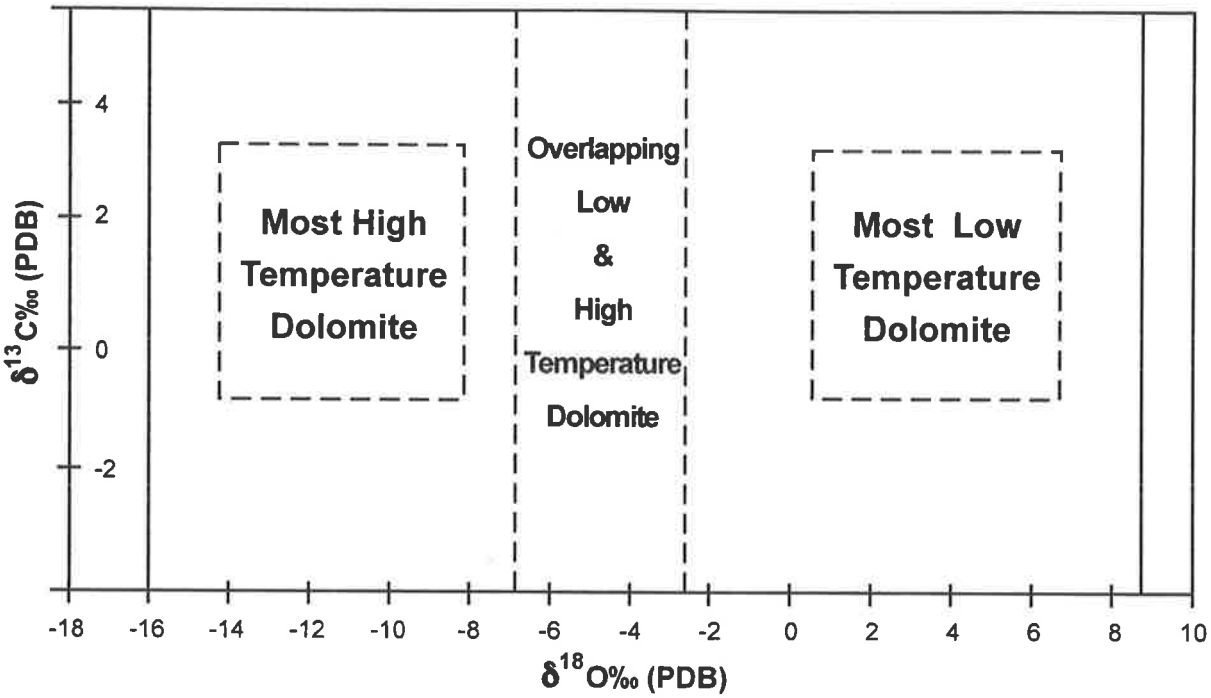

Figure 5.9: Formation temperatures of various dolomite types compiled from various studies. From Allan and Wiggings, 1993.

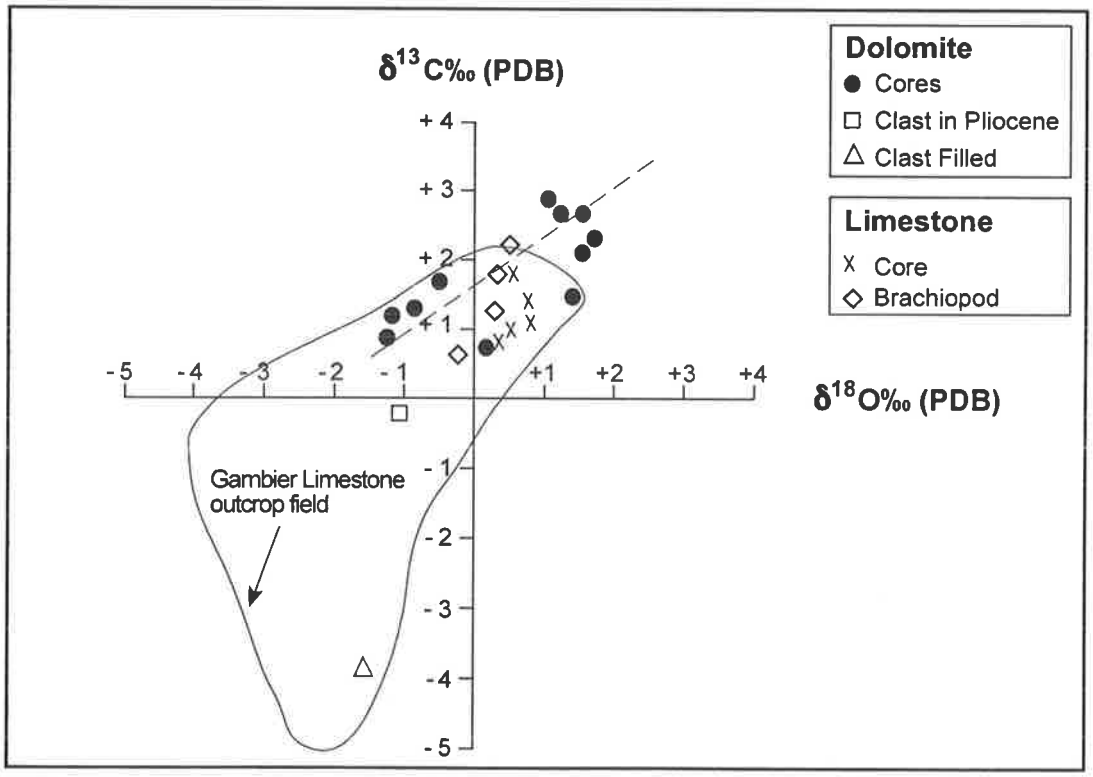

Figure 5.10: Carbon and oxygen isotope values in pure Gambier limestones and dolostones are presented here for comparison with values obtained for the dolostones and dolomitic limestone in the Port Vincent Limestone. From James et al., 1993.

5. DOLOMITE DIAGENESIS

5.1 Dissolution:

Non-stoichiometric dolomite is metastable (Folk and Land, 1975; Land, 1980; Tucker and Wright, 1990), and therefore more soluble and easily susceptible to secondary alteration (i.e. dedolomitisation). However, dedolomitisation is rare in the Port Vincent Limestone dolomite and is restricted to a few scattered rhombs. These appear to contain microdissolution voids as illustrated by SEM photomicrographs and back-scattered images (plate 5.7). Traces of calcite later precipitated in only a few intracrystalline micropores, in a two-step dedolomitisation process (cf. James et al., 1993).

Dolomite dissolution commonly affects only small parts of the crystal. Complete rhomb dissolution as described in similar dolomite occurrences (Rosen and Holdren, 1986; Coniglio et al., 1988; James et al., 1993) was not observed. Dissolution is fabric selective, affecting crystal cores and specific concentric zones that contain concentrations of iron slightly higher than that in the remainder parts of the crystal (Figs. 5.3, 5.5; Table-5.1; plate 5.2). This differential dissolution is a result of mineral-controlled diagenesis (James and Choquette, 1990a), and is caused by variable solubilities between dolomite zones when they are affected by percolating freshwater. The resultant thin rhomb-shaped intracrystalline dissolution voids are empty or later partially filled with iron oxides (plates 5.2, 5.7). Recent surface weathering of the dolomite by dolomite-seawater interaction produces an iron hydroxide crust which gives the rusty yellowish brown coloured appearance seen on these dolomites (Al-Hashimi and Hemingway, 1973), especially on the dolostones at the modern strandline (plate 5.1-B). The rusty yellowish brown colour decreases landward, and disappears in the cliffs, which are beyond the reach of seawater during hightide.

Iron oxides and glaucony grains concentrate around dolomite crystals. They appear to be expelled outside the growing rhombohedra (plate 5.7-E) by partial or complete physical

displacement (cf. Al-Hashimi and Hemingway, 1973). This is also supported by the high Aluminium content which coincides with areas of high iron concentrations around the dolomite rhombs and in dissolution voids (Fig. 5.7).

Plate 5.7:

Dolomite dissolution is fabric selective (mineral-controlled diagenesis), affecting crystal cores and specific concentric zones that contain concentrations of iron slightly higher than that in the remainder parts of the crystal. The back-scattered images A, B, C, and D (sample 2, section 4) show a number of dolomite crystals with thin rhomb-shaped intracrystalline dissolution voids, which are empty or later partially filled with iron oxides (arrows).

E- Iron oxides and glaucony grains from the precursor limestone are concentrated around dolomite crystals after being expelled outside the growing rhombohedra by partial or complete physical displacement. The dolomite is completely replacing the test of a large benthic foraminifer (arrow). Thin section photomicrograph under plain light. Sample 7, section 4.

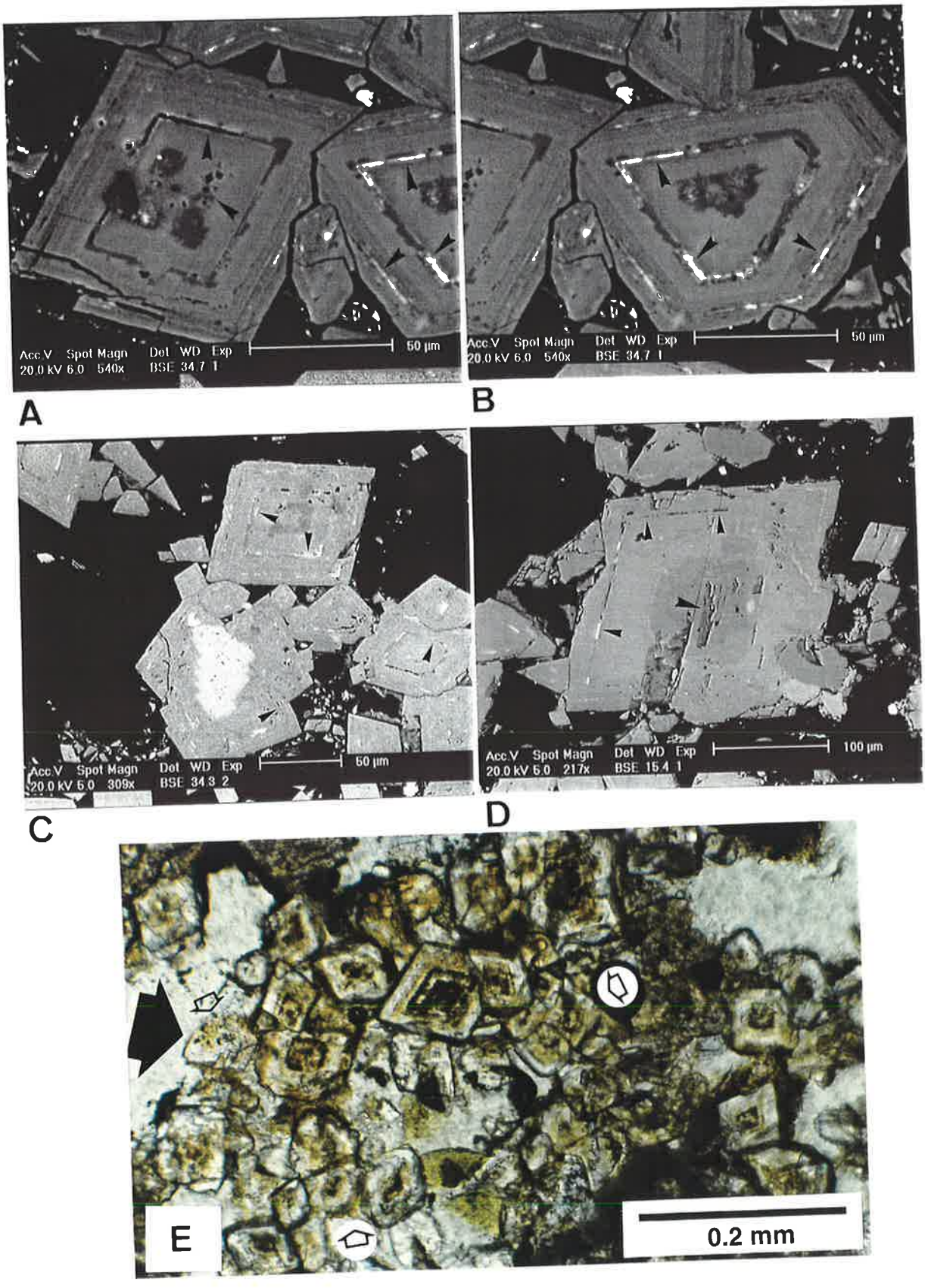
Acc.V Spot Magn Det WD Exp
20.0 kV 6.0 540x BSE 34.7 1
50 µm
A
Acc.V Spot Magn Det WD Exp
20.0 kV 6.0 540x BSE 34.7 1
50 µm
B
Acc.V Spot Magn Det WD Exp
20.0 kV 6.0 309x BSE 34.3 2
50 µm
C
Acc.V Spot Magn Det WD Exp
20.0 kV 5.0 217x BSE 15.4 1
100 µm
D
E
0.2 mm

Chapter 6

SUMMARY AND CONCLUSIONS

SUMMARY AND CONCLUSIONS

Over the past two decades, many characteristics of cool-water carbonate sediments and the settings in which they are produced have been acknowledged. Particular emphasis were drawn on contrasts which distinguished these carbonates from their extensively studied warm-water "tropical" counterparts, to point out the invalidity of directly applying the concepts of aragonite-dominated warm-water carbonate models to the interpretation of calcite-dominated cool-water carbonates. As a result, several models were proposed to explain the style of sedimentation in cool-water carbonate settings. This study presents a new contribution to the rapidly evolving research interest on the genesis of cool-water carbonate sediments, their characteristics, and their response to various diagenetic modifications through time. A model is proposed, based on facies analysis, for the style of deposition and cyclicity of the cool-water, Oligocene-Miocene, Port Vincent Limestone. The fundamental depositional unit is a metre-scale, warming-upward, hardground-bounded, subtidal cycle formed by extrinsic controls (mainly climatic changes and sealevel fluctuations), which governed several intrinsic controls (mainly seafloor cementation). Comparison with Cenozoic and modern high-energy, swell-dominated, open shelf models around southern Australia and New Zealand reveal that the Port Vincent Limestone, though deposited in an enclosed intracratonic basin, show little differences in it's general facies and diagenetic characteristics with those of the open shelf examples. Main differences are attributed to the size of the depositional platform (St. Vincent Basin being smaller and shallower) as well as depth related factors which governed the hydrodynamic controls on sediment production and accumulation. Depths in the St. Vincent Basin have not been reported to exceed 130 m. Therefore, unlike deposits of high-energy open shelves, the Port Vincent Limestone lacks deep open-shelf facies belts (shelf edge and deeper) that are enriched with fine intensively reworked bioclastic sand and mud, extensive biostromal and biohermal deposits, and deep low-diversity assemblages of bryozoan growth-forms. Instead shallow inner ramp to outer middle ramp facies belts composed of bryozoan-

echinoid-foraminiferal-bivalve grainstones and rudstones dominate the Port Vincent Limestone. The lithological, faunal, floral, textural, and mineralogical characteristics of these facies belts are similar in most aspects to those deposited on the shallow parts of open shelves between the strandline and shelf edge (< 130 m). Perhaps the most obvious difference is in the condensed sized facies belts resulting from the narrow size of the St. Vincent Basin, and the decrease in percentages of planktonics in the Port Vincent Limestone possibly caused by the presence of Kangaroo Island. Furthermore, despite proximity to the land mass, terrigenous sediment content is low in the Port Vincent Limestone compared to that contained in shallow open shelf sediments, which could well be an indication to the reduced effect of lowstand events in small basins. Overall, the facies pattern is unlike that described from cool-water shelves in the North Atlantic (Wilson, 1979; Scoffin et al., 1980) and the cold Nordic sea (Henrich et al., 1995). There are no barnacle and serpulid rich facies as in the North Atlantic example, nor are there any reefal coralline algal frameworks as in the inner shelves along the coast of Troms District in northern Norway and the northern Brittany coast.

Textural relationships between digenetic fabrics revealed the diagenetic history of the Port Vincent Limestone rock body. One of the main cited views on cool-water carbonate diagenesis is their lack of synsedimentary marine cements, due mainly to temperate waters being colder and bearing lower carbonate saturations compared to tropical waters. This property lead to the suggestion that diagenesis in cool-water settings is "destructive" involving processes such as maceration, grain bioerosion and dissolution rather than cementation. As a result, the taphonomic loss due to rapid dissolution would occlude the development of marine carbonate cement precipitation. Contrary to these earlier notions, this study shows that only minor evidence of chemical carbonate dissolution occurs, and that synsedimentary marine cement is locally developed in cool-water carbonate deposits of the Port Vincent Limestone, particularly within hardgrounds at the top of the warming-upward, subtidal carbonate cycles. The cement is present as isopachous, non-luminescent rinds, lining both intergranular and intragranular pores. Crystals are Fe-, Mn-poor, and low

Mg-calcite, but relatively higher in Mg content than their surrounding substrates and later cements. The general requirements for cement precipitation in these cool-water settings were satisfied during times of relatively lowered sea level. Lowering sea level will elevate temperatures of the water column above the sea floor due to shallowing, and will subject the sea floor to high energy circulation enough to provide the required efficient pumping system through the sediments for cement precipitation. Since marine cement is actively forming in cool-water carbonate settings, then the magnitude of "destructive" diagenesis is much lower than earlier suggested. This leads to the conclusion that the gap between net carbonate production and gross production caused by loss due to destructive diagenesis is much smaller than assumed, and thus views on rates of production and accumulation in cool-water carbonate settings should be adjusted accordingly.

Unlike tropical carbonates, which are mainly dominated by aragonitic components, sediments in cool-water systems are dominated by calcitic components which contain variable amounts of magnesium and therefore have a low diagenetic potential. As a result, rapid transformation of cool-water carbonate sediments to rocks, by series of dissolution-reprecipitation of cements in the meteoric environment is insignificant, and therefore the majority of cool-water carbonate deposits remain friable and highly porous.

Localised, fabric destructive, sucrosic dolomite was formed under shallow burial conditions, replacing calcite-dominated cool-water carbonate components. Dedolomitisation is not well developed, despite common dolomite dissolution and presence of narrow rhomb-shaped intracrystalline voids.

The Port Vincent Limestone model provides essential environmental information which is critical for the interpretation of other cool-water carbonate sequences in the rock record. It is also anticipated that this study complements other studies of Cenozoic cool-water carbonates in the Australia-New Zealand region in providing a link between modern cool-water carbonates and older deposits. Many older shallow-water carbonate deposits, though not necessarily produced in typical cool-water environments, may poses similar

characteristics of Cenozoic cool-water carbonates. For example, many early to middle Palaeozoic sediments are composed mostly of calcitic components and lack a reefal framework, thus being subjected to conditions similar to those acting on unrimmed platforms. Therefore, unravelling the depositional and diagenetic environments of such ancient deposits may well be achieved based on concepts derived from the cool-water carbonate model.

The depositional and diagenetic characteristics of the Port Vincent Limestone can be summarised in the following points:

1- The Port Vincent Limestone is intermittently exposed for approximately 50 km along the east coast of Yorke Peninsula, on the western margin of the St. Vincent Basin in South Australia. The sediments accumulated during the uppermost Early Oligocene to Early Miocene time when the St. Vincent Basin was lying south of latitude 50° S.

2- Rocks are mainly soft and friable with several massive well-lithified marine hardgrounds punctuating the sequence. Hardground surfaces are mechanically and biologically eroded and stained with red-brown iron oxides. Transition from friable to hard lithologies were brought about by a facies change, which stimulated subsequent selective diagenesis in the form of cementation and internal micrite precipitation.

3- The limestone is a bryozoan-dominated, cool-water calcarenite, locally enriched in foraminifers, echinoids, coralline algae, bivalves, gastropods and brachiopods. Nonskeletal grains are absent. Depositional textures are mainly grain-supported.

4- There are six major facies which are grouped into three informal members. The lower member is comprised of two facies, which represent a transgressive phase of deposition. The middle member is comprised of five warming-upward, metre-scale, hardground-bounded, subtidal, carbonate cycles, and two shallowing-upward wholly cool-water cycles. Warming was brought about by an overall temperature rise in the environment

(climatic changes and/or oceanic currents), acting in concert with relative sealevel fall. The upper member is comprised of one single facies.

5- The warming-upward carbonate cycles are capped by biologically and mechanically eroded hardgrounds that are stained by red-brown iron oxides. The bulk of all cycles (basal and middle units) are formed from largely similar bryozoan facies. Basal units consist of shallow, high-energy bryozoan calcirudite associated with epifaunal organisms, all characteristic of hard substrates. Middle units are mainly well-sorted bryozoan grainstones dominated by delicate branching cyclostomes and articulated branching cheilostomes. The upper units are composed of bryozoan-*Amphistegina* hardground facies. The style and cause of cyclicity in the Port Vincent Limestone is similar to that found in other Tertiary cool-water carbonates elsewhere, with the exception of the bryozoan-*Amphistegina* hardground cap. The cyclicity can be explained in terms of processes operating in the modern environment today in the same geographic area.

6- Rocks of the Port Vincent Limestone underwent various diagenetic alterations since their deposition, with cementation and dolomitisation being of particular importance. Cement is limited and precipitated in three diagenetic environments: the seafloor, shallow-burial, and meteoric. Seafloor cementation was synsedimentary, affecting each warming-upward carbonate depositional cycle separately (phase-1); whereas later shallow-burial and meteoric cementation affected the three members of the entire succession together (phase-2).

7- Marine dissolution in the cool-water Port Vincent Limestone is a significant early diagenetic process which contributes to the supply of $CaCO_3$ for cementation. Little cement is produced by mild intergranular pressure solution as evident from slightly- to non-sutured grain contacts. This paucity is expected since the rocks have only undergone shallow burial. Meteoric dissolution is an additional sources for cement, as evident from numerous moulds of aragonitic bivalves and bryozoans in the rocks.

8- Dolomitisation was local, replacing only a small volume of the Port Vincent Limestone, within Early Oligocene beds. The dolomite is non-pseudomorphic, has a planar-e texture, and forms an idiotopic sucrosic mosaic with an estimated intercrystalline and intracrystalline porosity reaching 40%. The process was early and occurred shortly after deposition as indicated by petrography and isotope data. All original components were dolomitised regardless of their mineralogy (mainly LMC and IMC), suggesting a high saturation state of the dolomitising fluid. The Port Vincent Limestone dolomite precipitated from moderately reducing pore fluids, such as that present in shallow-burial environments below the sediment-seawater interface.

9- Dolomite dissolution was common affecting only small parts of the crystal, and producing rhomb-shaped intracrystalline voids. Dedolomitisation, however, is rare and restricted to a few scattered rhombs which appear to contain microdissolution voids. Recent surface weathering of the dolomite by dolomite-seawater interaction produces an iron hydroxide crust which gives the Port Vincent Limestone dolomite its rusty yellowish brown coloured appearance.

10- Lateral and vertical facies analysis of the Port Vincent Limestone indicates deposition during a transgressive phase, on a cool-water carbonate ramp, characterised by environments ranging from a shallow inner ramp to the deeper outer part of a middle ramp. The warming-upward carbonate cycles represent fourth-order parasequences that developed during high frequency fourth-order sealevel fluctuations and are superimposed on the longer term third-order cycle. Each parasequence resembles a mini third-order cycle in it's systems tracts components. The three building units (facies) of each warming-upward cycle represent three distinctive systems tracts.

REFERENCES

REFERENCES

ADAMS, J. E. AND RHODES, M. L., 1960, Dolomitization by seepage refluxion: American Association of Petroleum Geologists Bulletin, v. 44, p. 1912 - 1920.

ADAMS, C. G., LEE, D. E., AND ROSEN, B. R., 1990, Conflicting isotopic and biotic evidence for tropical sea-surface temperatures during the Tertiary: Palaeogeography, Palaeoclimatology, and palaecology, v. 77, p. 289 - 313.

AHR, W.M., 1973, The carbonate ramp: an alternative to the carbonate shelf model: Transactions of the Gulf Coast Association of Geological Societies, v. 23, p. 221-225.

AL-HASHIMI, W. S., 1976, Significance of strontium distribution in some carbonate rocks in the Carboniferous of Northumberland, England: Journal of Sedimentary Petrology, v. 46, p. 369 - 376.

AL-HASHIMI, W. S., 1977, Recent carbonate cementation from seawater in some weathered dolostones, Northumberland, England: Journal of Sedimentary Petrology, v. 47, p. 1375 - 1391.

AL-HASHIMI, W. S. AND HEMINGWAY, J. E., 1973, Recent dedolomitization and the origin of the Rusty Crusts of Northumberland: Journal of Sedimentary Petrology, v. 43, p. 82 - 91.

ALEXANDERSSON, E.T., 1978, Destructive diagenesis of carbonate sediments in the eastern Skagerrak, North Sea: Geology, v. 6, p. 324-327.

ALEXANDERSSON, E.T., 1979, Marine maceration of skeletal carbonates in the eastern Skagerrak, North Sea: Sedimentology, v. 26, p. 845-852.

ALLAN, J. R. AND WIGGINS, W. D., 1993, Dolomite reservoirs, geochemical techniques for evaluating origin and distr1963) Petroleum Geologists, continuing education course note series 36, 129 p.

ALLEY, N. F. AND CLARKE, J. D. A., 1992, Stratigraphy and palynology of Mesozoic sediments from the Great Australian Bight area, southern Australia: BMR Journal of Australian Geology and Geophysics, v. 13, p. 113 - 129.

ALLEY, N. F. AND LINDSAY, J. M., 1995, Tertiary, *in* Drexel, J. F. and Preiss, W. V., eds., The geology of South Australia - Volume 2 The Phanerozoic: Mines and Energy, South Australia, p. 151 - 218.

AMIEUX, P., BERNIER, P., DALONGEVILLE, R., AND MEDWECKI, V., 1989, Cathodoluminescence of carbonate-cemented Holocene beachrock from the Togo coastline (West Africa): an approach to early diagenesis: Sedimentary Geology, v. 65, p. 261-272.

BADIOZAMANI, K., 1973, The Dorag dolomitization model, Application to the Middle Ordovician of Wisconsin: Journal of Sedimentary Petrology, v. 43, p. 965 - 984.

BANDY, O. L., 1964, Foraminiferal biofacies in sediments of Gulf of Batabano, their geological significance: American Association of Petroleum Geologists Bulletin, v. 48, p. 1666-1679.

BANNER, J. L., 1995, Application of the trace element and isotope geochemistry of strontium to studies of carbonate diagenesis: Sedimentology, v. 42, p. 805 - 824.

BATHURST, R. G. C., 1975, Carbonate Sediments and Their Diagenesis (2nd ed.): Amsterdam, Developments in Sedimentology 12, Elsevier, 658 p.

BEHRENS, E. W. AND LAND, L. S., 1972, Subtidal Holocene dolomite, Buffin Bay, Texas: Journal of Sedimentary Petrology, v. 42, p. 155 - 161.

BENSON, W. N., 1911, Note descriptive of a stereogram of the Mount Lofty Ranges, South Australia: Transactions of The Royal Society of South Australia, v. 35, p. 108 - 111.

BERGGREN, W. A. AND PROTHERO, D. R., 1992, Eocene-Oligocene climatic and biotic evolution: an overview, *in* Prothero, D. R, and Berggren, W. A., eds., Eocene-Oligocene climatic and biotic evolution: Princeton University Press, Princeton, p. 1-28.

BERNECKER, T., WEBB, J. A., AND PARTRIDGE, A. D., 1995, Carbonate Deposition of the Seaspray Group in the offshore Gippsland Basin (abs.): Cool and cold water carbonate conference, 14th-19th January Geelong, Victoria, Australia, p. 5 - 6.

BETJEMAN, K. J., 1969, Recent foraminifera from the western continental shelf of western Australia: Contribution Cushman Foundation of Foraminiferal Research, v. 20, p. 119-138.

BETZLER, C. AND CHAPRONIERE, G. C. H., 1993, Paleogene and Neogene larger foraminifers from the Queensland Plateau: Biostratigraphy and environmental significance: Proceedings of the Ocean Drilling Program, Scientific Results, v. 133, p. 51-66.

BIGNOT, G., 1985, Elements of Micropalaeontology: London, Graham and Trotman Limited, Sterling House, 217 p.

BLOM, W.M. AND ALSOP, D.B., 1988, Carbonate mud sedimentation on a temperate shelf: Bass Basin, Southeastern Australia, *in* Nelson C.S., ed., Non-tropical Shelf Carbonates-Modern and Ancient: Sedimentary Geology, v. 60, p. 301-322.

BMR, 1979, BMR Earth Science Atlas: Canberra, Australia Bureau of Mineral Resources, Geology and Geophysics.

BOARDMAN, R. S., CHEETHAM, A. H., AND ROWELL, A. J., 1987. Fossil Invertebrates. Blackwell Scientific Publications, 713 p.

BONE, Y., JAMES, N. P., AND KYSER, T. K., 1992, Synsedimentary detrital dolomite in Quaternary cool-water sediments, Lacepede Shelf, southern Australia: Geology, v. 20, p. 109 - 112.

BONE, Y. AND JAMES, N. P., 1993, Bryozoans as carbonate sediment producers on the cool-water Lacepede Shelf, southern Australia: Sedimentary Geology, v. 86, p. 247-271.

BONE, Y., CLARKE, J. A., AND JAMES, N. P., 1994, Carbonate sediments of the Woody Island, Esperance region, Western Australia (abs.): Perth, Geological Society of Australia, 12th Australian Geological Convention, p. 34.

BOREEN, T. D., 1993, Cenozoic Cool-Water Carbonates, southeastern Australia: Unpublished Ph.D. Thesis, Queen's University, Kingston, Ontario, Canada, 198 p.

BOREEN, T., JAMES, N. P., WILSON, C., AND HEGGIE, D., 1993, Surficial cool-water carbonate sediments on the Otway continental margin, southeastern Australia: Marine Geology, v. 112, p. 35 - 56.

BOREEN, T. D. AND JAMES, N. P., 1995, Stratigraphic sedimentology of Tertiary cool-water limestones, SE Australia: Journal of Sedimentary Research, v. B65, no. 1, p. 142 - 159.

BRAND, U. AND VEIZER, J., 1980, Chemical diagenesis of a multicomponent carbonate system-1, trace elements: Journal of Sedimentary Petrology, v. 50, no. 4, p. 1219-1236.

BROOKFIELD, M. E., 1988, A mid-Ordovician temperate carbonate shelf-the Black River and Trenton Limestone Groups of southern Ontario, Canada, *in* Nelson, C.S., ed., Non-tropical Shelf Carbonates - Modern and Ancient: Sedimentary Geology, v. 60, p. 137-153.

BRUCKSCHEN, P., NEUSER, R. D., AND RICHTER, D. K., 1992, Cement stratigraphy in Triassic and Jurassic limestones of the Weserbergland (northwestern Germany): Sedimentary Geology, v. 81, p. 195-214.

BRUHN, F., BRUCKSCHEN, P., RICHTER, D. K., MEIJER, J., STEPHAN, A., AND VEIZER, J., 1994, Diagenetic history of sedimentary carbonates: Constraints from combined cathodoluminescence and trace element analyses by micro-PIXE: Proceedings of the 4th International Conference on Nuclear Microprobe Technology and Applications, Shanghai, October 1994, (Nuclear Instruments and Methods in Physics, Research B)

BUDD, D. A., 1992, Dissolution of high-Mg calcite fossils and the formation of biomolds during mineralogical stabilization: Carbonates and Evaporites, v. 7, no. 1, p. 74-81

BUDD, D. A. AND HIATT, E. E. , 1993, Mineralogical stabilization of high-Mg calcite: Geochemical evidence for intracrystal recrystallization within Holocene porcellaneous foraminifera: Journal of Sedimentary Petrology, v. 63, no. 2, p. 261-274.

BURCHETTE, T.P. AND WRIGHT, V.P., 1992, Carbonate ramp depositional systems, *in* Sellwood, B.W., ed., Ramps and Reefs: Sedimentary Geology, v. 79, p. 3-57.

BURKE, W. H., DENISON, R. E., HETHERINGTON, E. A., KOEPNICK, R. B., NELSON, H. F., AND OTTO, J. B., 1982, Variation of seawater $^{87}Sr/^{86}Sr$ throughout Phanerozoic time: Geology, v. 10, p. 516 - 519.

CAMPANA, B. AND WILSON, B., 1954, The geology of Jervis and Yankalilla Military Sheets: Reports investigation and geological survey, South Australia, 3, p. 1 - 24.

CAREY, J. S., MOSLOW, T. F., AND BARRIE J. V., 1995, Origin and Distribution of Holocene Temperate Carbonates, Hecate Strait, Western Canada Continental Shelf: Journal of Sedimentary Research, v. A65, no. 1, p. 185-194.

CARPENTER, S. J. AND LOHMANN, K. C., 1992, Sr/Mg ratios of modern marine calcites: Empirical indicators of ocean chemistry and precipitation rate: Geochimica et Cosmochimica Acta, v. 56, p. 1837 - 1849.

CHAVE, K. E., 1967, Recent carbonate sediments: an unconventional view: Journal of Geological Education, v. 15, p. 200 - 204.

CHOQUETTE, P. W. AND PRAY, L. C., 1970, Geologic nomenclature and classification of porosity in sedimentary carbonates: American Association of Petroleum Geologists Bulletin, v. 54, p. 207-250.

CHOQUETTE, P. W. AND JAMES, N. P., 1990, Limestones-The Burial Diagenetic Environment, *in* McIlreath, I. A. and Morrow, D. W., eds., Diagenesis: Geoscience Canada Reprint Series 4, p. 75-112.

CHRISTIE-BLICK, N., 1991, Onlap, offlap, and the origin of unconformity-bounded depositional sequences: Marine Geology, v. 97, p. 35 - 56.

CLARKSON, E. N. K., 1993. Invertebrate Palaeontology and Evolution. Third edition, Chapman and Hall, 434 p.

COLLINS, L. B., 1988, Sediments and History of the Rottnest Shelf, southwest Australia: a swell - dominated, non tropical carbonate margin, *in* Nelson, C. S., ed., Non-tropical Shelf Carbonates - Modern and Ancient: Sedimentary Geology, v. 60, p. 15 - 50.

CONIGLIO, M., JAMES, N. P., AND AISSAOUI, D. M., 1988, Dolomitization of Miocene carbonates, Gulf of Suez, Egypt: Journal of Sedimentary Petrology, v. 58, p. 100-119.

CONOLLY, J. R. AND von der BORCH, C. C., 1967, Sedimentation and Physiography of the sea floor south of Australia: Sedimentary Geology, v. 1, p. 181-220.

COOPER, B. J., 1977, New revised stratigraphic nomenclature in the Willunga Embayment: Quarterly Notes of the Geological Survey of South Australia, v. 64, p. 2 - 5.

COOPER, B. J., 1985, The Cainozoic St. Vincent Basin - tectonics, structure, stratigraphy: Adelaide, South Australian Department of Mines and Energy, Special Publication 5, p. 35-49.

COOPER, B. J. AND LINDSAY, J. M., 1978, Marine entrance to the Cainozoic St. Vincent Basin: Quarterly Geological Notes, Geological Survey of South Australia, v. 67, p. 4-6.

CRAWFORD, A. R., 1965, The Geology of Yorke Peninsula: Adelaide, Geological Survey of South Australia Bulletin 39, 96 p.

CUSHMAN, J. A., 1950, Foraminifera, Their Classification and Economic Use (4th ed.): Cambridge, Harvard University press, 650 p.

DAILY, B., FIRMAN, J. B., FORBES, B. G., AND LINDSAY, J. M., 1976, Geology, *in* Twidale, C. R., Tyler, M. J., and Webb, B. P., eds., Natural History of the Adelaide Region: Adelaide, Royal Society of South Australia, p. 5-42.

DAILY, B., MILNES, A. R., TWIDALE, C. R., AND BOURNE, J. A., 1979, Geology and Geomorphology, *in* Tyler, M. J., Twidale, C. R., and Ling, J. K., eds., Natural History of Kangaroo Island: Royal Society of South Australia, Adelaide, South Australia, p. 1-38.

DEVEREUX, I., 1967, Oxygen isotope palaeotemperature measurements on New Zealand Tertiary fossils. New Zealand Journal of Science, v. 10, p. 988-1011.

DEWERS, T. AND ORTOLEVA, P., 1994, Formation of stylolites, marl/limestone alternations, and dissolution (clay) seams by unstable chemical compaction of argillaceous carbonates: *in* Wolf, K. H., and Chilingarian, G. V., eds., Diagenesis IV: Developments in Sedimentology 51, Elsevier, p. 155-216.

DICKSON, J. A. D., 1966, Carbonate identification and genesis as revealed by staining: Journal of Sedimentary Petrology, v. 36, p. 491-505.

DOROBEK, S. L., 1987, Petrography, geochemistry, and origin of burial diagenetic facies, Siluro-Devonian Helderberg Group (Carbonate Rocks), Central Appalachians: American Association of Petroleum Geologists Bulletin, v. 71, p. 492-514.

DROMGOOLE, E. L. AND WALTER, L. M., 1990, Iron and manganese incorporation into calcite: Effects of growth kinetics, temperature and solution chemistry: Chemical geology, v. 81, p. 311 - 336.

DROOGER, C. W. AND KAASSCHIETER, J. P. H., 1958, Foraminifera of the Orinoco-Trinidad-Paria Shelf, *in* Larsen, A. R., 1976, Studies of Recent *Amphistegina,* Taxonomy and some Ecological Aspects: Israel Journal of Earth Sciences, v. 25, p. 1-26.

DUNHAM, R. J., 1962, Classification of carbonate rocks according to depositional texture, *in* Ham, W. E., ed., Classification of Carbonate Rocks: Tulsa, American Association of Petroleum Geologists Memoir 1, p. 108-121.

EMERY, D. AND DICKSON, J. A. D., 1989, A syndepositional meteoric phreatic lens in the Middle Jurassic Lincolnshire Limest986) Geology, v. 65, p. 273-284.

EVAMY, B. D. AND SHEARMAN, D. J., 1965, The development of overgrowths from echinoderm fragments: Sedimentology, v. 5, p. 211-233.

EVAMY, B. D. AND SHEARMAN, D. J., 1969, Early stages in development of overgrowths on echinoderm fragments in limestones: Sedimentology, v. 12, p. 317-322.

FENNER, C., 1927, Adelaide South Australia: a study in human geography: Transactions of The Royal Society of South Australia, v. 51, p. 193 - 236.

FENNER, C., 1930, The major structural and physiographic features of South Australia: Transactions of The Royal Society of South Australia, v. 54, p. 1 - 36.

FLÜGEL, E., 1982, Microfacies Analysis of Limestones (Translated by K. Christenson): Berlin, Springer-Verlag, 633 p.

FOLK, R. L., 1959, Practical classification of limestones: American Association of Petroleum Geologists Bulletin, v. 43, p. 1-38.

FOLK, R. L. AND LAND, L. S., 1975, Mg/Ca ratio and salinity: Two controles over crystallization of dolomite: American Association of Petroleum Geologists Bulletin, v. 59, p. 60 - 68.

FRAKES, L. A., 1986. Mesozoic-Cenozoic Climatic History and Causes of the Glaciation. Reprinted from Mesozoic and Cenozoic Oceans, Geodynamics Series, American Geophysical Union, v. 15, p 33.

FRANK, J. R., CARPENTER, A. B., AND OGLESBY, T. W., 1982, Cathodoluminescence and composition of calcite cement in the Taum Sauk Limestone (Upper Cambrian), Southeast Missouri: Journal of Sedimentary Petrology, v. 52, p. 631-638.

FRASER, D. G., FELTHAM, D., AND WHITEMAN, M., 1989, High-resolution scanning proton microprobe studies of micron-scale trace element zoning in a secondary dolomite: implications for studies of redox behaviour in dolomites: Sedimentary Geology, v. 65, p. 223-232.

FRIEDMAN, G. M., 1964, Early diagenesis and lithification in carbonate sediments: Journal of Sedimentary Petrology, v. 34, p. 777-813.

FULLER, M. K., BONE, Y., GOSTIN, V. A., AND von der BORCH, C. C., 1994, Holocene cool-water carbonate and terrigenous sediments from southern Spencer Gulf, South Australia: Australian Journal of Earth Science, v. 41, p. 353-363.

GALLOWAY, W. E., 1989, Genetic stratigraphic sequences in basin analysis I: architecture and genesis of flooding-surface bounded depositional units. American Association of Petroleum Geologists, Bulletin 73, p. 125 - 142.

GINSBURG, R. N., 1971, Landward movement of carbonate mud: New model for regressive cycles in carbonates [abs]: American Association of petroleum Geologists Bulletin, v. 55, p. 340.

GINSBURG, R.N. AND JAMES, N.P., 1974, Holocene carbonate sediments of continental margins, *in* Burke, C.A., and Drake C.L., eds., The geology of continental margins: New York, Springer-Verlag, p. 137-155.

GLAESSNER, M. F., 1953, Some problems of Tertiary geology in southern Australia: Proceedings of the Royal Society of New South Wales, v. 87, p.31 - 45.

GLAESSNER, M. F., 1959, Tertiary stratigraphic correlation in the Indo-Pacific region and Australia: Journal of the Geological Society of India, v. 1, p. 153 - 157

GLAESSNER, M. F. AND WADE, M., 1958, The St. Vincent Basin, *in* Glaessner, M. F. and Parkin, L.W., ed., The Geology of South Australia: Journal of the Geological Society of Australia, v. 5, p. 115-126.

GOLDSMITH, J. R., GRAF, D. L., AND HEARD, H. C., 1961, Lattice constants of the calcium-magnesium carbonates: American Mineralogist, v. 46, p. 453 - 457.

GÖRÜR, N., 1979, Downward development of overgrowths from echinoderm fragments in a submarine environment: Sedimentology, v. 26, p. 605-608.

GOSTIN, V. A., BELPERIO, A. P., AND CANN, J. H., 1988, The Holocene non-tropical coastal and shelf carbonate province of southern Australia, *in* Nelson, C. S., ed., Non-tropical Shelf Carbonates-Modern and Ancient: Sedimentary Geology, v. 60, p. 51-70.

GROVER, J., JR. AND READ, J. F., 1983, Paleoaquifer and Deep Burial Related Cements Defined by Regional Cathodoluminescence Patterns, Middle Ordovician Carbonates, Virginia: American Association of Petroleum Geologists Bulletin, v. 67, p. 1275-1303.

HALLEY, R. B. AND HARRIS, P. M. , 1979, Fresh water cementation of a 1,000-year-old oolite: Journal of Sedimentary Petrology, v.49, p. 969-988.

HALLOCK, P., 1979, Trends in test shape with depth in large symbiont-bearing foraminifera: Journal of Foraminiferal Research, v. 9, p. 61-69.

HALLOCK, P., 1981, Light dependence in *Amphistegina*: Journal of Foraminiferal Research, v. 11, p. 40-46.

HALLOCK, P., FORWARD, L. B., AND HANSEN, H. J., 1986, Influence of environment on the test shape of *Amphistegina*: Journal of Foraminiferal Research, v. 16, p. 224-231.

HANDFORD, C.R. AND LOUCKS, R.G., 1993, Carbonate depositional sequences and systems tracts. Responces of carbonate platforms to relative sea level changes, *in* Loucks, R. G., and Fredrick, J. Sarg, eds., Carbonate sequence strtigraphy-recent developments and applications: American Association of Petroleum Geologists, Memoir 57, p. 3-41.

HANSEN, H. J. AND BUCHARDT, B., 1977, Depth distribution of *Amphistegina* in the Gulf of Elat, Israel: Utrecht Micropaleontological Bulletins, v. 15, p. 205-224.

HANSHAW, B. B., BACK, W., AND DIEKE, R. G., 1971, a geochemical hypothesis for dolomitization by groundwater: Economic geology, v. 66, p. 710 - 724.

HAQ, B. U., HARDENBOL, J., AND VAIL, P. R., 1987, Chronology of fluctuating sea levels since the Triassic: Science, v. 235, p 1156 - 1167.

HAQ, B. U., HARDENBOL, J., AND VAIL, P. R., 1988, Mesozoic and Cenozoic chronostratigraphy and cycles of sea level changes, *in* Wilgus, C. K., Hastings, B. S., Kendall, C. G. St. C., Posamentier, H. W., Ross, C. A., and Van Wagoner, J. C., eds., Sea Level Changes: An Integrated Approach: SEPM Special Publication No. 42, p. 71 - 109.

HARRIS, W. K., 1966, New and redefined names in South Australian Lower Tertiary stratigraphy: Quarterly notes of the geological survey of South Australia, v. 20, p. 1-3.

HARRIS, W. K., 1985, Middle to Late Eocene depositional cycles and dynoflagellate zones in southern Australia: Special Publication, South Australian Department of Mines and Energy, no. 5, p. 133 - 144.

HARTMANN, M., MULLER, P. J., SUESS, E., AND Van der WEIJDEN, C. H., 1976, Chemistry of late Quaternary sediments and their interstitial waters from the N. W. African continental margin: Meteor-Supply Pap. Geological Survey, 24, p. 1-67.

HEATH, R. S. AND McGOWRAN, B., 1984, Neogene datum planes: foraminiferal successions in Australia with reference sections from the Ninety-east Ridge and the Ontong-Java Plateau, *in* Ikebe N. and Tsuchi R. (eds.), Pacific Neogene datum Planes: Contributions to Biostratigraphy and Chronology, University of Tokyo Press, Tokyo, p. 187 - 192.

HENRICH, R., FREIWALD, A., BETZLER, C., BADER, B., SCHAFER, P., SAMTLEBEN, C., BRACHERT, T. C., WEHRMANN, A., ZANKL, H., AND KUHLMANN, D., H., H., 1995. Controls on modern carbonate sedimentation on warm-temperate to Arctic-coasts, shelves and seamounds in the northern hemisphere: Implications for fossil counterparts: Facies, v. 32, pp. 71 - 108.

HORBURY, A. D. AND ADAMS, A. E., 1989, Meteoric phreatic diagenesis in cyclic late Dinantian carbonates, northwest England: Sedimentary Geology, v. 65, p. 319-344.

HORNIBROOK, N. de B., 1968, Distribution of some warm water benthic foraminifera in the New Zealand Tertiary: Tuatara, v. 16, p 11-15.

HORNIBROOK, N. de B., 1971. New Zealand Tertiary climate. Reports of the New Zealand Geological Survey no. 47.

HOWCHIN, W., 1886, Remarks on a geological section at the New Graving Dock, Glanville, with special reference to a supposed old land surface now below sea level: Transactions of the Royal Society of South Australia, v. X, p. 31-35.

HOWCHIN, W., 1903, Further notes on the geology of Kangaroo Island: Transactions of the Royal Society of South Australia, v. 27, p. 75-90.

HOWCHIN, W., 1911, Description of a disturbed area of Cainozoic rocks in South Australia with remarks on its geological significance: Transactions of the Royal Society of South Australia, v. 35, p. 47 - 59.

HOWCHIN, W. AND PARR, W. J., 1938, Notes on the geological features and the foraminiferal fauna of the Metropolitat Abbattoirs Bore, Adelaide: Transaction of the Royal Society of South Australia, v. 62, p. 287 - 317.

ILLING, L. V., WELLS, A. J., AND TAYLOR, J. C. M., 1965, Penecontemporaneous dolomite in the Persian Gulf, *in* Murray, R. C. and Pray, L. C., ed., dolomitization and limestone diagenesis: Special Publication Society of Economic Palaeontologists and Mineralogists, v. 13, p. 89 - 111.

JACOBSON, R. L. AND USDOWSKI, H. E., 1976, Partitionong of strontium between calcite, dolomite and liquids: an experemental study under higher temperature diagenetic conditions and the model for the prediction of mineral pairs for geothermometry: Contributions to Mineralogy and Petrology, v. 59, p. 171 - 185.

JAMES, N. P., 1995. Paleozoic cryocarbonates: charlatans in the mist ? (abs.): Cool and cold water carbonate conference, 14th-19th January Geelong, Victoria, Australia, p. 43.

JAMES, N. P. AND BONE, Y., 1989, Petrogenesis of Cenozoic, temperate water calcarenites, South Australia: A model for meteoric/shallow burial diagenesis of shallow water calcite sediments: Journal of Sedimentary Petrology, v. 59, no. 2, p. 191-203.

JAMES, N. P. AND BONE, Y., 1991, Origin of a cool-water, Oligo-Miocene deep shelf limestone, Eucla Platform, southern Australia: Sedimentology, v. 38, p. 323-341.

JAMES, N. P. AND BONE, Y., 1992, Synsedimentary cemented calcarenite layers in Oligo-Miocene cool-water shelf limestones, Eucla Platform, Southern Australia: Journal of Sedimentary Petrology, v. 62, no. 5, p. 860-872.

JAMES, N. P. AND BONE, Y., 1994, Paleoecology of cool-water, subtidal cycles in Mid-Cenozoic limestones, Eucla Platform, Southern Australia: Palaios, v. 9, p. 457-476.

JAMES, N. P. AND CHOQUETTE, P.W., eds., 1988, Paleokarst: Springer-Verlag, New York, 416 p.

JAMES, N. P. AND CHOQUETTE, P.W., 1990a, Limestones-The Sea-Floor Diagenetic Environment, *in* McIlreath, I. A. and Morrow, D. W., eds., Diagenesis: Geoscience Canada, Reprint Series 4, p. 13-34.

JAMES, N. P. AND CHOQUETTE, P.W., 1990b, Limestones-The Meteoric Diagenetic Environment, *in* McIlreath, I. A. and Morrow, D. W., eds., Diagenesis: Geoscience Canada, Reprint Series 4, p. 35-74.

JAMES, N. P. AND GINSBURG, R. N., 1979, The seaward margin of Belize barrier and atoll reefs: International Association of Sedimentologists, Special Publication 3, 199p.

JAMES, N. P. AND KENDALL, A. C. 1992. Introduction to carbonate and evaporite facies models, *in* Walker R.G. and N.P. James, eds., Facies models-response to sea level change: Geological Association of Canada, pp. 265 - 275.

JAMES, N. P., BONE, Y., von der. BORCH C. C., AND GOSTIN, V. A., 1992, Modern carbonate and terrigenous clastic sediments on a cool-water, high energy, mid-latitude shelf: Lacepede, southern Australia: Sedimentology, v. 39, p. 877-903.

JAMES, N. P., BONE, Y., AND KYSER, T. K., 1993, Shallow burial dolomitization and dedolomitization of Mid-Cenozoic, cool-water, calcitic, deep-shelf limestones, Southern Australia: Journal of Sedimentary Petrology, v. 63, p. 528-538.

JAMES, N. P., BOREEN T. D., BONE, Y., AND FEARY D. A., 1994, Holocene carbonate sedimentation on the west Eucla Shelf, Great Australian Bight: a shaved shelf: Sedimentary Geology, v. 90, p. 161-177.

JENNINGS, J.N., 1985, Karst geomorphology: Oxford, Basil Blackwell, 293 p.

JONES, B. AND DESROCHERS, A., 1992, Shallow platform carbonates, *in* Walker, R.G., and James, N.P., eds., Facies models-response to sea level change: Geological Association of Canada, 15, p. 277 - 301.

JONES, H. A. AND DAVIES, P. J., 1983, Superficial sediments of the Tasmanian continental shelf and part of Bass Strait: Bulletin of the Bureau of Mineral Resources, Geology and Geophysics, v. 218, 25 P.

KAMP, P. J. J., WAGHOM, D. B., AND NELSON, C. S., 1990, Late Eocene-Early Oligocene integrated isotope stratigraphy and biostratigraphy for paleoshelf sequences in southern Australia: paleoceanographic implications: Palaeogeography, palaeoclimatology, palaeoecology, v. 80, p. 311-323.

KATZ, A. AND MATTHEWS, A., 1977, The dolomitization of $CaCO_3$: an experemental study at 252 - 295°C: Geochimica et Cosmochimica Acta, v. 41, p. 297 - 308.

KEMP, E. M., 1978, Tertiary climatic evolution and vegetation history in the southeast Indian Ocean region: Palaeogeography, Palaeoclimatology, Palaeoecology, v. 24, p. 169 - 208.

KENNETT, J. P. AND BARKER, P. F., 1990, Latest Cretaceous to Cenozoic climate and oceanographic developments in the Weddell Sea, Antarctica: an ocean-drilling project , in Barker, P. F., and Kennett, J. P., eds., Proceedings of the Ocean Drilling Program, Scientific Results, v. 113, p. 937 - 960.

KERANS, C., HURLEY, N. F., AND PLAYFORD, P. E., 1986, Marine diagenesis in Devonian reef complexes of the Canning Basin, western Australia, *in* J. H. Schroeder and B. H. Purser, eds., Reef Diagenesis: Springer-Verlag, New York, p. 357-380.

KING, D., 1956, On a Reconnaissance geological Survey of the Proterozoic-Cambrian Succession of Yorke Peninsula with reference to Oil Exploration in the Cambrian System: South Australian Department of Mines and Energy, envelope 45, R.B. 492.

KINSMAN, D. J. J., 1969, Interpretation of Sr^{+2} concentrations in carbonate minerals and rocks: Journal of Sedimentary Petrology, v. 39, p. 486 - 508.

KINSMAN, D. J. J. AND HOLLAND, H. D., 1969, The co-precipitation of cations with $CaCO_3$ IV. The co-precipitation of Sr^{2+} with aragonite between 16° and 96°C: Geochimica et Cosmochimica Acta, v. 33, p. 1 - 17.

KRETZ, R., 1982, A model for the distribution of trace elements between calcite and dolomite: Geochimica et Cosmochimica Acta, v. 46, p. 1979 - 1981.

KRUSE, P. D., AND PHILIP, G. M., 1985. Tertiary species of the echinoid genus *Eupatagus* from southern Australia. special publication, South Australian department of Mines and Energy, No. 5, p. 167-185.

LAND, L. S. AND HOOPS, G. K., 1973, Sodium in carbonate sediments and rocks: a possible index to salinity of diagenetic solutions: Journal of Sedimentary Petrology, v. 43, p. 614 - 617.

LAND, L. S., 1980, The isotopic and trace element geochemistry of dolomite: the state of the art, *in* Zenger, D. H., Dunham, J. B., and Ethington, R. L., eds., Concepts and models of dolomitization: Society of Economic Paleontologists and Mineralogists, Special Publication, 28, p. 87-110.

LAND, L. S., 1985, The origin of massive dolomite: Journal of Geological Education, v. 33, p. 112 - 125.

LAND, L. S., 1991, Dolomitization of the Hope Gate Formation (north Jamaica) by seawater: Reassessment of mixing-zone dolomite, *in* Taylor, H. P. Jr., O'Neil, J. R., and Kaplan, I. R., eds., Stable Isotope

Geochemistry: A tribute to Samuel Epstein: The Geochemical Society Special Publication 3, p. 121 - 133.

LARSEN, A. R., 1976, Studies of Recent *Amphistegina,* Taxonomy and some Ecological Aspects: Israel Journal of Earth Sciences, v. 25, p. 1-26.

LARSEN, G. AND CHILINGAR, G. V., 1979, Diagenesis of sediments and rocks, *in* Larsen, G. and Chilingar, G. V., eds., Diagenesis in sediments and sedimentary rocks: Amsterdam, Developments in Sedimentology 25A, Elsevier, p. 1-29.

LEES, A. AND BULLER A. T., 1972, Modern temperate-water and warm-water carbonate sediments contrasted: Marine Geology, v. 13, M67 - M73.

LI, Q. AND McGOWRAN, B., 1994, Miocene upwelling events: Neritic foraminiferal evidence from southern Australia: Australian Journal of Earth Sciences, v. 41, p. 593-603.

LI, Q., McGOWRAN, B., JAMES, N. P., AND BONE, Y., 1996, Foraminiferal biofacies on the mid-latitude Lincoln Shelf, South Australia: oceanic and sedimentological implications: Marine Geology, v. 129, p. 285 - 312.

LINDSAY, J. M., 1967, Foraminifera and stratigraphy of the type section of Port Willunga Beds, Aldinga Bay, South Australia: Transactions of The Royal Society of South Australia, v. 91, p. 93 - 109.

LINDSAY, J. M., 1969, Cainozoic foraminifera and stratigraphy of the Adelaide Plains Sub-Basin, South Australia: Bulliten geological survey of South Australia, 42.

LINDSAY, J. M., 1972, Two Cainozoic fossiliferous sands from Waterloo Bay, Yorke Peninsula, South Australia: South Australian Department of Mines and Energy, report no. 72/190 (unpublished).

LINDSAY, J. M., 1981. Tertiary Stratigraphy and Foraminifera of the Adelaide City area, St. Vincent Basin, South Australia. Unpublished Ph.D. Thesis, Department of Geology and Geophysics, University of Adelaide, 900 p.

LINDSAY, J. M., 1983, Late Eocene to Late Oligocene age of the Kingskote Limestone, Kangaroo Island, South Australia: Transactions of The Royal Society of South Australia, v. 107, p. 127-128.

LINDSAY, J. M., 1985, Aspects of South Australian Tertiary foraminiferal biostratigraphy, with emphasis on studies of *Massilina* and *Subbotina*, *in* Lindsay, J. M., ed., Stratigraphy, Palaeontology and Malacology: Special Publications South Australian Department of Mines and Energy no. 5, p. 187-231.

LINDSAY, J. M. AND McGOWRAN, B. , 1986, Eocene/Oligocene boundary, Adelaide region, South Australia, *in* Pomerol, C. and Premoli - Silva, I., eds., Terminal Eocene Events: Developments in Palaeontology and Stratigraphy Series 9, Elsevier, Amsterdam, p. 165 - 173.

LONGMAN, M. W., 1980, Carbonate diagenetic textures from nearshore diagenetic environments: Bulletin American Association of Petroleum Geologists, v. 64, p. 461-487.

LUCIA, F. J., 1962, Diagenesis of a crinoidal sediment: Journal of Sedimentary Petrology, v. 32, p. 848-865.

LUDBROOK, N. H., 1954, The molluscan fauna of the Pliocene strata underlying the Adelaide Plains-Part 1: Transactions of The Royal Society of South Australia, v. 77, p. 42 - 64.

LUDBROOK, N. H., 1961a, Subsurface stratigraphy and micropalaeontology: Minlaton and Stansbury Stratigraphic Bores, palaeontology report no 7/61, report book no. 667, S.R. 11/5/12, G.S. no. 2093, envelope No. 47, core library, South Australian Department of Mines and Energy.

LUDBROOK, N. H., 1961b, Stratigraphy of the Murray Basin in South Australia, Geological Survey South Australia, Bulletin No. 36, 96 p.

LUDBROOK, N. H., 1963a, Correlation of the Tertiary rocks of South Australia: Transactions of The Royal Society of South Australia, v. 87, p. 5-15.

LUDBROOK, N. H., 1963b, Subsurface stratigraphy: Troubridge Island Borehole No. 1 stratigraphic well, O.E.L 24, envelope No. 324, core library, South Australian Department of Mines and Energy.

LUDBROOK, N. H., 1964, Subsurface stratigraphy and micropalaeontological study: Beach Petroleum N. L., Black Point No. 1A stratigraphic well, palaeontology report no 7/64, report book no. 711, S.R. 11/5/153, G.S. no. 3047, envelope no. 439, core library, South Australian Department of Mines and Energy.

LUDBROOK, N. H., 1967, Correlation of Tertiary rocks of the Australasian region, *in* Hatki K., ed., Tertiary correlation's and climatic changes in the Pacific: Symposium no. 25, The Eleventh Pacific Science Congress, Tokyo, Sasaki Printing and publishing Company Ltd., Sendai, Japan, p. 7 - 19.

LUDBROOK, N. H., 1980, A Guide to the Geology and Mineral Resources of South Australia: Adelaide, Department of Mines and Energy, South Australia, Goverment Printer, 230 p.

LUDBROOK, N. H., 1984, Quaternary molluscs of South Australia: Handbook, South Australian Department of Mines and Energy, no. 9, 327p.

M'RABET, A., 1981, Differentiation of environments of dolomite formation, Lower Cretaceous of central Tunisia: Sedimentology, v. 28, p. 331 - 352.

MACHEL, H.-G., 1985, Cathodoluminescence in calcite and dolomite and its chemical interpretation: Geoscience Canada 12, p. 139-147.

MACHEL, H.-G. AND BURTON, E. A., 1991, Factors governing cathodoluminescence in calcite and dolomite, and their implications for studies of carbonate diagenesis, *in* Barker, C. E., and Kopp, O. C., eds., Luminescence Microscopy: Quantitative and Qualitative Aspects: Society of Economic Palaeontology Mineralogy, short course, 25, p. 37-57.

MACHEL, H.-G., MASON, R. A., MARIANO, A. N., AND MUCCI, A., 1991, Causes and emission of luminescence in calcite and dolomite, *in* Barker, C. E., and Kopp, O. C., eds., Luminescence Microscopy: Quantitative and Qualitative Aspects: Society of Economic Palaeontology Mineralogy, short course, 25, p. 9-25.

MANHEIM, F. T. AND BISCHOFF, J. L., 1969, Geochemistry of pore waters from Shell Oil Company drill holes on the continental slope of the Northern Gulf of Mexico: Chemical Geology, v. 4, p. 63-82.

MARTIN, H. A., 1991, Tertiary stratigraphic palynology and palaeoclimate of the inland river systems in New South Wales, in Williams, M. A. J., De Deckker, P., and Kershaw, A. P., eds., The Cainozoic of the Australian region: Geological Society of Australia, Special Publication 18, p. 181 - 194.

MAZZOLENI, A. G., BONE, Y., AND GOSTIN, V. A., 1995, Cathodoluminescence of aragonitic gastropods and cement in Old Man Lake thrombolites, southeastern South Australia: Australian Journal of Earth Sciences, v. 42, p. 497 - 500.

McGOWRAN, B., 1973, Rifting and drift of Australia and the migration of mammals: Science, v. 180, p. 759-761.

McGOWRAN, B., 1978, The Tertiary of Australia: Stratigraphic sequences and episodic geohistory, 3rd regional conference on geology and mineral resources of Southeast Asia, Bangkok, Thailand 14-18 November, p. 73-80.

McGOWRAN, B., 1979, The Tertiary of Australia: Foraminiferal overview: Marine Micropalaeontology, v. 4, p. 235 - 264.

McGOWRAN, B., 1986, Cainozoic Oceanic and Climatic Events: The Indo-Pacific Foraminiferal Biostratigraphic Record: Palaeogeography, Palaeoclimatology, Palaeoecology, v. 55, p. 247 - 265.

McGOWRAN, B., 1989a, The later Eocene transgressions in southern Australia: Alcheringa, v. 13, p. 45 - 68.

McGOWRAN, B., 1989b, Silica burp in the Eocene ocean: Geology, v. 17, p. 857 - 860.

McGOWRAN, B., 1991, Maastrichtian and early Cainozoic, southern Australia: planktonic foraminiferal biostratigraphy: Geological Society of South Australia, Special publication 18, p. 79 - 98.

McGOWRAN, B. AND BEECROFT, A., 1985, Guembelitria in the Early Tertiary of southern Australia and its palaeoceanographic significance, *in* Lindsay, J. M., ed., Stratigraphy, Palaeontology and Malacology: Adelaide, South Australian Department of Mines and Energy, Special Publication 5, p. 247 261.

McGOWRAN, B. AND BEECROFT, A., 1986, Foraminiferal Biofacies in a Silica-Rich Neritic Sediment, Late Eocene, South Australia: Palaeogeography, Palaeoclimatology, Palaeoecology, v. 52, p. 321 - 345.

McGOWRAN, B., MOSS, G., AND BEECROFT, A., 1992, Late Eocene and Early Oligocene in southern Australia: local neritic signals of global oceanic changes, *in* Prothero, D. R., and Berggren, W. A., eds., Eocene - Oligocene climatic and biotic evolution. Princeton University Press, Princeton, p. 178 - 201.

McGOWRAN, B. AND LI, Q., 1994, The Miocene oscillation in southern Australia: Records of the South Australian Museum, v. 27, p. 197-212.

McGOWRAN, B., LI, Q., AND MOSS, G., 1996, The Cenozoic neritic record in southern Australia: The biogeohistorical framework, in James, N. p., and Clarke, J., eds., Cool-water carbonates, Special Publication, Society of Economic Palaeontologists and Mineralogists, in press.

McINTIRE, W. L., 1963, Trace element partition coefficient-a review of theory and applications to geology: Geochimica et Cosmochimica Acta, v. 27, p. 1209-1264.

McNAMARA, K. J., PHILIP, G. M., AND KRUSE, P. D., 1986. Tertiary brissid echinoids of southern Australia. Alcheringa, 10, p. 55-84.

MEYERS, W. J., 1974, Carbonate cement stratigraphy of the Lake Valley Formation (Mississippian) Sacramento Mountains, New Mexico: Journal of Sedimentary Petrology, v. 44, p. 837-861.

MEYERS, W. J., 1978, Carbonate cements: their regional distribution and interpretation in Mississippian limestone's of southeastern New Mexico: Sedimentology, v. 25, p. 371-400.

MIALL, A. D., 1990, Principles of Sedimentary Basin Analysis (2nd ed.): New York, Springer-Verlag, 668p.

MILLER, K. G., 1992, Middle Eocene to Oligocene stable isotopes, climate, and deep-water history: the Terminal Eocene Event?, *in* Prothero, D. R, and Berggren, W. A., eds., Eocene-Oligocene climatic and biotic evolution: Princeton University Press, Princeton, p. 160-177.

MILLIMAN, J. D., 1974, Recent Sedimentary Carbonates: Berlin, Springer-Verlag, 375 p.

MILNES, A. R. LUDBROOK, N. H., LINDSAY, J. M., AND COOPER, B. J., 1983, The succession of Cainozoic marine sediments on Kangaroo Island, South Australia: Transactions of The Royal Society of South Australia, v. 107 (1), p. 1-35.

MOHAMAD, A. H. AND TUCKER, E. V., 1992, Diagenetic history of the Aymestry Limestone Beds (High Gorstian Stage), Ludlow Series, Welsh Borderland, U.K., *in* K. H., Wolf and G. V., Chilingarian, eds., Diagenesis III: Developments in Sedimentology 47, Elsevier, p. 317-385.

MOSS, G. D., 1995, The Oligocene of Southern Australia: Ecostratigraphy and Taxic Overturn in Neritic Foraminifera: Ph.D. Thesis, Department of Geology and Geophysics, University of Adelaide, 158 p., (unpublished).

MURRAY, J. W., 1985. Atlas of invertebrate macrofossils. (The Palaeontological sociaty) Longman Group UK Limited, 241 P.

MURRAY, J. W., 1991, Ecology and Palaeoecology of Benthic Foraminifera: Essex, Longman Scientific and Technical, Longman Group UK Limited, 397 p.

NELSON, C. S., 1978. Temperate shelf carbonate sediments in the Cenozoic of New Zealand: Sedimentology, v. 25, p. 737 - 771.

NELSON, C. S., 1988, An introductory perspective on non-tropical shelf carbonates, *in* Nelson, C. S., ed., Non-tropical Shelf Carbonates - Modern and Ancient: Sedimentary Geology, v. 60, p. 3-12.

NELSON, C. S., HANCOCK, G. E., AND KAMP, J. J., 1982, Shelf to basin, temperate skeletal carbonate sediments, Three Kings Plateau, New Zealand: Journal of Sedimentary Petrology, v. 53, p. 717-732.

NELSON, C. S., KEANE, S. L., AND HEAD, P.S., 1988a, Non-tropical carbonate deposits on the modern New Zealand shelf, *in* Nelson, C. S., ed., Non-tropical Shelf Carbonates - Modern and Ancient: Sedimentary Geology, v. 60, p. 71 - 94.

NELSON, C. S., HYDEN, F. M., KEANE, S. L., LEASK, W. L., AND GORDON, D. P., 1988b, Application of bryozoan zoarial growth-form studies in facies analysis of non-tropical carbonate

deposits in New Zealand, *in* Nelson, C. S., ed., Non-tropical Shelf Carbonates - Modern and Ancient: Sedimentary Geology, v. 60, p. 301-322.

NELSON, C. S., HARRIS, G. J., AND YOUNG, H. R., 1988c, Burial dominated cementation in non-tropical carbonates of the Oligocene Te Kuiti Group, New Zealand, *in* Nelson, C.S., ed., Non-tropical Shelf Carbonates - Modern and Ancient: Sedimentary Geology, v. 60, p. 233-250.

NICOLAIDES, S., 1995, Cementation in Oligo-Miocene non-tropical shelf limestones, Otway Basin, Australia: Sedimentary Geology, v. 95, p. 97-121.

ODIN, G. S., 1988, Green marine clays, ed.: Amsterdam, Developments in Sedimentology 45, Elsevier, p. 445.

ODIN, G. S. AND HUNZIKER, J.C., 1982, Radiometric dating of the Albian-Cenomanian boundary, *in* Odin, G. S., ed., Numerical dating in Stratigraphy: Chichester, John Wiley and Sons Publications, p. 537-556.

ODIN, G. S. AND FULLAGAR, P. D., 1988, Geological significance of the glaucony facies, *in* Odin, G. S., ed., Green Marine Clays: Amsterdam, Developments in Sedimentology 45, Elsevier, p. 295-332.

ODIN, G. S., RENARD, M., AND VERGNAUD-GRAZZINI, C., 1982, Geochemical events as a mean of correlation, *in* Odin, G. S., ed., Numerical dating in Stratigraphy: John Wiley and Sons Publication, Chichester, p. 37-71.

OGDEN, A. E., 1984, Discharge and seasonal effects on the water chemistry of the San Marcos Springs, Edwards Aquifer, Texas. GSA Abstract, program 16, p. 111.

OPDYKE, B. AND BIRD, M., 1996, The Scott Plateau: a paleoceanographic target for monitoring the Indonesian throughflow and evolution of deep water in the eastern Indian Ocean, *in* Stagg, H. M. J. and Symonds, P. A., eds., Australia and the Ocean Drilling Program: Canberra, The 13th Australian Geological Convention, Record 1996/4, AGSO, p. 58-60.

OSLEGER, D., 1991, Subtidal carbonate cycles: Implications for allocyclic vs. autocyclic controls: Geology, v. 19, p. 917-920.

PAQUETTE, J., WARD, W. B., AND REEDER, R. J., 1993, Compositional zoning and crystal growth mechanisms in carbonates: A new look at microfabrics imaged by cathodoluminescence microscopy, *in* Rezak R. and Lavoie D., eds., Carbonate microfabrics: Springer-Verlag, p. 243-252.

PHLEGER, F. AND PARKER F. L., 1951, Foraminifera species: Boulder, Geological Society of America Memoir 46, Part II, p. 2-26.

PIERSON, B. J. AND SHINN, E. A., 1985, Cement distribution and carbonate mineral stabilization in Pleistocene Limestones of Hogsty Reef, Bahamas, *in* N. Schneidermann and P. Harris, eds., Carbonate Cements: Society of Economic Paleontologists and Mineralogists, special publication No. 36, p. 153-168.

PINGITORE Jr., N. E., 1982, The role of diffusion during carbonate diagenesis: Journal of Sedimentary Petrology, v. 52, p. 27-39.

POSAMENITIER, H. W. AND VAIL, P. R., 1988, Eustatic controles on clastic deposition II-sequence and systems tract models, *in* Wilgus, C. K., Hastings, B. S., Kendall, C. G. St. C., Posamentier, H. W., Ross, C. A., and Van Wagoner, J. C., eds., Sea Level Changes: An Integrated Approach: SEPM Special Publication No. 42, p. 125 - 154.

POSAMENITIER, H. W., JERVEY, M. T., AND VAIL, P. R., 1988, Eustatic controles on clastic deposition I-conceptual framework, *in* Wilgus, C. K., Hastings, B. S., Kendall, C. G. St. C., Posamentier, H. W., Ross, C. A., and Van Wagoner, J. C., eds., Sea Level Changes: An Integrated Approach: SEPM Special Publication No. 42, p. 109 - 124.

PYTKOWICZ, R. M., 1983, Equilibria, Nonequilibria, and Natural Waters, v. 1: John Wiley, New York, 351 p.

RAO, C . P., 1981a, Criteria for recognition of cold-water carbonate sedimentation: Berriedale Limestone (Lower Permian), Tasmania, Australia: Journal of Sedimentary Petrology, v. 51, p. 491 - 506.

RAO, C . P., 1981b, Cementation of cold-water bryozoan sand, Tasmania, Australia: Marine Geology, v. 40, M23-M33.

RAO, C . P. AND ADABI, M. H., 1992, Carbonate minerals, major and minor elements and oxygen and carbon isotopes and their variation with water depth in cool, temperate carbonates, western Tasmania, Australia: Marine Geology, v. 103, p. 249 - 272.

RAO, C . P. AND JAYAWARDANE, M. P. J., 1994, Major minerals, elemental and isotopic composition in modern temperate shelf carbonates, eastern Tasmania, Australia: Implications for occurrence of extensive ancient non-tropical carbonates: Palaeogeography, Palaeoclimatology, Palaeoecology, v. 107, p. 49 - 63.

READ, J. F., 1980, Carbonate ramp to basin transitions and foreland basin evolution, Middle Ordovician, Virginia Appalachians: American Association of Petroleum Geologists Bulletin, v. 64, p. 1575-1612.

READ, J. F., 1985, Carbonate platform facies models: American Association of Petroleum Geologists Bulletin, v. 66, p. 860-878.

REECKMANN, S. A., 1988, Diagenetic alterations in temperate shelf carbonates from southern Australia, *in* Nelson, C. S., ed., Non-tropical Shelf Carbonates - Modern and Ancient: Sedimentary Geology, v. 60, p. 209-219.

REEDER, R. J. AND PROSKY, J. L., 1986, Compositional sector zoning in dolomite: Journal of Sedimentary Petrology, v. 56, p. 237-247.

REEDER, R. J. AND PAQUETTE, J., 1989, Sector zoning in natural and synthetic calcites: Sedimentary Geology, v. 65, p. 239-247.

REID R. P., MACINTYRE, I. G., AND JAMES, N. P., 1990, Internal precipitation of microcrystalline carbonate: a fundamental problem for sedimentologists: Sedimentary Geology, v. 68, p. 163-170.

REIJERS, T. J. A. AND HSÜ, 1986, Manual of Carbonate Sedimentology: A Lexicographical Approach: Academic press Inc. (London), 302p.

REISS, Z. AND HOTTINGER, L., 1984, The Gulf of Aqaba, Ecological Micropaleontology: Berlin, Springer-Verlag, Ecological studies-50, 354 p.

REYNOLDS, M. A., 1953, The Cainozoic Succession of Maslin and Aldinga Bays, South Australia: Transactions of The Royal Society of South Australia, v. 76, p. 114-140.

RICHTER, D. K. AND FÜCHTBAUER, H., 1978, Ferroan calcite replacement indicates former magnesian calcite skeleton: Sedimentology, v. 25, p. 843-860.

ROSEN, M. R. AND HOLDREN, G. R., 1986, Origin of dolomite cements in Chesapeake Group (Miocene) siliciclastic sediments: an alternative model to burial dolomitization: Journal of Sedimentary Petrology, v. 56, p. 788 - 798.

ROSEN, M. R., MISER, D. E., STARCHER, M. A., AND WARREN, J. K., 1989, Formation of dolomite in the Coorong region, South Australia: Geochimica et Cosmochimica Acta, v. 53, p. 661 - 669.

SARG, J. F., 1988, Carbonate sequence stratigraphy, *in* Wilgus, C. K., Hastings, B. S., Kendall, C. G. St. C., Posamentier, H. W., Ross, C. A., and Van Wagoner, J. C., eds., Sea Level Changes: An Integrated Approach: SEPM Special Publication No. 42, p. 155 - 181.

SAVARD, M. M., 1991, Calcite cements in carbonates of the Sverdrup Basin, Canadian Arctic Archipelago (unpublished Ph.D. thesis, University of Ottawa, 209 p.), *in* Savard et al., 1995, Cathodoluminescence

at low Fe and Mn concentrations: A SIMS study of zones in natural calcites: Journal of Sedimentary Research, v. A65, no. 1, p. 208-213.

SAVARD, M. M., VEIZER, J., AND HINTON, R., 1995, Cathodoluminescence at low Fe and Mn concentrations: A SIMS study of zones in natural calcites: Journal of Sedimentary Research, v. A65, no. 1, p. 208-213.

SCHLAGER, W., 1981, The paradox of drowned reefs and carbonate platforms: Geological Society of America Bulletin, Part I, v. 92, p. 197 -211.

SCHLAGER, W., 1991, Depositional bias and environmental change - important factors in sequence stratigraphy: Sedimentary Geology, v. 70, p. 109 - 130.

SCHLAGER, W., 1992, Sedimentology and Sequence Stratigraphy of Reefs and Carbonate Platforms: American Association of Petroleum Geologists, continuing education course note series 34, 71 p.

SCHLANGER, S. O. AND DOUGLAS, R. G., 1974, The pelagic ooze-chalk-limestone transition and its implications for marine stratigraphy, *in* Hsu, K. J. and Jenkyns, H. C., eds., Pelagic Sediments on Land and Under the Sea: International Association of Sedimentologists, Special Publication 1, p. 117 - 148.

SCOFFIN, T. P., ALEXANDERSSON, E. T., BOWES, G. E., CLOKIE, J. J., FARROW, G. E., AND MILLIMAN, J.D., 1980, Recent temperate, sub-photic, carbonate sedimentation: Rockall Bank, northeast Atlantic. Journal of Sedimentary Petrology, v. 50, p. 331-356.

SCOFFIN, T. P., 1988, The environments of production and deposition of calcareous sediments on the shelf west of Scotland, *in* Nelson, C.S., ed., Non-tropical Shelf Carbonates - Modern and Ancient: Sedimentary Geology, v. 60, p. 107 - 124.

SEIGLIE, G. A., 1968, Relationships between the distribution of *Amphistegina* and the submerged Pleistocene reefs off western Puerto Rico: New Orleans, Tulane studies in geology, Tulane University, v. 6, p. 139-147.

SHACKELTON, N. J., 1986, Paleogene stable isotope events: Palaeogeography, Palaeoclimatology, Palaeoecology, v. 57, p. 91 - 102.

SHACKELTON, N. J., AND KENNETT, J. P., 1975, Palaeotemperature history of the Cenozoic and the initiation of Antarctic glaciation: oxygen and carbon isotope analysis in DSDP Sites 277, 279, and 281, *in* Kennett, J. P., Houtz, R. E., et al., eds., Initial Reports of the Deep Sea Drilling Project, v. 29, U. S. Government Printing Office, Washington, D.C., p. 743 - 755.

SHEPHERD, S. A., 1982, The marine environment, *in* Shepherd, S. A. and Thomas, I. M., eds., Marine Invertebrates of Southern Australia: Adelaide, D. J. Woolman, p. 11-25.

SHINN, E. A., GINSBURG, R. N., AND LLOYD, R. M., 1965, recent supratidal dolomite from Andros Island, Bahamas, *in* Murray, R. C. and Pray, L. C., ed., dolomitization and limestone diagenesis: Special Publication Society of Economic Palaeontologists and Mineralogists, v. 13, p. 112 - 123.

SHIRMOHAMMADI, N. H. AND SHEARMAN, D. J., 1966, On the distribution of strontium in some dolomitised and dedolomitised limestones from the French Jura (abs.): Proceedings of the Mineralogical Society of London: Mineral Magazine, v. 35, p. LXXII.

SHUBBER, B., BONE, Y., McGOWRAN, B., AND JAMES, N. P., 1995, Facies analysis of a cool-water carbonate formation: The Oligocene-Miocene Port Vincent Limestone, St. Vincent Basin, South Australia (abs.): Geelong, Cool and Cold Water Carbonate Conference, p. 71-72.

SHUBBER, B., BONE, Y., JAMES, N. P., AND McGOWRAN, B., 1996, Shallow Burial Dolomitization in the Tertiary Cool-water Port Vincent Limestone, St. Vincent Basin, South Australia: 13th Australian Geological Convention, Geological Society of Australia, abstracts no. 41, p. 393.

SIBLEY, D. F. AND GREGG, J. M., 1987, Classification of dolomite rock texture: Journal of Sedimentary Petrology, v. 57, p. 967-975.

SMITH, A., 1984. Echinoid Palaeobiology. George Allen & Unwin (publishers) Ltd., London. 190P.

SPENCER, R. J. AND DEMICCO, R. V. 1989, Computer models of carbonate platform cycles driven by subsidence and eustacy: Geology, v. 17, p. 165-168.

STAFFORD, B., 1987, The geological history, stratigraphy, structure and field geology of the east coast of central and southern Yorke Peninsula: Unpublished M. Sc. thesis, University of South Australia, 73 p.

STEEL, T. M., 1963, Subsurface stratigraphy, Port Vincent No. 1 Stratigraphic Well. Beach Petroleum N. L., report no 5/63, report book no. 686, S.R. 11/5/95, G.S. no. 2573, core library, South Australian Department of Mines and Energy.

STUART, W. J. Jr., 1969, Stratigraphy and structural development of the St. Vincent Tertiary Basin, South Australia: Unpublished Ph.D. Dissertation, University of Adelaide, Adelaide, 260 p.

STUART, W. J. Jr., 1970, The Cainozoic stratigraphy of the eastern coastal area of Yorke Peninsula, South Australia: Transactions of the Royal Society of South Australia, v. 94, p. 151-178.

TATE, R., 1888, Descriptions of some new species of marine mollusca from South Australia and Victoria: Transaction of the Royal Society of South Australia, v. XI, p. 60-66.

TATE, R., 1890, The stratigraphical relations of the Tertiary Formations about Adelaide with especial reference to the Croydon bore: Transaction of the Royal Society of South Australia, v. 13, p. 180-184.

TEPPER, J. G. O., 1879, Introduction to the cliffs and rocks at Ardrossan, Yorke's Peninsula: Transaction of the Royal Society of South Australia, v. 2, p. 71 - 79.

THOMSON, B. P., 1969, The Kanmantoo Group and early Palaeozoic tectonics: *in* Parkin, L. W., ed., Handbook of South Australian Geology: Geological Survey of South Australia, p. 97-108.

TUCKER, M. E., 1991, Sequence stratigraphy of carbonate-evaporite basins: models and application to the Upper Permian (Zechstein) of northeast England and adjoining North Sea: Journal of the Geological Society of London, v. 148, p. 1019 - 1036.

TUCKER, M. E., AND WRIGHT, V. P., 1990. Carbonate Sedimentology (1992 reprint), Blackwell Scientific Publications, 482 p.

VAIL, P. R., MITCHUM, R. M., JR., TODD, R. G., WIDMIER, J. M., THOMPSON, S., III, SANGREE, J. B., BUBB, J. N., AND HATLELID, W. G., 1977, Seismic stratigraphy and global changes of sea level (11 parts), *in* Payton, C. E., ed., Seismic stratigraphy - Applications to Hydrocarbon Exploration: American Association of Petroleum Geologist, Memoir 26, p. 49 - 212.

VAIL, P. R., AUDEMARD, F., BOWMAN, S. A., EISNER, P. N., AND PEREZ-CRUZ, C, 1991, The stratigraphic signature of tectonics, ecstasy and sedimentology-an overview, *in* Einsele G., Ricken W., and Seilacher A., eds., Cycles and Events in Stratigraphy, Springer-Verlag, Berlin, p. 617 - 618.

VAN WAGONER, J. C., POSAMENTIER, H. W., MITCHUM, R. M., JR., VAIL, P. R., SARG, J. F., LOUTIT, T. S., AND HARDENBOL, J., 1988, An overview of the fundamentals of sequence stratigraphy and key definitions, *in* Wilgus, C. K., Hastings, B. S., Kendall, C. G. St. C, Posamentier, H. W., Ross, C. A., and Van Wagoner, J. C., eds., Sea-level Changes - An integrated Approach: Society of Economic Paleontologists and Mineralogists, Special Publication 42, p. 39 - 46.

VAN WAGONER, J. C., MITCHUM, R. M., CAMPION, K. M., AND RAHMANIAN, V. D., 1990, Siliciclastic Sequence Stratigraphy in Well Logs, Cores, and Outcrops: Concepts for High-Resolution Correlation of Time and Facies: American Association of Petroleum Geologist, Methods in Exploration Series, No. 7, 55 p.

VEEVERS, J.J., POWELL, C.McA., AND ROOTS, S.R., 1991, Review of Seafloor Spreading around Australia - I, Synthesis of the pattern of spreading: Australian Journal of Earth Science, v. 38, p. 373-389.

VEIZER, J., 1983, Chemical diagenesis of carbonates: theory and application of trace element technique, *in* Arthur, M. A., and Anderson, T. F., ed., Stable Isotopes in Sedimentary Geology: Society of Economic Palaeontologists and Mineralogists, short course no. 10, Chapter 3, p. 1 - 100.

VEIZER, J. AND COMPSTON, W., 1974, $^{87}Sr/^{86}Sr$ composition of seawater during the Phanerozoic: Geochimica et Cosmochimica Acta, v. 38, p. 1461-1484.

VEIZER, J., LEMIEUX, J., JONES, B., GIBLING, M. R., AND SAVELLE, J., 1977, Sodium: Paleosalinity indicator in ancient carbonate rocks: Geology, v. 5, p. 177 - 179.

VEIZER, J., LEMIEUX, J., JONES, B., GIBLING, M. R., AND SAVELLE, J., 1978, Paleosalinity and dolomitization of a Lower Palaeozoic carbonate sequence, Somerset and Prince of Wales Islands, Arctic Canada: Canadian Journal of Earth Science, v. 15, p. 1448 - 1461.

WADE, M. 1959, The morphological and stratigraphical analysis of foraminiferal faunas of the Tertiary basins of South Australia: Unpublished Ph.D. Thesis, University of Adelaide, South Australia, 200 p.

WALKDEN, G. M. AND BERRY, J. R., 1984, Syntaxial overgrowths in muddy crinoidal limestone's: cathodoluminescence sheds new light on an old problem: Sedimentology, v. 31, p. 251-267.

WALKER, R. G., 1992. Facies, facies models and modern stratigraphic concepts, *in* Walker R.G. and N.P. James, eds., Facies models-response to sea level change: Geological Association of Canada, Saint Johns, Newfoundland, p. 1-14.

WASS, R. E., CONOLLY, J. R., AND MACLNTYRE, R. J., 1970, Bryozoan carbonate sand continuous along southern Australia: Marine Geology, v. 9, p. 63-73.

WATTS, T. R. AND GAUSDEN, J., 1966, Stansbury West No. 1 Well. Well completion report, Beach Petroleum N. L. open file envelope, core library, South Australian Department of Mines and Energy.

WEBB, J. A., 1995, Cool-water Carbonates of the Northeastern Otway Basin, Southeastern Australia: Excursion Guide for Cool and Cold-water Carbonate Conference, Geelong, Victoria, 14-19 January. Geological Society of Australia, Australian Sedimentologists Group, Field Guide Series No. 6, 60 p.

WEI, W., 1991. Evedence for an earliest Oligocene abrupt cooling in the surface waters of the Southern Ocean. Jour. Geology, Vol. 19, pp. 780-783.

WILSON J. L., 1975, Carbonate Facies in Geologic History: Springer-Verlag, 471 p.

WILSON J. B., 1979, Biogenic carbonate sediments on the Scottish Continental Shelf and Rockall Bank. Marine Geology, 33, M85-M93.

WOLFE, J. A. AND POORE, R. Z., 1982, Tertiary marine and nonmarine climatic trends, *in* Berger, W. H. and Crowell, J. C., eds., Climate in earth history: Washington, D. C., National Research Council, National Academy of Sciences, p. 154-158.

WOODRUFF, F. AND SAVIN, S., M., 1985, $\delta^{13}C$ values of Miocene Pacific benthic foraminifera: Correlations with sea level and biological productivity: Geology, v. 13, p. 119 - 122.

ZIMIRI, A., KAHAN, D., HOCHSTEIN, S., AND REISS, Z., 1974, Phototaxis and thermotaxis in some species of *Amphistegina* (Foraminifera): Journal of Protozoology, v. 21, p. 133-138.

APPENDICES

APPENDIX A-1

Bryozoan Classification Scheme: *"The Growth-Form Approach"*

Bryozoans were identified using the bryozoan growth-form classification of Bone and James (1993) (Fig. 1.4). In order to apply this morphology-based classification to thin section samples of the Port Vincent Limestone, selected rock samples were gently crushed and the bryozoan fraction separated using wet sieving. Oriented thin sections of these bryozoans were then prepared, for each confirmed growth form, and employed for comparison and identification. Interpretation of depositional environments were essentially based on their bryozoan growth-form associations. However, limitations do arise, especially when dealing with certain growth forms that have a wide environmental adaptability range that overlaps ranges of other growth forms, so that at the end an aerial extent of a subjectively chosen facies is spread out beyond its true extent. As a result, environmental geographic boundaries (e.g., inner ramp, middle shelf) may be valid, but with variable positions. To reduce the ambiguity of boundary locations in such situations, it is essential to support this morphology based classification with studies of other associated major biogenic constituents.

APPENDIX A-2

Cathodoluminescence, *a brief introduction:*

Cathodoluminescence petrography (CL) is increasingly used in diagenetic studies, particularly for documenting crystal growth in calcite and dolomite cements. This allows the deduction of pore water evolution between diagenetic sequences. Luminescent zonation in carbonate cements is induced by changes in fluid chemistry across successive stages of crystal growth. Zones are detected by many excitation methods including cathodoluminescence, electro-, radio-, chemo-, thermo-, and others.

A number of trace elements is responsible for activating or suppressing cathodoluminescence in carbonates. Among them Mn^{2+} and Fe^{2+} in solid solution, are the key activator and suppresser (Machel, 1985; Machel and Burton, 1991; Machel et al., 1991). The amount of Mn^{2+} and Fe^{2+} incorporated in calcite and dolomite crystals is related to the prevailing environmental conditions acting on the rocks. Approximately 20 ppm Mn^{2+} is required to activate luminescence, whereas a content of Fe^{2+} in excess of approximately 1400 ppm (regardless of the Mn^{2+} concentration) is sufficient to cause partial quenching (Savard et al., 1995). Both Fe/Mn ratio as well as absolute concentrations of either cation, control luminescent intensity (Bruhn et al., 1994). An exception is when Fe^{2+} concentrations fall below 1400 ppm, then luminescent intensity becomes a function of Mn^{2+} concentration alone (Savard et al., 1995). Ratios and concentrations may vary throughout growth stages of a single crystal, producing concentric luminescent zones, sectoral zones, and intrasectoral zones (Reeder and Paquette, 1989; Machel and Burton, 1991; Paquette et al., 1993). Generally, luminescent zonation reflects different diagenetic sequences and may be grouped into three categories, which are employed as analogues for comparison with the studied cements.

1- Non-luminescent zones (black or extinguished) represent precipitation from oxidising pore waters of meteoric or marine origin (Meyers, 1978; Machel, 1985; Amieux et al., 1989; Emery and Dickson, 1989; Horbury and Adams, 1989); here Mn^{2+} and Fe^{2+} are minimal or absent in the positive Eh solution (Frank et al., 1982). Occasionally, thin luminescent subzones occur in this zone; they reflect short periods of pore water stagnation or diminished fresh water supply, and precipitation of Mn^{2+} bearing cement (James and Choquette, 1990; Bruckschen et al., 1992). Synsedimentary marine cements are non-luminescent, since they lack Mn^{2+} and precipitate from waters that have a positive Eh (Tucker and Wright, 1990; Mazzoleni et al., 1995).

2- Luminescent zones (bright to moderate yellow or orange) represent precipitation from moderately reducing pore waters upon shallow burial. Mn^{2+} ions are present and easily

incorporated into the carbonate lattice, but Fe^{2+} ions decline as they are progressively extracted to form a sulphide through the reduction of SO_4^{2-} (Grover and Read, 1983; Dorobek, 1987; Tucker and Wright, 1990).

3- Dull-luminescent zones (brown, dark brown and very dull) represent precipitation from reducing pore waters during deeper burial. These cements are often ferroan calcite precipitated from more negative Eh water below the stability field of FeS_2 (Frank et al., 1982; Tucker and Wright, 1990; Bruckschen et al., 1992). Often times dull-luminescent cements may not show compositional zonation.

It must be stressed that in many cases these contrasting luminescent zonations, though representing different pore water chemistry, do not necessarily indicate that the sediments were hosted by different diagenetic environments and vice versa. For example, a particular cement fabric undergoing progressive burial, may show different luminescent intensities correlating to each stage of burial. These can be deduced from their cement stratigraphy (cf. Meyers, 1974) as: an early non-luminescent sequence, through an intermediate bright, to a late dull-luminescent sequence (Choquette and James, 1990). In other cases, the same type of luminescence (non, dull, or luminescent) may be produced in any of the meteoric, marine, or burial diagenetic environments under varying conditions (see Frank et al., 1982; Savard, 1991). However, waters from different environments vary in their trace element concentrations (e.g., Sr, Mg, Fe, Mn, Na). With combined trace element data and CL interpretations, the reconstruction of diagenetic cement sequences is facilitated and the broader pattern of diagenesis can then be predicted from the regional geology.

APPENDIX B-1

Mineralogy of Various Constituents of the Port Vincent Limestone

XRD Analysis

The mineralogy of the following constituents was identified by XRD. All samples were spiked with quartz to provide a reference peak for accurate measurements of the calcite peak. Positions of peaks were measured to the nearest 0.01° 2-theta, using the computer program XPLOT. The derived angular values were then entered into a computer program to obtain the mole % $MgCO_3$ proportions within the calcite. Calibration is based on Goldsmith et al. (1961).

Constituent	Mineralogy (mole% $MgCO_3$)	Sample No.
1- Delicate branching growth form (cyclostome)	1.5	5/6
2- Delicate branching growth form (cyclostome)	2.0	8/7
3- Articulated branching growth form (cheilostome)	2.0	12/6
4- Robust branching growth form	2.5	12/6
5- Internal micrite	2.5	16/6
6- Internal micrite	2.5	8/7
7- Syntaxial cement	1.5	8/7
8- Whole rock Sample	1.5	5/6 (friable)
9- Whole rock Sample	2.0	10/6 (friable)
10- Whole rock Sample	3.0	16/6 (hardground)

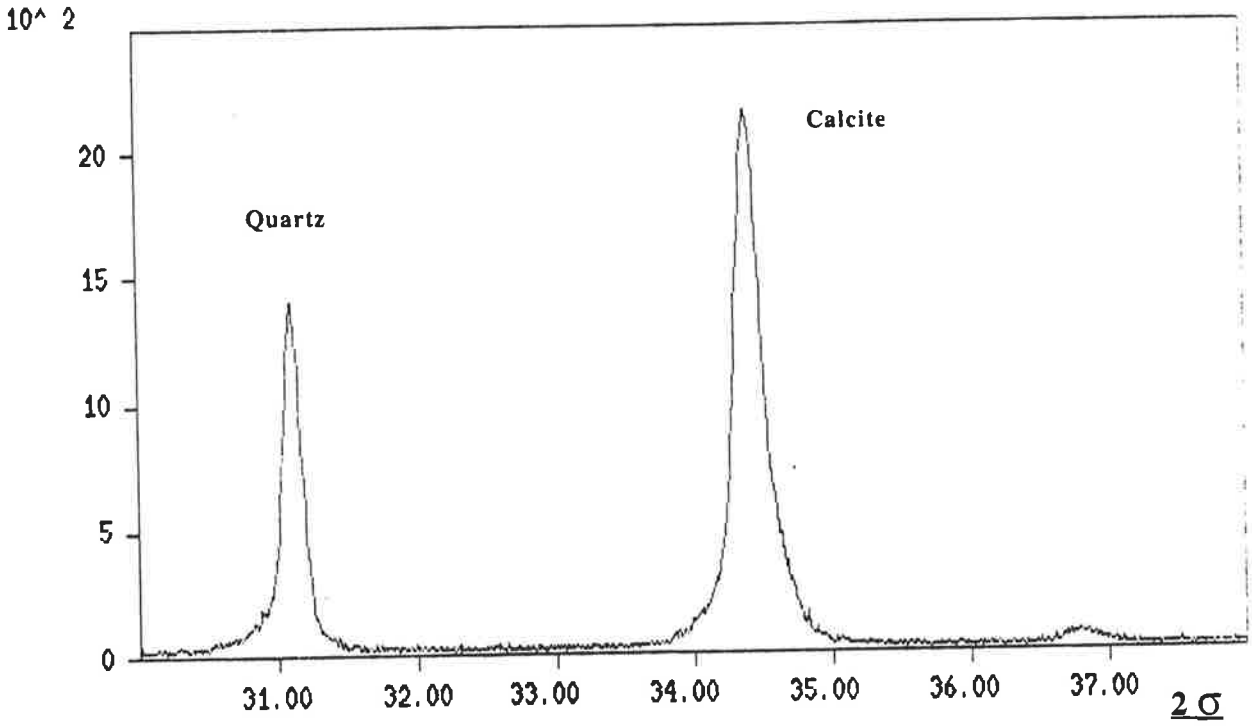

Constituent	Mineralogy (mole% $MgCO_3$)	Sample No.
1- Delicate branching growth form (cyclostome)	1.5	5/6

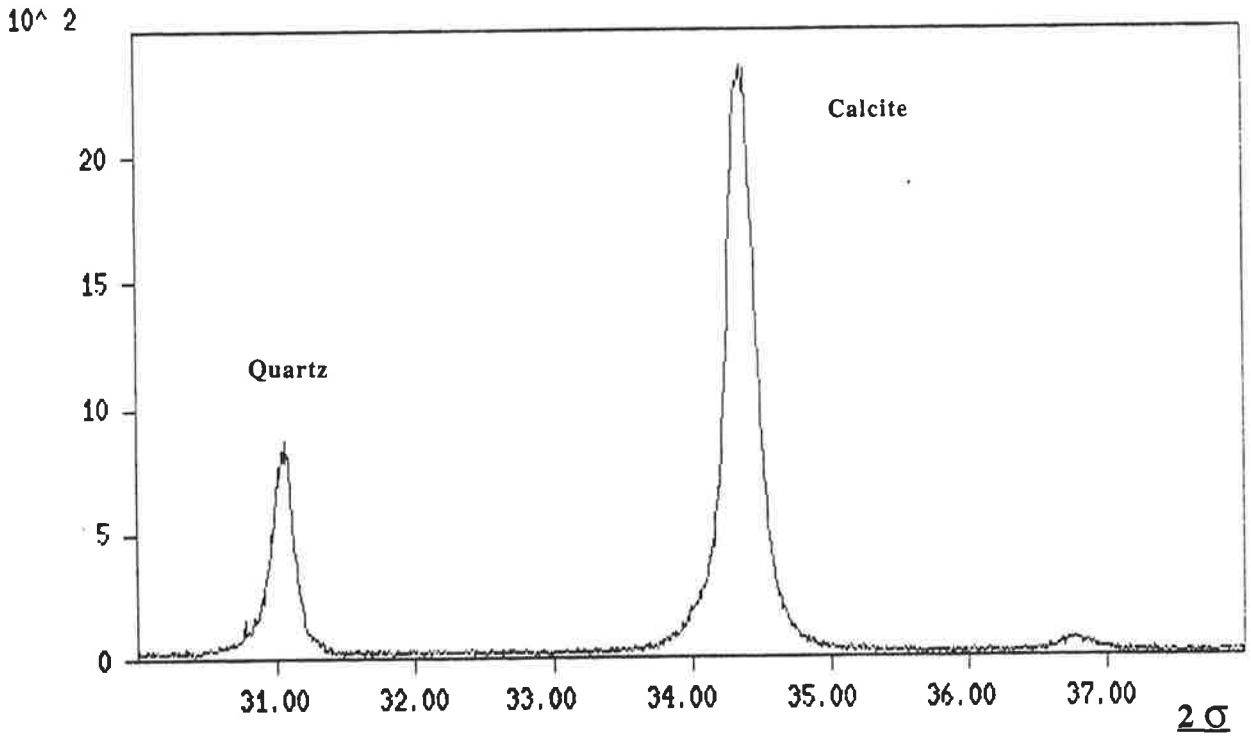

Constituent	Mineralogy (mole% $MgCO_3$)	Sample No.
2- Delicate branching growth form (cyclostome)	2.0	8/7

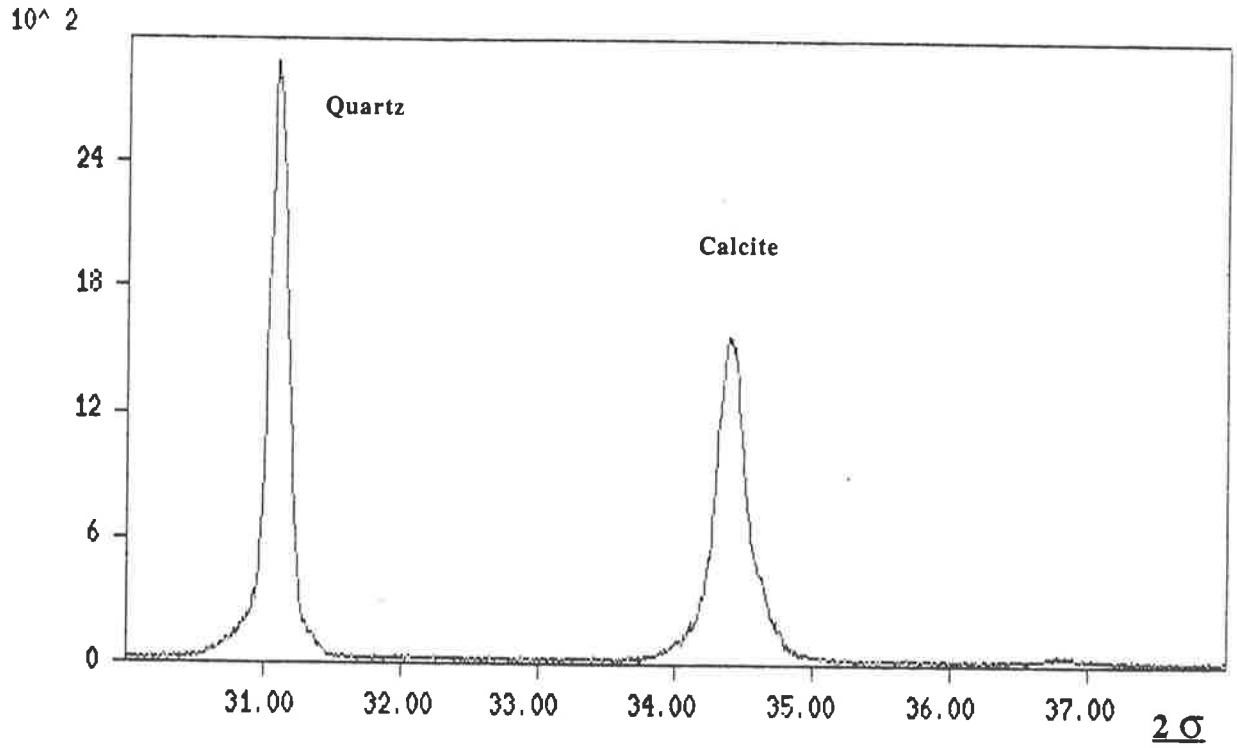

Constituent	Mineralogy (mole% $MgCO_3$)	Sample No.
3- Articulated branching growth form (cheilostome)	2.0	12/6

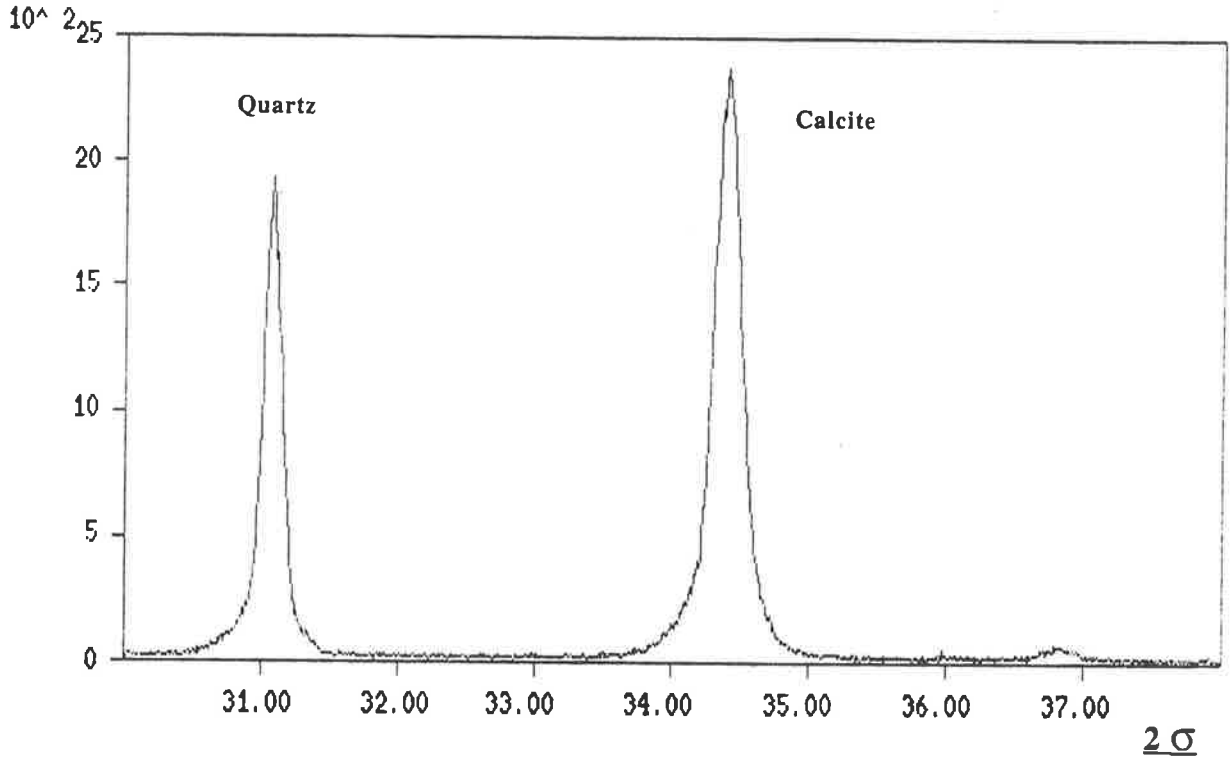

Constituent	Mineralogy (mole% $MgCO_3$)	Sample No.
4- Robust branching	2.5	12/6

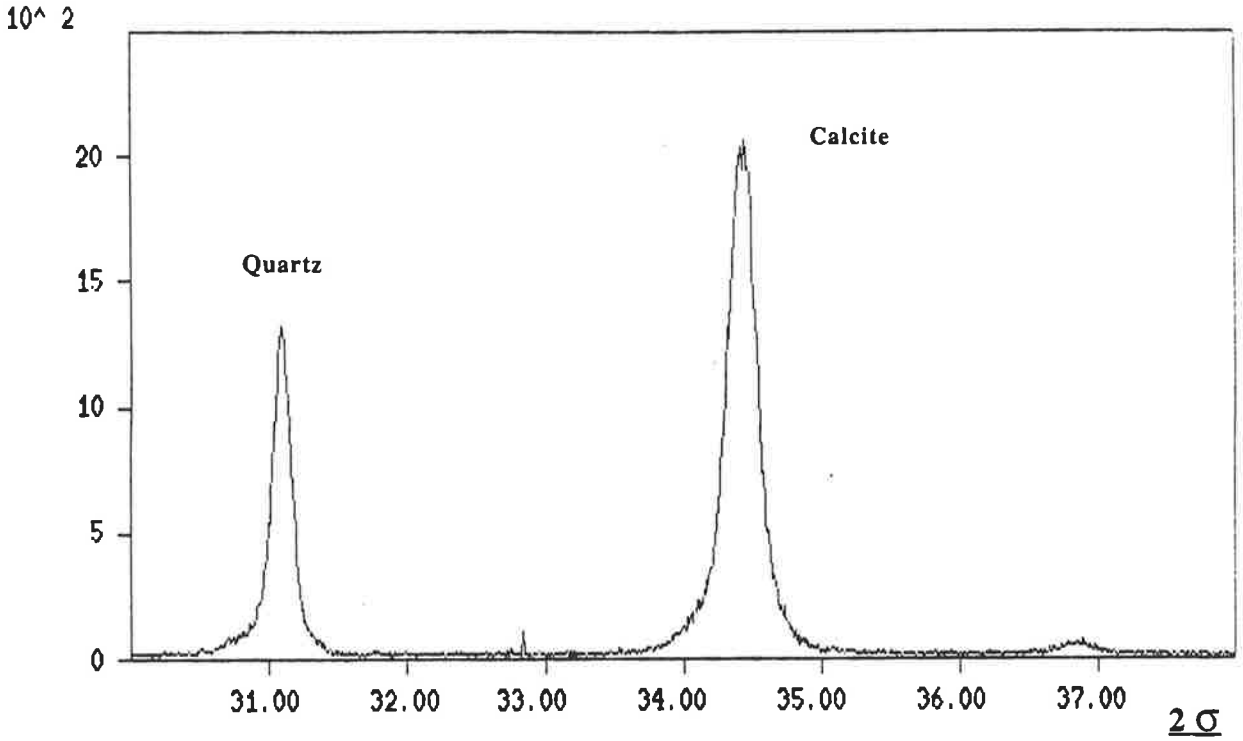

Constituent	Mineralogy (mole% $MgCO_3$)	Sample No.
5- Internal micrite	2.5	16/6

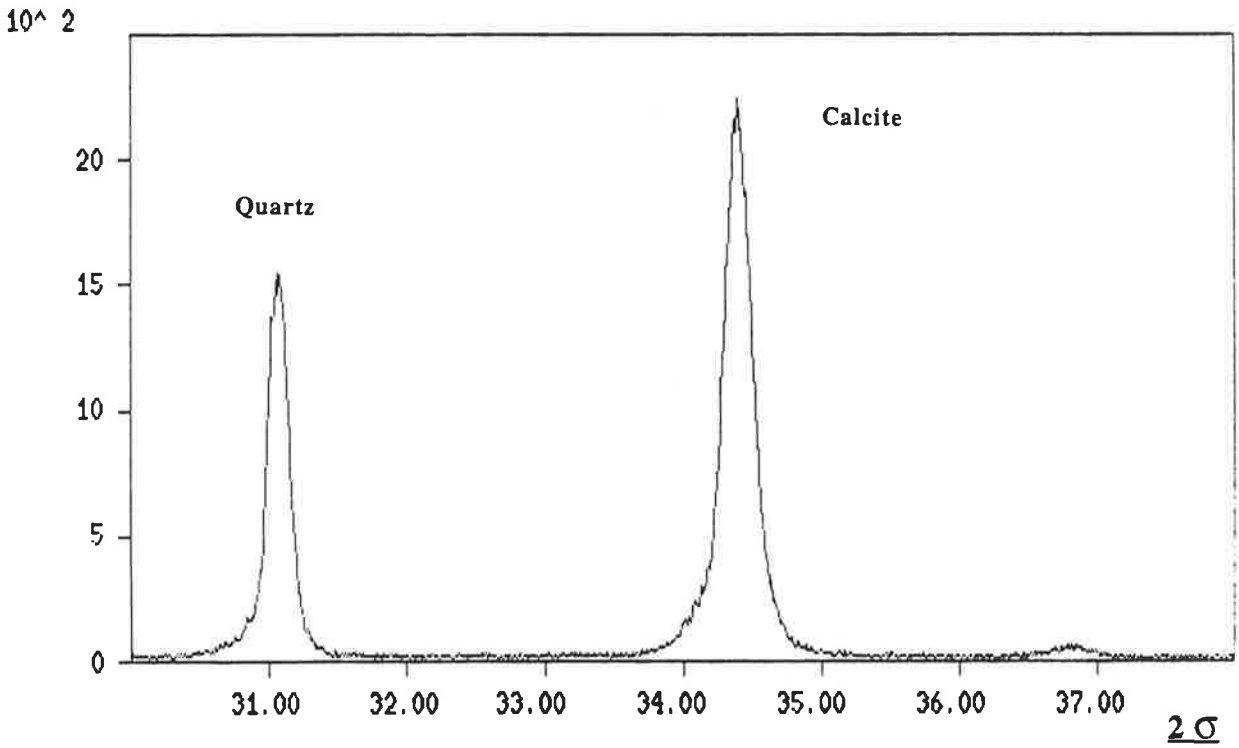

Constituent	Mineralogy (mole% $MgCO_3$)	Sample No.
6- Internal micrite	2.5	8/7

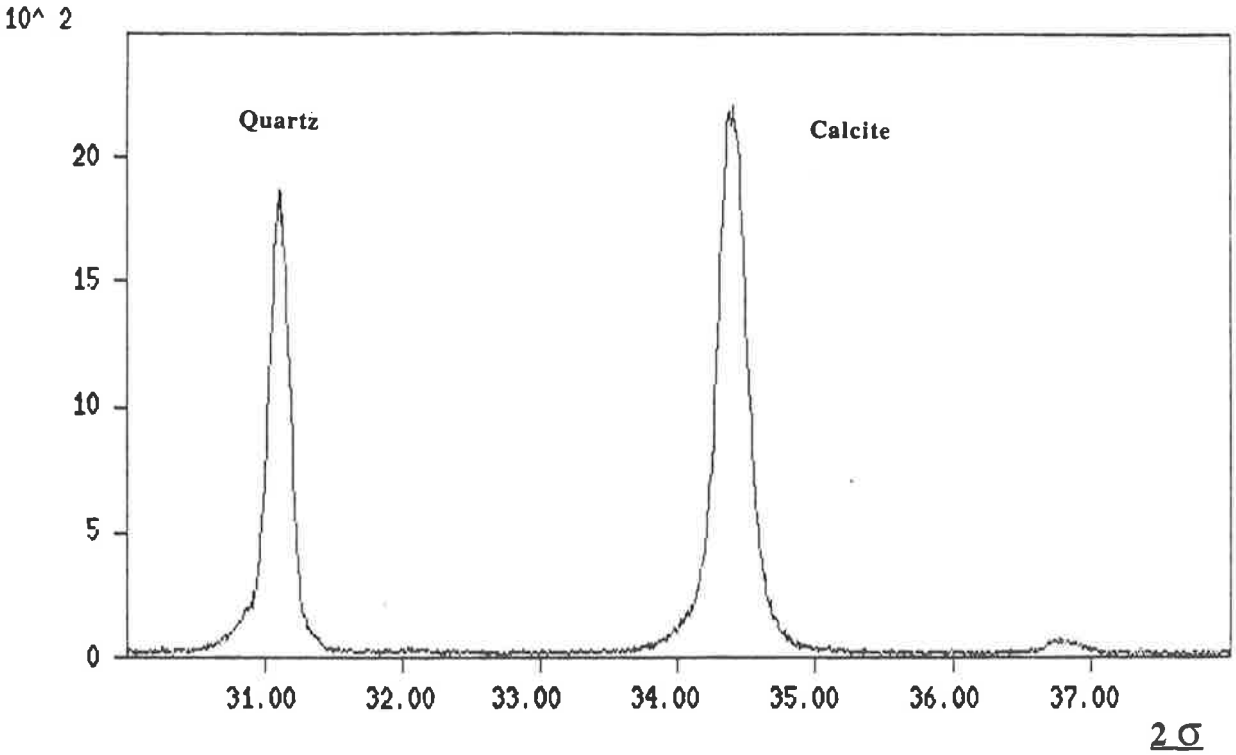

Constituent	Mineralogy (mole% $MgCO_3$)	Sample No.
7- Syntaxial cement	1.5	8/7

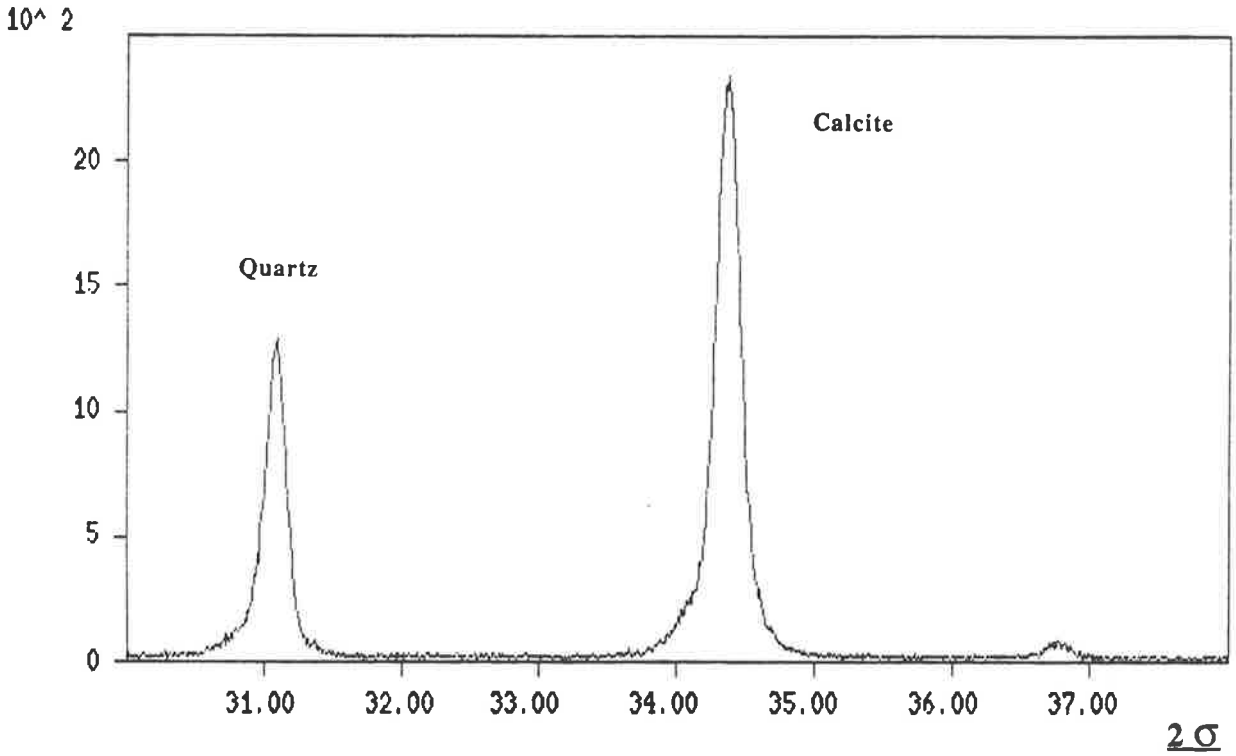

Constituent	Mineralogy (mole% $MgCO_3$)	Sample No.
8- Whole rock Sample	1.5	5/6 (friable)

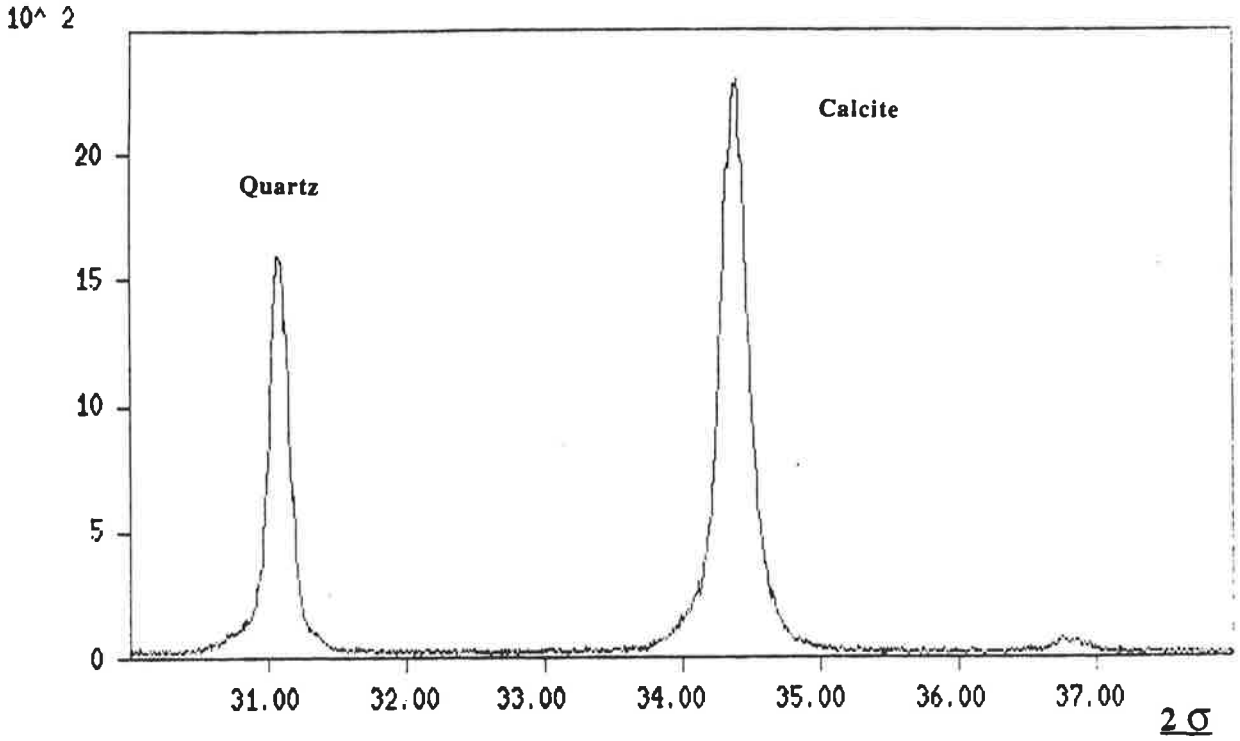

Constituent	Mineralogy (mole% $MgCO_3$)	Sample No.
9- Whole rock Sample	2.0	10/6 (friable)

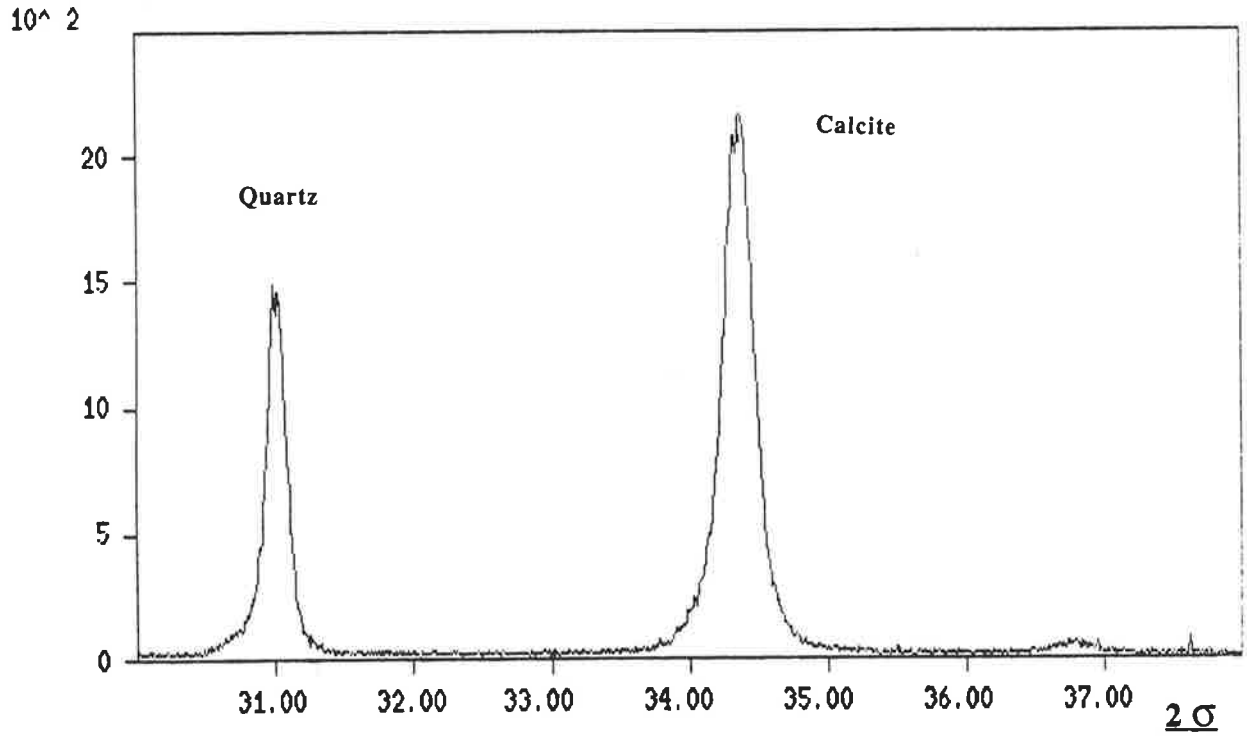

Constituent	Mineralogy (mole% $MgCO_3$)	Sample No.
10- Whole rock Sample	3.0	16/6 (hardground)

APPENDIX B-2

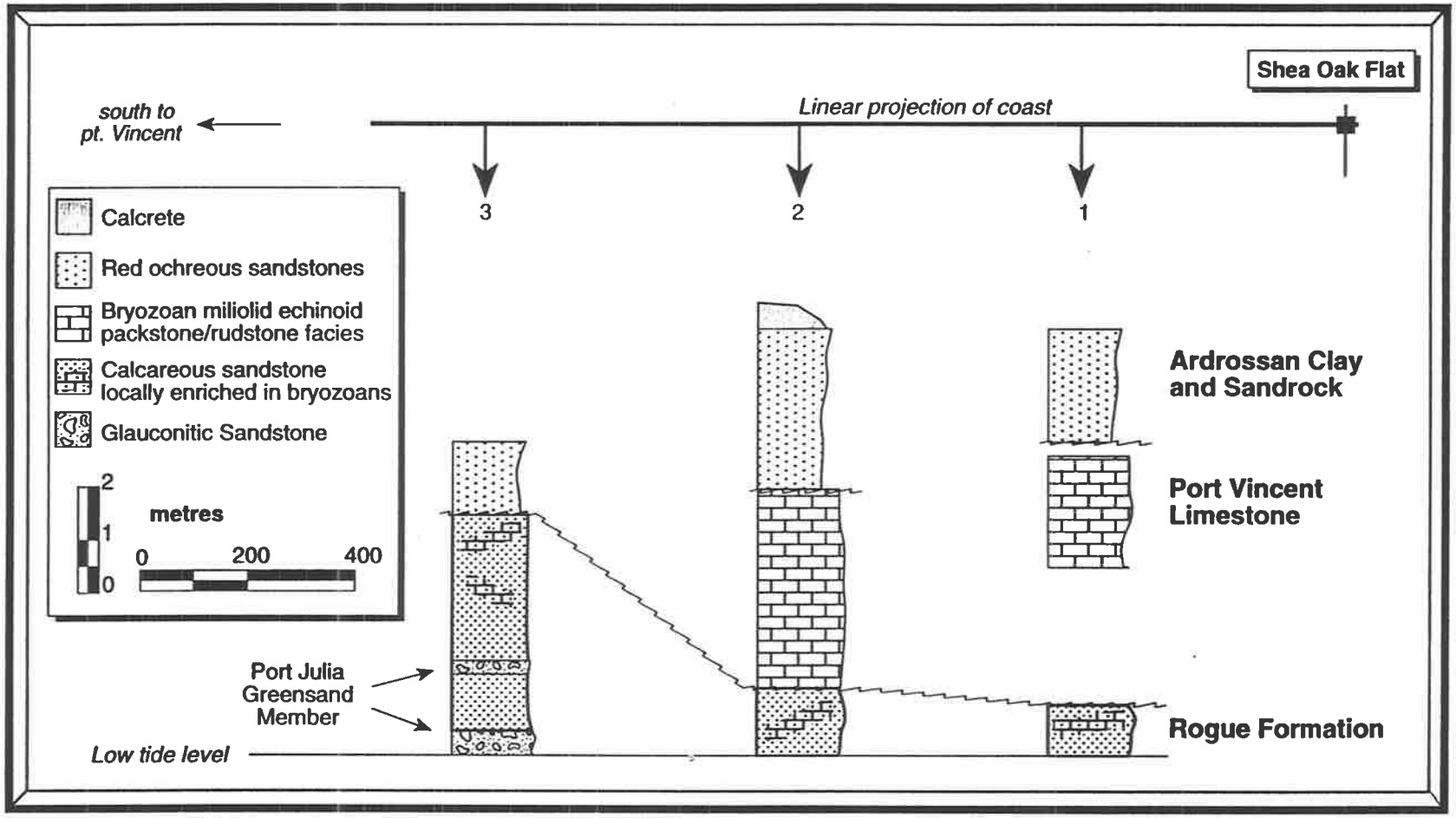

Stratigraphic coloumns of sections 1, 2, and 3 in the coastal cliffs south of Shea Oak Flat

APPENDIX B-3

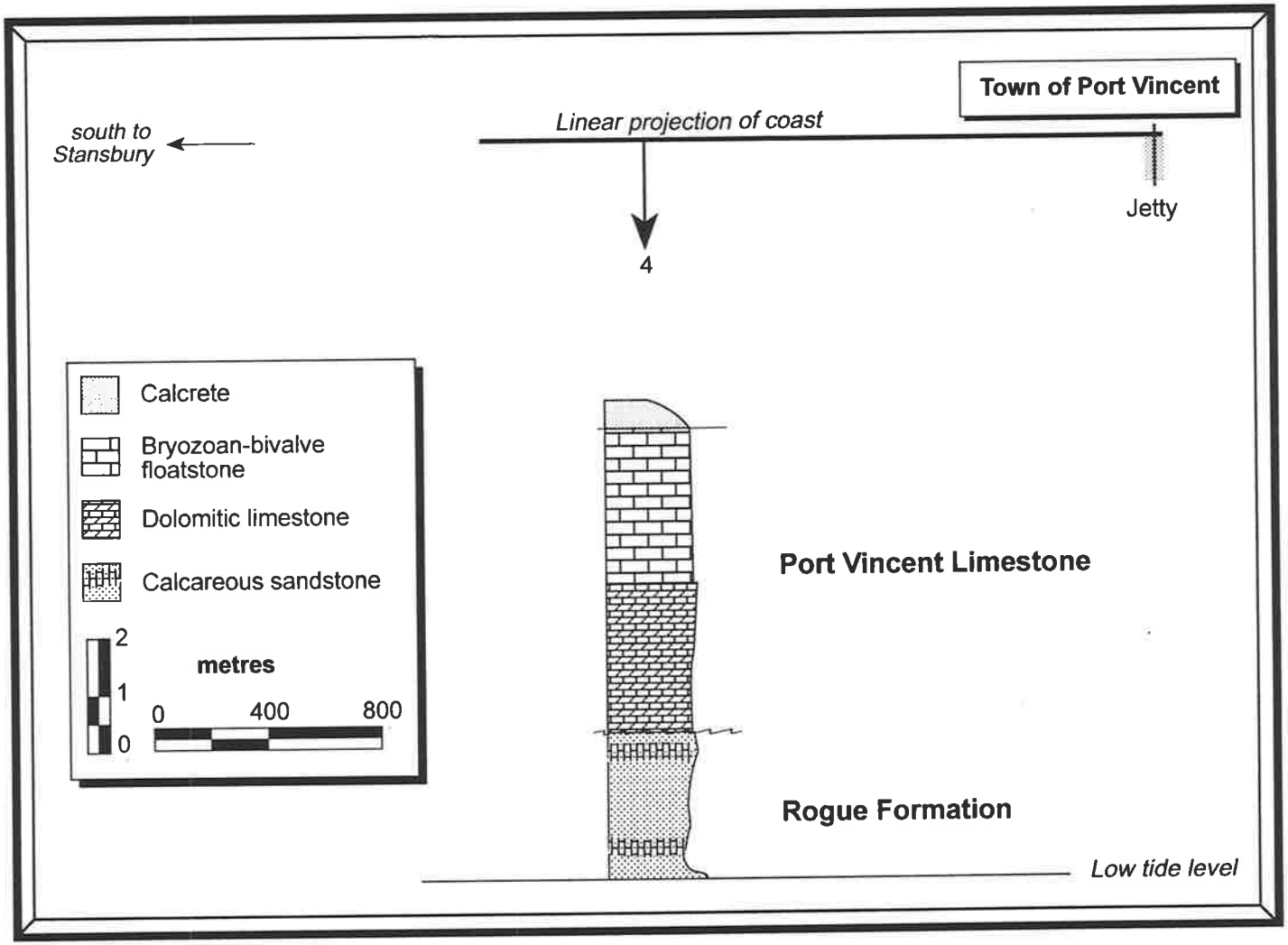

Stratigraphic coloumn of section 4 in the coastal cliffs south of Port Vincent Township

APPENDIX B-4

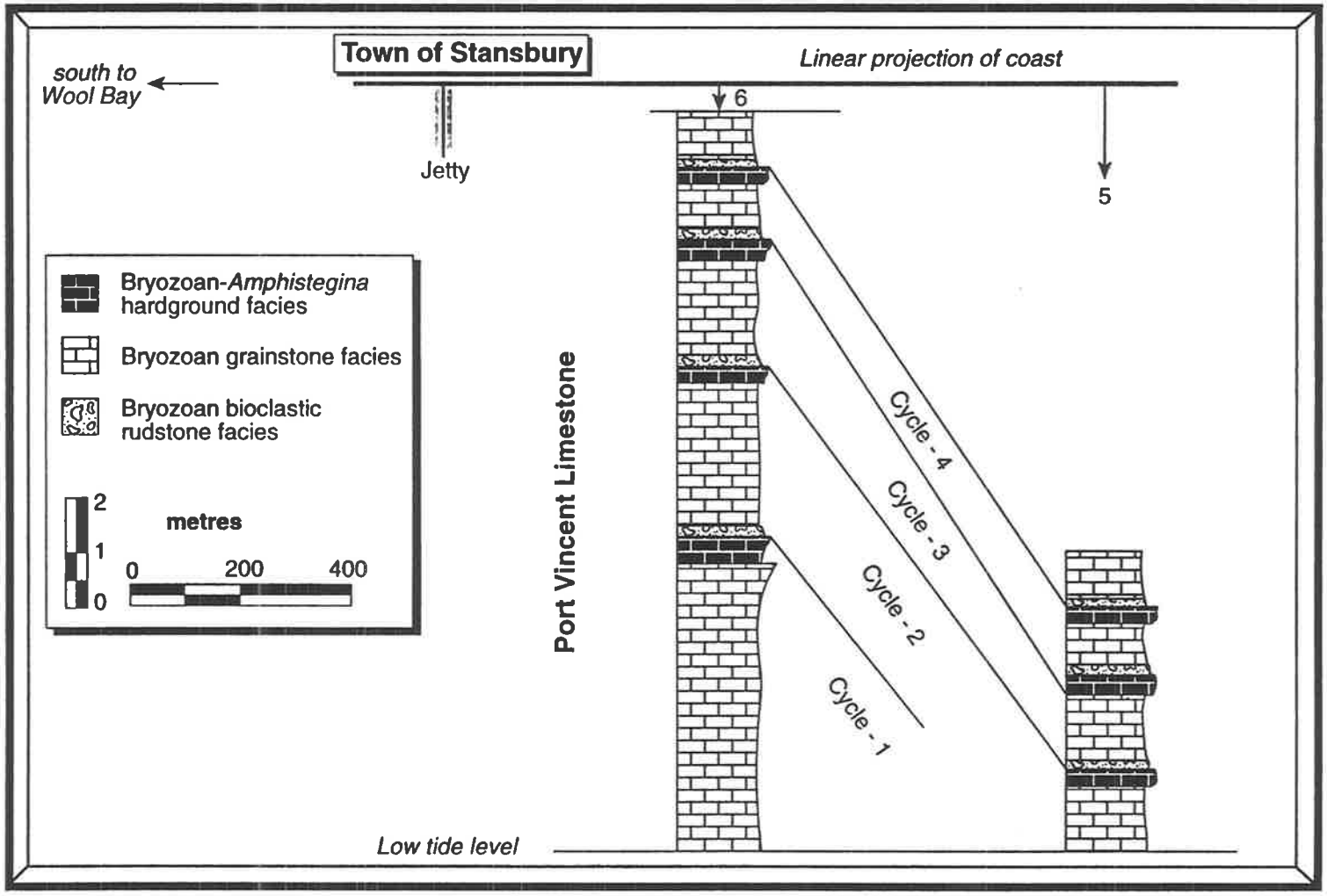

Stratigraphic coloumns of sections 5 and 6 in the coastal cliffs north of Stansbury

APPENDIX B-5

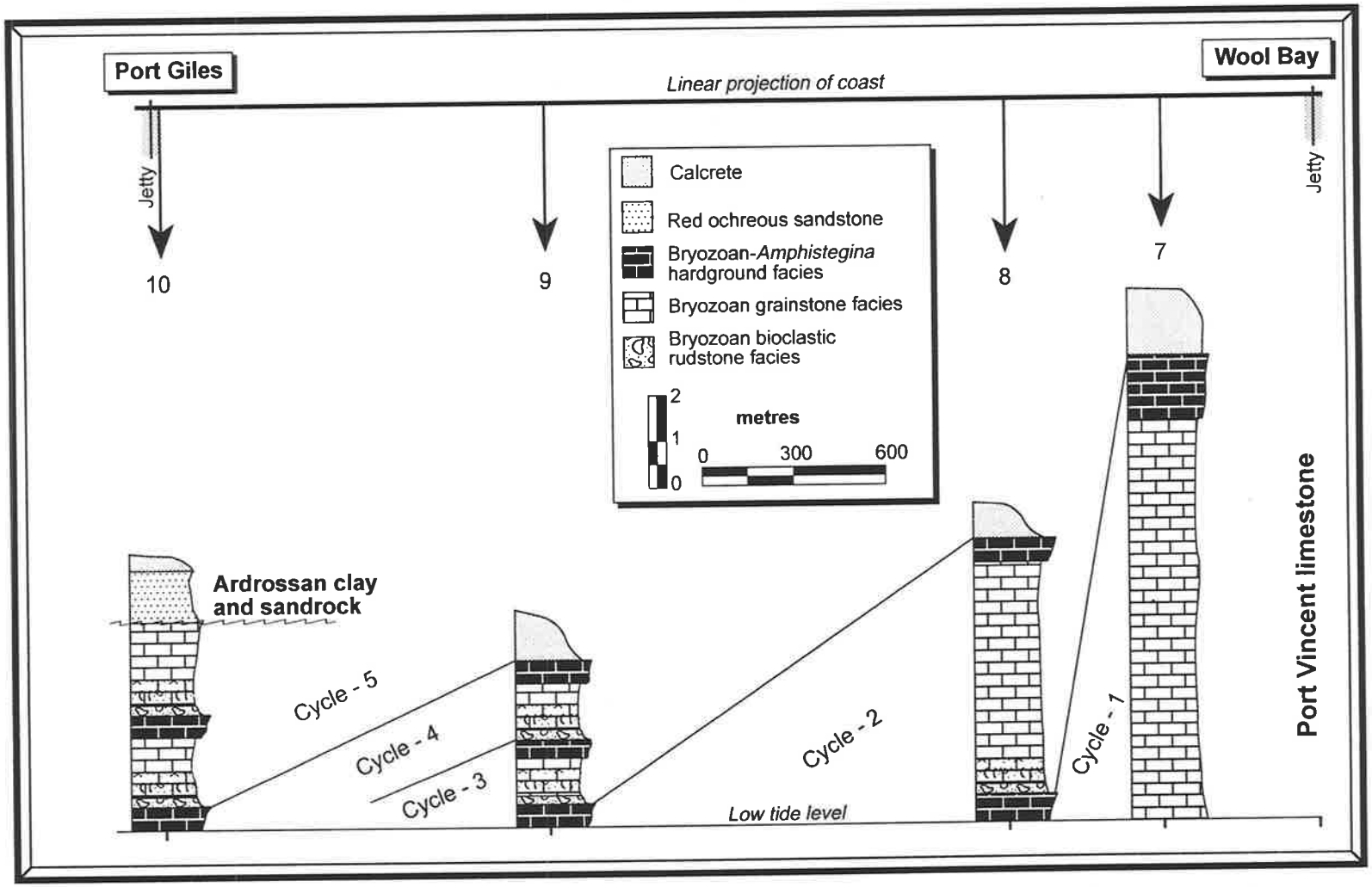

Stratigraphic coloumns of sections 7, 8, 9 and 10 in the coastal cliffs between Wool Bay and Port Giles

APPENDIX B-6

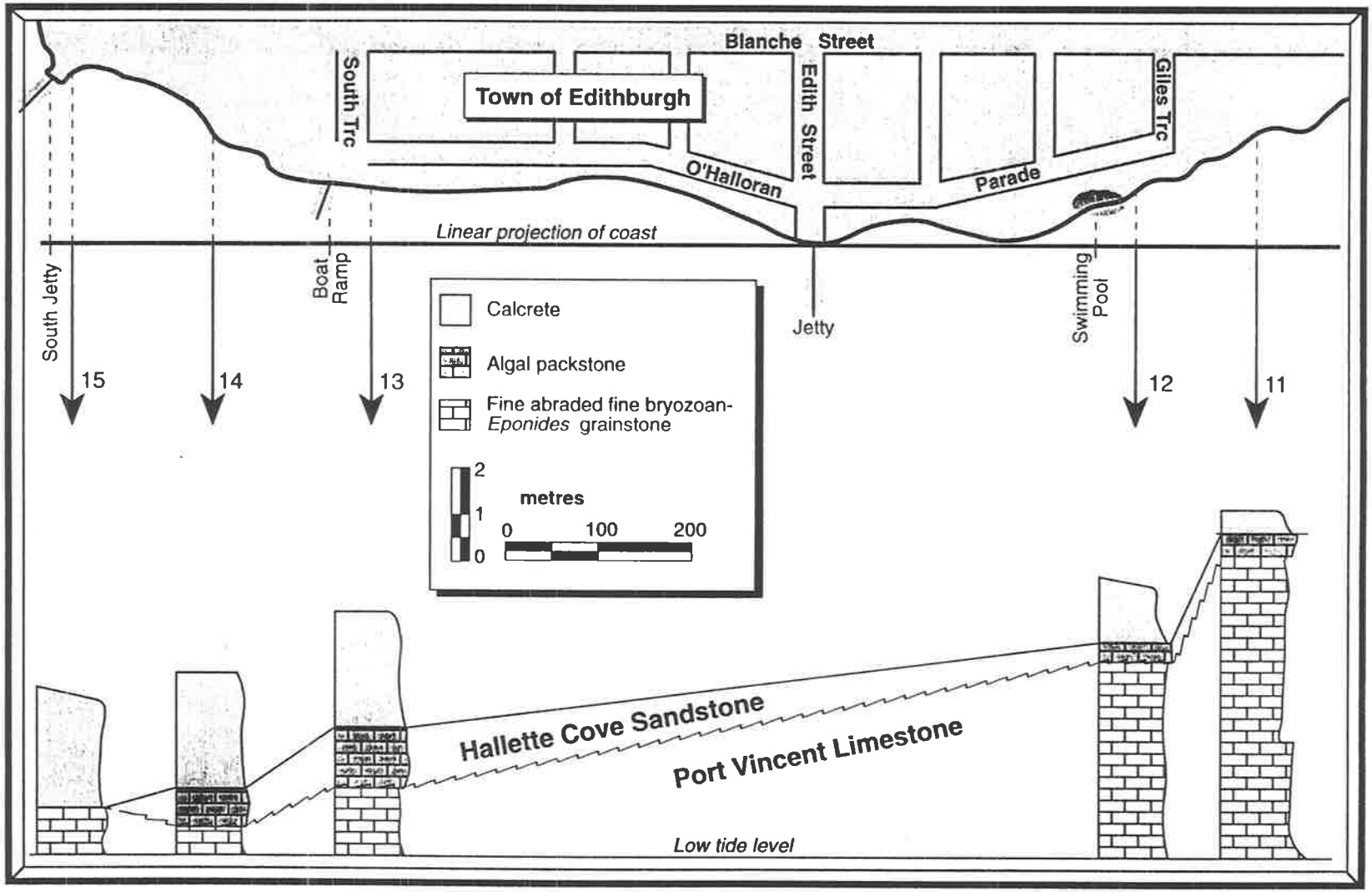

Stratigraphic coloumns of sections 11, 12, 13, 14, and 15 in the coastal cliffs north and south of Edithburgh

APPENDIX B-7

Frequency analysis by grain bulk (gives volume %, Dunham, 1962) for selected samples from section 6, north of Stansbury.

Sample No. / Variables%	1/6 counts	1/6 %	2/6 counts	2/6 %	3/6 counts	3/6 %	4/6 counts	4/6 %	5/6 counts	5/6 %
ERde cy	207	31.36	118	18.58	128	19.78	54	8.307	97	16.16
artic-branch ch	135	20.45	203	31.96	238	36.78	66	10.15	70	11.66
ERro ch	18	2.727	44	6.929	6	0.927	2	0.307	50	8.333
EN cy					5	0.772			6	1
EN ch	36	5.454	21	3.307	7	1.081	5	0.769	14	2.333
ERfe cy										
ERfe ch	4	0.606					2	0.307	7	1.166
EFartc-zo cy										
EFart-zo ch										
Vagrant					4	0.618	3	0.461	3	0.5
FO							1	0.153	42	7
Bryoz-bioclasts	61	9.242	14	2.204	27	4.173	142	21.84	86	14.33
Echinoids	57	8.636	73	11.49	46	7.109	32	4.923	61	10.16
Bivalves	2	0.303							2	0.333
Coral										
Serpulids										
Cibicides					8	1.236	8	1.230	2	0.333
Elphedium										
Milio/Textularid							2	0.307		
Bigenerina										
Spirilina										
Amphistigina										
Other Benthics			1	0.157	3	0.463	6	0.923	1	0.166
Bioclasts			1	0.157	2	0.309			1	0.166
Algae					4	0.618	3	0.461		
Groundmass							11	1.692	3	0.5
Porosity intergra	98	14.84	95	14.96	137	21.17	169	26	70	11.66
Syntax. cement	26	3.939	49	7.716	9	1.391	47	7.230	50	8.333
Intergra-cement	10	1.515			4	0.618	2	0.307	22	3.666
Glauconite	5	0.757	5	0.787	10	1.545	18	2.769	7	1.166
Quartz	1	0.151	3	0.472	8	1.236	77	11.84	6	1
Peloids										
TOTAL count	**660**		**635**		**647**		**650**		**600**	

The following intragranular variables are not included in the total count (out of count). They are listed for the interest of researchers seeking frequency analyses tests by grain solid (gives wt%, Dunham, 1962).

pores-ERde cy	8		4		1				3	
pores-artic-bra ch	40		27		34		2		13	
pores-ERro ch	3		7		1					
pores-EN ch	2		3		1				3	
pores-FO									8	
pores-ERfe ch	1								3	
cement ERde cy	3								4	
cement artic ch	7									
cement ERro ch									1	
cement EN ch									2	
cement -FO									1	
Matrix ERde cy										
Matrix artic-br ch										
Matrix ERro ch										

Sample No. Variables%	6/6 counts	%	7/6 counts	%	8/6 counts	%	9/6 counts	%	10/6 counts	%
ERde cy	218	33.38	102	15.57	149	22.92	121	20.86	114	18.78
artic-branch ch	149	22.81	143	21.83	118	18.15	73	12.58	158	26.02
ERro ch			1	0.152	7	1.076	2	0.344	5	0.823
EN cy										
EN ch	1	0.153	49	7.480	21	3.230	19	3.275	71	11.69
ERfe cy										
ERfe ch					2	0.307				
EFartc-zo cy										
EFartic-zo ch										
Vagrant	2	0.306			2	0.307				
FO										
Bryoz-bioclasts	24	3.675	19	2.900	23	3.538	15	2.586	25	4.118
Echinoids	60	9.188	40	6.106	58	8.923	77	13.27	41	6.754
Bivalves							1	0.172	4	0.658
Coral									1	0.164
Serpulids	1	0.153	2	0.305	1	0.153			3	0.494
Cibicides	13	1.990	9	1.374	14	2.153	17	2.931	12	1.976
Elphedium	1	0.153	2	0.305						
Milio/Textularid	1	0.153			2	0.307	4	0.689	3	0.494
Bigenerina							1	0.172		
Spirilina							1	0.172		
Amphistigina									2	0.329
Other Benthics	3	0.459	1	0.152	5	0.769	10	1.724	4	0.658
Bioclasts	3	0.459	3	0.458					1	0.164
Algae	4	0.612	45	6.870	37	5.692	30	5.172	16	2.635
Groundmass									55	9.060
Porosity intergra	111	16.99	182	27.78	94	14.46	66	11.37	67	11.03
Syntax. cement	45	6.891	16	2.442	3	0.461	7	1.206	9	1.482
Intergra-cement	5	0.765	23	3.511	112	17.23	131	22.58	14	2.306
Glauconite	7	1.071	9	1.374			2	0.344	2	0.329
Quartz	5	0.765	9	1.374	1	0.153	3	0.517		
TOTAL count	**653**		**655**		**650**		**580**		**607**	

The following intragranular variables are not included in the total count (out of count). They are listed for the interest of researchers seeking frequency analyses tests by grain solid (gives wt%, Dunham, 1962).

pores-ERde cy	14		4						5	
pores-artic-bra ch	36		30		3		1		16	
pores-ERro ch					1					
pores-EN ch			4		3				6	
cement Erde cy			5		5		6		2	
cement artic ch			5		9		11		1	
cement ERro ch										
cement EN ch			1		2		3		3	
cement (other)							1 Benthic			
Matrix ERde cy										
Matrix artic ch										
Matrix ERro ch										
Matrix EN ch										

Sample No. / Variables%	11/6 counts	%	12/6 counts	%	13/6 counts	%	16/6 counts	%	17/6 counts	%
ERde cy	151	23.63	48	8.727	148	23.27	76	12.64	58	10.74
artic-branch ch	174	27.23	85	15.45	199	31.28	33	5.490	114	21.11
ERro ch	15	2.347	22	4	8	1.257	3	0.499		
EN cy										
EN ch	17	2.660	35	6.363	21	3.301	16	2.662	56	10.37
ERfe cy										
ERfe ch	11	1.721								
EFartc-zo cy										
EFart-zo ch										
Vagrant	5	0.782							2	0.370
FO							9	1.497		
Bryoz-bioclasts	54	8.450	16	2.909	67	10.53	61	10.14	31	5.740
Echinoids	71	11.11	30	5.454	66	10.37	39	6.489	69	12.77
Bivalves			3	0.545			4	0.665	1	0.185
Coral			2	0.363						
Serpulids			2	0.363			3	0.499		
Cibicides	3	0.469	2	0.363	4	0.628	15	2.495	14	2.592
Elphedium										
Milio/Textularid			1	0.181			1	0.166	2	0.370
Bigenerina										
Spirilina										
Amphistigina			2	0.363					4	0.740
Other Benthics			1	0.181	2	0.314	3	0.499	12	2.222
Bioclasts							3	0.499	3	0.555
Algae			3	0.545			11	1.830	3	0.555
Groundmass			263	47.81			48	7.986	117	21.66
Porosity intergr	88	13.77	13	2.363	78	12.26	66	10.98	9	1.666
Syntax. cement	32	5.007	5	0.909	32	5.031	27	4.492	6	1.111
Intergra-cement	18	2.816	11	2	11	1.729	173	28.78	38	7.037
Glauconite			3	0.545			7	1.164		
Quartz			1	0.181			1	0.166	1	0.185
Peloids							2	0.332		
TOTAL count	**639**		**550**		**636**		**601**		**540**	

The following intragranular variables are not included in the total count (out of count). They are listed for the interest of researchers seeking frequency analyses tests by grain solid (gives wt%, Dunham, 1962).

pores-ERde cy	13				9					
pores-artic-bra ch	22		2		29				2	
pores-ERro ch	2		1							
pores-EN ch							2			
Pores uniden-Bry							1			
cement ERde cy	2				2		1		2	
cement artic ch	5				7		5		5	
cement ERro ch			1							
cement EN ch					1		4			
cement										
cement unide-Bry							2			
Matrix ERde cy										
Matrix artic-br ch			15						11	
Matrix ERro ch			8							
Matrix EN ch			8						1	

APPENDIX C-1a

Microprobe quantitative analysis showing elemental composition (%) of the non-luminescent synsedimentary (marine) cement and internal micrite. The analysis was conducted along traverse 1 in figure 4.2 on page 102. Graphical representation is illustrated in figure 4.3 on page 103. To convert to PPM multiply by 10,000.

Points	CaO	MgO	FeO	MnO	Al2O3	SrO	Total
Low Mg Calcite Cement							
1	54.84	0.036	0	0.072	0.025	0.051	55.024
2	55.54	0	0.012	0.005	0.008	0.023	55.588
3	56.97	0.101	0	0.006	0.01	0.03	57.117
4	54.92	0.224	0	0.008	0	0.029	55.181
5	54.66	0.041	0.037	0.057	0.004	0.039	54.838
6	57.15	0.037	0	0.072	0	0.054	57.313
7	53.95	0.054	0.024	0.072	0.015	0.035	54.15
8	55.99	0.637	0	0.021	0	0.053	56.701
9	55.91	0	0.061	0.174	0	0.03	56.175
10	58.31	0	0	0.021	0.007	0.012	58.35
11	55.66	0	0	0	0	0.054	55.714
Non-Luminescent Synsedimentary (Marine) Cement							
12	54.98	0.837	0.024	0.044	0.013	0.059	55.957
13	60.09	0.874	0.012	0	0	0.083	61.059
14	54.67	0.593	0.016	0.011	0	0.067	55.357
15	55.66	0.595	0.016	0.004	0	0.048	56.323
16	54.67	0.466	0.02	0.023	0	0.056	55.235
17	58.33	0.54	0.012	0.012	0.005	0.034	58.933
18	57.24	0.595	0.047	0	0	0.034	57.916
19	62.41	0.867	0.002	0	0.002	0.032	63.313
20	57.08	0.551	0.053	0	0	0.031	57.715
21	57.12	1.025	0	0	0.001	0.042	58.188
Internal Micrite Precipitate							
22	53.88	0	0	0.011	0	0	53.891
23	50.29	0.229	0.098	0.021	0.023	0.069	50.73
24	50.7	0.02	0.071	0	0.022	0.029	50.842
25	54.46	0.242	0.008	0.026	0.017	0.043	54.796
26	53.51	0.19	0.349	0.056	0.164	0.028	54.297
27	51.88	0.503	0.284	0.056	0.228	0.099	53.05
28	53.56	0.409	0.41	0.018	0.502	0.075	54.974
29	48.91	0.34	0.852	0.038	1.009	0.052	51.201
30	46.12	0.612	1.618	0.056	1.858	0.041	50.305
31	51.06	0.355	0.687	0.057	0.546	0.03	52.735
32	46.96	0.408	1.966	0.068	1.277	0.017	50.696
33	52.95	0.298	0.351	0.014	0.256	0.031	53.9
34	51.63	0.457	0.887	0.088	0.454	0.046	53.562
35	55.51	0.546	0.135	0.055	0.091	0.074	56.411
36	51.59	0.252	0.353	0.054	0.246	0.023	52.518
37	49.56	0.29	0.909	0.065	0.58	0.011	51.415
38	50.56	0.29	0.634	0.064	0.488	0.026	52.062

APPENDIX C-1b

Microprobe quantitative analysis showing elemental composition (%) of a bryozoan fragment, non-luminescent synsedimentary (marine) cement and internal micrite. The analysis was conducted along traverse 2 in figure 4.2 on page 102. Graphical representation is illustrated in figure 4.3 on page 103. To convert to PPM multiply by 10,000.

Points	CaO	MgO	FeO	MnO	Al2O3	SrO	Na2O	Total
Bryozoan Fragment								
1	56.75	0.418	0.006	0.071	0.038	0.048	0.004	58.335
2	59.66	0.504	0.016	0.084	0	0.048	0.041	60.353
3	56.09	0.397	0.014	0.065	0	0.041	0.032	56.639
4	58.39	0.206	0.002	0.027	0.014	0.042	0.015	58.696
5	58.02	0.107	0	0.053	0	0	0.043	58.223
6	58.41	0.167	0.01	0.099	0.013	0.045	0.635	59.379
7	59.04	0.184	0	0.07	0.004	0.033	0.164	59.495
Non-Luminescent Synsedimentary (Marine) Cement								
8	59.8	0.777	0	0.028	0.024	0.033	0.021	60.683
9	62.87	0.63	0.422	0.056	0.085	0.056	0.111	64.23
10	57.97	0.618	0.22	0.041	0.057	0.046	0.027	58.979
11	56.3	1.002	0.018	0.055	0	0.105	0.048	57.528
12	60.96	1.162	0	0.027	0.003	0.072	0.04	62.264
13	55.19	1.029	0	0.016	0	0.034	0.14	56.409
14	65.72	0.869	0.202	0.037	0.044	0.082	0.171	67.125
15	55.72	0.944	0.008	0.011	0	0.075	0.045	56.803
16	64.74	1.068	0.123	0.067	0.016	0.068	0.09	66.172
Internal Micrite Precipitate								
17	54.91	0.545	0.063	0.056	0	0.057	0.009	55.64
18	61.39	0.518	0.025	0.051	0.005	0.054	0.048	62.091
19	55.67	0.566	0.016	0.006	0.008	0.114	0.259	56.639
20	56.36	0.433	0	0.213	0.024	0.06	0.029	57.119
21	62.97	0.087	0	0.461	0	0.042	0.215	63.775
22	55.88	0.154	0	0.251	0	0.045	0.131	56.461
23	56.34	0.206	0	0.054	0.011	0.062	0.118	56.791
24	59.68	0.221	0.008	0.043	0	0.092	0.075	60.119
25	55.2	0.108	0	0.071	0.003	0.062	0.041	55.485
26	59.15	0.525	0	0.145	0	0.078	0.049	59.947
27	55.12	0.267	0.698	0.065	0.773	0.046	0.047	57.016
28	50.62	0.304	0.649	0.03	0.658	0.065	0.064	52.39
29	49.74	0.215	1.226	0.055	0.704	0.02	0.028	51.988
30	48.48	0.271	0.953	0.106	0.976	0.016	0.029	50.831
31	49.61	0.304	1.09	0.093	0.693	0.036	0.044	51.87
32	51.83	0.393	1.142	0.079	0.466	0.086	0.035	54.031
33	47.83	0.366	0.666	0.072	1.466	0.02	0.063	50.483
34	29.01	0.735	1.371	0.032	7.145	0	0.116	38.409
35	48.91	0.253	0.673	0.048	1.085	0.02	0.063	51.052
36	52.01	0.231	0.419	0.058	0.293	0.048	0.051	53.11
37	51.21	0.221	0.359	0.039	0.393	0.056	0.051	52.329
38	49.9	0.282	0.639	0.048	0.696	0.038	0.029	51.632

Points	CaO	MgO	FeO	MnO	Al2O3	SrO	Na2O	Total
39	50.64	0.28	1.134	0.074	0.422	0.043	0.043	52.636
40	51.84	0.366	0.463	0.026	0.365	0.034	0.008	53.102
41	49.73	0.264	0.743	0.018	0.569	0.015	0.039	51.378
42	49.36	0.335	0.718	0.054	0.882	0.016	0.037	51.402
43	45.38	0.378	2.137	0.061	0.943	0.034	0.05	48.983

APPENDIX C-2

Microprobe quantitative analysis showing elemental composition (%)of the three types of synaxial cements illustrated in plate 4.7 on page 107. To convert to PPM multiply by 10,000.

Spots	CaO	MgO	FeO	Al2O3	MnO	SrO	Na2O
non-luminescent marine							
1	58.2	0.403	0	0	0.124	0.032	0.028
2	52.312	0	0.071	0.069	0.017	0.025	0.23
3	58.541	0	0.022	0	0.019	0.053	0.017
4	57.237	0.022	0	0.01	0.031	0.035	0.004
5	59.23	0	0	0	0.024	0.059	0.029
6	58.979	0	0.006	0	0.008	0.058	0
7	57.133	0.147	0	0.01	0.286	0.028	0.029
8	57.053	0	0	0.003	0	0	0.041
9	57.833	0	0.035	0.002	0.021	0.029	0.103
bright-luminescent shallow-burial							
10	56.302	0	0	0.01	1.868	0.044	0.039
11	56.079	0	0	0	0.876	0.036	0.021
12	55.632	0	0.018	0.038	1.303	0.024	0
13	58.478	0	0.012	0	1.742	0.068	0.007
14	58.563	0	0.067	0	0.526	0.079	0.007
15	57.761	0	0.006	0	0.238	0.052	0.021
16	58.08	0	0.006	0.017	0.133	0.028	0.027
non-luminescent meteoric with several bright-luminescent zones							
17	58.05	0	0.043	0	0.03	0.043	0.041
18	58.37	0	0	0.01	0.021	0.039	0.027
19	58.42	0	0	0.001	0.024	0.031	0
20	57.245	0	0	0	0.001	0.049	0.032
21	58.924	0	0.049	0.019	0.034	0.06	0.045
22	52.009	0	0.043	0.048	0.016	0.026	0.161
23	57.34	0	0.031	0.005	0.011	0.033	0
24	56.795	0	0.01	0.035	0	0.024	0
25	57.988	0	0	0.013	0	0.014	0.056
26	57.4	0	0	0.003	0.029	0.05	0.04
27	57.85	0	0	0.002	0	0.027	0.013

Spots	CaO	MgO	FeO	Al2O3	MnO	SrO	Na2O
28	58.181	0	0.047	0.014	0.02	0.007	0.024
29	58.308	0	0.022	0	0.016	0.03	0.021
30	58.442	0	0.008	0.013	0.013	0.04	0.017
31	56.481	0	0	0.01	0.026	0.08	0.004
32	58.901	0	0	0	0.03	0.029	0.009
33	57.254	0	0.037	0.01	0	0.029	0.041
34	56.548	0	0	0.015	0.039	0.004	0.049
35	57.392	0	0.029	0	0.016	0.09	0.036
36	58.379	0	0.012	0.003	0	0.007	0.033
37	57.752	0	0.027	0.009	0.006	0.047	0.024
38	56.764	0	0	0.024	0	0.089	0.019
39	57.487	0	0.004	0	0	0.064	0.02
40	58.183	0	0.006	0	0.056	0.036	0.027
41	57.825	0	0	0	0	0.026	0.012
42	58.535	0	0	0	0.034	0.066	0.028
43	58.168	0	0.01	0	0	0	0.008
44	58.453	0	0.031	0.001	0.017	0.04	0.1
45	57.62	0	0.006	0.011	0	0.024	0.009
46	58.14	0	0.039	0.013	0.034	0	0.02
47	58.67	0	0.039	0.129	0.14	0.025	0.019
48	58.82	0	0.043	0.012	0.015	0.052	0.029
49	56.923	0	0.051	0	0.065	0.027	0.044
50	52.741	0.906	0.296	0.176	0.014	0.066	0.08

APPENDIX D-1

Dolomite stoichiometry was identified by XRD. All samples were spiked with quartz to provide a reference peak for accurate measurements. Positions of peaks were measured to the nearest 0.01° 2-theta, using the computer program XPLOT. Whole dolostone samples show them to contain on average $Ca_{(53\ mole\%)}\ Mg_{(41.6)}\ Fe_{(5.4)}\ (CO_3)2$.

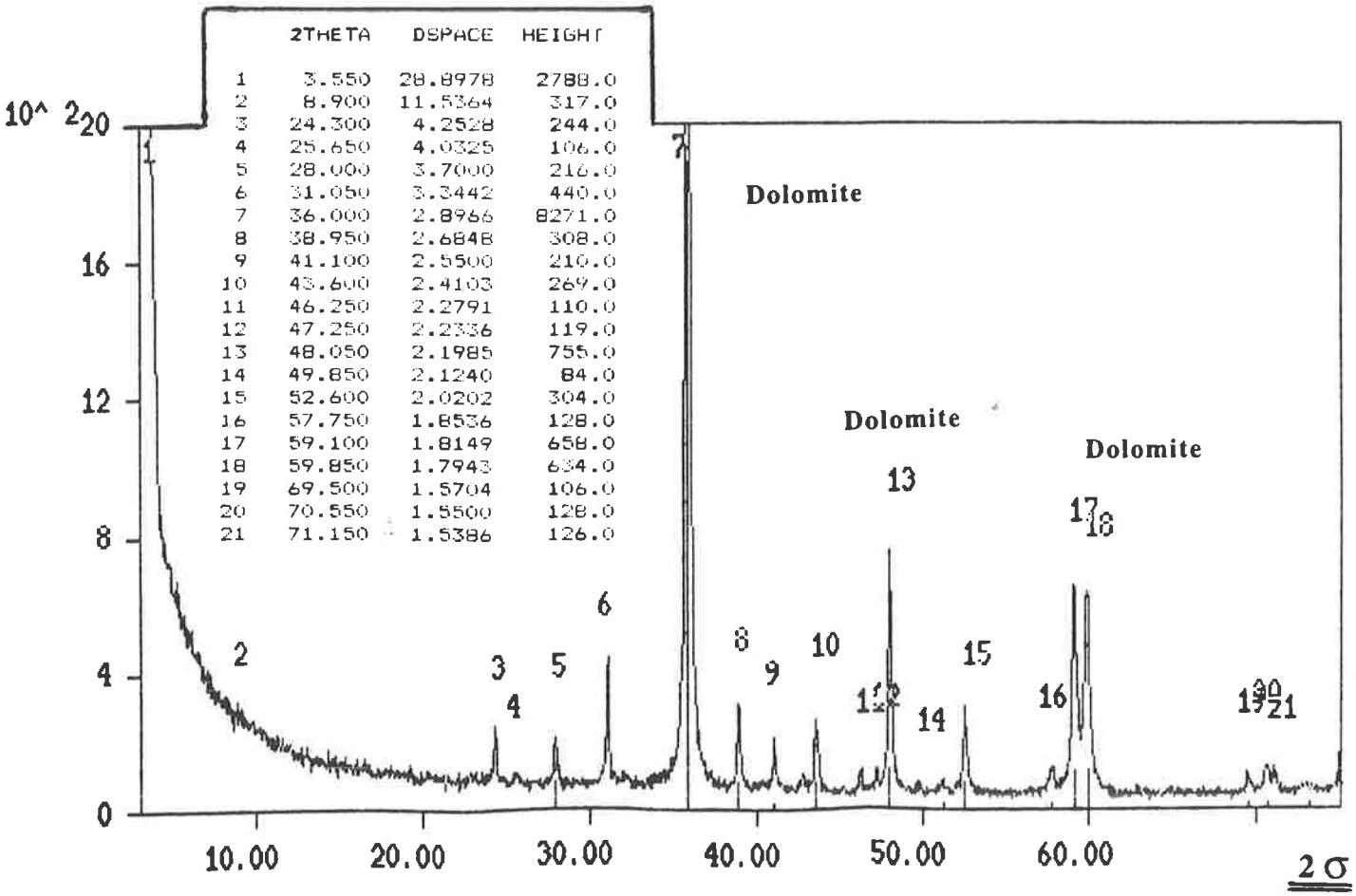

APPENDIX D-2

Microprobe quantitative analysis showing Fe and Mn content (ppm) in the dolomite crystal illustrated in figures 5.3, 5.4, 5.5 and plate 5,2 on page 140.

Spots	FeO	MnO
1	3840	620
2	3980	4160
3	3530	2300
4	3730	3140
5	3250	210
6	23160	21240
7	14310	55300
8	22960	23780
9	23810	41100
10	18530	980
11	25510	0
12	11970	150
13	11600	170
14	36570	0
15	21420	120
16	35920	990
17	36940	780
18	35940	1470
19	30910	1260
20	36190	890
21	15630	900
22	11840	460
23	39630	2270
24	122230	410
25	171990	170
26	34860	760
27	31460	1600
28	30020	1850
29	28980	1790
30	29370	1300
31	2440	0
32	1690	0
33	1710	1300
34	2240	0
35	1320	0

APPENDIX D-3

X-ray analysis (XRD) for three brachiopod specimens from the Port Vincent Limestone dolomite used for isotope analysis (figure 5.8 - page 156). The three specimens belong to the same species*Stethothyris sufflata,* and they all contain approximately 0 mole % $MgCO_3$.

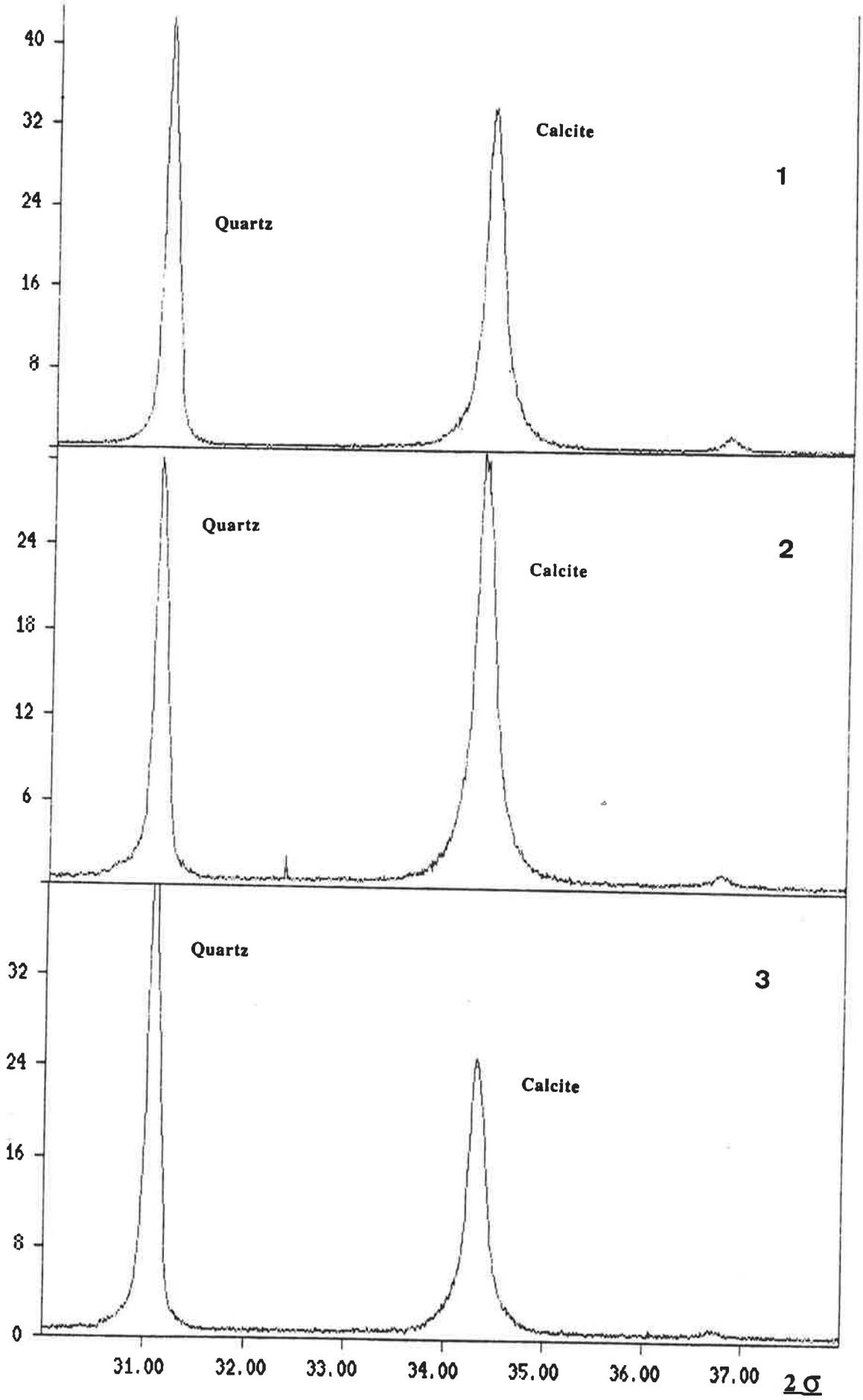
40
32
24
16
8
Quartz
Calcite
1
24
18
12
6
Quartz
Calcite
2
32
24
16
8
0
Quartz
Calcite
3
31.00
32.00
33.00
34.00
35.00
36.00
37.00
2σ

B. Shubber, Y. Bone, B. McGowran and N.P. James (1995) Facies analysis of a cool-water carbonate formation: The Oligocene-Miocene Port Vincent Limestone, St. Vincent Basin - South Australia.
Cool and Cold-Water Carbonate Conference held Geelong, Victoria, pp. 71-72, 1995

B. Shubber, Y. Bone, B. McGowran and N.P. James (1996) Cementation in cool-water subtidal carbonate cycles: the Tertiary Port Vincent Limestone, St. Vincent Basin, South Australia.
13th Australian Geological Convention, Canberra, 19-23 February 1996 [GSA Abstract no. 41]

B. Shubber, Y. Bone, B. McGowran and N.P. James (1996) Shallow burial dolomitization in the Tertiary Cool-water Port Vincent Limestone, St. Vincent Basin, South Australia.
13th Australian Geological Convention, Canberra, 19-23 February 1996
[GSA Abstract no. 41]